PRECURSOR ROUTES TO CONDUCTING POLYMERS FROM THE RING-OPENING METATHESIS POLYMERIZATION OF CYCLIC OLEFINS

Thesis by

Timothy Manning Swager

In Partial Fulfillment of the Requirements

For the Degree of

Doctor of Philosophy

California Institute of Technology

Pasadena, California

1988

(Submitted May 16, 1988)

ELECTRONS TALK TO ME!

Oh elusive electron
how can I set thee free?
I'll unlock your chains
just show me the key.

Should I destroy your captors
those localized bonds?
Or would you like something else
should I search beyond?

I want to let you run
and move about with ease.
And you may travel in pairs
or alone if you please.

Lead me the way
to that magic superconductive state.
And I will do my best
to try to accommodate.

I'll build you a band
of whatever width you desire.
And with my friend polymer chemistry
I'll fashion you a wire.

You hold the secrets
that can make the world a better place.
And I have become curious
and decided to join the chase.

Oh magnificent electrons hear my plea
I have come to set you free.

Timothy M. Swager 1988

ACKNOWLEDGMENTS

First and foremost, I want to thank my wife and best friend Anne for her undaunting support and companionship. I cannot imagine life without her and her influence has made me a happier and stronger person.

To my research advisor Bob Grubbs, I owe considerable gratitude and thanks. His guidance will have lasting influence over my career as a chemist. Bob has allowed me to chase many pipe dreams in his laboratory, yet given me the necessary guidance to keep my research on course. I appreciate the fact that he has tolerated all my crazy ideas and allowed me to discover things for myself. It has been a pleasure working in his group. I thank Dennis Dougherty for his interest in my work and his patience as chairman of my committee.

To my parents I owe the most thanks of all. They raised me with the mind-set that I can be successful and that education is indeed a virtue. Their support for my career has been the basis of much of my motivation and for that I will be forever grateful.

There are many other people that I feel gratitude toward for my experience at Caltech. Working in an atmosphere of people who love to talk science and are so willing to think about each other's projects has made a major contribution to my scientific background.

ABSTRACT

Chapter 1 provides an introduction to the field of conductive polymers. The perspective is that of a chemist who is also interested in the physics of conductive polymers. The concepts discussed in this chapter are referred to throughout the other chapters, and should be a good primer for newcomers to this field as well as a reference to the literature for others. This chapter sets the stage for the theme of this thesis, which is the use of soluble precursor polymers in the synthesis of conductive polymers. Recent work was cited in this chapter which is not available in existing reviews of conductive polymers.

The method of ring-opening metathesis polymerization (**ROMP**) is discussed in Chapter 2. The concepts discussed therein are again referred to throughout the following chapters. The ideas of catalyst matching for different monomers are discussed, and particular emphasis is given to the steric requirements of the catalysts.

The **ROMP** of derivatives of dimethylene cyclobutene is discussed in Chapter 3. However, the primary focus of the chapter is on the polymer polydiisopropylidenecyclobutene. This material is distinctly different from other conductive polymers in the fact that it has a structure consisting of triene units that are mutually orthogonal to each other. A detailed study of this material with a variety of spectroscopies and measurements is presented.

The synthesis of polybenzvalene, and the isomerization of this material to polyacetylene, is discussed in Chapter 4. This work constitutes a new precursor method to this fundamentally important polymer, as well as a demonstration of the far reaching scope of **ROMP**. Polybenzvalene is also a high energy material and has unusual explosive properties which are also discussed.

In Chapter 5, new precursor routes to conductive polymers based on the elimination and hydrolysis of ketals are presented. This work has been primarily focused

on structural chemistry and how to best transform the precursor polymers into conductive polymers. The majority of the effort has been focused on the poly(quinone bisketals); however, another example of this concept is presented briefly.

TABLE OF CONTENTS

LIST OF TABLES

page

LIST OF FIGURES, SCHEMES AND EQUATIONS

page

Chapter 1

Chapter 2

Chapter 3

Chapter 1

AN INTRODUCTION TO CONDUCTIVE POLYMERS: A CHEMICAL PERSPECTIVE

INTRODUCTION:

The study of electrical conduction in extensively conjugated polymers, known as conductive polymers, has seen considerable effort over the last decade.[1] Examples of conductive polymers exhibiting high conductivities (σ's) are shown in Figure 1.1. These materials are intrinsically wide band semiconductors and high conductivities are only attainable with oxidation or reduction. This redox treatment has been termed doping in analogy to semiconductors, and oxidative and reductive modifications are referred to as p- and n-doping, respectively. A logarithmic scale of conductivities of various materials is given in Figure 1.2 to put these materials in perspective.

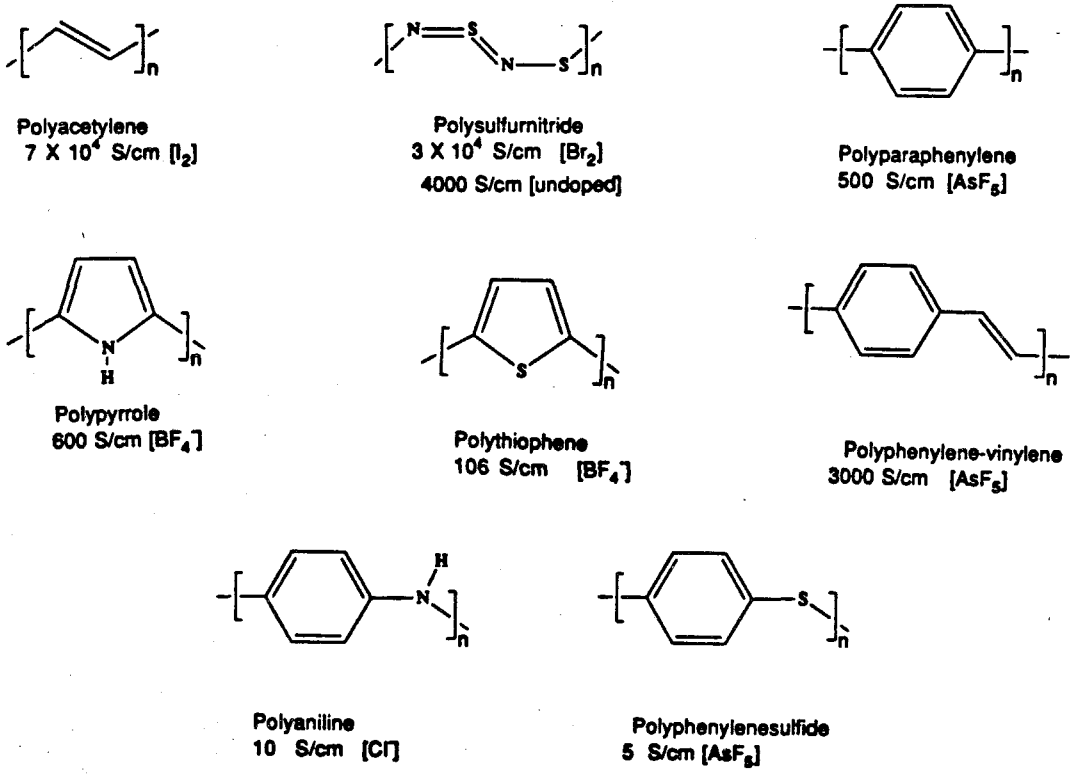

Figure 1.1. Well-known conductive polymers and their conductivities. The chemical oxidant for which the conductivity corresponds is shown in brackets. S=Ω^{-1}. Electrochemical doping is signified with a (*) and in these cases the counterion is in brackets.

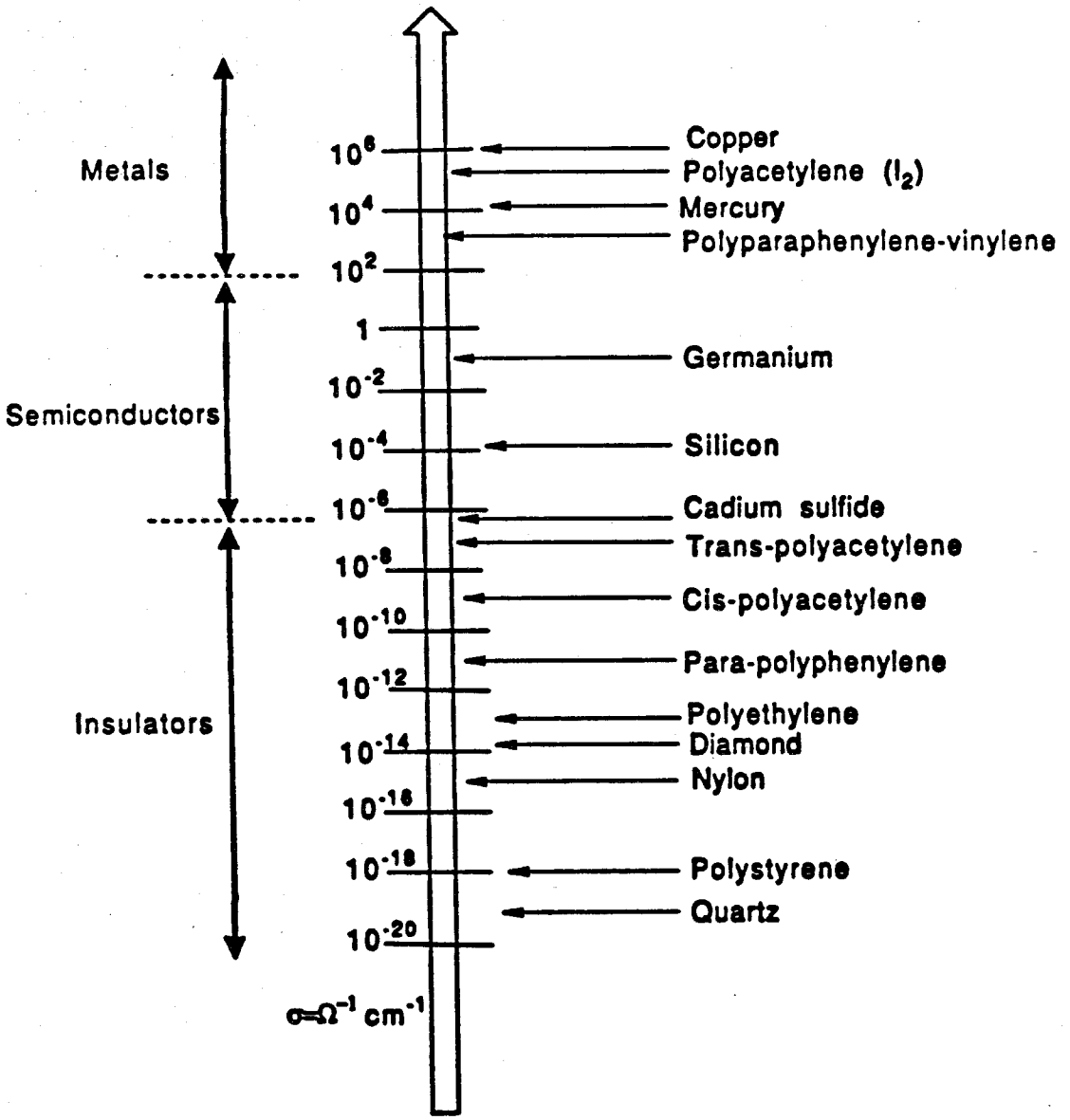

Figure 1.2. A logarithmic plot of the conductivities of various materials, and the general ranges of insulators, semiconductors, and metals are shown.

Much of the interest in CPs has been fostered by the general intrigue of many scientists (the author included) with designing, synthesizing, and studying organic electrical conductors. However, these materials also have many potential applications. In general, polymers have been replacing metals in many structural applications. It is possible that this may someday be the case for conductors. In addition, CPs exhibit phenomena not offered by metals, and hence they may be much more than just metal substitutes. The ability to use standard polymer processing and fabrication techniques is perhaps the most appealing economic feature of CPs . Fiber and sheet processing techniques can potentially lead to materials of prescribed crystallinity and mechanical properties,[2] for a fraction of the cost that it takes to process metals. Imagine spinning wire as if it were polyester, maufacturing conductive sheeting as if it were sandwich wrap, or mold injecting battery storage plates. As a result of their light weight and reversible redox behavior, CPs may soon see commercial application as light-weight rechargeable battery materials.[3] The conductivity of CPs may be varied with doping all the way from an insulator to a metal (Figure 1.2). This variable conductivity with doping provides a mechanism for electrochemical switching, and has been shown to be be effective in the formation of molecule-based devices.[4] Molecular conductors will likely be key components in the realization of the currently speculative field of molecular electronics.[5] CPs have been shown to behave as sensors in both an optical[5c] and chemical capacity.[6] In addition, these materials have also been shown to exhibit non-linear optical responses[7] and hence may have applications in optical signal processing.[8]

HISTORY:

Polysulfurnitride $(SN)_x$ was the first CP to be studied in detail.[9] This material is an intrinsic conductor (i.e., doesn't require doping to become conductive) and has the added feature that it becomes superconductive at .35°K .[9] To date,

this material is the only known polymeric superconductor. However, interest in this material has diminished as a result of the occasional violent explosions that occur in its synthesis. Polysulfurnitride is an inorganic **CP** and in the rest of this discussion only organic **CPs** are considered.

The current interest in organic conductive polymers was sparked by a historic discovery by Shirakawa and Ikeda in 1971.[10] They observed the formation of films of polyacetylene (**PA**) when the surface of concentrated solutions of the Ziegler-Natta catalyst $Ti(OC_4H_9)$:$AlEt_3$ was exposed to acetylene. This method has been widely used for **PA** preparation and is commonly referred to as the "Shirakawa method." These **PA** films were subsequently shown in 1977 to exhibit conductivities comparable to metals ($\approx 10^2\Omega^{-1}cm^{-1}$) when doped with I_2.[11] Soon after this disclosure, high conductivity in polypyrrole[12] and polyparaphenylene[13] were reported.

ELECTRONIC STRUCTURES:

An intuitive "chemical" understanding of the electronic states of some well-known conductive polymers will aid in predicting the properties of new materials. The reader that is interested in a more "physical" discussion is referred to the literature.[14] **PA** is the simplest and most conductive **CP**, and hence has received the most study.[15] **PA** and most conductive polymers are considered one-dimensional materials since the strongest electronic interactions are between orbitals within a given polymer chain. In the limit of an infinite polymer chain, the orbitals form a continuum of electronic states which are referred to as bands. The highest energy occupied bands and lowest energy unoccupied bands are π bands which are responsible for the conductive properties of these materials. In theory if all the C-C bond lengths of **PA** were equal in length, the conduction band and valence band (LUMO and HOMO) would be degenerate at the band

edge. If this were the case **PA** would be a metal and have a half-filled band as shown in Figure 1.3a. However, one-dimensional metals are intrinsically unstable with respect to a lattice deformation that breaks this degeneracy and lowers the energy (Figure 1.3b). This instability is called a Peierls instability[16] and results in a "dimerization" of the **PA** unit cell, with alternating shorter and longer C-C bonds. This bond length distortion in one-dimensional metals is analogous to the symmetry lowering Jahn-Teller distortion that is exhibited in transition metal complexes with degenerate HOMOs.[17] Both Jahn-Teller and Peierls distortions raise the energy of the LUMO and lower that of the HOMO. In *trans*-**PA** this energy lowering is substantial and leads to the formation of a 1.8 eV band gap between the valence band and the conduction band. The origin of this band gap is readily seen by considering the orbitals at the top of the valence band (**1**) and the bottom of the conduction band (**2**). In **1** the bonding interaction is between the shorter C-C bond and the antibonding interaction is between the longer C-C bond, thus maximizing the bonding and minimizing the antibonding. The result of alternating bond lengths is therefore a net lowering of the energy of orbitals at the top of the valence band. For **2** the opposite is true since the antibonding interactions exist across the shorter bands, while bonding is diminished by the longer bond lengths. Thus, the energy of the bottom of the conduction band is raised.

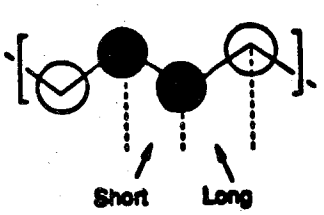

1

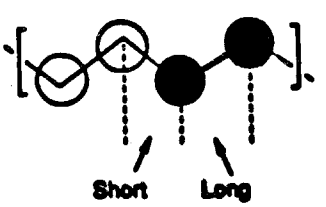

2

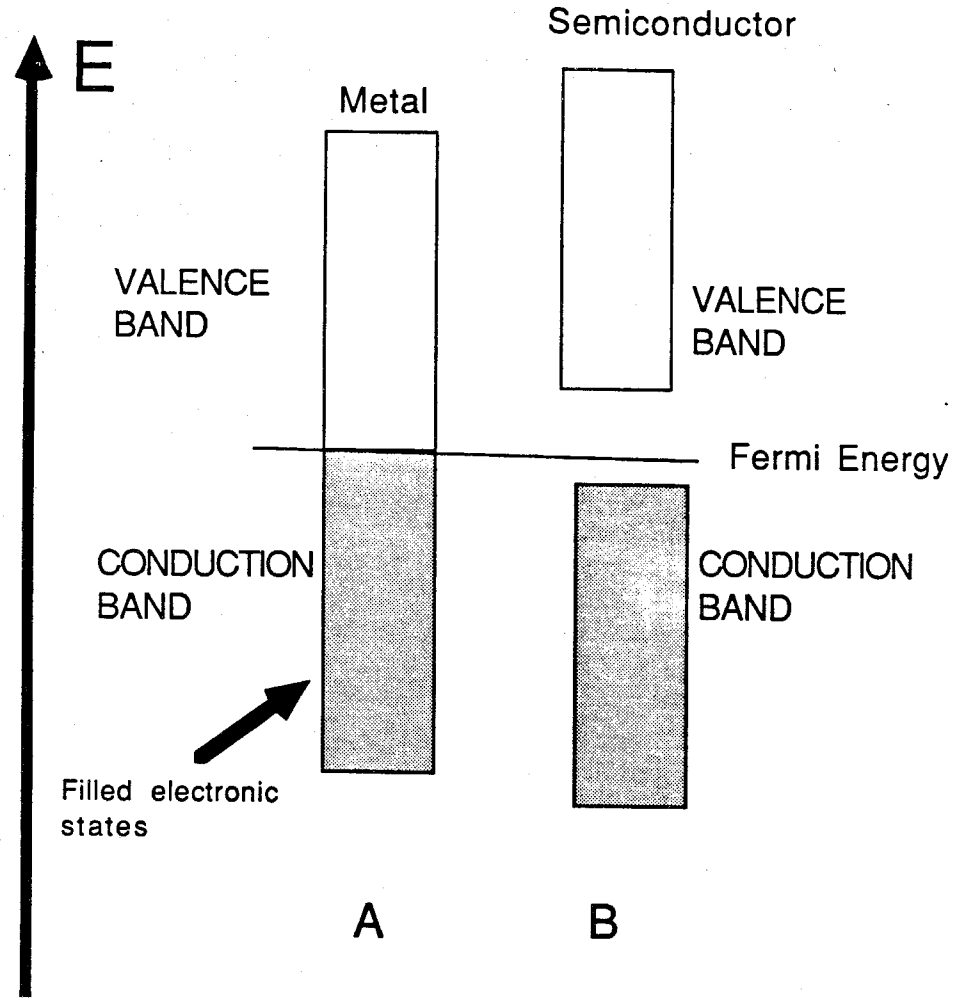

Figure 1.3 (a) Energy bands for metallic **PA** with equal bond lengths. (b) Energy bands for the dimerized **PA**, which is a wide band gap semiconductor.

In general, band gaps in **CPs** can be qualitatively thought about in terms of bond length alternation in the polymer.[18] The incorporation of aromatic groups in the polymer backbone results in particularly large bond alternation as a consequence of the preferred aromatic resonance form. For example, in polyparaphenylene the aromatic resonance form **3** is strongly preferred over the quinoid form **4**. This leads to a lengthening of the bond between phenyl rings and a band gap of 3.2 eV.

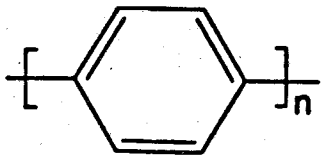

3

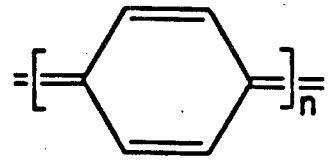

4

A clever exploitation of this bond length alternation concept has been reported by Wudl.[19] It was rationalized that benzannelating polythiophene to give polyisothianaphthene would result in a lower band gap as a result of a contribution from both resonance forms **5** and **6**. Some aromatic character is present in both **5** and **6**; hence, one resonant form will not dominate the electronic structure, and bond alternation will be diminished.[19] In fact, the band gap for polyisothianaphthene is $\approx$ 1 eV, which is the lowest "undisputed" band gap to be reported.[20] However, while the above reasoning was successful, recent theoretical studies have shown that a more accurate description of this effect is found in the orbital mixing and intrinsic electronic structures of this material.[21]

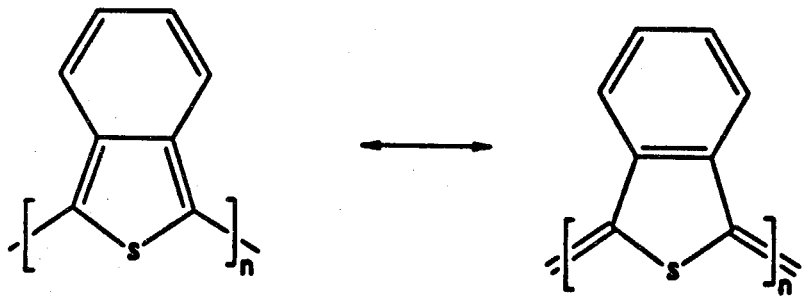

5 6

CARRIERS AND DOPED MATERIALS:

A fundamental understanding of charge transport mechanisms is useful in the design of efficient conductors. The mechanism of charge transport in **PA** has been a subject of intense study and debate.[1] The carriers in **PA** are viewed as mobile localized lattice deformations that may move along the polymer backbone. The transfer of carriers between polymer chains is less well understood. In *trans*-**PA** these carriers may be neutral (**7**), cationic (**8**), and anionic (**9**) and are present in undoped, p-doped, and n-doped **PA** respectively.

7

8

9

In the language of solid state physics the carriers in *trans*-**PA** fit the criteria of the quasi-particles called *solitons*.[22] The features necessary for this characterization are namely that the charged carriers have no spin, the neutral carrier has spin, and that the domain of the carrier has one maximum (i.e., a solitary wave packet). In the language of chemistry these carriers can be thought of as mobile delocalized radicals, carbocations, and carbanions. By convention the physics nomenclature will be used throughout this thesis. These carriers exist as localized electronic states in the middle of the bandgap of *trans*-**PA**.[22] The dimensions of the structural distortions created by solitons are considered to be approximately 12-14 carbons by most researchers.[22] However, on the basis of ENDOR measurements they have been proposed to be as large as 50 carbons.[23] There is a fundamental difference between the carriers in *cis*- and *trans*-**PA** . *Trans*-**PA** is a degenerate conductor since it has two resonance structures with the same energy. This can

be shown by considering the case of an infinite polyene where all the bond lengths are equal. Inspection reveals that both resonance structures **10** and **11** are of equal energy, for *cis*-**PA** **12** and **13** are not of equal energy and hence are not degenerate.

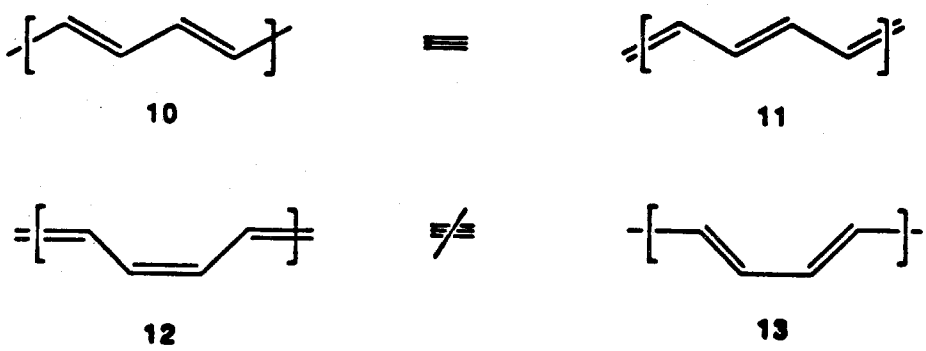

10 **11**

12 **13**

A degenerate structure like that of *trans*-**PA** is a requirement for a material to support soliton carriers. This is a consequence of a soliton presenting a topological kink which shifts the π bonds by one carbon. If the structure is degenerate then the polyene on either side of the kink is of equal energy. This degeneracy can be the result of symmetry, as is the case of *trans*-**PA** , or can be accidental. A recent theoretical study by Pranata, Grubbs, and Dougherty has found the two resonance forms of polyfulvene-vinylene **14** and **15** to be nearly degenerate.[21]

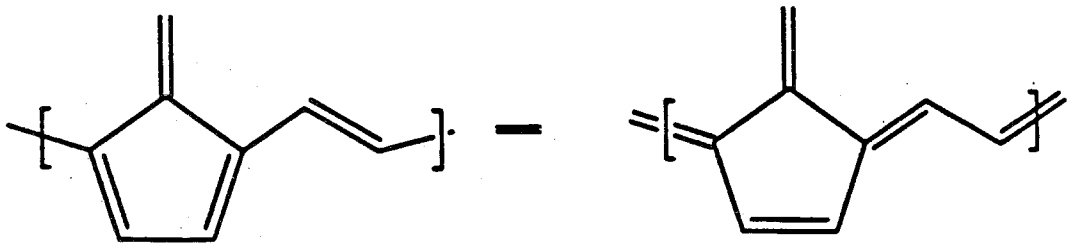

14 **15**

It is the case that most CPs have electronic structures that are not degenerate. As a consequence of this non-degenerate electronic structure the carriers in these materials cannot be solitons. This can be readily deduced by considering an example. Polythiophene, like polyparaphenylene, discussed in the previous section, is strongly biased toward the aromatic resonance form over the quinoid form. The formation of a lone cation in this material results in an aromatic resonance structure on one side of the charge, and a quinoid resonance form on the other (**16**). As a result of the energetically unfavorable quinoid resonance form, the polymer localizes the "quinoid-like" bond alternation and adopts an open shell structure **17**. For polythiophene the distortions are distributed over approximately three rings. Further oxidation can be thought to produce more radical-cation species which combine to form the analogous dication carriers **18**.

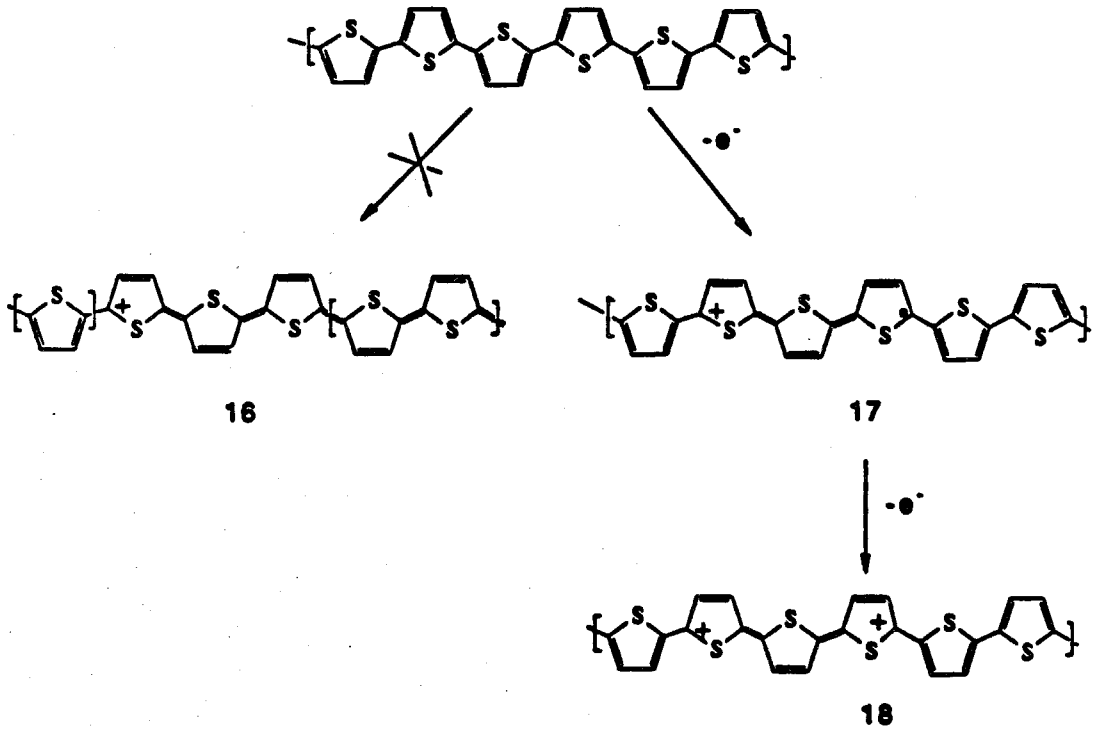

16 **17** **18**

These carriers fit the description of the quasiparticles called *polarons* (**17**) and *bipolarons* (**18**).[24] Polarons have charge and spin, and bipolarons have a charge of 2 but no spin. These carriers, like solitons, have localized energy states in the band gap; however, there are two states for each carrier and these states are not at midgap.[24] These types of carriers are quite general, and formalization of a polaron and bipolaron distortion in polyphenylene-vinylidene can be done in the same way.

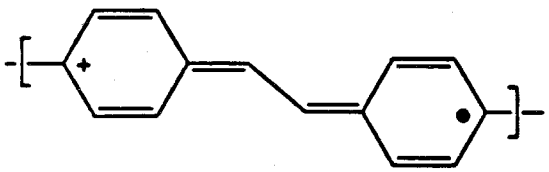

POLARON

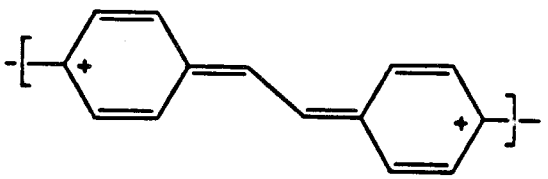

BIPOLARON

Bipolarons are closed shell species and hence their movement through a **CP** can be illustrated through resonating bonds. Hence, intuitively an organic chemist can visualize a bipolaron moving through polythiophene as shown below.

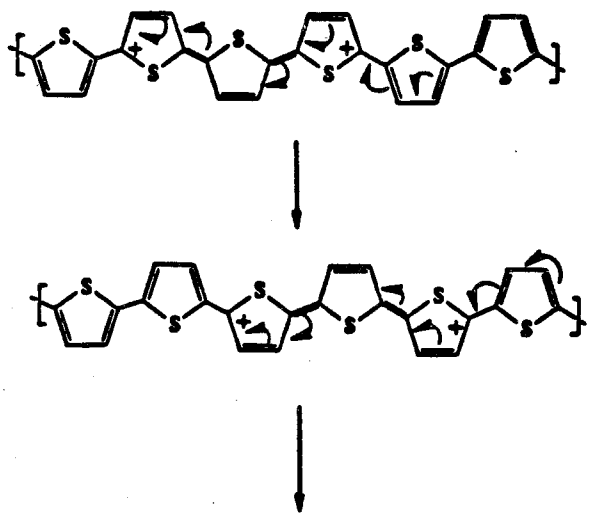

ETC.

Polyaniline is a material that is distinctly different than the other CPs discussed above.[25] The acid doping of the electrochemically deposited emeraldine form of polyaniline (**19**) leads to the most conductive form of this material (**20**).

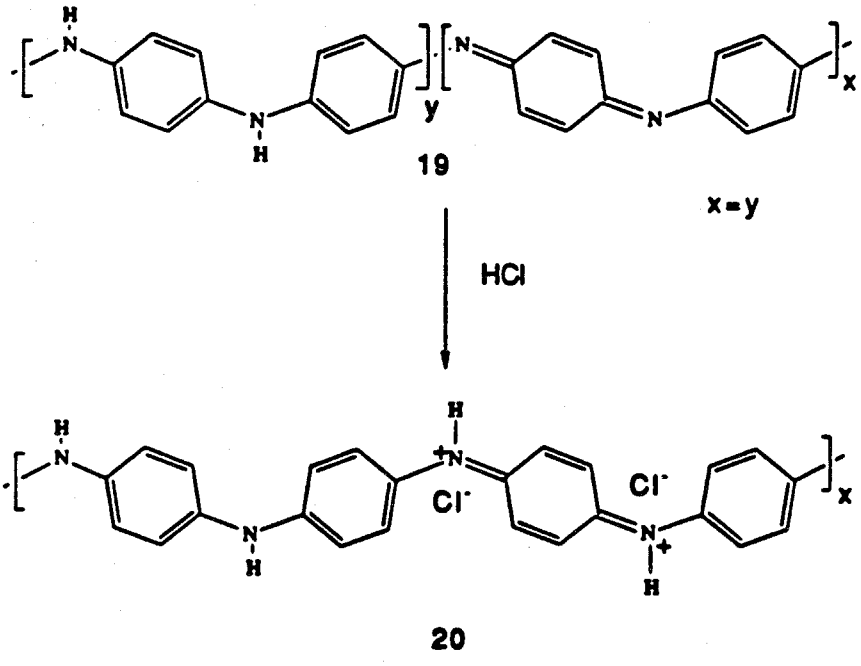

19 x=y

20

Further oxidation of polyaniline leads to a reduction of the conductivity and the liberation of protons.[25] This reversible drop in the conductivity at high oxidation levels is unique to polyaniline. Other CPs studied to date exhibit their maximun conductivity at their highest doping level (that is in the absence of decomposition).[1] The exact nature of the carrier species is yet to be determined. However, the polymer exhibits free spins suggesting the existence of polarons.[26] The number of free electrons is less than the number of protons added. Polarons (**21** and **22**) and bipolarons (**23**) have been proposed.[26] However, the "jury is still out" with respect to the definitive nature of the conductive state.

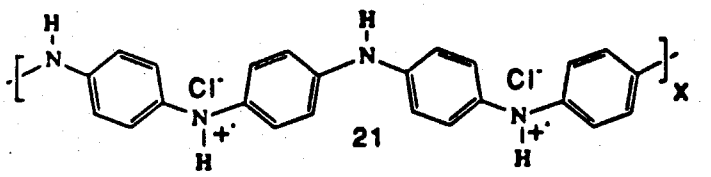

21

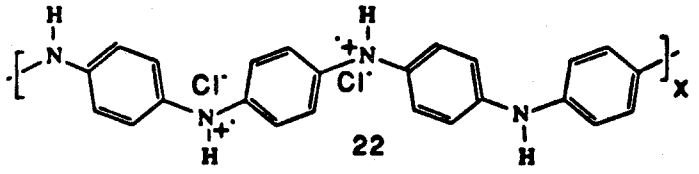

22

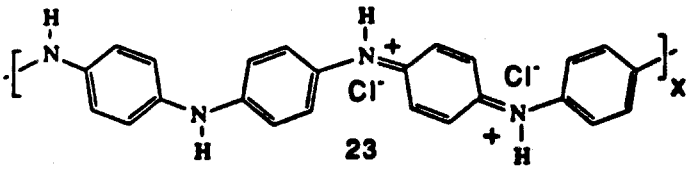

23

Intrachain carrier transport is generally thought to be more facile than interchain transport. This notion is supported by the observation that stretched (oriented) polymers exhibit higher conductivities along the direction of stretching ($\sigma \parallel$). However, interchain conduction is certainly very important. Both $\sigma \parallel$ and $\sigma \perp$ in **PA** show a temperature dependence, but the ratio of $\sigma \parallel$ to $\sigma \perp$ is temperature independent.[27] From this result it has been concluded that both $\sigma \parallel$ and $\sigma \perp$ are limited by the same processes.

THE METALLIC STATE:

The existence of a true metallic state for a **CP** has yet to be undisputably proven. However, there is strong evidence for its existence. In a classical metal there are unoccupied states at energies infinitesimally higher than those that are occupied. That is, there is a density of states at the Fermi level (see Figure 1.3a). As a result, carriers in a metal require no activation to move about the material. The limiting factor in metallic type conduction is the scattering of the carriers by lattice vibrations. Thus, in a true metal the conductivity increases with decreasing

temperature, since lower temperatures decrease thermal vibrations which scatter the carriers. In an undoped semiconductor, the Fermi level is between the conduction band and valence band (Figure 1.3b). Carriers are generated by thermal activation of electrons into the conduction band, which also produces holes in the valence band. The conductivity is an activated process, and hence conductivity increases with increasing temperature.[15]

Doping a **CP** produces carrier bands within the band gap. With further doping these bands widen, and upon overlapping with the valence band a metallic state is formed. However, a metallic temperature dependence in the conductivity has yet to be obtained for a **CP**. Heavily doped materials exhibit a very small activation energy ($\approx 10^{-3}$ eV for **PA**),[15] but conductivities have not been observed to increase with decreasing temperature as would be expected for a "true" metal. This anomalous behavior has been attributed to imperfect materials, in which hopping must occur between particles or crystallites.[28]

Another characteristic of metals which has been used as evidence of the metallic state is the observation of Pauli paramagnetism.[26,28,29] A material exhibits Pauli paramagnetism when there is a density of states at the Fermi level. This component of the total magnetic susceptibility (χ_t) is independent of temperature and its magnitude is proportional to the density of states at the Fermi level.[16] Therefore, measuring the Pauli susceptibility (χ_p) has been used to determine the density of states of **CPs** at the Fermi level.[26,28,29] The magnitude of χ_p is generally extracted from the χ_t by fitting the temperature dependent data to the following formula:

$$\chi_t(T) = \chi_c(T) + \chi_d + \chi_p$$

In this formula, χ_c is the Curie susceptibility, which has a 1/T dependence, and χ_d is the diamagnetic susceptibility which is negative and temperature independent. The origin of the χ_p is illustrated by considering the density of states of a metal at the Fermi level with respect to spin. In the absence of magnetic fields, the population of spin up states is equal to spin down states (Figure 1.4a). However, when a magnetic field is applied the energy of the spin states parallel are lowered and the energy of the states antiparallel are raised. This energy difference leads to an increase in the number of states parallel and a decrease in the number of states antiparallel (Figure 1.4b). The difference in the shaded regions of Figure 1.4b represents the χ_p.

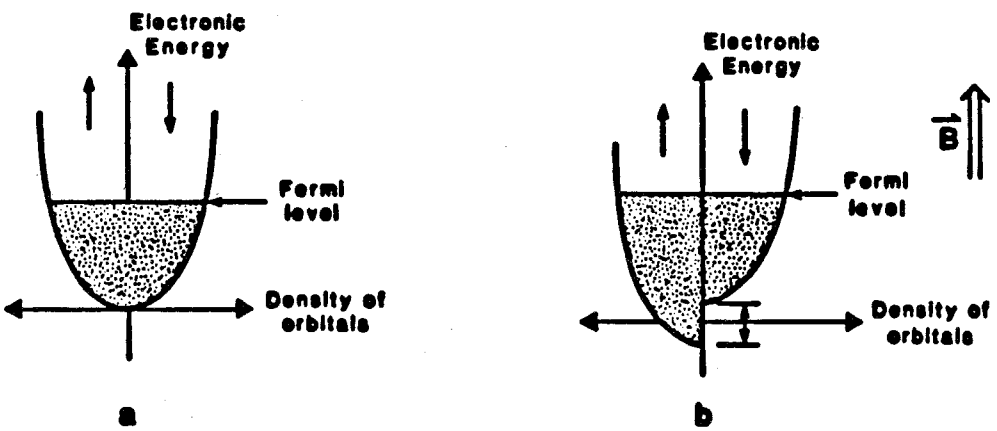

Figure 1.4. The origin of χ_p is illustrated by considering the density of spin states, in the absence of a magnetic field (a), and with an applied magnetic field (b). Shaded regions represent filled electronic states.

SYNTHESIS AND PROCESSING:

Polymers may have a variety of morphologies depending on the material and the processing technique used. Processing polymers into stretched fibers or films is an effective method to produce a highly crystalline morphology. **CPs** are extremely sensitive to crystallinity, and a highly crystalline **CP** may have a conductivity that is three to four orders of magnitude higher than the same material in a low crystallinity state. This increase in conductivity with crystallinity is primarily a consequence of increased carrier mobility. Higher mobilities are intrinsic to a more rigid lattice and longer conjugation lengths, which are characteristics of highly crystalline materials.

Conductive polymers by their very nature are generally intractable, infusible materials. These properties of **CPs** have been the biggest obstacle to processing these materials into useful shapes and highly ordered crystalline morphologies. Such characteristics are a result of the inherent rigidity of a conjugated polymer backbone and the tendency of these materials toward crystallization. Indeed, the significance of the Shirakawa method of **PA** synthesis was the fact that it produced a *continuous highly crystalline film.* **PA** before that time had only been available as an intractable powder.[30] Characteristics of **PA** prepared by the Shirakawa method are a low density (.4 g/cm^3), a high surface area, and a fibular morphology.[14] Once formed, this material can only be slightly stretched (l/l_o = 3 for *cis*-**PA**), and further shaping and manipulation of the morphology is not possible. A significant improvement in the Shirakawa method has recently been reported by Naarmann.[31] In this modified procedure the catalyst is heated at (aged) 120°C in silicone oil, cooled, and treated with butyl lithium, prior to acetylene polymerization. These modifications result in a higher density (.8 g/cm^3), improved conductivity ($\approx 10^5 \Omega^{-1}\text{cm}^{-1}$ (I_2)), and *air stability.* Naarmann was able to stretch his polyacetylene over 500% (l/l_o=6), which is also an improvement over

the Shirakawa method. The nearly 10^3 fold increase in the conductivity of I_2 doped **PA** is rationalized by a lower (undetectable) amount of sp^3 defects in "Naarmann **PA**." Highly oriented **PA** has been produced with the Shirakawa method in a liquid crystalline matrix aligned with a magnetic field.[32] Materials produced by this method display conductivities of $10^4\Omega^{-1}cm^{-1}$. **PA** wire has been processed by polymerization of acetylene in a polyethylene gel, and then drawing the composite material into fibers which exhibit conductivities of $\approx 10^4\Omega^{-1}cm^{-1}$.[33]

Of the other direct syntheses of **CPs**, the most notable is the oxidative electrochemical deposition polymerization of aromatic monomers on electrodes.[34] In this process, it is believed that electrochemical oxidation produces radical cations of the monomers which couple and liberate protons. Such a step-growth polymerization is illustrated for polypyrrole below.

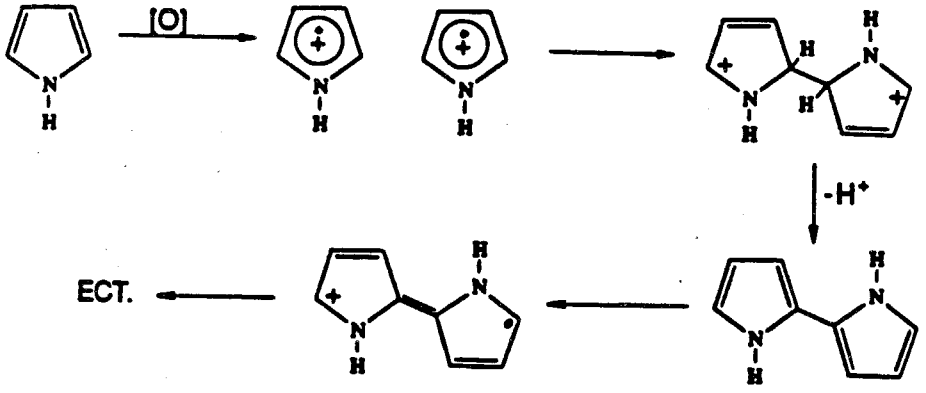

The growing polymer chains precipitate on the electrode surface as a continuous amorphous film. This method is the preferred method of synthesis for polypyrrole, polythiophene, and polyaniline. The porosity and texture of the deposited film can be varied by choice of electrolyte. However, further manipulation of the morphology is extremely limited. These polymers are not stretchable and crystalline morphologies have yet to be attained. However, interesting morphologies have been produced in polypyrrole by using surfactants as the electrolyte.[35] This modification has led to a layered structure (**24**) as evidenced by X-ray diffraction, which correlates the layer separation with the chain length of the surfactant.[35]

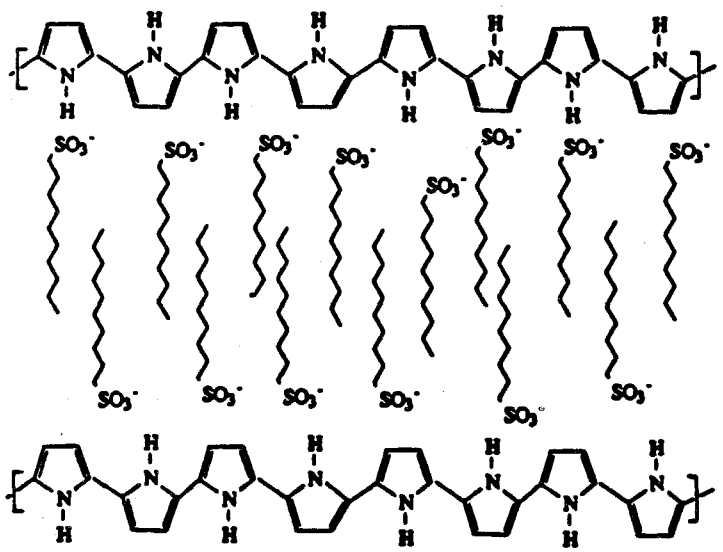

24

Another interesting modification of electrochemical deposition was recently demonstrated by the polymerization of pyrrole in the inorganic layered compound FeOCl.[36] This method produces layers of polypyrrole in between the inorganic layers, with the pyrrole rings perpendicular to the planes of the host material (**25**). The inorganic host can then be dissolved to leave behind the layers of polypyrrole.

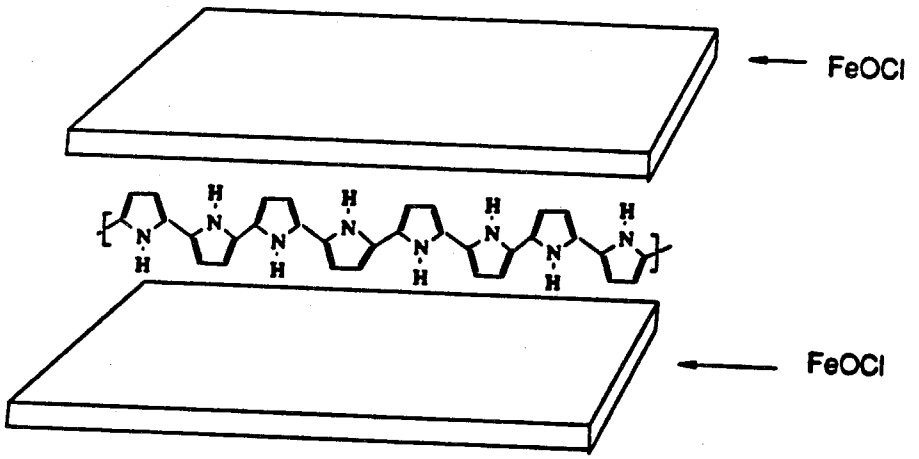

25

While the above methods of CP synthesis have been successful at producing highly conductive continuous films, they in general prohibit the use of conventional polymer processing. Melt or solution processing can lead to the production of a wide range of morphologies, mechanical properties, and useful shapes of these materials. CPs with highly crystalline ansiotropic morphologies through processing may ultimately lead to the highest possible conductivities. Reduction of the surface area through processing can also result in improved air stability.

One approach to this processing problem is to solubilize the CPs by attaching side groups to the polymers. A wide variety of soluble substituted polyacetylenes have been studied (**26**).[34] However, the steric requirements of the side groups induce twisting of the polymer backbone, which precludes high conductivity in these polymers. These substituted polyacetylenes have been observed to reversibly absorb and desorb I_2 and only exhibit a moderate conductivity (10^{-5}-10^{-4} $\Omega^{-1}cm^{-1}$) under an atmosphere of I_2. N-methyl substitution of polypyrrole (**27**) also results in twisting of the polymer backbone, and the conductivity decreases five orders of magnitude from that of polypyrrole.[38] However, substitution at the β-position in polythiophene has been successful at the production of soluble conductive polymers without significant loss of conductivity.[39] β-substitution does not produce steric crowding and hence long conjugation lengths are permitted. This method has led to both aqueous (**28**) and organic soluble (**29**) materials. However, the exploitation of the processability of these polymers to produce highly oriented or crystalline materials has not been reported. Solubilizing groups will undoubtedly decrease the crystallinity of the resulting materials, and hence limit the ultimate conductivities of these materials.

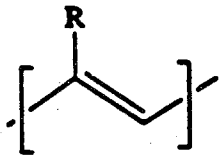

26

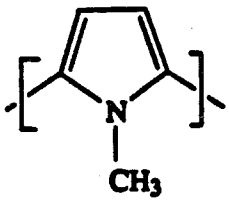

27

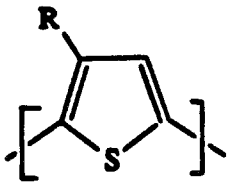

28 R= $(CH_2)_5CH_3$

29 R= $(CH_2)_4SO_3^-$

Potentially the best method to deal with the processability problem posed by **CPs** is known as a precursor route. In this method, a *processable precursor polymer* is synthesized that can be chemically or thermally transformed into an insoluble crystalline conductive polymer. Manipulation of the material into the desired morphology can be done at the precursor stage, or during the transformation to the **CP**. The most notable application of the precursor technique is the Feast route to **PA**.[40] In this process a precursor polymer (**30**) is synthesized by ring opening metathesis polymerization of a cyclobutene derivative. Once synthesized, the precursor polymer can undergo a thermally promoted, retro-Diels Alder reaction to extrude an aromatic fragment and produce **PA**. Material so produced has been called "Durham **PA** " after the University where the work was performed. This method has resulted in high quality **PA** that is of lower crystallinity than was previously available. Polarized infrared spectroscopy of oriented Durham **PA** reveals a higher anisotropy in the polymer chains than could be produced with Shirakawa **PA**.[41] However, Durham **PA** has yet to exhibit conductivities as high as Shirakawa **PA**.

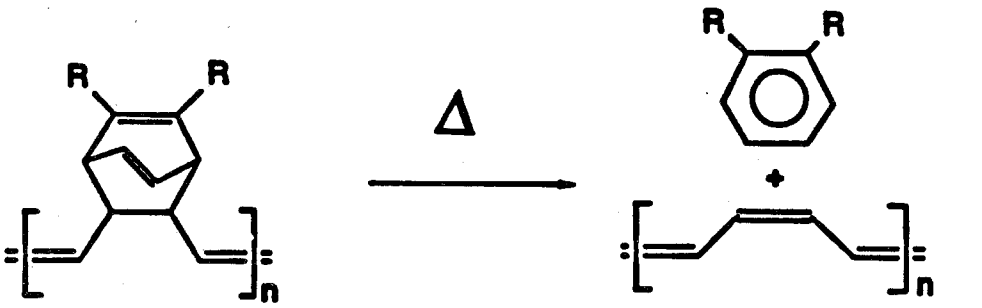

30 **Durham Polyacetylene**

Elimination reactions are perhaps the most common method for the synthesis of olefins in organic chemistry. Elimination reactions have also been employed in the conversion of precursor polymers into conductive polymers. Ballard has developed a method for the synthesis of polyparaphenylene in which the starting material is a bacterially oxidized benzene derivative (5,6-dihydroxycyclohexa-1,3-diene).[42] Radical polymerization of the diester (**31**) gives 1,4-addition product (**32**) with ≈ 80% selectivity over the 1,2-addition product and elimination thus gives about 80% polyparaphenylene.[42,43]

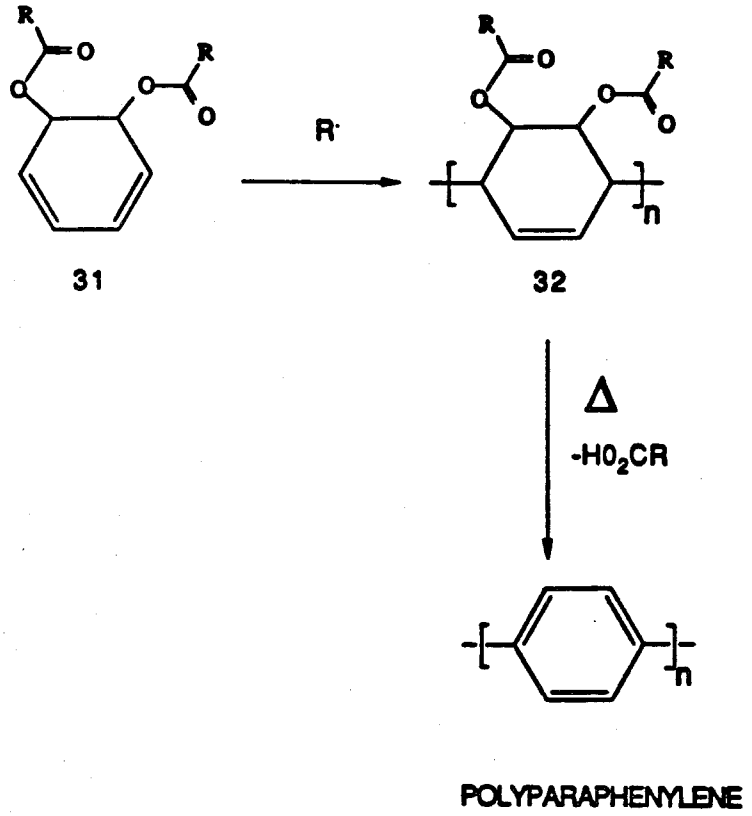

Elimination of sulfonium groups has proved to be an efficient method for the conversion of precursor polymers into CPs. This method, as illustrated for polyparaphenylene-vinylene,[44] first involves a polymerization of **33**, which results in the elimination of one sulfonium group per repeat to give soluble **34**. Heat-

ing this ionic polymer (**34**) results in elimination reactions and the formation of polyphenylene-vinylene. This method has been used in conjunction with stretching to produce paraphenylene-vinylene with a conductivity of 3000 $\Omega^{-1}cm^{-1}$ (AsF_5).[44] Unoriented material produced by this method has a conductivity of 1 $\Omega^{-1}cm^{-1}$ (AsF_5). Detailed studies of the thermal eliminations in this process reveal that the elimination reactions in the formation of polyphenylene-vinylene occur in two stages.[45] The first stage below 180°C results in the elimination of Me_2S and HBr with some MeBr. The production of the highest conductivity material requires thermolysis at 370°C , which results in elimination of the residual MeSH.

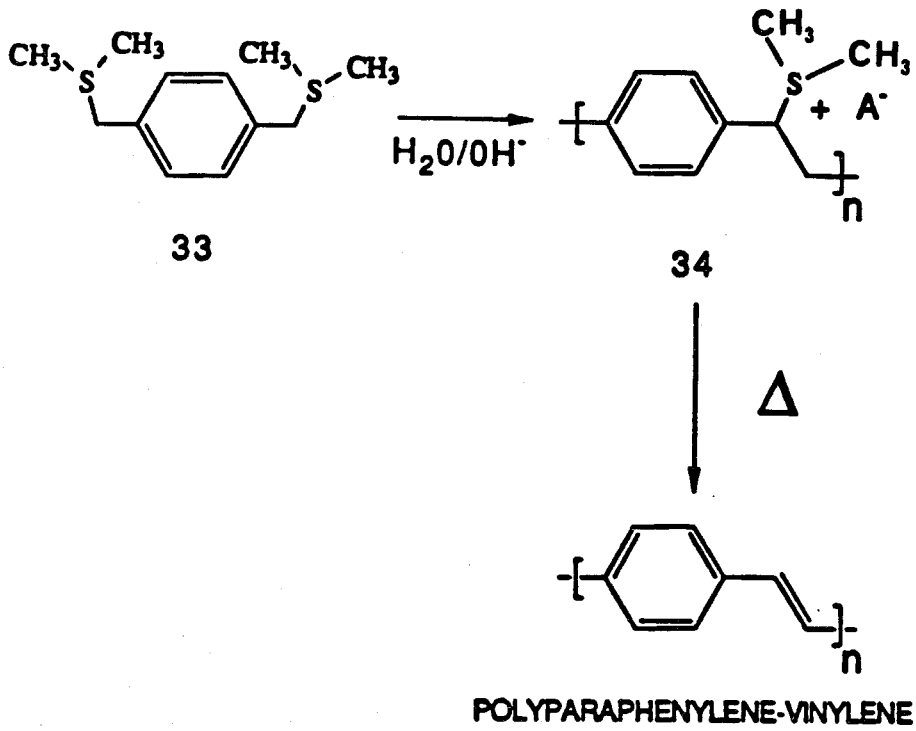

33 **34**

POLYPARAPHENYLENE-VINYLENE

This method has also been successful in the production of other polyaryl-vinylenes. Polynapthalene-vinylene (**35**),[46] polydimethoxyphenylene-vinylene (**36**),[47] polythienylene-vinylene (**37**),[48] and polyfurandiyl-vinylene (**38**)[49] were all produced by this method.

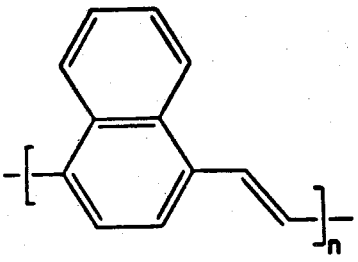

35

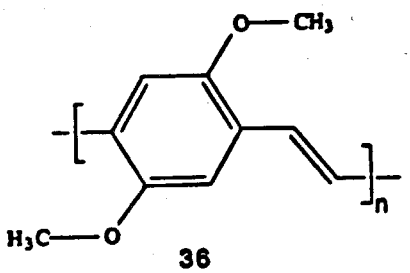

36

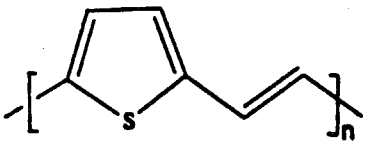

37

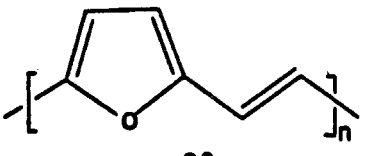

38

CONDUCTIVITY, CONCEPTS AND MEASUREMENT:

The most important property of CPs is their conductivity (σ). Conductivity ($\Omega^{-1}cm^{-1}$) is a measure of the ease of current flow through a material with an applied potential. Measurement of the conductivity is performed by determining the resistance of a sample and multiplying by geometrical corrections. The geometrical corrections are needed to extract the bulk σ from a given sample which may have a variety of sizes and shapes. A general equation for σ is given below where I = current, V = applied potential, D = distance over which the current must flow, and A_c = the cross-sectional area of the sample.[50]

$$\sigma = \left(\frac{I}{V}\right)\left(\frac{D(cm)}{A_c(cm)}\right)$$

Conductivity on a more fundamental level is the product of the number of carriers η (cm^{-3}) and their mobility μ ($cm^2V^{-1}sec^{-1}$). Since there may be more than one kind of carrier a summation over all species and the charge of each carrier q are needed.

$$\sigma = \sum_{i}^{n} q_i \mu_i \eta_i$$

This relationship is useful for determining the number of carriers by measuring the μ and σ; μ can be measured directly by the Hall effect. For CPs, little information is available with respect to μ. However, its magnitude is on the order of .1-10 $cm^2V^{-1}sec^{-1}$. For comparison, semiconductors have μ's that are on the order of 10^3 $cm^2V^{-1}sec^{-1}$ or higher.[15] In general CPs have considerably slower carriers than their semiconductor counterparts. This is compensated by much higher carrier densities (η) to achieve high conductivity.

A discussion of the sample configurations and conductivity calculations used to determine the σ's is necessary. For high resistivity samples ($\sigma \leq 10^{-5}$ $\Omega^{-1}cm^{-1}$) a two-point measurement was performed. Samples usually consisted of polymer films which were glued with colloidal graphite to platinum wires. The sample configuration used is shown in Figure 1.5. The overall probe apparatus (only a portion of the apparatus is shown, see appendix B) is a modified version of that discussed by Chien.[15] In this apparatus the sample is enclosed in a glass chamber which is capable of holding a high vacuum. This presents a controlled environment in which the sample can be exposed with dopant vapor while continuously monitoring σ. A voltage is applied to the sample through the attached wires, and the current is measured by an inline ammeter. The current, voltage and geometrical parameters (D and A_c) are then substituted into the equation given above to obtain σ.

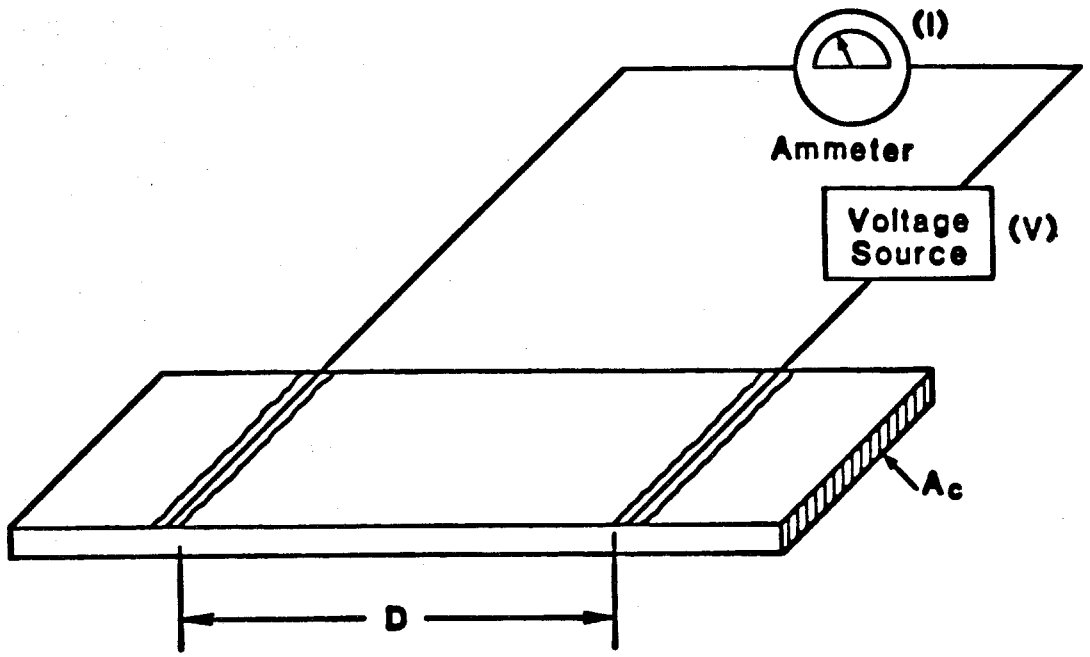

Figure 1.5. A schematic illustration of a two-point conductivity measurement is shown. A film of a CP is glued to Pt wires with conductive paste. D is the distance between the conductive paste and A_c is the shaded cross-sectional area.

Theoretically, a two-point measurement will allways give a σ lower than the true value. This is a result of the contact resistance which is present between the electrodes and the sample. In practice contact resistances of as high as 10^4 Ω have been observed. For samples in which the resistance of the sample is greater than the contact resistance a two-point measurement is reliable. However, with low resistance samples (high σ) a four-point measurement is necessary to factor out the contact resistance. The sample configuration for a four-point measurement is shown in Figure 1.6.

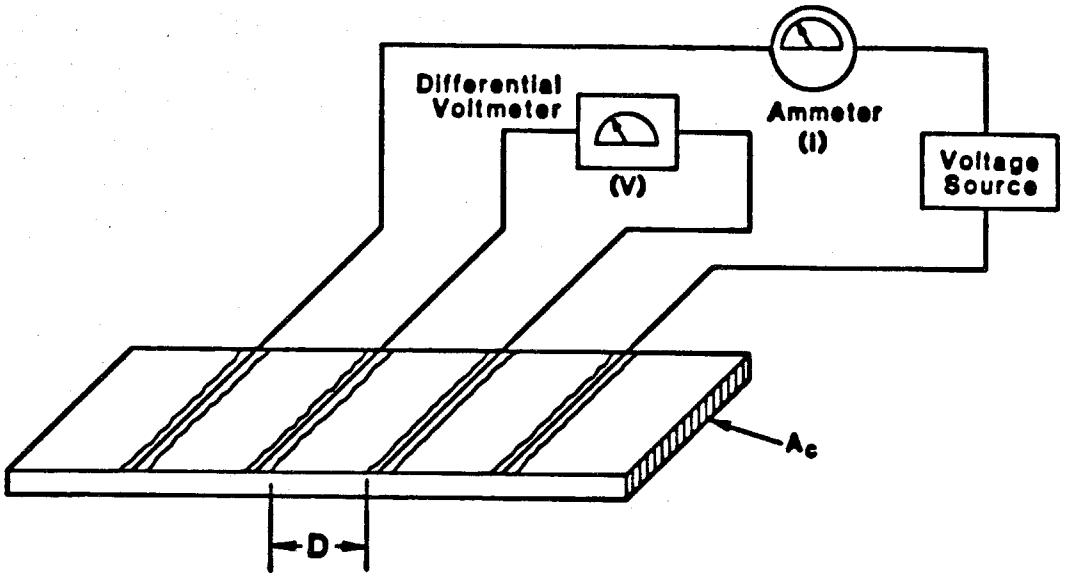

Figure 1.6. A schematic of a four-point conductivity measurement is shown. The parameters identified are those used in the equation given for σ.

In this measurement a known current is passed through the outer two leads of the sample, and the potential difference is measured across the inner leads. By using a high impedance differential voltmeter, the voltage measurement is a "currentless" measurement, and therefore does not include a contribution from the contact resistance.

Another sample configuration used to measure σ is commonly called a sheet resistivity measurement.[50] This method is the standard measurement for semiconductor wafers and involves a pressed contact of four colinear contacts on the surface of a sample as shown in Figure 1.7. An advantage of this apparatus is that the samples can be on a glass substrate or may be a pressed pellet, and hence it is not limited to free-standing films like the probe discussed above.

This apparatus is also most suitable for investigating a larger number of samples. However, this measurement is in general less accurate since it involves lower currents and has smaller dimensions than the first probe. For air sensitive materials the measurements can be made in a glove box. In the case that the ratio of the thickness of the sample (δ) to probe spacing (s) is less than 0.4 then the conductivity is readily calculated from the equation below.

$$\sigma = \left(\frac{I}{V}\right)\left(\frac{.22}{\delta}\right)$$

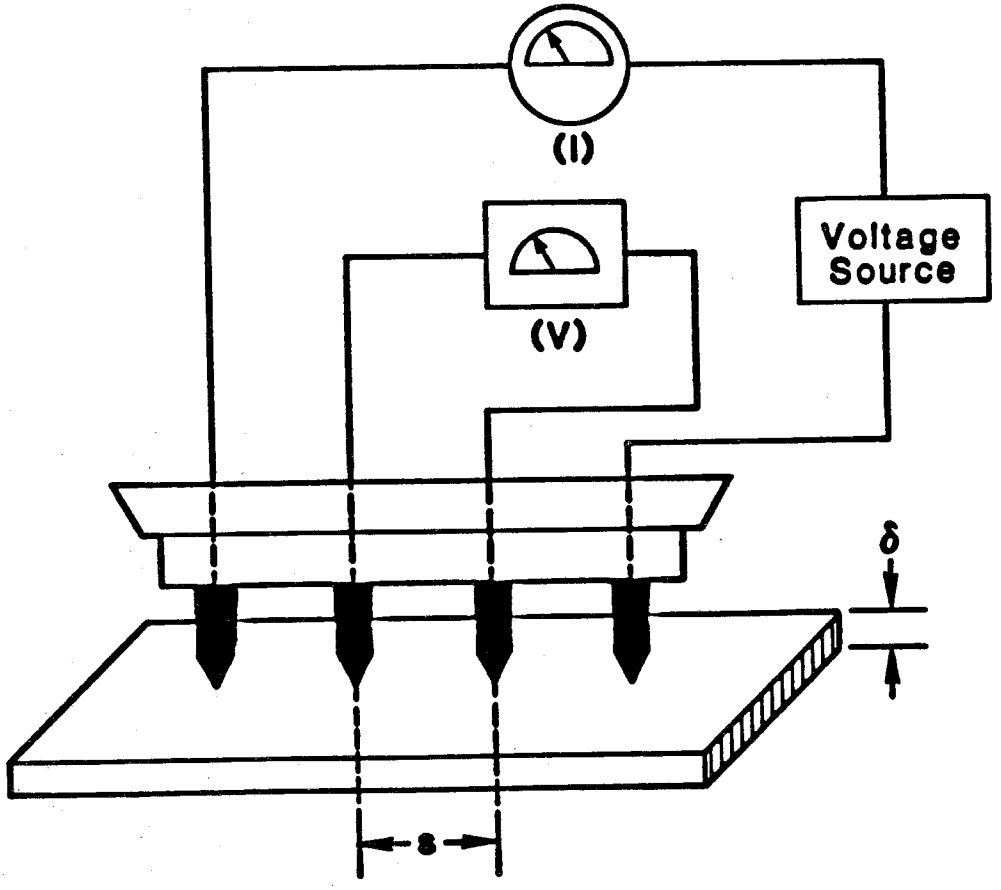

Figure 1.7. A schematic illustration of a four-point sheet resistivity measurement is shown. Spring loaded probe tips provide the electrical contact with the surface of the sample.

When making electrical measurements, grounding and shielding has been found to be very important. In general, shielded cables were used, with the shields carefully grounded. In the 4-point configuration the cable shields from both loops were grounded separately. Conductivity measurements can be tricky and if not done carefully anomalous readings may be obtained. It is advisable to have a standard sample of known conductivity to test whether or not the equipment is assembled correctly. As a test of the reliablity of a given reading, it is recommended that measurements be made at different applied voltages (the conductivity should be independent of the voltage), and the conductivity should not vary with the polarity of the applied potential. Capacitance currents were also sometimes observed when making measurements. In this case a larger current is observed with initial application of a potential, which decayed over the course of 10 - 20 seconds. A reliable measurement should be stable for long periods of time.

Future Outlook:

While problems still exist with many of the currently available **CPs**, significant progress has been made in the field in the last decade. Air instability persists with many of the materials. However, Naarmann's results demonstrate that conductive polymers may not be inherently unstable to air.[31] Environmental stability may also be accomplished through better processing. The processing problems currently faced by **CPs** will be overcome by new precursor routes and the development of soluble and melt processable polymers. In addition, only a very few structural types of **CPs** have been synthesized.[1] Considering the potential structures that organic chemistry can offer, effort in the synthesis of new structural types of conductive polymers is in order.

References:

1. *Handbook of Conducting Polymers*; Skotheim, T. J. (ed.); Dekker: New York, 1986.

2. Billmeyer, F. W. *Textbook Of Polymer Science* 3rd ed. John Wiley and Sons, 1984.

3. See MacDiarmid, A. G. and Kaner, R. B. in reference 1.

4. (a) Turner, E. T.; Chyan, O. M.; Wrighton, M. S. *J. Am. Chem. Soc.* **1987**, 109, 5526. (b) Loften, E. P.; Thackeray, J. W.; Wrighton, M. S. *J. Phys. Chem.* **1986**, 90, 6080. (c) Kittlesen, G. P.; White, H. S.; Wrighton, M. S. *J. Am. Chem. Soc* **1984**, 106, 7389. (d) White, H. S.; Kittlesen, G. P.; Wrighton, M. S. *J. Am. Chem. Soc.* **1984**, 106, 5375.

5. (a) *Molecular Electronic Devices*; Carter, F. L. (ed.); Marcel Dekker, **1982**. (b) *Molecular Electronic Devices II*; Carter, F. L. (ed.); Marcel Dekker, **1987**. (c) See the special issue on molecular electronics: *IEE Proc. I* **1983**, 130. 197-263.

6. Thackeray, J. W.; Wrighton, M. S. *J. Phys. Chem.* **1986**, 90, 6674.

7. Heeger, A. J. *Synthetic Metals* **1986**, 15, 95.

8. Williams, D. J. *Angew. Chem. Int. Ed. Engl.*, **1984**, 23, 690.

9. Gill, W. D.; Clarke, T. C.; Street, G. B. *Appl. Phys. Comm.* **1982-3**, 2(4), 211 and references therein.

10. Shirakawa, H.; Ikeda, S. *Polymer J.* **1971**, 2, 231.

11. (a) Shirakawa, H.; Louis, E. J.; MacDiarmid, A. G.; Chaing, C. K.; Heeger, A. J. *J. Chem. Soc. Chem. Commum.* **1977**, 578. (b) Chiang C. K.; Park, Y. W.; Heeger. A. J.; Shirakawa, H.; Louis, E.J.; MacDiarmid, A. G. *Phys. Rev. Lett.* **1977**, 39, 1098.

12. Kanazawa, K. K.; Diaz, A. F.; Gill, W. D.; Grant, P. M. Street, G. B., Gardini, G. P.; Kwak, J. F. *Synth. Met.* **1980**, 1, 329.

13. Ivory, D. M.; Miller, G. G.; Sowa, J. M.; Shacklette, L. W.; Chance, R. R.; Braughman, R. H. *J. Chem. Phys.* **1979**, 71, 1506.

14. See articles in reference 1.

15. Chien, J. C. W. *Polyacetylene: Chemistry, Physics, and Material Science* Academic Press 1984.

16. Kittle, C. *Introduction To Solid State Physics* 5th ed., John Wiley and Sons 1976.

17. Figgis B. N. *Introduction to Ligand Fields* New York Interscience, 1966.

18. Bredas, J. L. *J. Phys. Chem.* **1985**, 82, 3808.

19. (a) Wudl, F.; Kobayashi, M.; Heeger, A. J. *J. Org. Chem.* **1984**, 49, 3382. (b) Kobayashi, M.; Colaneri, N.; Boysel, M.; Wudl, F.; Heeger, A. J. *J. Chem. Phys.* **1985**, 82, 5717. (c) Colaneri, N.; Kobayashi, M.; Heeger, A. J.; Wudl, F. *Synthetic Metals*, **1986**, 14, 45. (d) Bredas, J. L.; Heeger, A. J.; Wudl, F. *J. Chem. Phys.* **1986**, 85, 4673.

20. **CPs** with smaller band gaps have been reported: Jenekhe, S. A. *Nature (London)* **1986**, 322, 345. Jenekhe, S. A. *Macromolecules* **1986**, 19, 2663. Jenekhe, S. A. *Polym. Prep. (Am. Chem. Soc., Div. Polym. Chem.)* **1986**, 27, 74. However, a recent reinvestigation has shown this work to be suspect: Patil, A. O.; Wudl, F. *Macromolecules* **1988**, 21, 540.

21. Pranata, J.; Grubbs, R. H.; Dougherty, D. A.; *J. Am. Chem. Soc.*, in press.

22. Su, W. P.; Schrieffer, J. R.; Heeger, A. J. *Phy. Rev. B* **1980**, 22, 2099. See also articles by Heeger, A. J. and Su, W. P. in reference 1.

23. See article by Thomann, H.; Dalton, L. R. in reference 1.

24. Bredas, J. L.; Street, G. B. *Acc. Chem. Res.* **1985**, 18, 309. See also articles in reference 1.

25. MacDiarmid, A. G.; Chiang, J. C.; Richter, A. F.; Epstein, A. J. *Synthetic Metals* **1987**, 18, 285.

26. Epstein, A. J.; Ginder, J. M.; Zuo, F.; Bigelow, R. W.; Woo, H. S.; Tanner, D. B.; Richter, A. F.; Huang, W. S.; MacDiarmid, A. G. *Synthetic Metals* **1987**, 18, 303.

27. Baughman, R. H.; Shacklette, L. W. *Synthetic Metals* **1987**, 173.

28. Moraes, F.; Davidov, D.; Kobayashi, M.; Chung, T. C.; Chen, J.; Heeger, A. J.; Wudl, F. *Synthetic Metals* **1985**, 169.

29. (a) Chung, T. C.; Moraes, F.; Flood, J. D.; Heeger, A. J. *Phys. Rev. B* **1984**, 29, 2341. (b) Ikehata, S.; Kaufer, J.; Woerner, T.; Pron, A.; Dury, M.; Sivak, A.; Heeger, A. J.; MacDiarmid, A. G. *Phys. Rev. Lett.* **1980**, 45, 1123.

30. Natta, G.; Mazzanti, G.; Corradini, P; *Atti. Accad. Naz. Lincei, Cl. Sci. Fis. Mat. Nat. Rend.* **1958**, 25, 2.

31. Naarmann, H.; Theophilou, N. *Synthetic Metals* **1987** 22, 1.

32. (a) Akagi, K.; S. Katayama, S.; Shirakawa, H.; Araya, K.; Mukoh, A.; Narahara, T. *Synthetic Metals*, **1987**, 17, 241. (b) Yamashita, Y.; Shimamura, K.; Kasahara, H.; Monobe, K. *Synthetic Metals* **1987**, 17, 253.

33. Wudl, F. disclosure at Cal. State LA seminar on Jan. 5, 1988.

34. See article by Diaz, A. F.; Bargon, J. in reference 1.

35. Wenger, G. disclosure at J.P.L. seminar Jan. 1988.

36. Kanatzidis, M. G.; Tonge, L. M.; Marks, T. J.; Marcy, H. O.; Kannewurf, C. R. *J. Am. Chem. Soc.* **1987**, 109, 3797.

37. See article by Gibson, H. W. in reference 1.

38. See article by Street, G. B. in reference 1.

39. (a) Jen, K. Y.; Oboodi, R.; Elsenbaumer, R. L. *Proc. of Am. Chem. Soc.; Div. of Poly. Mat. Sci. and Eng.* **1985**, 53, 79. (b) Sato, M.; Tanaka, S.; Kaeriyama, K. *J. Chem. Soc., Chem. Comm.* **1986**, 873. (c) Patil, A. O.; Ikenoue, Y.; Wudl, F.; Heeger, A. J. *J. Am Chem. Soc.* **1987**, 109, 1858.

40. (a) Edwards, J. H.; Feast, W. J. *Polymer* **1980**, 21, 595. (b) Bott, D. C. et al. *Synthetic Metals* **1986**, 14, 245 and references therein.

41. Bott, D. C.; Brown, C. S.; Winter, J. N.; Barker, J. *Polymer* **1987**, 28, 601 and references therein.

42. Ballard, D. G.; Couris, A.; Shirley, I. M.; Taylor, S. C. *J. Chem. Soc. Chem. Commun.* **1983**, 954.

43. (a) McKean, D. R.; Stille, J. K. *Macromolecules* **1987**, 20, 1787. (b) Stille, J. K.; McKean, D. R. *Polym. Prep. (Am. Chem. Soc., Div. Polym. Chem.)* **1987**, 28(1), 65.

44. (a) Gagnon, D. R.; Karasz, F. E.; Thomas, E. L.; Lenz, R. W. *Synthetic Metals* **1987**, 20, 85. (b) Karasz, F. E.; Capistran, J. D.; Gagnon, D. R.; Lenz, R. W. *Molec. Cryst. Liq. Cryst.* **1982**, 118, 567.

45. Gragnon, D. R.; Capistran, J. D.; Karasz, F. E.; Lenz, R. W.; Antoun, S. *Polymer J.* **1987**, 28, 567.

46. Antoun, S.; Gragnon, D. R.; Karasz, F. E.; Lenz, R. W. *J. Polym. Sci. C, Polym. Lett.* **1986**, 24, 503.

47. (a) Han, C.; Lenz, R. W.; Karasz, F. E. *Polym. Comm.* **1987**, 28, 261. (b) Murase, I.; Ohnishi, T.; Noguchi, T.; Hirooka, M. *Polymer Comm.* **1985**, 26, 3624. (c) Jen, K.; Shacklette, L. W.; Elsenboumer, R. *Synthetic Metals* **1987**, 22, 179.

48. Murase, I.; Ohnishi, T.; Noguchi, T.; Hirooka, M. *Polymer J.* **1987**, 28(8), 229.

49. Jen, K.; Jow, T. R.; Elsenboumer, R. L. *J. Chem. Soc., Chem. Comm.* **1987**, 1113.

50. Wieder, H. H. *Laboratory Notes on Electrical and Galvanomagnetic Measurements* Elsevier Scientific Pub., 1979.

Chapter 2

RING OPENING METATHESIS POLYMERIZATION

Introduction To Olefin Metathesis:

The olefin metathesis reaction has been demonstrated to be among the most useful reactions offered by organometallic chemistry.[1,2,3] This process involves a 2+2 cycloaddition of an alkene and a metal alkylidene which may be reversible. A generic equilibria for this process is shown below in equation 2.1.

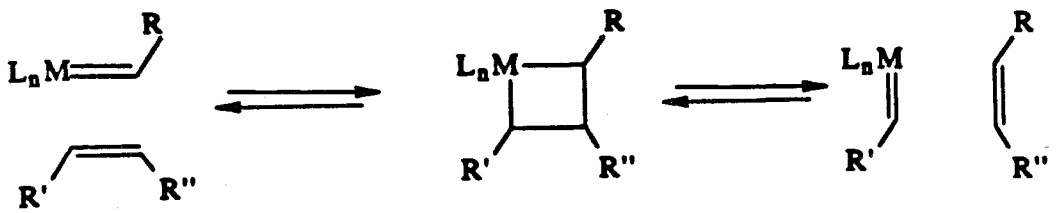

Equation 2.1

These equilibria may favor the metal alkylidene or metallacycle, depending on the olefin and metal. The most active metathesis catalysts are those of the early transition metals. However, late transition metals also exhibit metathesis activity.[4] The in situ generation of the active catalyst has been predominantly used.[2] These in situ catalysts are commonly called "classical catalysts" by researchers in the field. The early metal classical systems are comprised of high oxidation state metal halides and an alkyl-tin or alkyl-aluminum co-catalyst. Modifiers such as alcohols have also been employed, and serve to increase the catalyst homogeneity and to decrease the electrophilic nature of the metal center. An example of a early metal classical catalyst is: WCl_6:$EtAlCl_2$. These systems are highly Lewis acidic and have an extremely low tolerance for functional groups. A variety of late metal

catalysts are known. Particularly convenient catalysts are the late metal catalysts that are generated by heating a metal halide with the cyclic olefin and alcohol.[4] A typical procedure would be to heat MCl_3 (M= Ru, Ir, Os) at $\approx$ 55-60 °C in the presence of olefin, ethanol, and a solvent. Late metal catalysts have a greater functional group tolerance than the early metals. The mechanism of initiation in both systems is the in situ generation of a metal carbene.

Recently non-Lewis acidic, well-characterized metathesis catalysts have been isolated.[5,6,7,8,9] These catalysts allow the polymerization of cyclo-olefins with Lewis acid sensitive functionality. The use of these catalysts to synthesize conductive polymer precursors will be the focus of this thesis. These well-characterized metathesis catalysts are shown below in Figure 2.1. The majority of the work reported in the following chapters has been done with catalysts **1**, **2**, **3**, **4**, and **5**. Fischer carbenes have also been demonstrated to generate non-Lewis acidic catalysts.[10] However, these catalysts are of low activity and only are generated with prolonged heating (i.e., days).

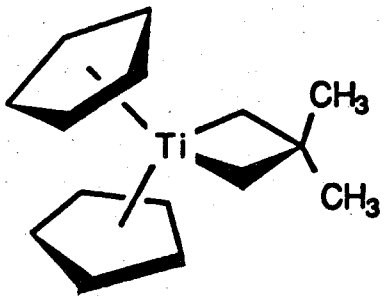

1
GRUBBS

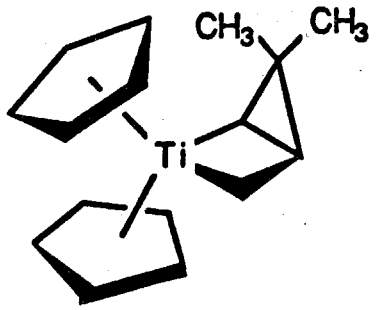

2
GRUBBS

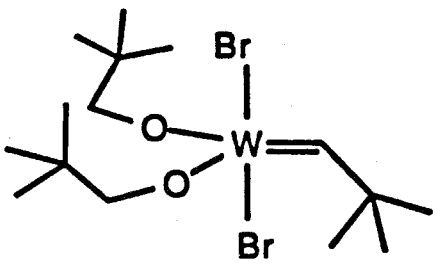

3
KRESS AND OSBORN

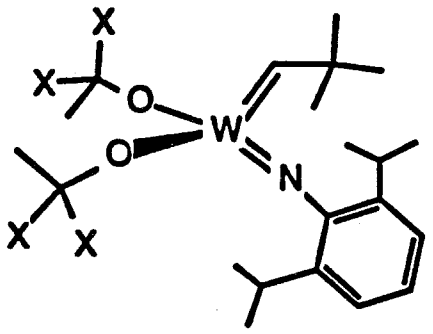

4 X= CF_3
5 X= CH_3
SCHROCK

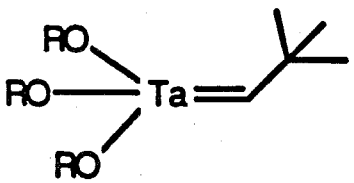

6 R= 2,6-DIMETHYLPHENYL
SCHROCK

Figure 2.1. Well-characterized metathesis catalysts what were used in this thesis research. The names of the principle investigators are given under the respective catalysts.

Ring Opening Metathesis Polymerization: "ROMP"

If the olefin in Equation 2.1 is cyclic, then there is the potential to produce a polymer by ring opening metathesis polymerization (**ROMP**).[3] The overall process results in the formal cleavage and reconnection of the olefin as shown in Equation 2.2. **ROMP** is an ideal polymerization method for the synthesis of highly unsaturated polymers since it doesn't require the sacrifice of an olefin as would be the case for anionic, Ziegler-Natta, radical, or cationic polymerization. Thus, **ROMP** provides an efficient method for the synthesis of highly unsaturated conductive polymers.

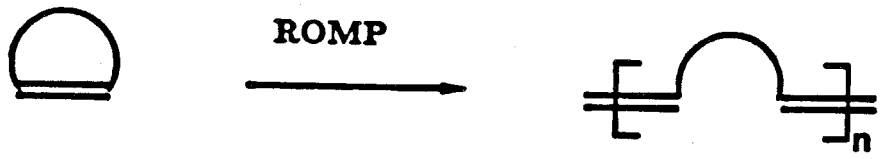

Equation 2.2

A generic reaction mechanism for **ROMP** is shown in Scheme 2.1. If the cyclic olefin has ring strain there is a strong thermodynamic driving force for polymerization. However, it is thermodynamically favorable to **ROMP** large low strain energy rings due to favorable entropy. In general ring strain is the most efficient driving force for **ROMP**. The steps in the mechanism of Scheme 2.1 are drawn as reversible equilibria. The effect of ring strain is to decrease (or eliminate) the reverse reactions. Work in the polymerization of low strain energy rings has been studied in the Grubbs laboratory by others and will not be discussed here.[11]

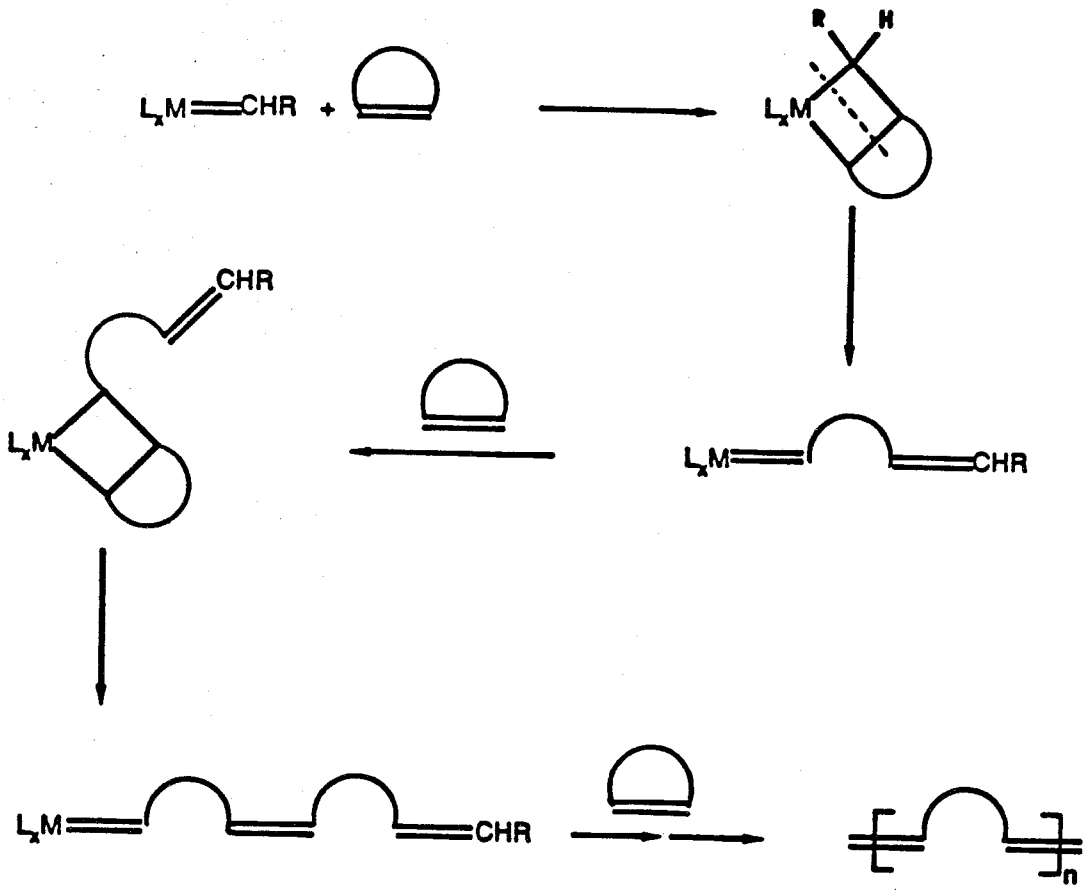

Scheme 2.1

Nature Of The Catalysts:

The polymerization activity of the catalysts from Figure 2.1 are the result of steric and electronic factors. Electronic effects may be considered to include the combined effects of the reactivity of the strained olefin and the activity of the metal center. One of the objectives in this thesis is to develop an understanding of the reactivity of the catalysts and monomers.

A living metathesis polymerization was first demonstrated by Gilliom and Grubbs with the titanium metallacycle catalysts **1** and **2** and norbornene.[12] **1** and **2** are sources of titanocene methylidene and titanocene alkylidene respectively, which are the active catalysts. Titanocene methylidene can also be generated by treating it's $(Me)_2AlCl$ complex (Tebbe's reagent) with a Lewis base. **1** and **2** only generate the active catalysts at temperatures where there is an equilibrium between the metallacycle and active catalyst.[5] The Tebbe reagent on the other hand can be used to generate titanocene methylidene at any desired temperature. Later studies by this group and others have also indicated that other catalysts can give living polymers.[13,14] A living polymerization is possible by the virtual absence of chain termination and chain transfer processes.[15] A monodispersed polymer is attained under these conditions if initiation is fast relative to propagation. Catalysts **1** and **2** have been demonstrated to afford monodispersed homopolymers[12] and block copolymers with low polydispersities.[16]

The intimate details of the mechanism of the olefin metathesis reaction for the titanium system have been studied theoretically,[17] and with chemical kinetics.[18] These studies indicate that it may be necessary for a pre-coordination of the olefin to the catalyst prior to metallacycle formation. This suggests by microscopic reversibility that the metallacycle may need to distort toward the olefin complex (**7**) before opening.

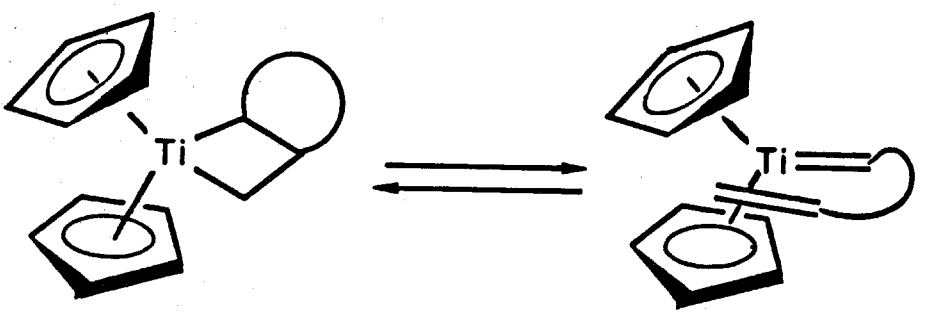

7

At the onset of this research the titanocene metallacyles were the only well-characterized catalysts available. The limitations of this catalyst system became apparent immediately with the author's first attempted polymerization: the **ROMP** of acenaplthene.

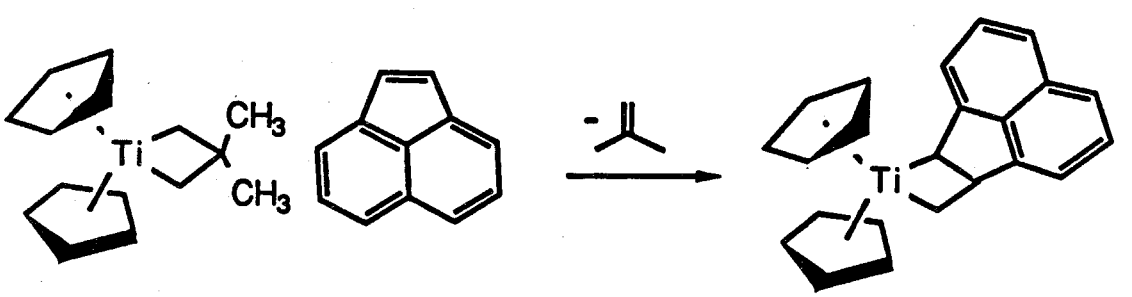

8

The acenaplthene metallacycle (**8**) is the most stable titanocene metallacycle that has been synthesized to date and only slowly decomposes at temperatures over 110 °C . This stability may be a result of the fact that **8** is not capable of opening due to the steric hindrance of the cyclopentadienyl rings as shown below. However, the need to distort toward an olefin metal complex like (**7**) may also play a role.

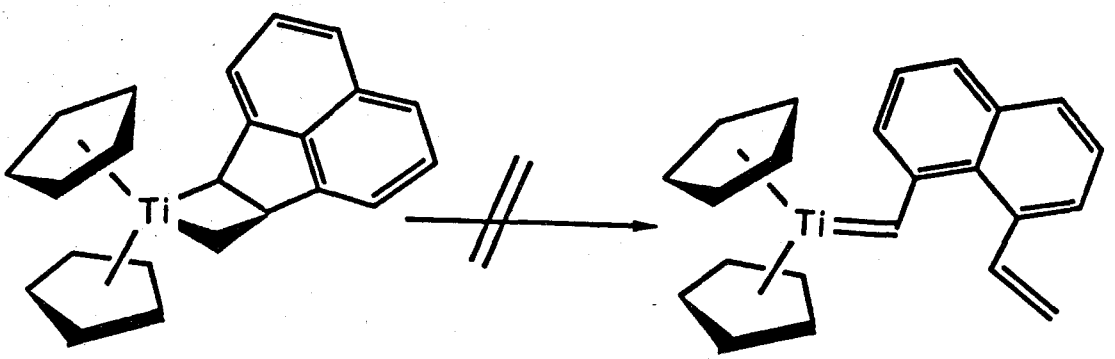

8

This steric effect is also apparent in **2**, which prefers the metallacycle over the alkylidene as a result of steric interactions of the gem dimethyl group. The metallacycle (**2**) incorporates 27 kcal/mole of strain energy from the cyclopropane ring to avoid the steric interactions of the alkylidene **9**. The tetramethylcyclobutene metallacycle **10** studied by Scott Virgil in this group was found to not give productive cleavage. For **10** these results must be steric in origin.

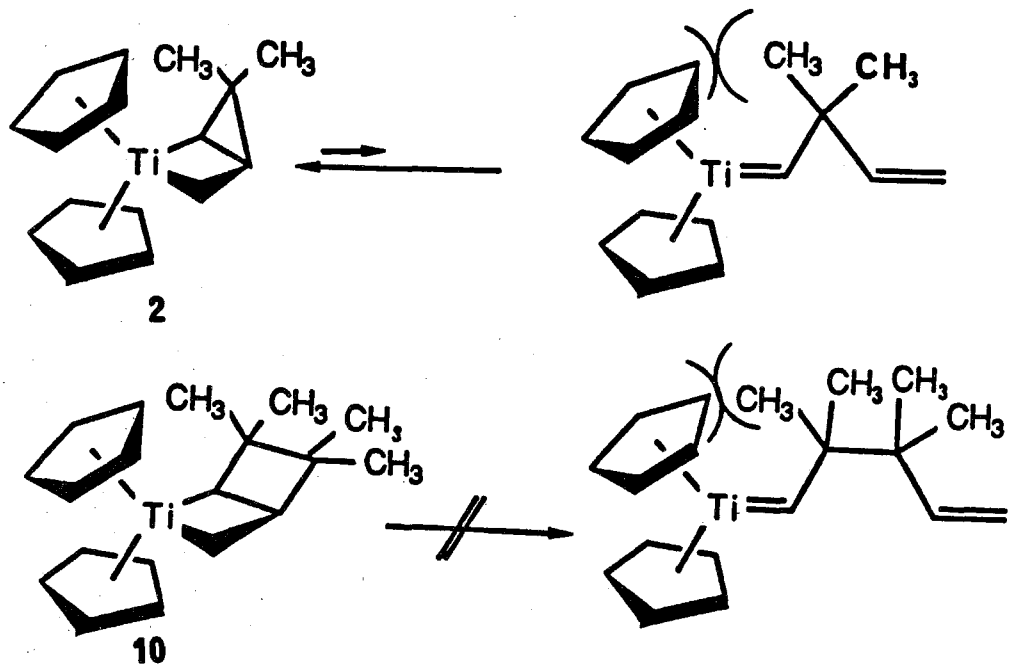

Catalyst **3** developed by Kress and Osborn was the first well-characterized tungsten alkylidene to be synthesized.[6] The preparation of **3** has not been published in detail and its synthesis was reproduced in this laboratory only after correspondence with J. Kress. A detailed experimental procedure for the synthesis of this catalyst is reproduced in the appendix. This procedure is essentially the one supplied by J. Kress with some minor, but effective modifications. The catalyst by itself is found to be a relatively low activity metathesis catalyst. However, the activity of this catalyst is greatly increased with the addition of Lewis acid cocatalysts. A long-lived (24-hr) catalyst was observed to be formed when the cocatalyst is $GaBr_3$.[20] The activity of the catayst has been correlated with conductivity measurements, suggesting that the catalyst must dissociate a ligand to a cationic state prior to reaction with an olefin as shown for norbornene below.[20]

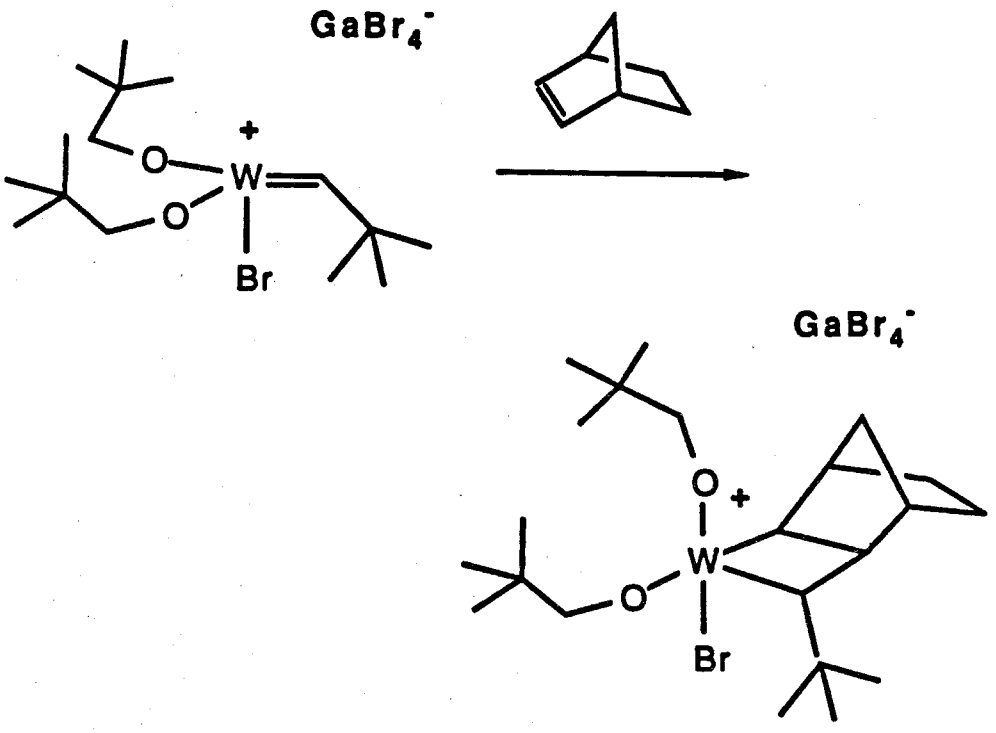

11

This need to form an open coordination site to form a metallacycle has been proposed to be necessary because octahedral tungsten metallacycles have not been observed and may not be stable.[21] Kress and Osborn have recently reported the observation of a cationic norbornene metallacycle **11** at low temperature.[22] **3** can also be activated by exchanging one of the bromides with a better leaving group such as a TfO^- or TsO^-. The triflate has been reported by Kress and Osborn[20] and the tosylate was synthesized by an analogous route and is reported in Chapter 4. The tosylate derivative has the advantage that it is a solid and thus is more easily handled than **3**, which is an oil. Further modification of this catalyst with electron donating and withdrawing groups was attempted but was unsuccessful. A similar catalyst **12** has been reported by Basset[7]. The greater electron donating ability of the ligands in this catalyst may facilitate the formation of a cationic species. This catalyst displays high activity without a need for a Lewis acid cocatalyst, but this catalyst has not been studied in this group.

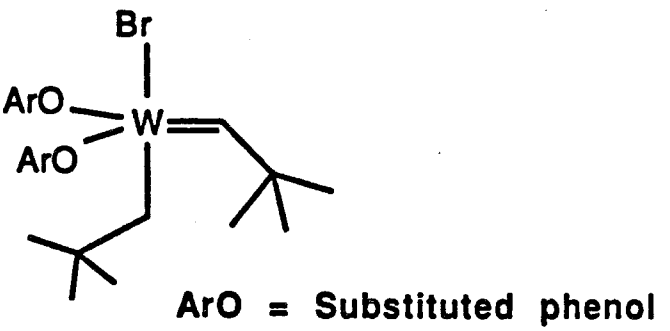

12

The four coordinate tungsten alkylidenes **4** and **5** synthesized by Schrock[8] are emerging as perhaps the most important catalysts for **ROMP**. These catalysts can readily form five-coordinate metallacycles upon addition of an olefin without ligand dissociation. The nature of the alkoxides has been observed to have a strong effect on the activity of the catalyst. For example; the hexafluoro-t-butylalkoxide derivative (**4**) polymerizes norbornene at -80 °C where the t-butylalkoxide catalyst (**5**) polymerizes norbornene slowly at R.T.[13] This activity difference between **4** and **5** is also manifested in the fact that **4** will metathesize unstrained olefins where **5** will only react with strained olefins. The price of the high activity of **4** is selectivity, and a living polymerization is not observed with **4** as a result of backbiting, chain transfer, and possibly decomposition processes.[13] The less reactive derivative **5** has been shown to provide a living polymerization of norbornene.[13] Both **4** and **5** have a low tolerance for carbonyl compounds. However, the molybdenum analogue has been used to produce narrow dispersity polymers with ester groups.[23]

The steric requirements of catalysts **4** and **5** are illustrated below in Figure 2.2. The large bulky alcohol groups promote *cis* double bond formation in the polymer. This arises from the cyclic olefin preferring an approach to the metal in which the ring is pointing away from the alkoxides. In the case that the monomer is sterically bulky, then the growing polymer will also present a large steric effect. If the polymer presents more steric bulk than the alkoxides, then steric interactions between the monomer and polymer may promote *trans* olefins as shown in Figure 2.2b. The large alkoxides of **4** give virtually 100% *cis*-polynorbornene at low temperature; **5** has a slight trans preference in the **ROMP** of norbornene.[13] The electrophilic nature of these catalysts is revealed by the fact that coordinating solvents such as ethers lower the polymerization rate.[8]

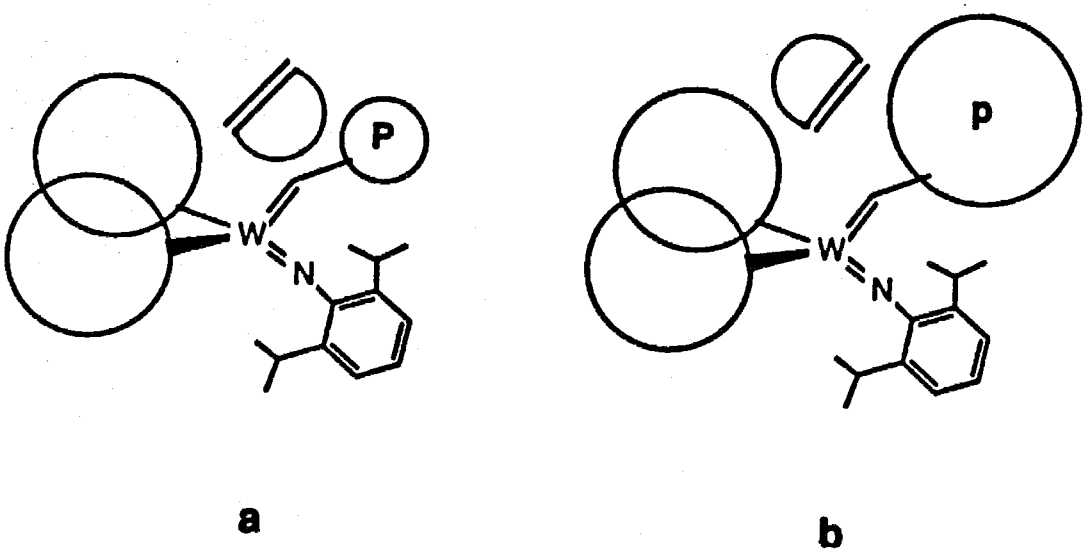

Figure 2.2. The sterics of the Schrock catalyst are shown. In (a) the sterics of the alkoxides dominate the monomer addition. In (b) the growing polymer directs the monomer addition.

The tantalum catalyst **6** polymerized norborene[15] at conditions similar to the titanocene catalyst discussed above (i.e., 65°C).[12] Both carbenes and metallacycles are observed in this system. The carbene is initially synthesized and when treated with norbornene, a norbornene metallacycle is formed. The metallacycle is the chain carrying species and **6** has been reported to give a living polymerization of norbornene. The norbornene polymerization with **6** is not as clean as observed for **1** and **2** and the catalyst is not as readily available. Therefore, this catalyst has not been found to have any advantage over the titanocene catalysts.

Prior to the work in this thesis, very few types of monomers had been **ROMP**ed, and the limitations of the catalysts from Figure 1 were not well defined. Thoughout the following chapters the performance of these catalysts relative to each other will be described.

References:

1. Grubbs, R. H. in *Comprehensive Organometallic Chemistry*; Wilkinson, G., Ed.; Pergamon Press, Ltd.: Oxford, 1982, Vol. 8, 499-551.

2. Collman, J.P.; Hegedus, L. S.; Norton, J. R.; Finke, R. G. *Principals and Applications of Organotransition Metal Chemistry*; 2nd ed. University Science Books, 1987.

3. (a) Ivin, K. J. *Olefin Metathesis*; Academic Press, 1983. (b) Draguton, V.; Balabon, A. T.; Dimonie, M. *Olefin Metathesis and Ring Opening Polymerization of Cyclo Olefins*; John Wiley and Sons, 1985.

4. Thoi, H. H.; Ivin, K. J.; Rooney, J. J. *J. Mol. Cat* **1982**, 15, 245-270.

5. (a) Strauss D. A.; Grubbs, R. H. *J. Mol. Cat.* **1985**, 28, 9 and references therein. (b) Gilliom, L. R.; Grubbs, R. H. *Organomatallics* **1986**, 5, 721.

6. (a) Kress, J.; Osborn, J. A. *J. Am. Chem. Soc.* **1983**, 105, 6346. (b) Aguero, A.; Kress, J.; Osborn, J. A. *J. Chem. Soc., Chem. Commun.* **1985**, 793. (c) Kress, J.; Osborn, J. A.; Green, R. M. E.; Ivin, K. J.; Rooney, J. J. *J. Chem. Soc., Chem. Commun.* **1985**, 874.

7. Quignard, F.; Leconte, M.; Basset, J. M. *J. Chem. Soc., Chem. Comm.* **1985**, 1816.

8. (a) Schaverin, C. J.; Dewan, J. C.; Schrock, R. R. *J. Am. Chem. Soc.* **1986**, 108, 2771. (b) Schrock, R. R.; Depue, R. T.; Feldman, J.; Schaverien, C. J.; Dewan, J. C.; Liu, A. H. *J. Am. Chem. Soc.*, **1988**, 110, 1423.

9. Wallace, K. C.; Dewan, J. C.; Schrock, R. R. *Organometallics* **1986**, 5, 2162.

10. Katz, T. J.; Savage, E. B.; Lee, S. J.; Nair, M. *J. Am. Chem. Soc.* **1980**, 102, 7940 and 7942.

11. Anslyn, E. V.; Cannizzo, L. F.; Grubbs, R. H. submitted for publication.

12. Gilliom, L. R.; Grubbs, R. H. *J. Am. Chem. Soc.* **1986**, 108, 733.

13. Schrock, R. R.; Feldman, J.; Cannizzo, L. F.; Grubbs, R. H. *Macromolecules* **1987**, 20, 1169.

14. Wallace, K. C.; Schrock, R. R. *Macromolecules* **1987**, 20, 448.

15. Szwarc, M. *Living Polymers and Mechanisms of Anionic Polymerizations: Advances in Polymer Science no. 49*; Springer Verlag, 1983.

16. Cannizzo, L. F.; Grubbs, R. H. *Macromolecules* in press.

17. Upton, T. H.; Rappe', A. K. *J. Am. Chem. Soc* **1985**, 107, 1206.

18. Anslyn, E. V.; Grubbs, R. H. *J. Am. Chem. Soc.* **1987**, 109, 4880.

19. Anslyn, E. V. personal communication.

20. Kress, J.; Aguero, A.; Osborn, J. A. *J. Mol. Cat.* **1986**, 36, 1.

21. Schrock, R. R. personal communication.

22. (a) Kress, J.; Osborn, J. A.; Green, R. M. E.; Ivin, K. J.; Rooney, J. J. *J. Am. Chem. Soc.* **1987**, 109, 899.

23. Murdzek, J. S.; Schrock, R. R. *Macromolecules* **1987**, 20, 2640.

Chapter 3

POLYMERS FROM THE RING-OPENING METATHESIS POLYMERIZATION OF DIMETHYLENECYCLOBUTENE AND ITS DERIVATIVES

POLYMERIZATION OF DIMETHYLENECYCLOBUTENE

INTRODUCTION:

The dimethylenecyclobutene ring system provides an opportunity in the synthesis of highly unsaturated polymers by ring-opening metathesis polymerization[1] (**ROMP**) of the cyclobutene olefin. The desired transformation as shown for dimethylenecyclobutene (**DMCB**) in Equation 3.1, would produce the ring opened polymer **1**.

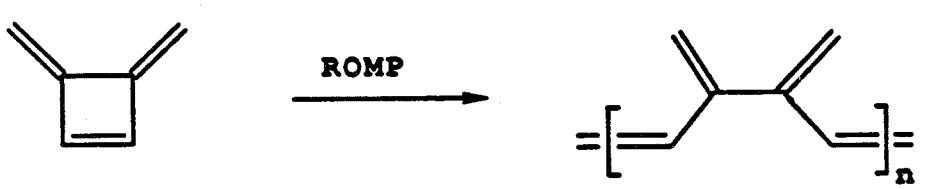

DMCB **1**

Equation 3.1

There is presently considerable interest in the synthesis of highly unsaturated polymers as conductive polymers.[2] Polymer **1** would be extensively unsaturated with a backbone comprosed totally of sp^2 carbons. Polymers of the structural class of **1** contain cross-conjugated olefins. Cross-conjugated conductive polymers such as **1** have not been studied. However, acetylene carbon monoxide copolymers have been reported by Chien.[3] In these copolymers the carbonyl groups are said to interrupt the conjugation, as evidenced by the color of the materials. Yet these materials when doped still lead to highly conductive materials. The results

and conclusions of Chien have not been eccepted by some researchers.[4] Cross-conjugated organic structures in general have interesting bonding,[5] and hence this effect on the conducting properties of these polymers is worthy of investigation.

If polymer **1** can be produced, then the possibility for an electrocyclic ring closure to form polymer **2** exists (Scheme 3.1). Such electrocyclic ring closures are well known[6] and for 1,3,5-hexatriene cyclization occur at $\approx 150^{\circ}C$. Therefore, the proposed chemistry is expected to occur under relatively mild conditions. **2** is essentially partially hydrogenated polyparaphenylene, and hence should be easily oxidized to polyparaphenylene as shown in Scheme 3.1. The value of such a precursor method is in the fact that only a few percent weight loss would be necessary in the conversion to the desired material. In contrast, the precursor route to polyparaphenylene developed by Ballard[7] (see Chapter 1, page 23) extrudes more than half the polymer's mass during the conversion. This extrusion limits the utility of this method in the fabrication and processing of materials, particularly as it relates to carbon composite structures.

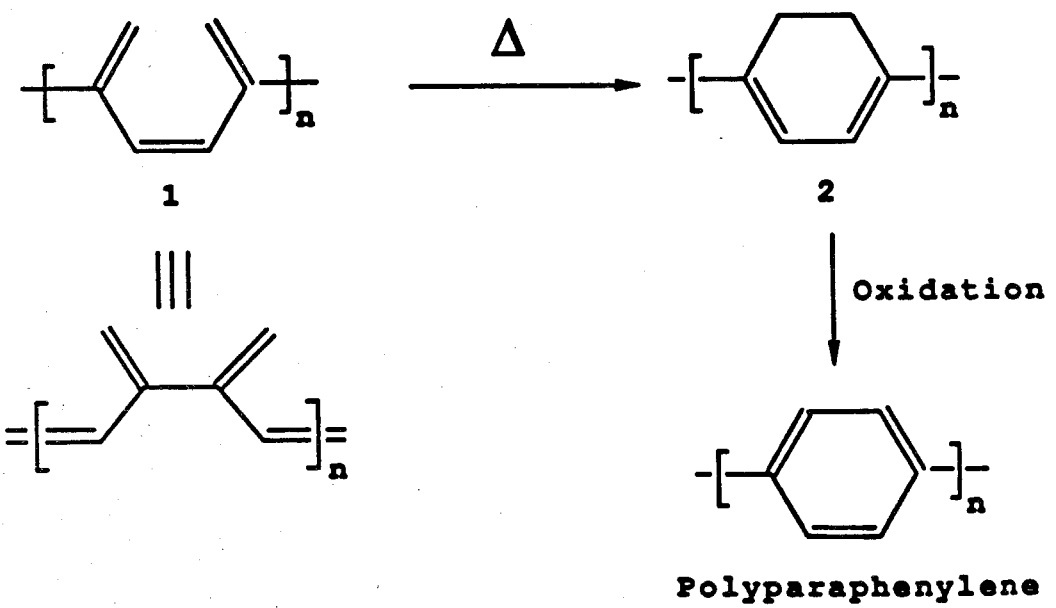

Scheme 3.1

RESULTS AND DISCUSSION:

Polymerization of DMCB:

There are a few routes by which **DMCB** can be synthesized.[8,9] The best synthesis is the thermal rearrangement of 1,5-hexadiyne shown below in Equation 3.2.[8] This transformation is quantitative and produces high purity material. Large scale preparation is conveniently performed by the vacuum pyrolysis of 1,5-hexadiyne vapor.[8] **DMCB** prepared by this method is slightly yellow, but only very minor impurity signals are observed in ^{1}H and ^{13}C NMR. Further purification by vacuum distillation from sodium hydride gave **DMCB** as a colorless liquid. **DMCB** is air sensitive and forms hazardous peroxide polymers with air exposure. **DMCB** is also prone to polymerization, and when stored at RT under inert atmosphere, polymer is formed. Therefore, for long-term storage, **1** was kept under inert atmosphere at -40°C .

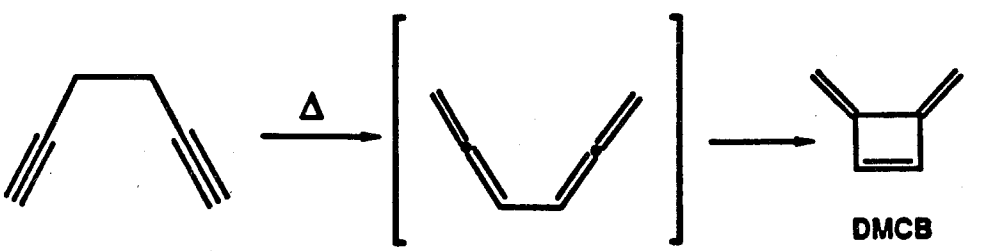

Equation 3.2

Initial attempts at the polymerization of **DMCB** were with the titanocene metallacyle catalysts that have been used extensively in this group.[10] Reaction of **DMCB** with titanocene methylidene sources was not effective at producing polymer. Observation of the reaction of **DMCB** with titanocene methylidene **3**[6] by ^{1}H NMR reveals the disappearance of the cyclopentadiene resonances. In addition, a small broad peak at 5.09 ppm (C_6D_6) is produced. However, peaks for

DMCB did not undergo a significant reduction with prolonged reaction or heating. The generation of the titanocene methylidene catalyst **3** at low temperature (-50°C with the Tebbe reagent) and higher temperature (50°C t-butyl metallacycle) was investigated, but both were unsuccessful at producing polymer. The loss of the cyclopentadiene peaks suggests that the metal may become paramagnetic. Titanium metallacyclobutenes are observed to undergo thermal decomposition to paramagnetic products.[11] Thus, it may be speculated that the decomposition reaction involves a titanocene metallacyclobutene intermediate. In considering the reaction between **3** and **DMCB** there is the possibility that the ring-opened metal akylidene can rearrange to a metallacyclobutene (**4**) as shown in Scheme 3.2. This reaction scheme is speculative, but interesting because it is the reverse of a widely cited yet not proven acetylene polymerization mechanism.[12]

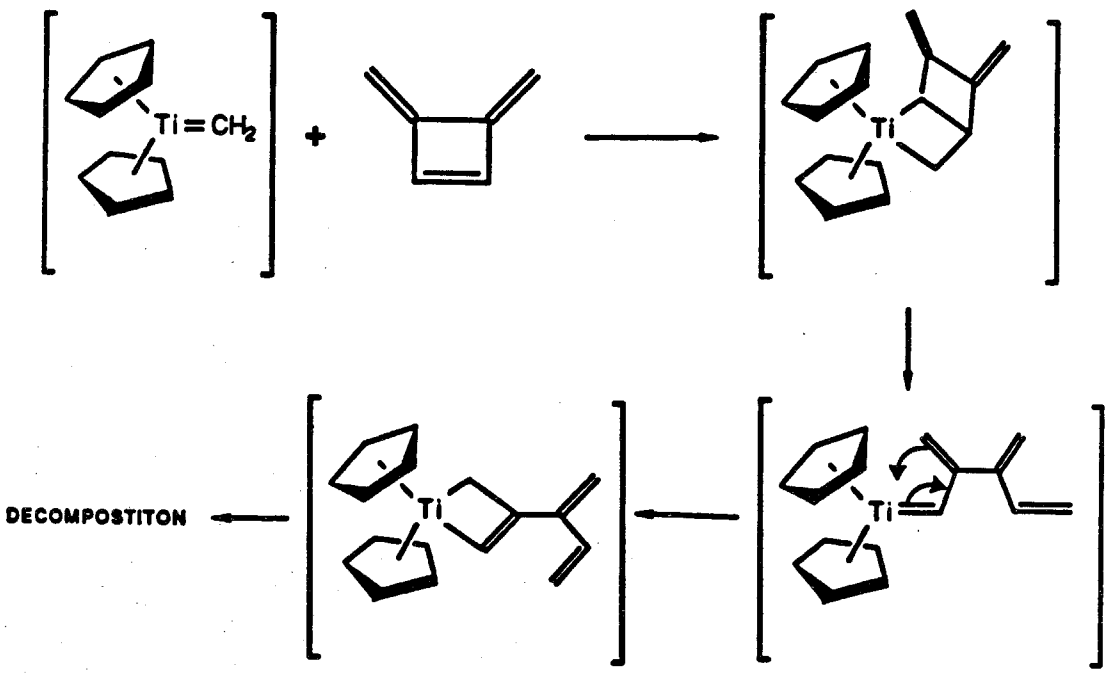

Scheme 3.2

DMCB can be polymerized with $WOCl_4$:$Sn(Me)_4$ and $WOCl_4$:$EtAlCl_2$ to give insoluble tan polymer as a precipitate in the reaction mixture. Dark purple WCl_6:$Sn(CH_3)_4$ solutions turn to light yellow upon addition of DMCB, but formed no polymer. Infrared spectroscopic analysis of these materials from the $WOCl_4$ catalysts indicates that these materials are very similar in chemical composition. The infrared spectra of these materials are shown in Figure 3.1.

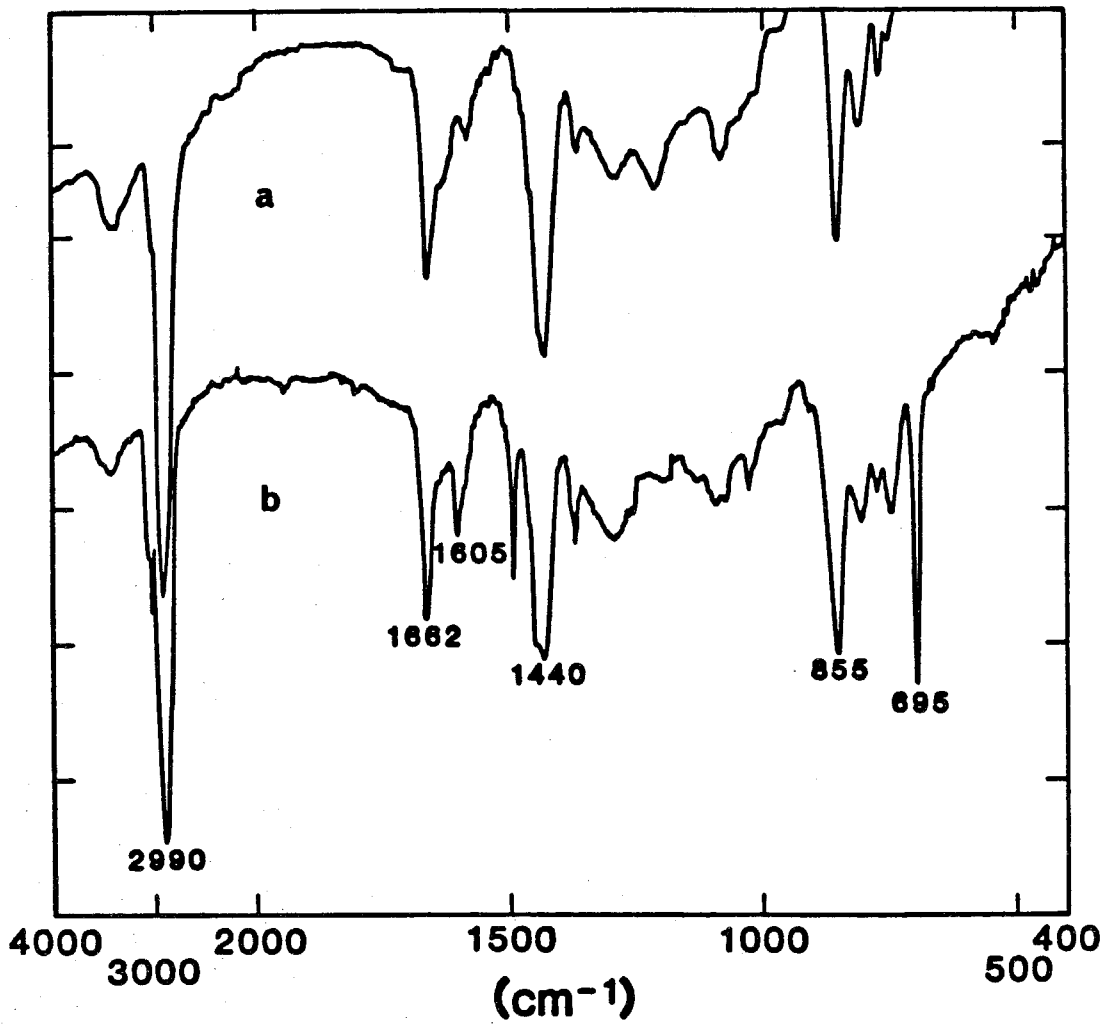

Figure 3.1. Infrared spectra of polymers of DMCB produced with $WOCl_4$:$Sn(CH_3)_4$ (a) and $WOCl_4$:$EtAlCl_2$ (b).

The infrared spectra of Figure 3.1 contain considerable information as to the structure of these materials.[13] Analysis of the infrared spectra is as follows. The C-H stretching band at 2990 cm^{-1} indicates saturated C-H groups. However, this band has a shoulder at 3010 cm^{-1} which indicates that this material also contains olefinic C-H units. The bonds at 1662 and 1605 cm^{-1} are characteristic of C=C stretching modes. The lower energy band at 1605 cm^{-1} is indicative of an assymmetric conjugated diene moiety. The band at 1440 cm^{-1} is a methylene scissoring mode. Other bands consistent with the presence of a methylene group are the twisting and wagging bands from $\approx$ 1150-1350 cm^{-1}, and a rocking mode at 740 cm^{-1}. The strong band at 855 cm^{-1} is indicative of a vinylene group. Other olefins are also present as evidenced by a *cis*-olefin band at 695 and trisubstituted olefin bands at 790-830 cm^{-1}. The large amount of saturation in this material indicates that the isolated polymer of the polymerizations with $WOCl_4$:$Sn(Me)_4$ and $WOCl_4$:$EtAlCl_2$ is not **1**.

Films of this material were prepared by coating the walls of a glass flask with a concentrated solution of the homogenous catalyst $((Me)_3CCH_2O)_2WOCl_2$:$EtAlCl_2$ and exposing it to a vapor of **DMCB** under vacuum. This process produced clear, slightly yellow films that display high reflectivity when viewed at an angle with a high intensity lamp. The infrared spectra of this material is virtually identical to that obtained with $WOCl_4$:$EtAlCl_2$. The mechanical properties of this material are poor, and the films were very fragile. This material was further studied with solid state cross-polarization magic angle spinning (CPMAS) ^{13}C NMR .[14] A CPMAS ^{13}C NMR spectrum of this material is shown in Figure 3.3 and complements the interpretation of the infrared spectra. A dipolar-dephasing experiment[15] indicated that the peaks at 126, 44, and 26 ppm are proton bearing carbons. The peak at 26 ppm is indicative of methylene groups, and the peak at 44 ppm confirms the presence of tertiary C-H groups.[16] The signals at 151, 139,

and 126 are assigned to olefinic carbons. Integration reveals that about 45 % of the polymer's carbon centers are saturated.

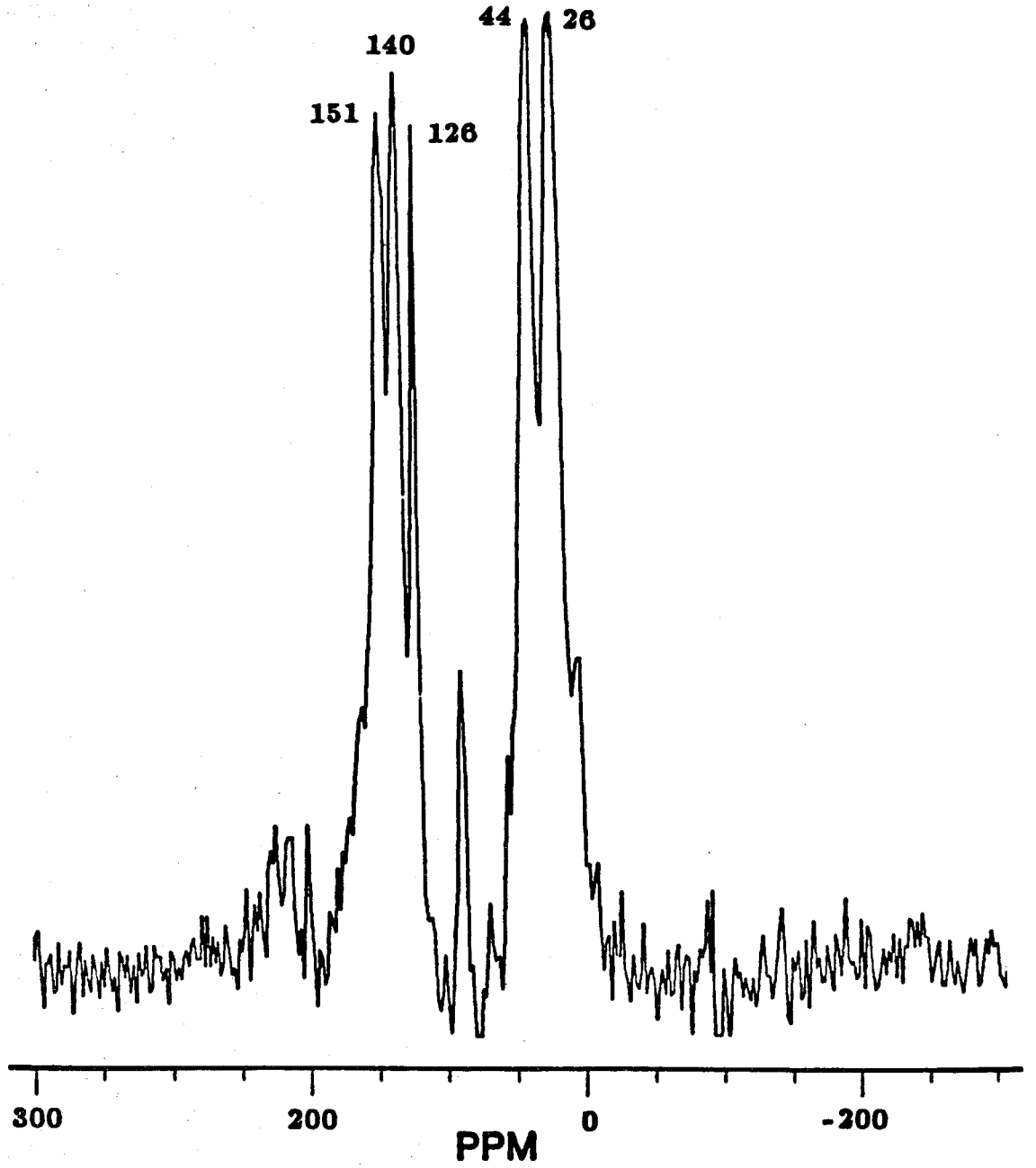

Figure 3.2. CPMAS ^{13}C NMR spectra of **1** polymerized as a film with the homogenous catalyst $((Me)_3CCH_2O)_2WOCl_2$:$EtAlCl_2$.

It was thought that the Lewis acidic nature of the $WOCl_4$ based catalysts may be causing the decomposition of **1** once it is formed. Thus, the polymerization of **DMCB** was investigated with other non-Lewis acidic tungsten alkylidene catalysts[17,18,19] shown below.

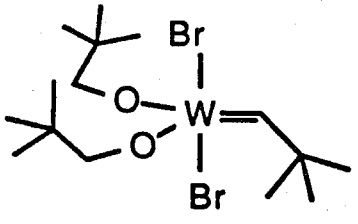

4

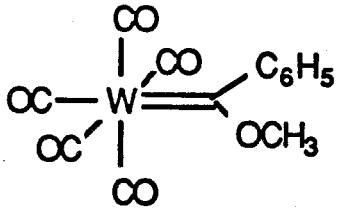

5

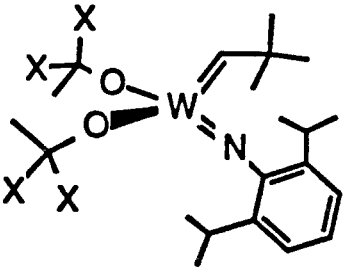

6 X= CF_3

7 X= CH_3

The reaction between **4**[17] and **DMCB** was followed by ^1H NMR. As **DMCB** was consumed, a new broad olefinic signal at 5.09 ppm (C_6D_6) was observed which is consistent with the formation of **1**. However, another broad signal at 2.73 ppm also appears with increasing time. This up-field signal indicates the formation of saturated carbon centers. Some polymer precipitate is observed in the reaction mixture, but the majority of the polymer remains in solution. Work-up of the reaction by precipitation in acetone produces a tan polymer gel. Further washing with acetone causes this material to become progressively darker and decrease in volume. When pumped to dryness, the material volume has decreased to about $\approx$ 1/20 the original size of the tan gel, and consists of dark red nuggets of polymer. These nuggets are hard and make a rattling noise when shaken against the side of the glass container. With the addition of benzene this material did not swell. Solid state CPMAS ^{13}C NMR of this material (Figure 3.3) is very similar to those

obtained with the Lewis acidic catalysts discussed above. The interpretation of these observations is as follows. Polymer is formed in solution and becomes slightly crosslinked, but not so crosslinked as to quanitatively precipitate or gel. Upon addition to acetone a precipitated crosslinked polymer gel is produced. This material is highly swollen with the polymerization reaction solvent which is benzene. As the benzene is washed away by the non-solvent (acetone), the gel collapses. The polymer chains are now closer together and further crosslinking is facilitated. Upon drying, the polymer continues to collapse and crosslink to give the material that was characterized. Crosslinking is also consistent with the observation that the polymer will not swell in solvent after drying. The polymerization of **DMCB** with **4** under more concentrated conditions or longer reaction times than reported in the experimental procedure produced gels without addition of acetone.

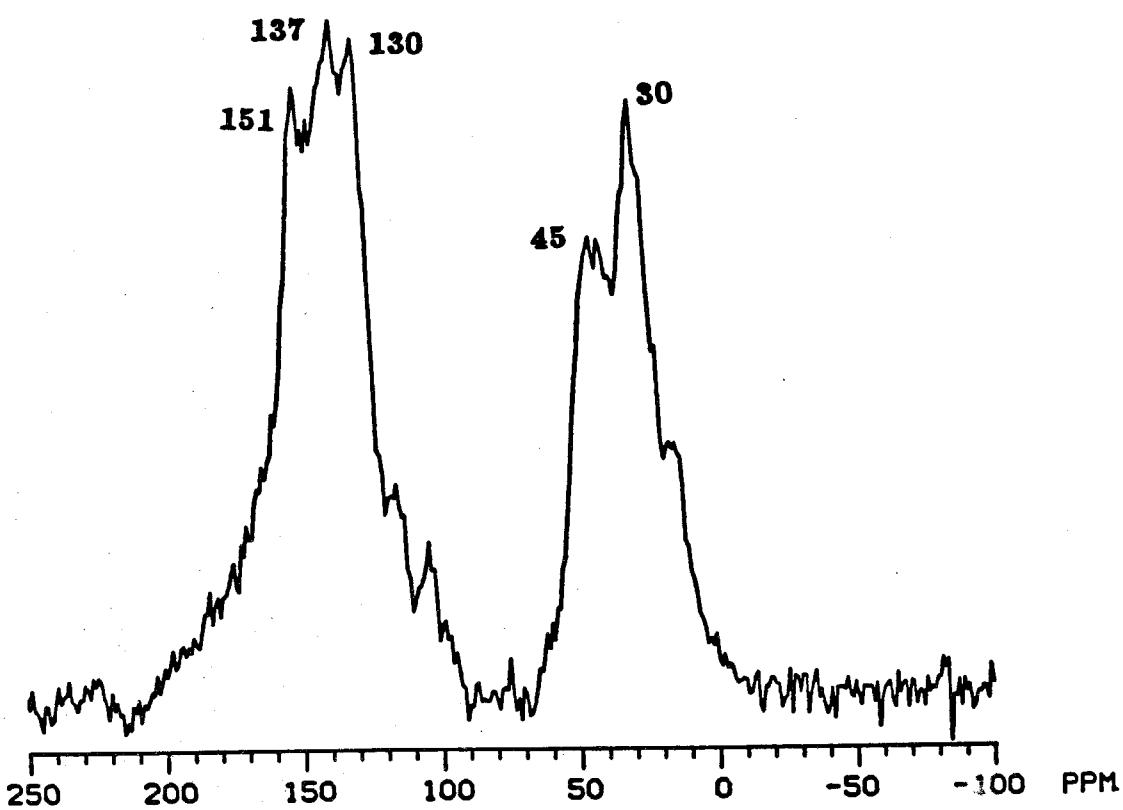

Figure 3.3. CPMAS ^{13}C NMR of DMCB polymerized in solution with 4.

The non-Lewis Fischer carbene (**5**) was also investigated. This catalyst was used in conjunction with a small amount of phenylacetylene as an initiator according to the procedure of Katz.[19] This catalyst will only produce polymer with the phenylacetylene initiator. The results for this catalyst were similar to those obtained with **4**. The polymer was precipitated as a highly swollen tan gel, which collapsed to give non-swellable red polymer nuggets upon drying. The infrared spectra of this material is nearly identical to that obtained for the material polymerized with $WOCl_4$:$EtAlCl_2$ shown in Figure 3.1.

Reaction of **DMCB** with the catalysts **6** and **7**[18] in dilute solution did not produce polymer. ^{1}H NMR investigation of this reaction revealed the decline of the metal-alkylidene signal and the appearance of a broad signal at 5.06 ppm similar to that seen in the polymerization with **4**. This broad signal is suggestive of polymer. Other peaks with complex coupling in the region of 2.2-3.7 ppm were also observed which may be the result of metallacycles. However, the complexity of these signals indicate that there is most likely more than one organometallic compound present. The catalyst consumed approximately five equivalents of **DMCB** under the conditions of the NMR experiment and would not react further, even with heating to 60°C. However, polymer was produced from these catalysts in bulk polymerizations. In this technique the catalyst is dissolved in neat monomer and the catalyst-monomer solution solidifies with further polymerization. Strong free-standing films of the polymer were obtained under these conditions with catalyst **6**, but with **7** the polymers precipitated during the polymerization and hence did not produce continuous films. The films from **6** were yellow in color and infrared spectroscopy gave resonances similar to those obtained for the other catalysts.

As a result of the high reactivity of **DMCB** the possibility that these polymerizations are not **ROMP** should be considered. Two likely alternative polymerizations are cationic or radical polymerization. There are three polymerization

pathways available for cationic or radical polymerization of DMCB as shown in Scheme 3.3. A 1,2-addition polymerization would produce polymer structures **8** and **9**. However, 1,4-polymerization can only lead to one polymer, structure **10**; **11** is unlikely since it contains the energetically unfavorable cyclobutadiene unit. The polymer structures **8**, **9**, and **10** all have a vinylene exo-cyclic to a four membered ring in their structure. Vinylenes of this type have a pronounced higher frequency C=C stretching band than other vinylenes.[9,13] This band for DMCB is at 1694 cm^{-1}, and methylene cyclobutene exhibits a stretching frequency of 1689 cm^{-1}.[20] The highest frequency C=C stretching band observed in materials synthesized is at 1662 cm^{-1}, which is too low for structures **8**, **9**, and **10**. Thus, it can be concluded that the materials described herein are not the products of cationic or radical polymerizations.

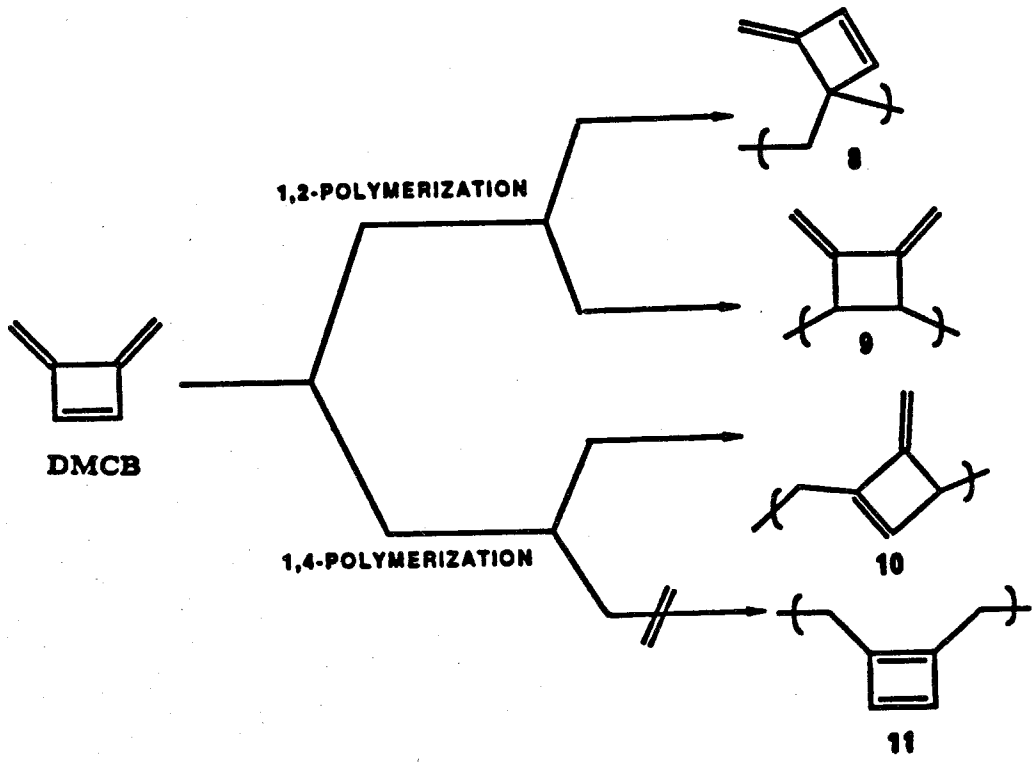

Scheme 3.3

Doping and Conductivity of Polymers:

When exposed to I_2 vapor in vacuum, the above polymers slowly became progressively darker. After 48 hr of I_2 exposure, the materials became black and shiny. This appearance is retained after prolonged evacuation. The conductivity of films and/or pressed pellets of materials saturated with I_2 were investigated. The conductivities of the films formed by bulk polymerization with **6** gave the highest conductivities which were 10^{-6} - 10^{-5} $\Omega^{-1}cm^{-1}$. The conductivities of all the other materials were below the limits of detection ($\approx 10^{-9}\Omega^{-1}cm^{-1}$). Initial capacitance currents were observed, indicating the presence of partially mobile ionic species in the polymers. Films produced with **6** were treated with AsF_5 and sodium naphthalinide to give dull brown materials that were insulators. Hence, the conductivities and doping of materials from the **ROMP** of **DMCB** were not studied further.

Thermogravimetric Analysis:

All the polymers obtained from **1** were studied with thermogravimetric analysis to explore the possibility of attaining materials with high thermal stablity. Polyparaphenylene has a particularly high thermal stability, decomposing only over 500°C .[21] However, the materials at hand need not produce polyparaphenlyene to be useful. Materials that give a high yield of carbon on heating are also of technological importance for composite manufacturing. The results for all the materials from the various catalysts are similar. Upon heating to 700°C under nitrogen atmosphere, these materials gave a 40 - 45 % char yield. The major weight loss occurred between 430 - 490 °C . Typical thermogravimetric curves are shown in Figure 3.4. Heating under ambient atmosphere reduces the char yield to 6%.

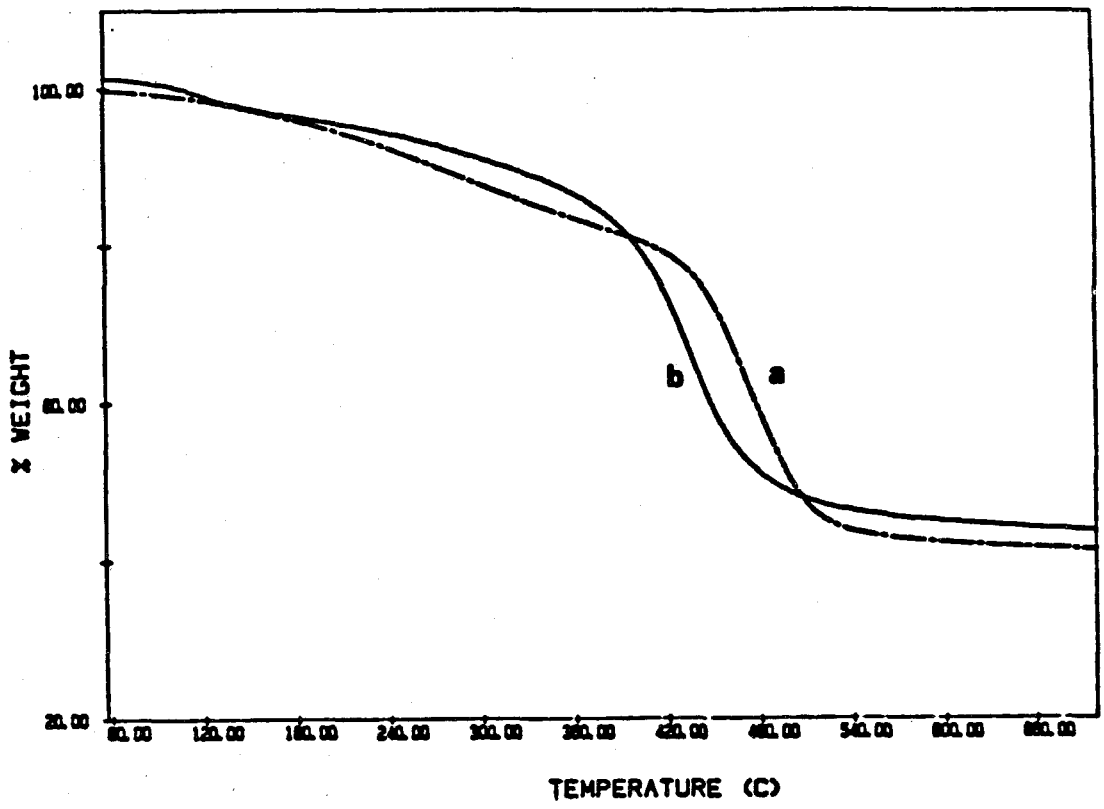

Figure 3.4. Thermogravimetric analysis of polymers of **1**. Curve (a) is polymer formed with the $((Me)_3CCH_2O)_2WOCl_2$:$EtAlCl_2$ catalyst, and curve (b) is that which has been formed with catalyst **7**.

CONCLUSIONS:

The polymerization of **DMCB** with a variety of metathesis catalysts has been shown to produce polymers with similar chemical compositions. The resulting polymer is not **1**, which would be produced by straightforward **ROMP** of **DMCB**, nor is it the product of radical or cationic polymerization. The polymerization reactions may be complicated by intramolecular reactions with the catalyst such as was proposed for the titanium catalysts in Scheme 3.2. This intramolecular reaction is not only limited to the titanium catalysts, but may apply to all the catalysts. The fact that catalysts **6** and **7** are efficient at producing polymer only in very concentrated solution is suggestive of intramolecular catalyst deactivation. In addition, these polymerizations may be complicated by reaction of the catalyst with the methylene groups of the monomer and the polymer to give chain transfer processes such as shown below in Equations 3.3 and 3.4.

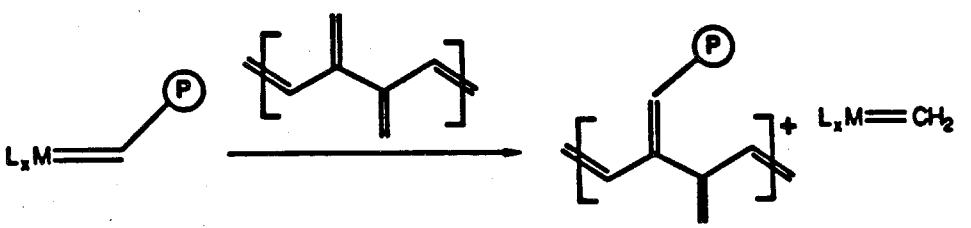

Equation 3.3

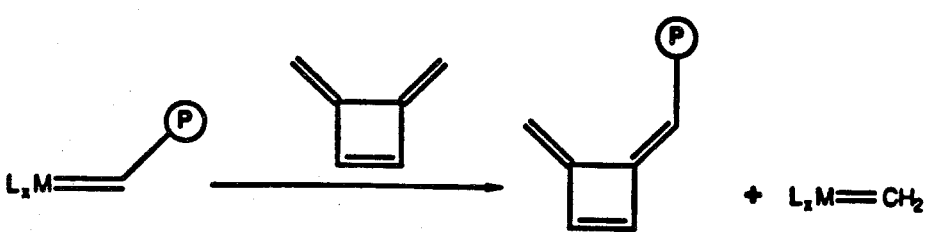

Equation 3.4

The solution polymerization of **DMCB** with **4**, **6**, and **7** was observed *in situ* by ^{1}H NMR to give signals consistent with a highly unsaturated polymer. However, this material appeared to undergo decomposition to an extremely crosslinked material upon isolation. The results presented suggest that polymer **1** may be initially formed in the polymerizations, but is unstable with respect to forming a highly crosslinked material. It is possibile that some of the observed saturation is the result of the desired cyclization shown in Scheme 3.1. However, the presence of a considerable amount of tertiary carbon indicates that the desired chemistry does not occur to a high degree. A variety of crosslinking reactions may be operative. Diels-Alder reactions may be facile in structures like **1**. Equation 3.5 illustrates one possible Diels-Alder crosslinking reaction that may be occurring.

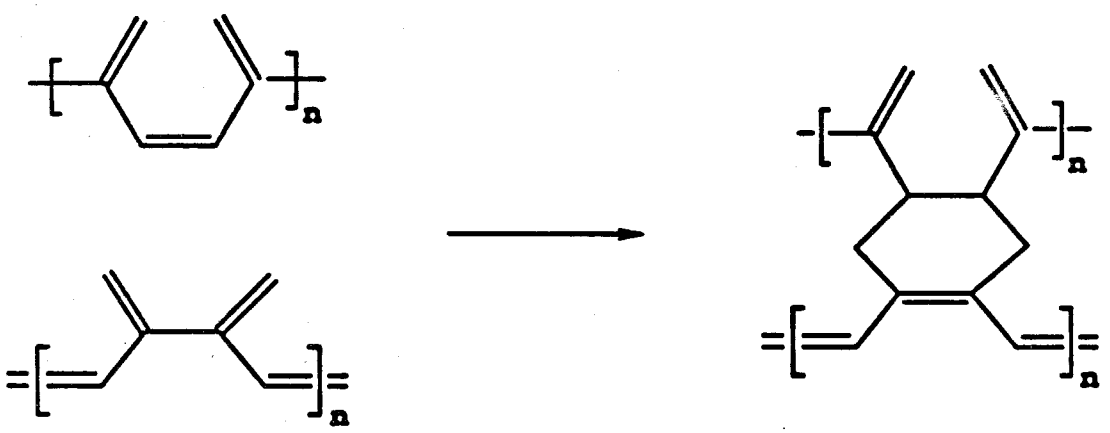

Equation 3.5

Radical initiated processes may also induce crosslinking in a random fashion. Figure 3.5 illustrates a possible crosslinked state that could come about from a radical reaction. The crosslinking reactions in addition will have some catalyst dependence, as a result of the *cis:trans* ratios and chemistry that may be initiated

by residual catalyst. Both the Diels-Alder and radical structures incorporate the functional groups observed in the spectroscopic analysis of these polymers.

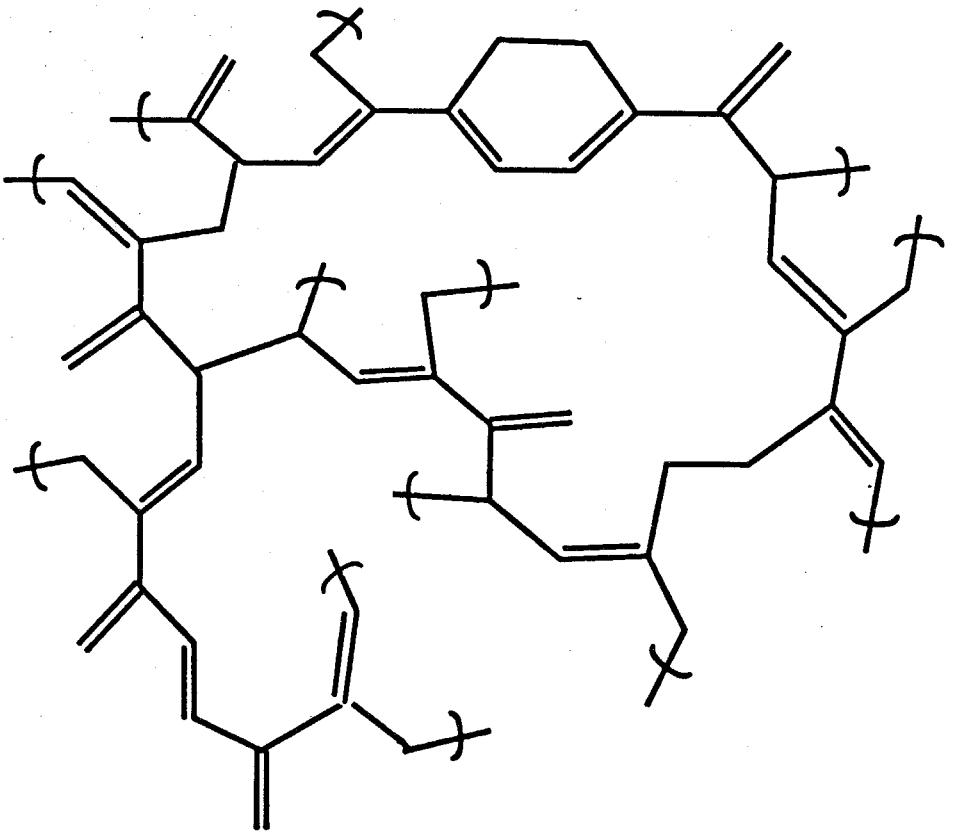

Figure 3.5. Proposed crosslinked structures for polymers obtained from **ROMP** of **1**.

This work demonstrates that the production of new extensively unsaturated materials may be severely limited by crosslinking. The preponderance of **1** to crosslink may be a direct result of its cross-conjugated electronic structure. The cross-conjugation will have a tendency to localize the electronic states of the polymer, and hence any radicals will be somewhat localized. Thus, the fact that localized radicals are much more reactive than delocalized radicals may be responsible for the high degree of crosslinking.

THE SYNTHESIS AND PROPERTIES OF POLY(3,4-DIISOPROPYLIDENECYCLOBUTENE)

INTRODUCTION:

Given the problems encountered in the **ROMP** of the parent monomer **DMCB**, other derivatives were considered. Substitution of the methylene groups of **DMCB** should reduce the potential for crosslinking and intramolecular catalyst deactivation that was discussed in the previous section. The tetramethyl-substituted monomer diisopropylidenecyclobutene (**DICB**) was therefore an attractive candidate for **ROMP**.

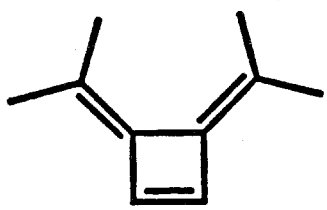

DICB

There are three acceptable syntheses of **DICB** in the literature.[8b,22,23] These syntheses were investigated in the course of this research and are summarized in Figure 3.6. Synthesis I was the first synthesis to be reported and is an extension of the thermolysis as was used in the synthesis of **1**.[8b] However, the 3,3,4,4-tetramethyl-1,5-hexadiyne is not readily available (i.e., 4 steps). Synthesis II provides a high yield and is a convenient method for the preparation of 10 to 20 gram quantities of **DICB**.[22] Synthesis III has been recently developed and is an elegant example of organometallic chemistry applied to organic synthesis.[23] This method was described as a better synthesis over other methods, and the reaction is catalytic in the presence of excess zinc. However, due to the large solvent volumes required and a tedious reaction workup, this method is not suitable for

the preparation of more than a few grams of **DICB**. Synthesis II was in general found to be the preferred synthesis and the majority of **DICB** was prepared by this route. **DICB**, like **DMCB**, is an air sensitive material which forms peroxide polymers upon air exposure. **DICB** was stored under inert atmosphere at -40°C

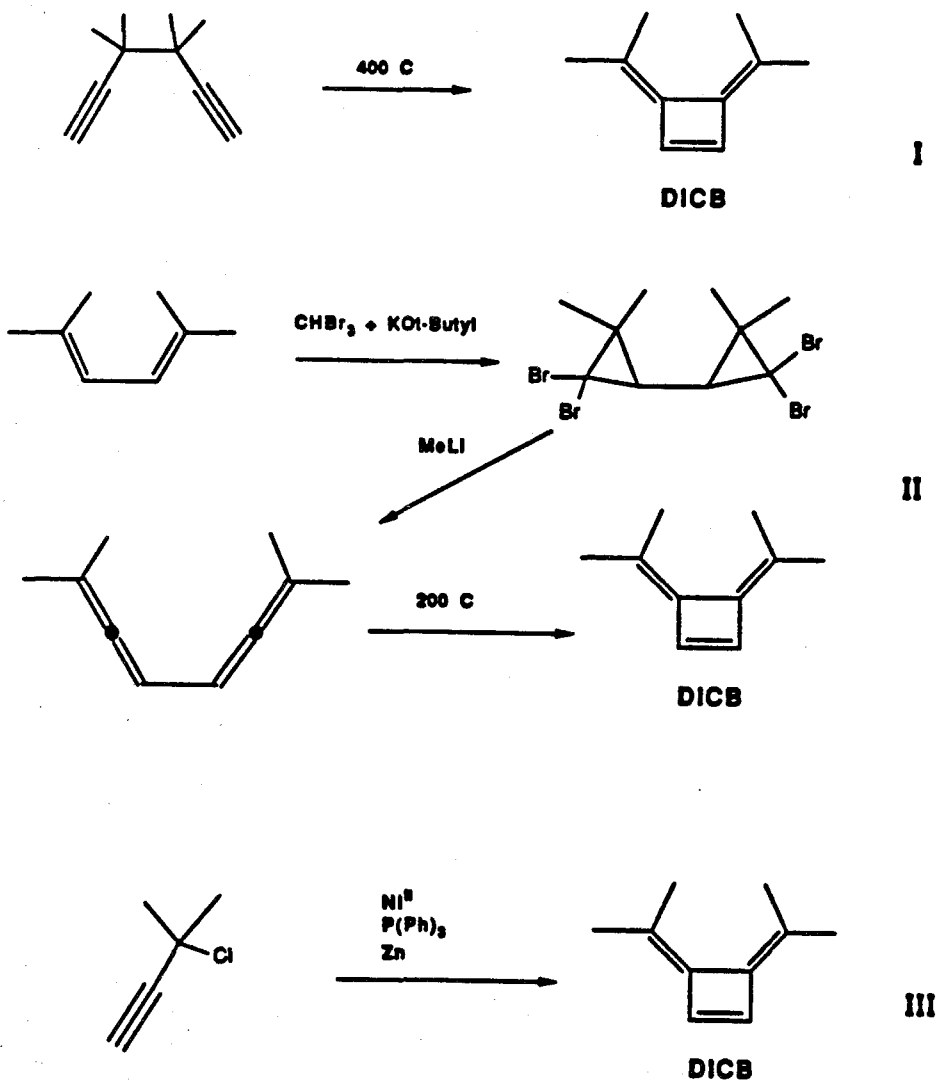

Figure 3.6. Syntheses I, II, III used in the preparation of **DICB** , as reported in references 8b, 22, and 23 respectively.

RESULTS AND DISCUSSION:

Polymerization of DICB:

DICB was found to undergo facile **ROMP** with a variety of metathesis catalysts. We have focused our studies on the **ROMP** of **DICB** titanocene catalysts[10] and the polymerization with **3** is shown below in Scheme 3.4. Poly(3,4-diisopropylidenecyclobutene) (**PDICB**) is obtained as a white powder when precipitated in methanol. This polymer is readily soluble in aromatic solvents and chloroform, and slightly soluble in hydrocarbon, tetrahydrofuran, ether, and methylene chloride. **PDICB** is air sensitive and within minutes of air exposure turns bright yellow to produce materials which were soluble in polar solvents. The ^{1}H and ^{13}C NMR shown in Figure 3.7 are consistent with the assigned structure of **PDICB**. The *trans*-olefin is confirmed by the presence of the C-H out of plane bending mode in the infrared spectra at 945 cm^{-1} (see Figure 3.18).[13]

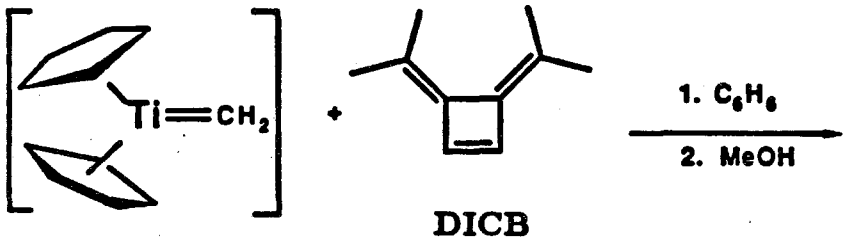

DICB

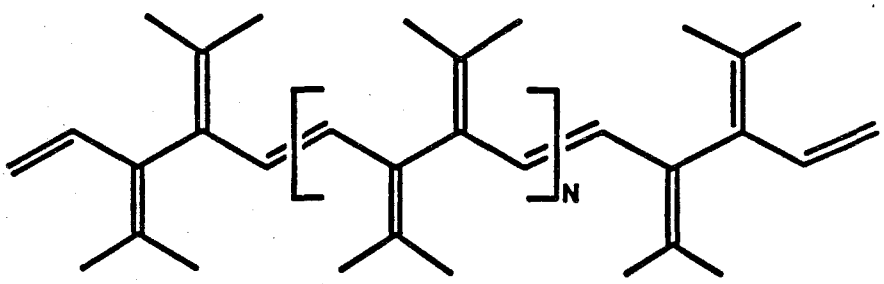

PDICB

Scheme 3.4

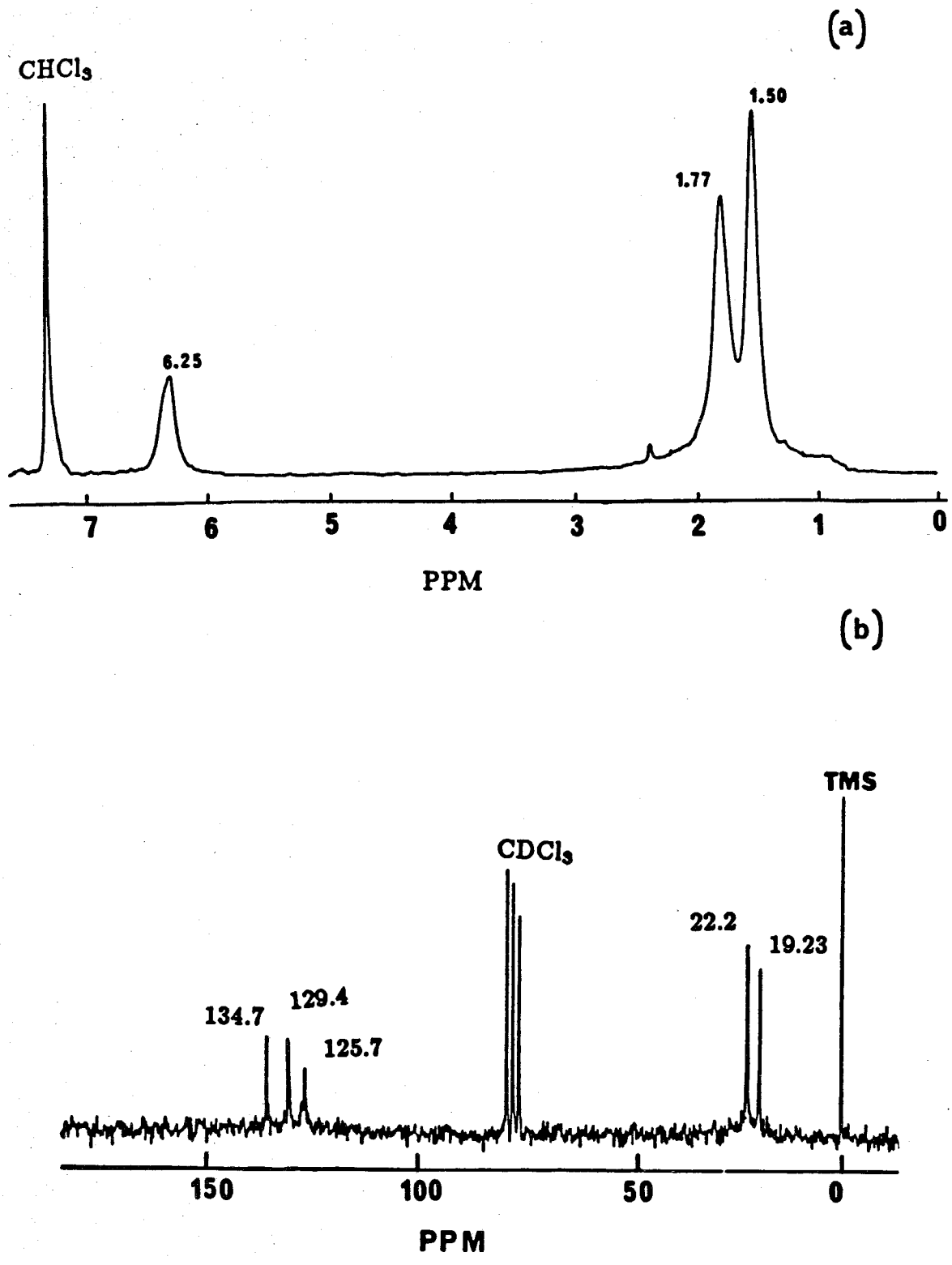

Figure 3.7. ^{1}H NMR (a) and ^{13}C NMR (b) of PDICB in $CDCl_3$.

Catalysts **4**, **6**, **7**, and WCl_6:$Sn(CH_3)_4$ were also found to produce polymer with infrared spectra identical to **PDICB** prepared with **3**. Materials polymerized with WCl_6:$Sn(CH_3)_4$ could not be redissolved after precipitation as a result of the high molecular weight and/or crosslinking. All the catalysts were found to produce purely *trans*-**PDICB**. This is likely a result of the sterics of the growing polymer directing the monomer addition as discussed for **6** and **7** in Chapter 2 (Figure 2.2). The titanocene metallacycle catalysts are more readily available than **4**,[17] **6**,[18] and **7**.[18] Thus, the results reported throughout this chapter will be for **PDICB** prepared with the titanium catalysts.[10]

It was found that **PDICB** was prone to gelation. Concentrated solutions ($\approx$100 mg/ml) gel in a matter of hours. This gelation is irreversible and is believed to be the result of crosslinking. Efforts were made to have the polymer in solution for a minimum length of time to minimize crosslinking. Even so, a small amount of polymer would typically not redissolve after precipitation. The amount of insolubie material was found to be reduced by shorter polymerization times. Typical polymerization conditions were .5 M **DICB**, .01 M catalyst, and a reaction time of 30 minutes. Under these conditions, the reaction mixture became noticeably warm as the result of the strain energy released from the cyclobutene ring with **ROMP**. Increasing the monomer to catalyst ratio above 100 resulted in lower yields of polymer, and the red color of the catalyst faded to light orange upon monomer addition. The yields of **PDICB** were also found to be variable depending on the lot of **DICB**. These observations are indications that the monomer as synthesized has impurities that cause catalyst decomposition. **DICB** is difficult to purify due to its air sensitivity, low melting point, and high solubility. Hence, further purification of this monomer was not pursued.

The presence of an impurity is also apparent in the gel permeation chromotographic (GPC)[24] analysis of **PDICB** which is shown in Figure 3.8. The tailing

at low molecular weights is suggestive of chain termination processes which may result from impurity decomposition of the growing polymer. In addition, the average molecular weights of the materials are higher than would be predicted. That is, every catalyst molecule does not produce a polymer molecule. Again, this result is consistent with decomposition of some of the catalyst by an impurity. GPC also supports the proposed crosslinking of the **PDICB** by the presence of the small peak at high molecular weight. This peak is reduced by shorter reaction times or low temperature polymerization (Figure 3.8b). Low temperature polymerization also increased the tailing to low molecular weight, suggesting that the polymerization rate is decreased with respect to catalyst deactivation by the impurity. The polydispersity index[24] for polymerizations at various conditions ranged from 5.4-2.2.[25] These results were somewhat dependent on the monomer purity which varied between lots. Procedures that yielded various dispersities are given in the experimental section.

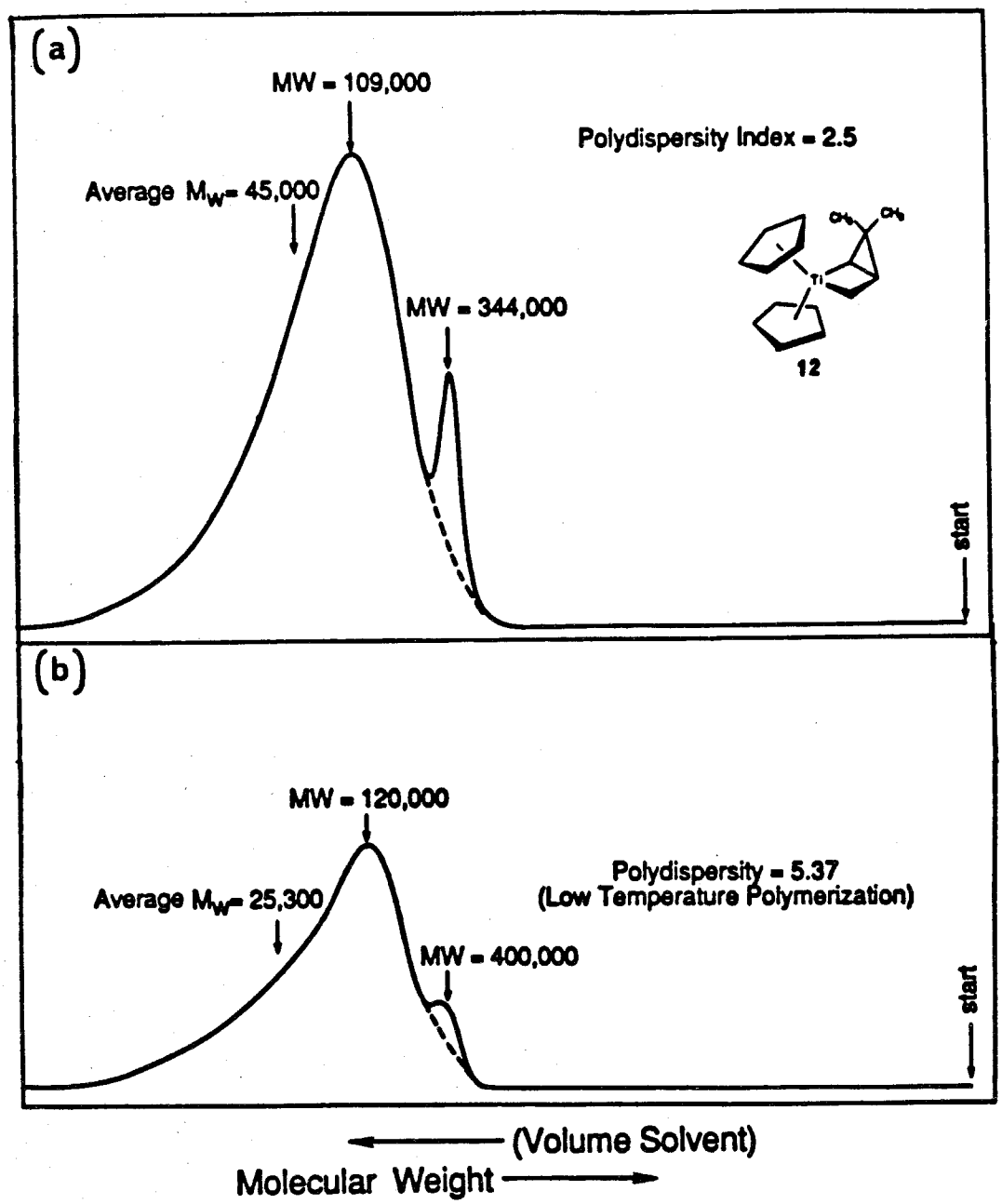

Figure 3.8. GPC trace (UV) of **PDICB** polymerized with catalyst **12** at RT (a) and the Tebbe reagent and pyridene at -30 to -20°C (b).

Block Copolymers:

ROMP allows the synthesis of block copolymers as a result of the fact that the chain carrying species is stable and presents for some monomers a living polymerization.[10,18,26] The titanocene metallacycle catalysts and **7** exhibit living polymerizations of norbornene,[10] and hence block copolymers can be readily synthesized between **PDICB** and polynorbornene.[27] Polynorbornene is a well-known elastomer and as a result these block copolymers may have superior mechanical properties. The titanocene metallacycle catalysts provide a convenient synthesis of these block copolymers by the following procedure. A low dispersity polynorbornene segment is polymerized at 65°C, and reaction is then cooled to room temperature. At this point the catalyst is unreactive and the solvent and excess monomer are removed *in vacuo*. The red rubbery mass consists of a polynorbornene segment of predetermined length with a titanocene metallacycle on the terminous **13** (Scheme 3.5). **13** is then redissolved in solvent and heated to 65°C to reactivate the catalyst and **DICB** is added and polymerized to give a block copolymer. The block copolymer is isolated by precipitation as a white solid with a very light red tint. This red color is indicative of residual metallacycles such as **13** which are known to be inert to methanol.[28] This observation indicates that some of the metallacycle did not reinitiate polymerization or that residual norbornene was present in the polymerization. The GPC trace shown in Figure 3.9 reveals a broad molecular weight distribution. This high polydispersity index is expected as a result of the comparatively slow initiation of **13** with respect to polymerization of **DICB**.[29] Attempts at improving the polydispersity by polymerizing the **DICB** first, adding the norbornene, and heating to 65°C produced only gels. Gelation is a result of the crosslinking of **PDICB** which occurs at the temperatures required to polymerize norbornene. This crosslinking is also evidenced in the GPC trace in Figure 3.9 which indicates a greater fraction of

the high molecular weight material than was observed for the PDICB homopolymer (Figure 3.8). However, the copolymers exhibit an improvement in solubility over the PDICB homopolymer and these materials displayed good viscoelastic properties. The ratio of polynorbornene to PDICB was determined by NMR integration of the olefinic resonances. A representative ^{1}H NMR spectra of a 1:1.5 block copolymer is shown in Figure 3.9.

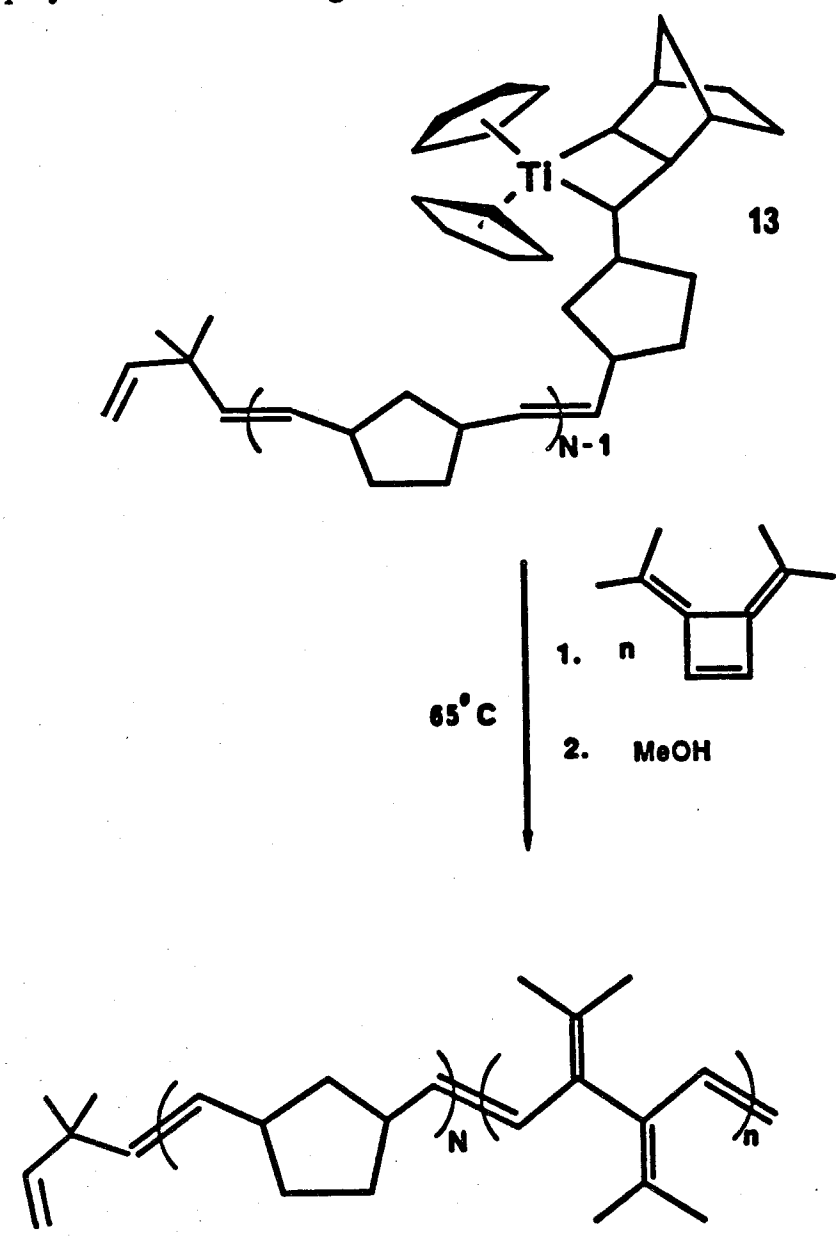

Scheme 3.5

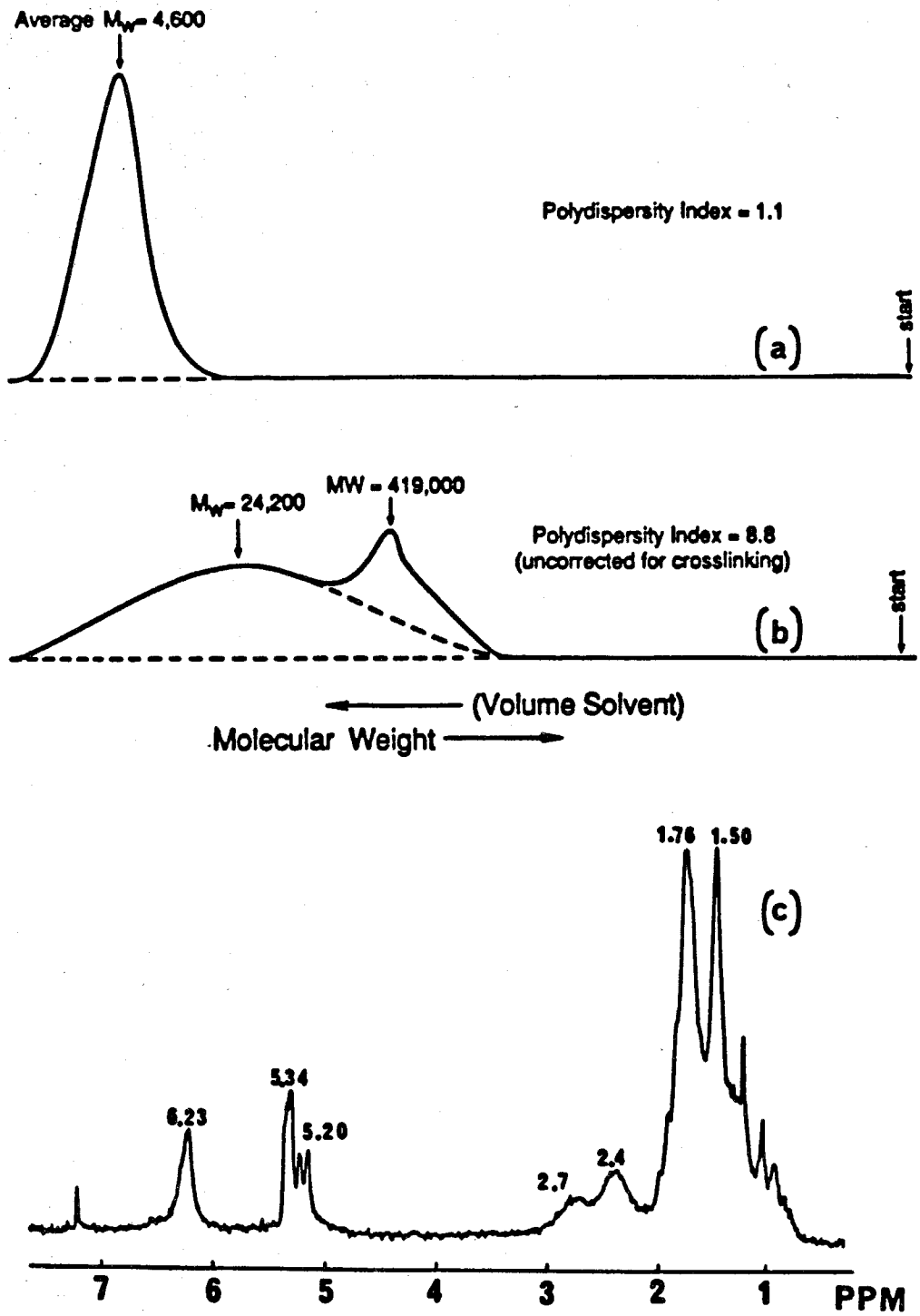

Figure 3.9. GPC trace of polynorbornene homopolymer (a); and the PDICB - polynorbornene block copolymer (b); ^{1}H NMR ($CDCl_3$) of PDICB : polynorbornene block copolymer (c).

Thermal properties:

Considering the rigidity of the unsaturated polymer backbone of **PDICB**, one would predict a high glass transition temperature. DSC of **PDICB** revealed no evidence for a glass transition upon scanning from 50 to 300°C. The DSC thermogram shown in Figure 3.10 displays a small exotherm at 150 and major exotherm peaking at 280°C. Therefore, the glass transition temperature is above the decomposition temperature of **PDICB**. Thermogravimetric analysis reveals only a slight weight loss up to 330°C as shown in Figure 3.11. However, at higher temperatures, nearly the entire weight of the sample is lost. Samples heated to 300°C produced brown tacky solids. No attempts were made to determine the nature of the decomposition.

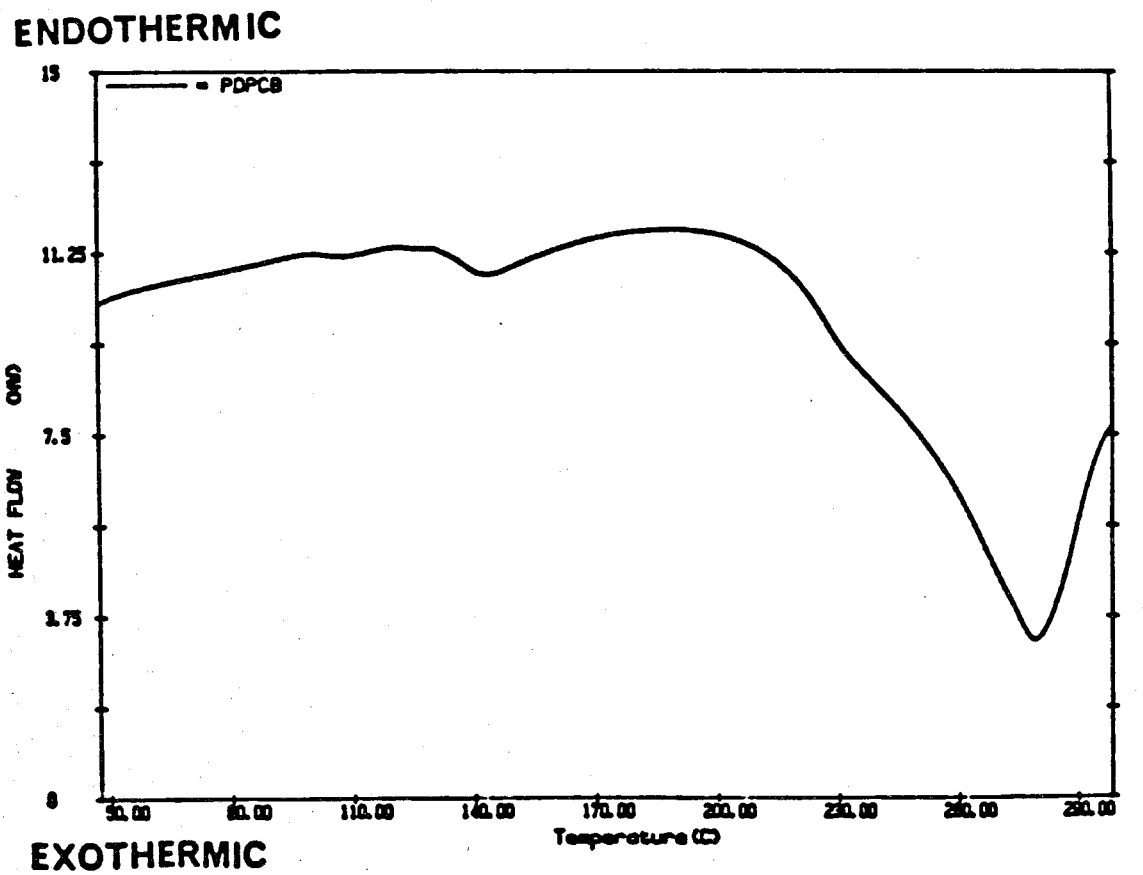

Figure 3.10. DSC thermogram of **PDICB**.

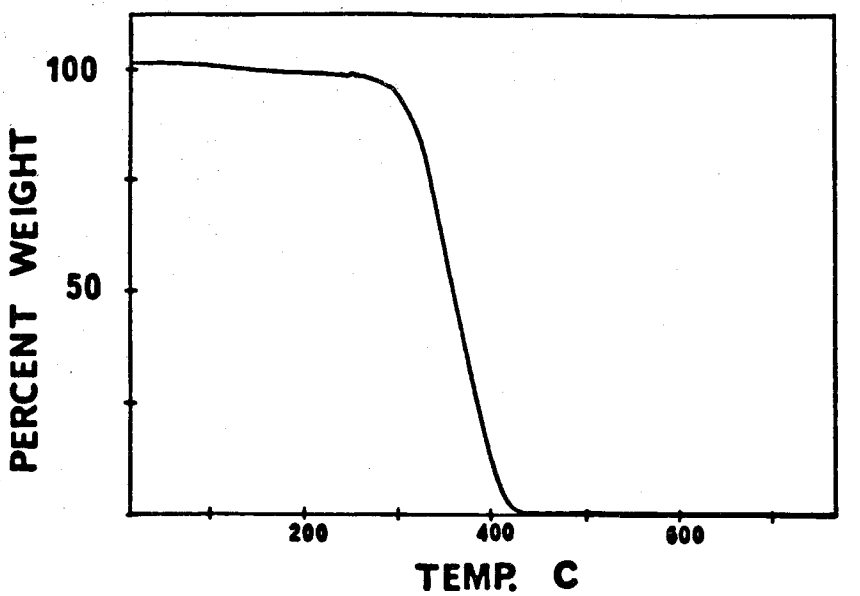

Figure 3.11. Thermogravimetric analysis of **PDICB.**

Conformational Properties of PDICB:

The UV-vis spectra of **PDICB** are very different from most other conductive polymers. A spectrum in $CHCl_3$ is shown in Figure 3.12 with $\lambda_{max} = 278$ nm. The onset of the absorption gives a band gap of 3.9 eV which is indicative of a low conjugation length. CPK molecular models of **PDICB** indicate that there are large steric interactions between the methyl groups and the olefinic protons as shown in Figure 3.13. As a result of these steric interactions, the backbone of **PDICB** cannot be planar. Models suggest that a 90° torsion about the bond between the cross-conjugated olefins leads to minimal steric interactions. An illustration of this conformation is shown in Figure 3.14. A conformation such as this leads to triene segments of the polymer that are coplanar, but are twisted 90°C with respect to the plane of the next triene. This structure is consistent with the UV-vis spectra which is appropriate for a substituted triene chromophore.[13] The molar extinction coefficient was calculated for **PDICB**, and found to be 20,000 $M^{-1}cm^{-1}$ per triene unit in $CHCl_3$. This extinction coefficient is again consistent with the triene moiety.[13]

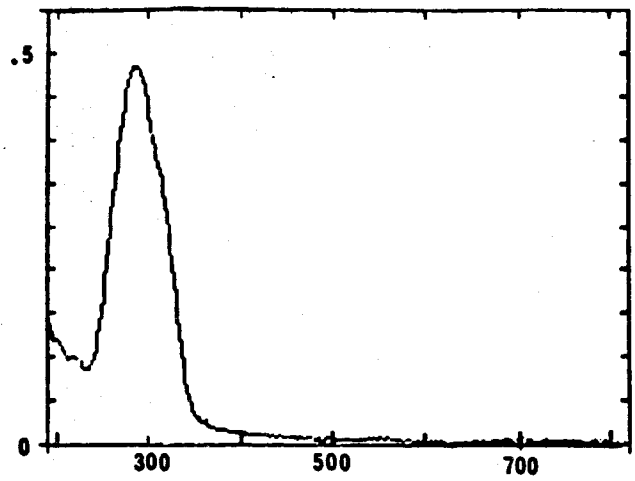

$\lambda_{max}^{CHCl_3}$ = 278 mn

E_m = 20,000 $M^{-1}cm^{-1}$ per triene unit

Figure 3.12. UV-vis spectrum of a $CHCl_3$ solution of PDICB.

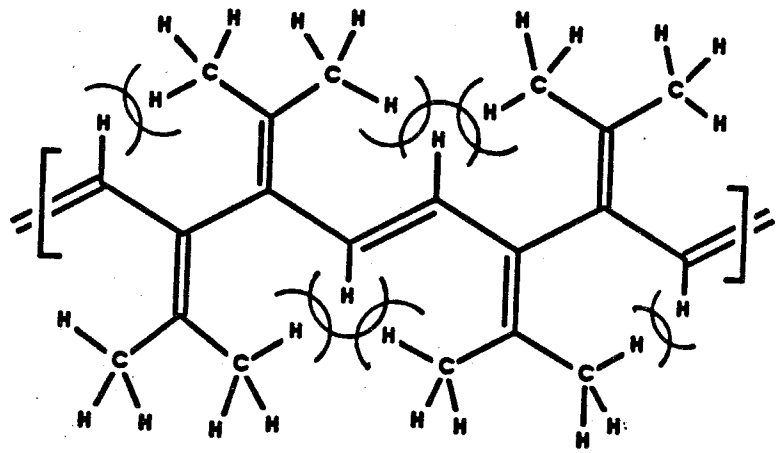

Figure 3.13. Illustration of the steric interactions in **PDICB** which lead to the non-planar conformation.

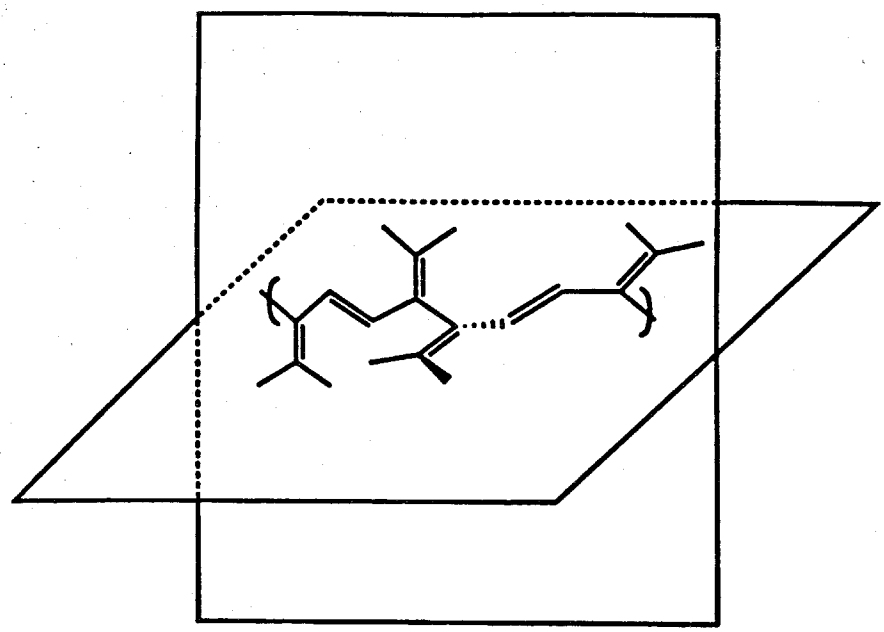

Figure 3.14. Proposed conformation of **PDICB** which minimizes the steric crowding.

For comparison, a polyacetylene substituted with isopropyl groups was synthesized (**14**).[30] The isopropyl groups will have a similar magnitude of steric interactions. Due to twisting of the polymer backbone this material is also a white material with a UV-vis with similar intensity maxima at 265 and 305 nm which is extremely similar to that of **PDICB** in energy. However, the extinction coefficient of **13** was found to be 3000 $M^{-1}cm^{-1}$ per triene which is almost 10 times smaller than that of **PDICB**. Thus, even though **14** has approximately the same band gap, it does not behave like an ensemble of non-interacting triene groups as does **PDICB**. This effect is most likely the result of a smooth twisting of the polymer backbone for **14** where in **PDICB** the deviation from planarity is localized in one major torsion between the crossconjugated olefins. It is interesting to note that substituted polyacetylenes such as **14** are not particularly air sensitive and may be stored for months in air without major decomposition.

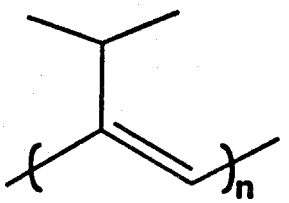

14

A recent theoretical study by Pranata and Dougherty considered the twisting of the polymer backbone of **PDICB**.[31] After consideration of model compounds, it was concluded that the polymer structure consisted of mutually orthogonal triene segments as suggested above. This low overlap makes for a very narrow valence bandwidth of .03 eV which is much lower than most conductive polymers.[32]

Morphology and Processing of PDICB:

As described in Chapter 1 the morphology is an important factor in determining the electrical properties of conductive polymers. Thus, the morphology of **PDICB** was investigated. Scanning electron microscopy of a film of **PDICB** cast from $CHCl_3$ revealed a smooth but not featureless texture. As shown in Figure 3.15, the polymer surface contains small circular raised areas. The origin of this structure is not known but it is most likely the result of surface tension that occurs with the evaporation of the solvent. The diameters of these raised areas ranged from .5 to 2 microns. X-ray diffraction of films and powders revealed that the polymer is totally amorphous yielding only a broad amorphous halo. It was found that fibers could be formed by elongation and precipitation of concentrated solutions. Further study of these fibers has not been performed. **PDICB** can not be stretched or melted as a result of its rigidity and high glass transition. Pellets formed at RT and preasures of 10,000 pounds cm^{-2} were transparent, indicating the **PDICB** can be fused under these pressures.

Figure 3.15. Scanning electron micrograph of PDICB at 1.1 X 10^4 magnification and a 60 °C angle to the surface.

Doping and Conductivity of PDICB:

In light of the "trieneic" nature of **PDICB** it is surprising that it is so easily oxidized. The high air sensitivity was particularly surprising. Prolonged exposure to air gave a material with elemental composition of $C_{10}H_{13.8}O_{3.1}$, which is approximately three oxygen atoms per repeating unit or one per olefin. The oxidized materials are soluble in polar solvents, and concentrated solutions are not viscous. The qualitatively low viscosity suggests that chain scission has occurred and that the oxidized materials are of low molecular weight.

PDICB readily absorbs I_2 to yield a black and shiny material. This change is rapid and, when exposed to I_2 in vacuum, occurs in less than a minute. Prolonged exposure (days) to I_2 was found to give a composition which is 55 to 60% by weight I_2 ($\approx$.6 I_3^-/repeat). Elemental analysis of material doped to 65 revealed that the carbon-hydrogen ratio remained unchanged. Thus, the abstraction of hydrogen to give HI is not observed. Once doped, materials became insoluble in all solvents.

The conductivity can be monitored while simultaneously doping by using a four-point probe conductivity apparatus similar to that described by Chien[33] (Figure 1.5). Conductivity measurements with I_2 doping reveal a peak conductivity of 2 X $10^{-3}\Omega^{-1}cm^{-1}$ for **PDICB**. A plot of the conductivity as a function of I_2 exposure is shown in Figure 3.16. The highest conductivities were attained under an atmosphere of I_2, and upon removal of excess I_2 *in vacuo* the conductivity is lowered to 10^{-4} to $10^{-5}\Omega^{-1}cm^{-1}$ depending on the duration of the evacuation. Prolonged evacuation gave materials that were 40 - 50% I_2 by weight. Conductivity measurements made with a sheet resistivity probe (Figure 1.6) in a glove box were 6 X $10^{-4}\Omega^{-1}cm^{-1}$ on samples saturated with I_2. Once doped, samples seemed to be reasonably air stable, and after 6 - 8 months of air exposure had conductivities of 10^{-5} to $10^{-6}\Omega^{-1}cm^{-1}$. The conductivity of these samples could be raised to $\approx$5 X $10^{-4}\Omega^{-1}cm^{-1}$ with re-exposure to I_2.

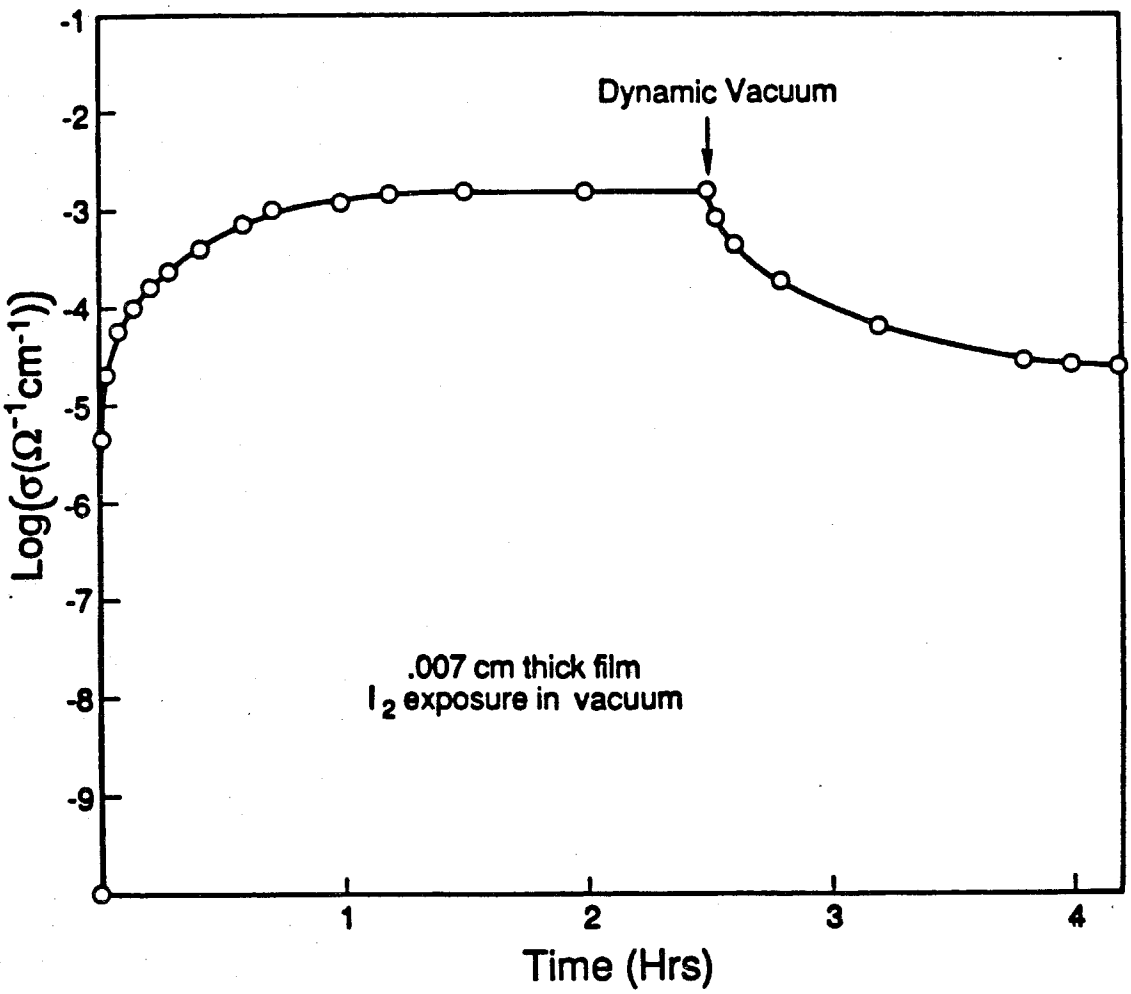

Figure 3.16. Plot of log(conductivity) of **PDICB** as a function of time of I_2 exposure. At ≈2.5 hours the I_2 source was shut off and a dynamic vacuum was applied.

AsF_5 is an extremely powerful oxidant and has been used extensively in the doping of conductive polymers.[2] Upon exposure to AsF_5 **PDICB** immediately turns to a bright red-orange color. This color persists and slowly turns to a brown-orange color. Black and shiny materials (45 to 66 % AsF_5) were only attained after long exposures to AsF_5 (c.a. 24 hr 300 torr). The resulting materials were not subjected to elemental analysis. However, vials in which heavily doped samples were stored (c.a. 50% AsF_5) became etched after weeks at RT. Thus, heavily doped materials slowly evolve HF gas. The AsF_5 forms diamagnetic products in the polymer and likely results in a mixed valence state with As^{V} and As^{III} centers. Thus, three AsF_5 may prehaps disproportionate to form 2 AsF_6^{-1} and one AsF_3. Such a process will lead to the removal of 2/3 of an electron per AsF_5. A doping level 45% AsF_5 is .64 AsF_5 per repeat and 66% is 1.5 AsF_5 per repeat. Based on the above hypothesis of AsF_5 products this corresponds to .43 and .1 electron per repeating unit respectively. AsF_5 doping of **PDICB** was found to give a conductivity of $\approx 10^{-5}\Omega^{-1}cm^{-1}$ when doped to 45% AsF_5. Further doping resulted in a decrease to $10^{-7}\Omega^{-1}cm^{-1}$ (60% AsF_5). **PDICB** has been found by others to give a conductivity of 6 X 10^{-3} with AsF_5 doping (51%).[34] These differences in conductivity are most likely a result of the high reactivity of AsF_5 which may lead to varied results depending on the conditions employed.

Other dopants that were investigated were Br_2 and $NOPF_6$.[2] These dopants did not produce materials with conductivities in the range that could be measured with the equipment at hand ($\approx 10^{-9}\Omega^{-1}cm^{-1}$). However, both materials displayed capacitance currents. Br_2 doping was found to give varied results. Exposure of powders of **PDICB** to Br_2 at low pressure gave blue materials with portions of yellow. However, doping at higher pressures gave materials similar in appearance to those obtained with I_2. Films of **PDICB** treated with solutions of $NOPF_6$ first turned red-orange and then black.

The mechanical properties of the doped materials are poor. Heavily doped films are extremely brittle and crack easily. The **DICB**-norborene block copolymers are found to have far superior properties and were flexible and slightly stretchable even when heavily doped. Materials in which the ratio of **PDICB** to polynorborene is 1.25 and .66 displayed conductivities of 5 X 10^{-4} $\Omega^{-1}cm^{-1}$ and 1 X $10^{-4}\Omega^{-1}cm^{-1}$ respectively when saturated with I_2. Thus, the decrease in conductivity appears to behave like a dilution effect. However, when the ratio of **PDICB** to polynorbornene was .15, the samples were not observed to become conductive with I_2 doping. Hence, at this ratio the amount of **PDICB** is below the percolation level and a continuous path through the sample is not available for conduction.

Characterization of Doped PDICB:

UV-vis absorption spectra of **PDICB** doped with I_2 and AsF_5 are shown in Figure 3.17. These absorption spectra display a distinct loss of intensity in the original "trieneic" absorption at 378, and the evolution of a broad absorbance at 401 nm (3.09 eV) and 484 nm (2.56 eV) for I_2 and AsF_5 respectively. There is also a small tailing of the absorbance into the near IR (i.e., above 820 nm) indicating the presence of low energy electronic transitions (i.e., 820 nm = 1.51 eV). The new absorbances indicate the formation of new bands in the band gap with oxidation. The exact nature of these bands is hard to deduce. The calculations of Pranata and Dougherty investigated the possibility of a relaxation of the torsion of the polymer's backbone with oxidation (Figure 3.14). However, they found the same conformation to be the minimum energy in model cationic compounds as was observed for the undoped polymer. There is the possibility that charge transfer processes may account for some of the oscillator strength in these optical transitions (especially for I_2 doping). If the absorptions were charge transfer bands, illumination would increase the conductivity by increasing

the number of carriers. Conductivity measurements of I_2 doped materials under illumination with a 350 watt Hg arc lamp resulted in an increase only 2 to 3 times that observed in normal room light. The relatively small observed effect with illumination indicates that these processes are not particularly important and most likely not responsible for the 401 nm absorption peak observed with I_2 doping. The observed absorbance spectra of the I_2 doped materials may also have contributions from I_3^-, I_5^-, and I_2, which have absorbances at 360 nm, 450 nm and 500 nm respectively.[35] However, the observed spectra (Figure 3.17b) do not show maxima at any of these wavelengths, indicating that these species are not major contributors to the absorption spectra.

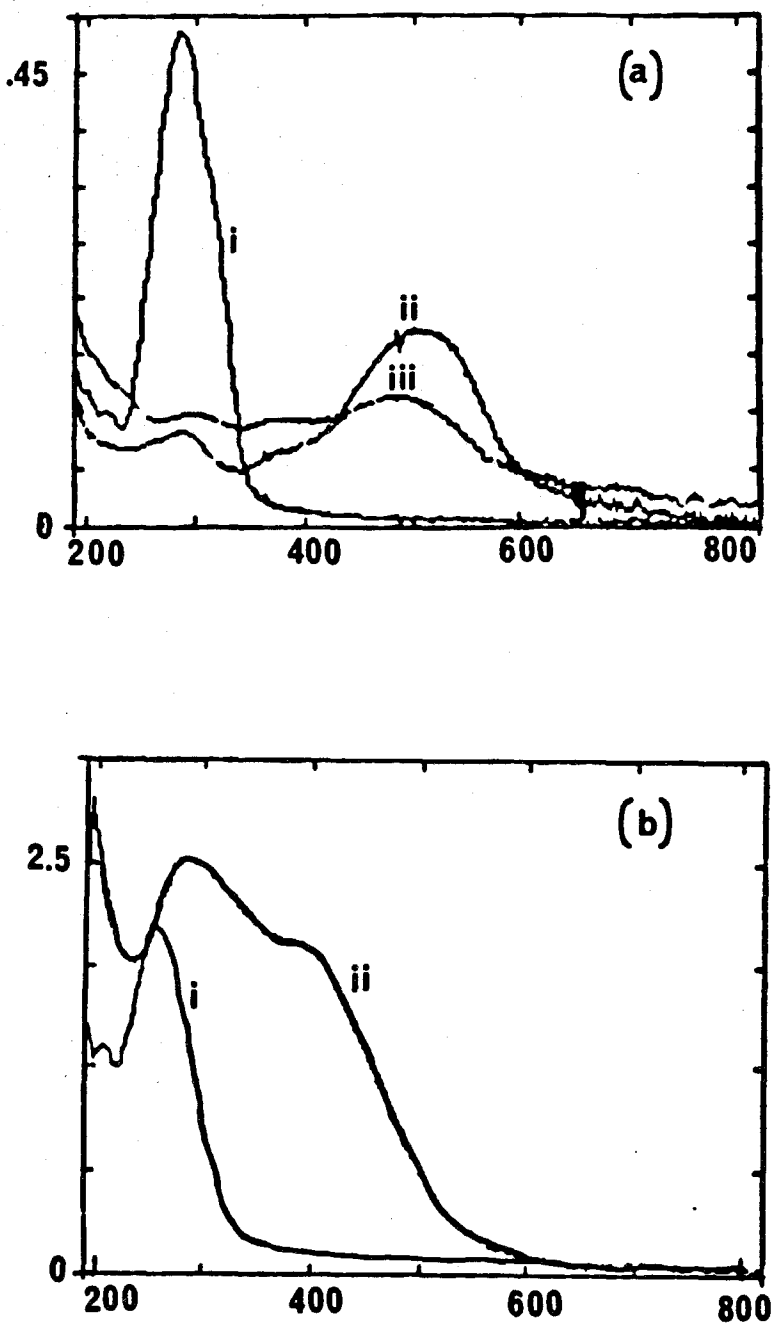

Figure 3.17. (a) UV-vis spectra of **PDICB** doped with AsF_5: (i) undoped polymer; (ii) 5 minute exposure to 30 mm AsF_5; (iii) 16 hour exposure to 30 mm AsF_5. (b) UV-vis spectra of **PDICB** doped with I_2: (i) undoped polymer; (ii) polymer saturated with I_2.

Infrared Characterization of Doped PDICB:

The infrared spectra of **PDICB** and materials that are obtained with I_2 and AsF_5 doping are shown in Figure 3.18. These spectra show a greatly increased absorbance in the region of 1400 cm^{-1}. Polyacetylene also shows a pronounced increase in this region with doping.[36] This strong band is thought to arise form C=C stretching modes which are shifted to lower energy as a result of doping weakening the double bonding.[36] The high intensity of this band can be thought to arise from the induction of a larger dipolar character in the olefins caused by having charge in the π system. The surface of the KBr plates used in this experiment showed small amounts of a white material. The bands at 1040 cm^{-1} and 700 cm^{-1} (Figure 3.18c) were also observed by treating the blank KBr plates with AsF_5.

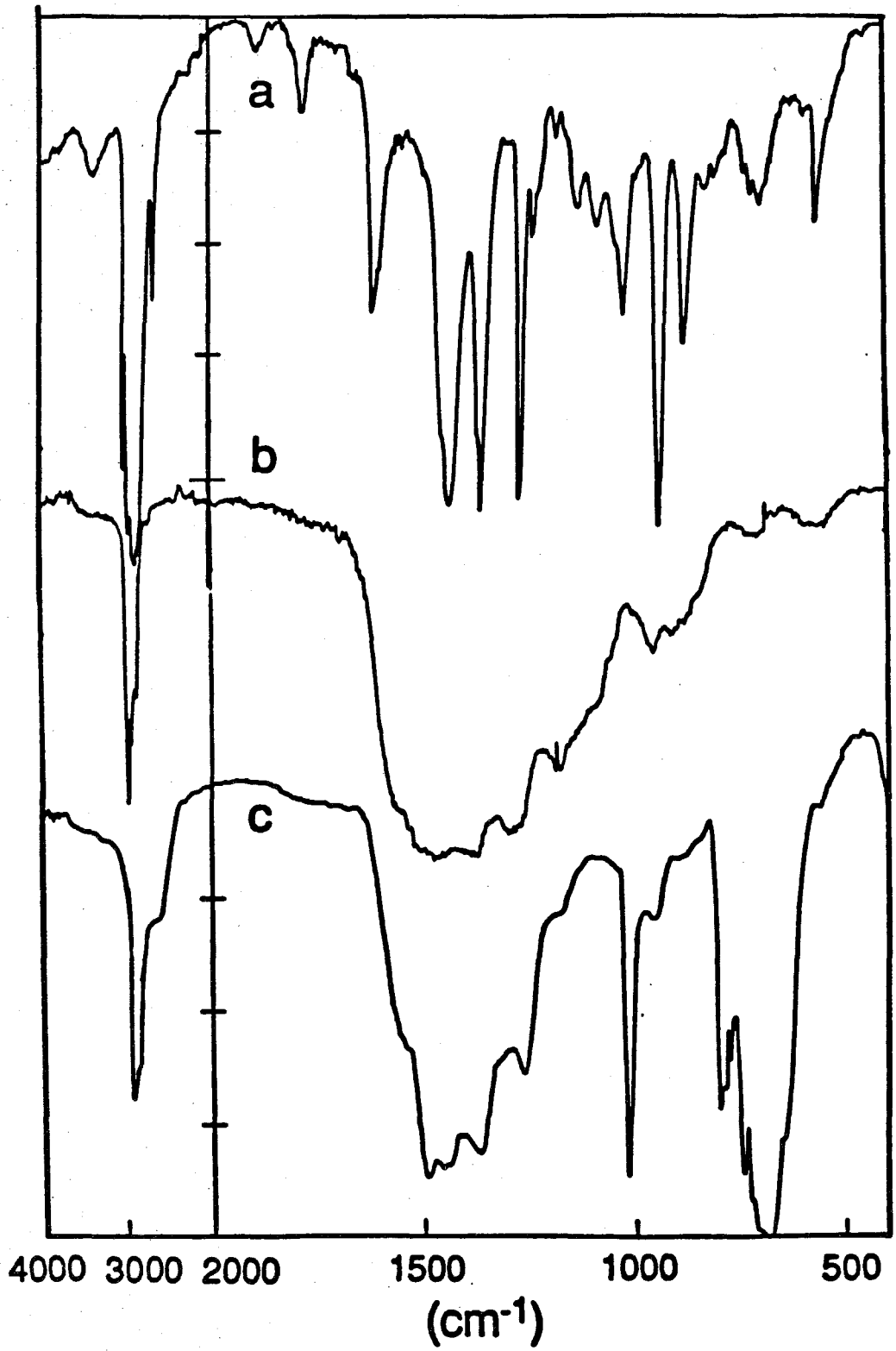

Figure 3.18. Infrared spectra of **PDICB** : undoped(a); saturated with I_2 (b); treated with AsF_5 for 1 hour, 400 torr (c).

Electron Spin Resonance Studies of PDICB:

As formed **PDICB** exhibits an ESR signal with a Gaussian lineshape with a peak to peak line width (H_{pp}) of 18 Gauss and g = 2.0027. This signal is characteristic of a stationary isolated electron which is inhomogeneously broadened by it's surroundings.[37] The existence of free spins in polymers has been used as an indication of the potential of materials as conductors. Double integration of the ESR signal of **PDICB** indicates that it contains $\approx 10^{-5}$ spins per monomer unit or 10^{18} per mole monomer. This spin concentration is slightly higher than the average values observed for substituted polyacetylenes.[38] With light I_2 doping ($\leq$13%), the spin concentration seems to be nearly independent of the dopant concentration, and the signal is the same as that of the undoped polymer. When heavily doped with iodine, the polymer exhibits an increase in paramagnetism and a narrowed isotropic ESR signal with H_{pp} = 8 Gauss and g = 2.0028 is observed. **PDICB** heavily doped with I_2 (56%) displays 2.5 X 10^{-3} spins per monomer. Figure 3.19 shows the ESR signals of the undoped and heavily doped (I_2) **PDICB** and the integrated lineshapes. The ESR signal of the material saturated with I_2 exhibits a narrowed Lorentzian line shape as shown in Figure 3.20.

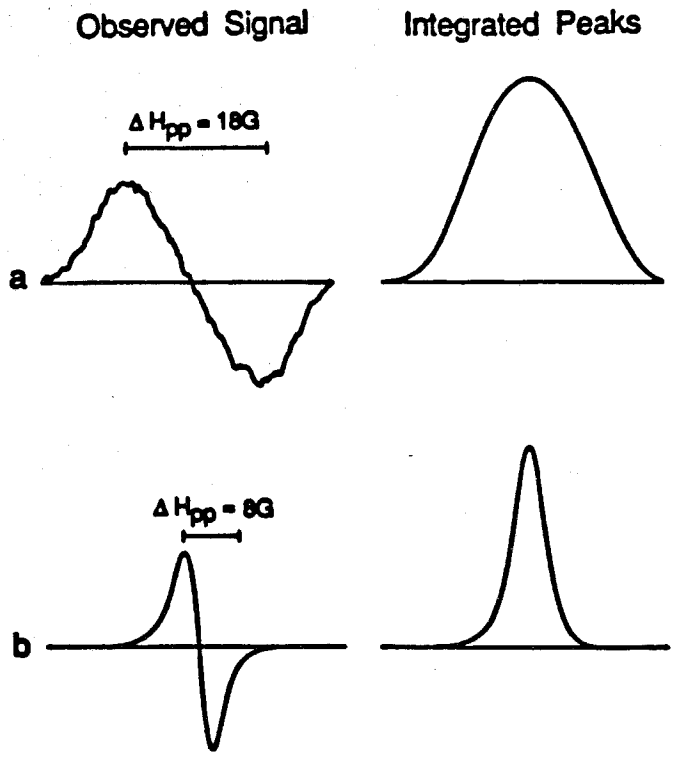

Figure 3.19. ESR signals for undoped **PDICB** (a) and **PDICB** heavily doped with Iodine (b).

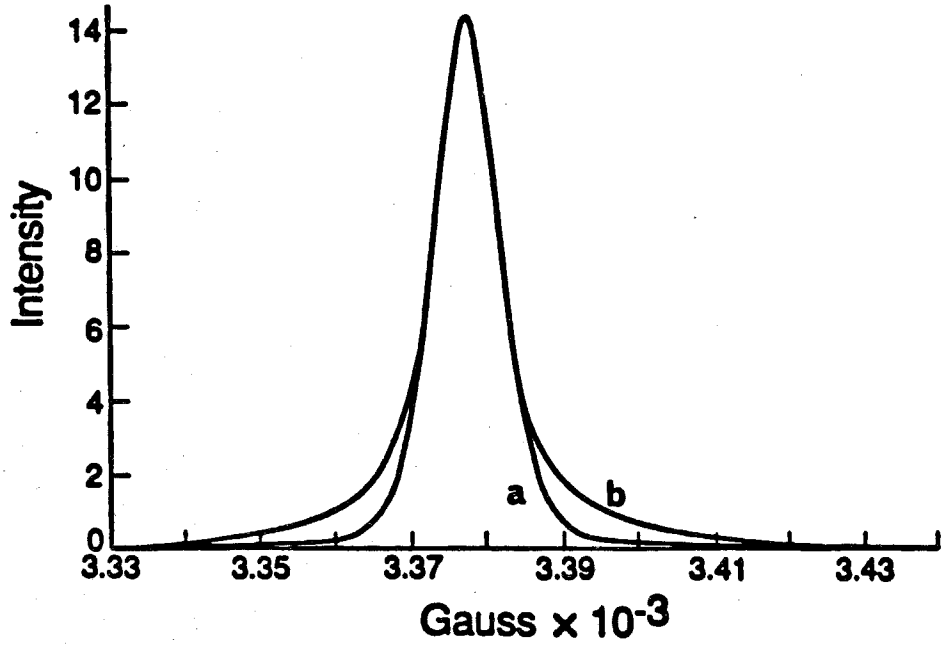

Figure 3.20. Comparison of the ESR lineshape of **PDICB** doped with I_2 (56%) (a) and a Lorentzian lineshape (b).

The narrowed lineshape of the ESR signal is an indication of exchange and/or motional processes.[37,39] Low temperature studies at 4 K showed the signal to broaden to 11 Gauss, indicating that there is an activation energy associated with this process.[40] Saturation studies of the ESR signals of **PDICB** doped to 29% and 55% I_2 are shown in Figure 3.21. These saturation curves demonstrate that the relaxation times of heavily doped **PDICB** (55%) are shorter than those of less heavily doped samples (29%).[41,42] In addition the data in Figure 3.21 indicate that at low temperatures the relaxation times become longer.[41] These results are again consistent with the motional and/or exchange narrowing of the ESR signal. The fact that the relaxation behavior is dependent on dopant concentration was not obvious from the line shape analysis, since the 29% I_2 and the 55% I_2 doped samples exhibit the same lineshapes.

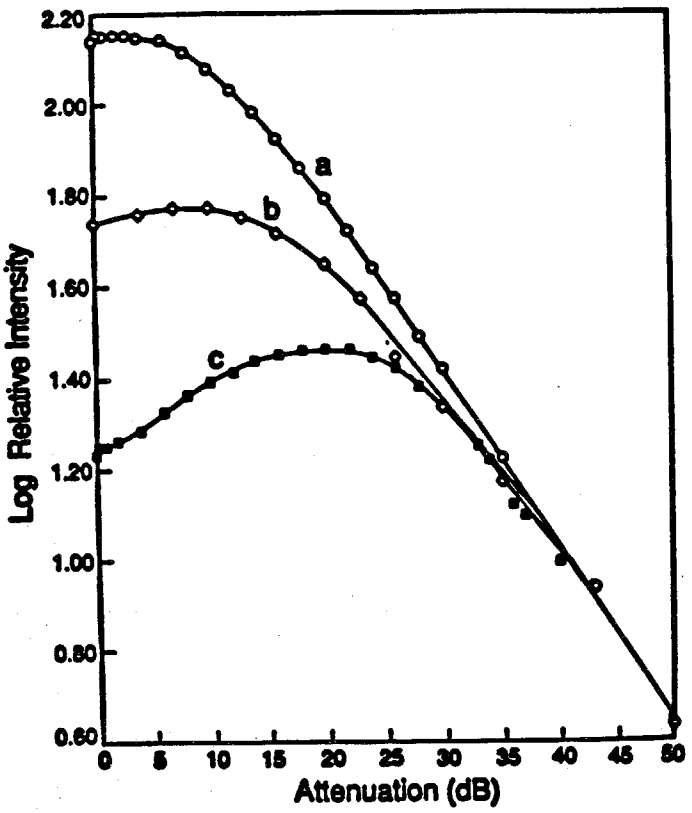

Figure 3.21. ESR saturation curves for **PDICB** : 55% I_2 at RT (a); and 29% I_2 at RT (b); 55% I_2 at 4 K (c).

Materials doped with AsF_5 were also studied with ESR spectroscopy. At an intermediate level of AsF_5 doping (15%), an asymmetric ESR signal is observed as shown in Figure 3.22. This signal is the superposition of a narrow and a broad signal. At high microwave power, the broad signal is saturated and the observed signal collapses to an isotropic signal (H_{pp}= 10.5 Gauss). The same narrow signal is also observed at higher AsF_5 doping levels (H_{pp}= 10.5 Gauss g = 2.0034). It has been shown by others that subtraction of the narrow signal from the composite signal shown in Figure 3.22 results in a seven line signal with a hyperfine coupling constant of 8.5 Gauss.[34] The signal attained at high doping levels has a Lorentzian lineshape which is again consistent with exchange and/or motional processes narrowing the signal. **PDICB** heavily doped with AsF_5 (55 to 62%) displays a spin concentration of $\approx 10^{-2}$ per monomer unit, which is about a factor of ten bigger than that obtained for I_2 doping.

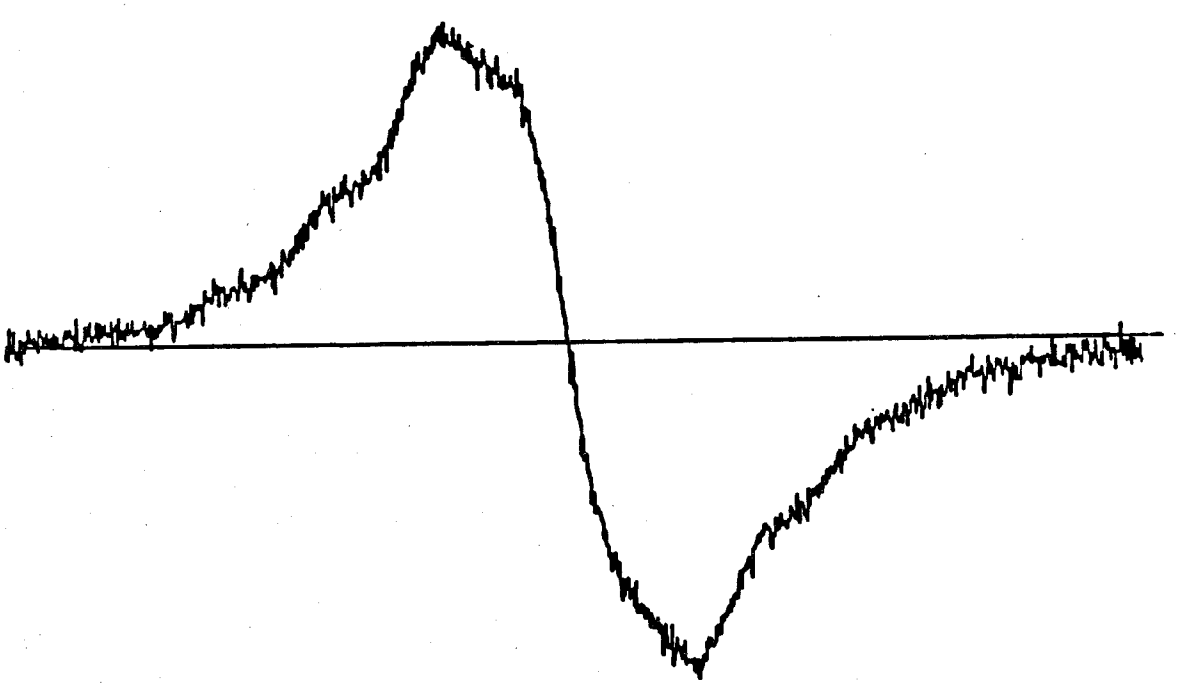

Figure 3.22. ESR signal of **PDICB** doped with 15% AsF_5.

Br_2 doping also produced a lineshape similar to that obtained with AsF_5. In this case, H_{pp} = 7 Gauss, which was slightly lower than that attained for iodine doping. A comparison of the lineshapes for **PDICB** doped with I_2, AsF_5, and Br_2 is shown below in Figure 3.23.

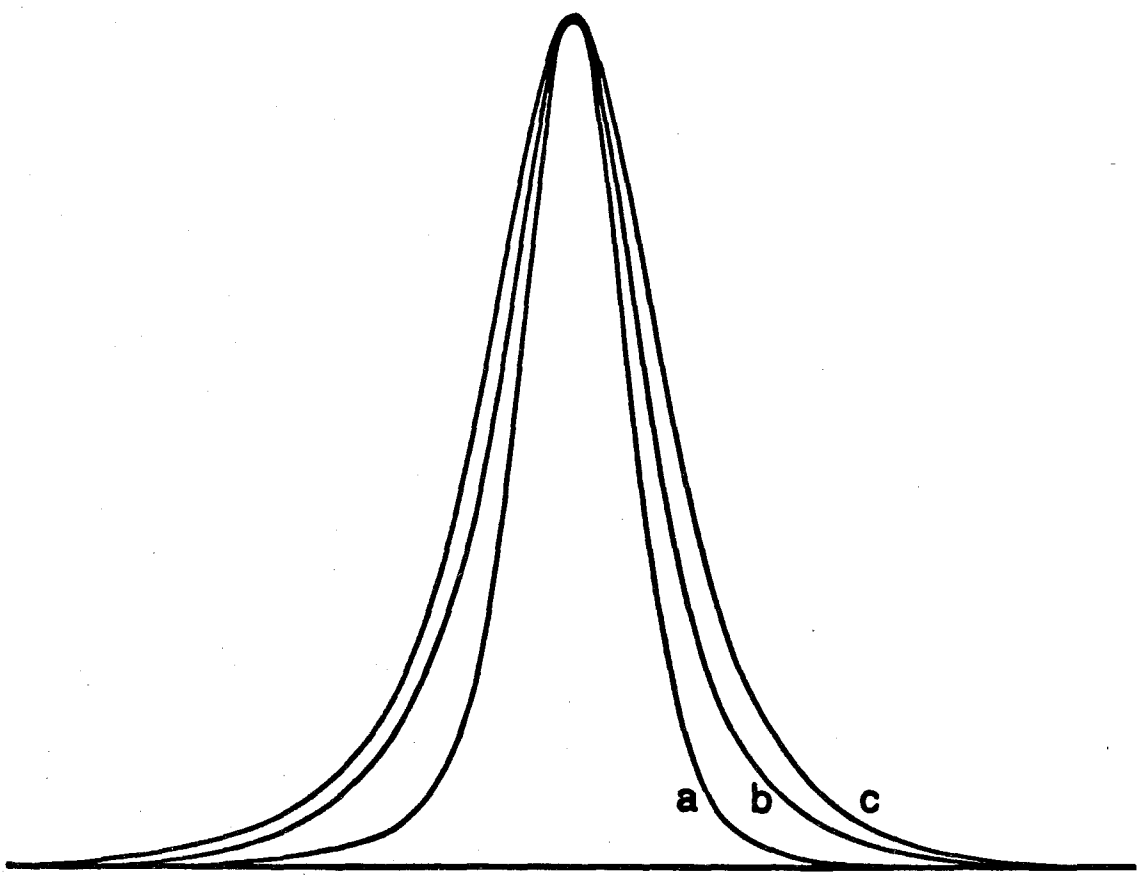

Figure 3.23. Integrated ESR signals for **PDICB** doped with I_2 56% (a); Br_2 60% (b); AsF_5 55% (c).

Magnetic Susceptibility of Doped PDICB:

The temperature dependence of the magnetic susceptibility is important with respect to the nature of the electronic states at the Fermi level. As discussed in Chapter 1, classical metals exhibit Pauli paramagnetism which is characterized by its temperature independent nature.[43,44] The temperature dependence of the total gram magnetic susceptibility (emu/g) of **PDICB** doped with AsF_5 and I_2 is shown in Figure 3.24. The total susceptibility (χ_T) is a composite of a diamagnetic core (χ_D), Pauli (χ_P), and Curie (χ_C) components.[43] χ_D is negative and χ_P and χ_C are positive. χ_C has a 1/T dependence, and is usually expressed in terms of a Curie constant (C).

$$\chi_T = \chi_D + \chi_P + \chi_C$$

The diamagnetic correction of the dopant ions is relatively large. A correction for iodine of -43 X 10^{-6} (emu/mole I) was used,[43e] and for AsF_5 a correction of - 88.5 X 10^{-6} (emu/mol AsF_5) was employed.[43f] The diamagnetic correction for the polymer core electrons is much smaller and was not applied. By applying a diamagnetic correction for the dopants the total spin susceptibility (χ_S) is obtained and is plotted for samples in Figure 3.25. χ_S is the combination of the $\chi_C + \chi_P$.

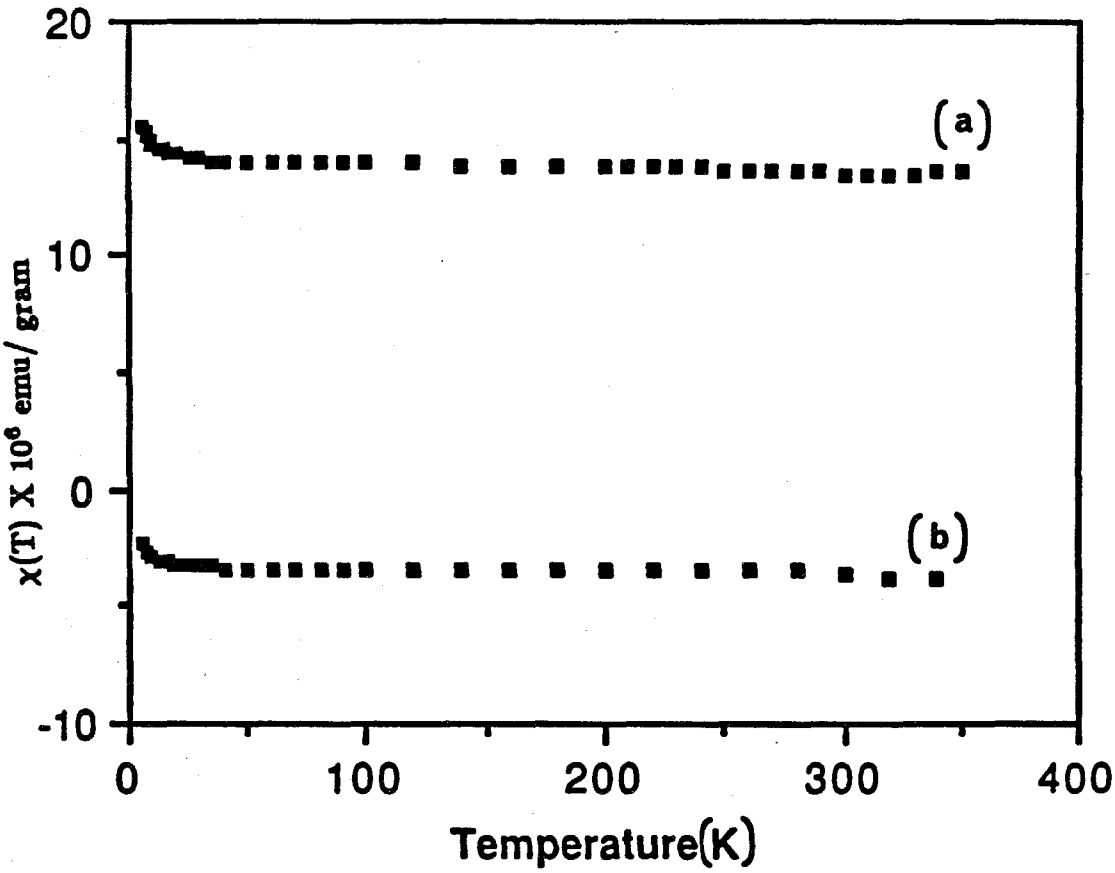

Figure 3.24. Temperature dependence of the total gram magnetic susceptibility (χ_T) of PDICB doped with 66% AsF_5 (a) and 64% I_2 (b).

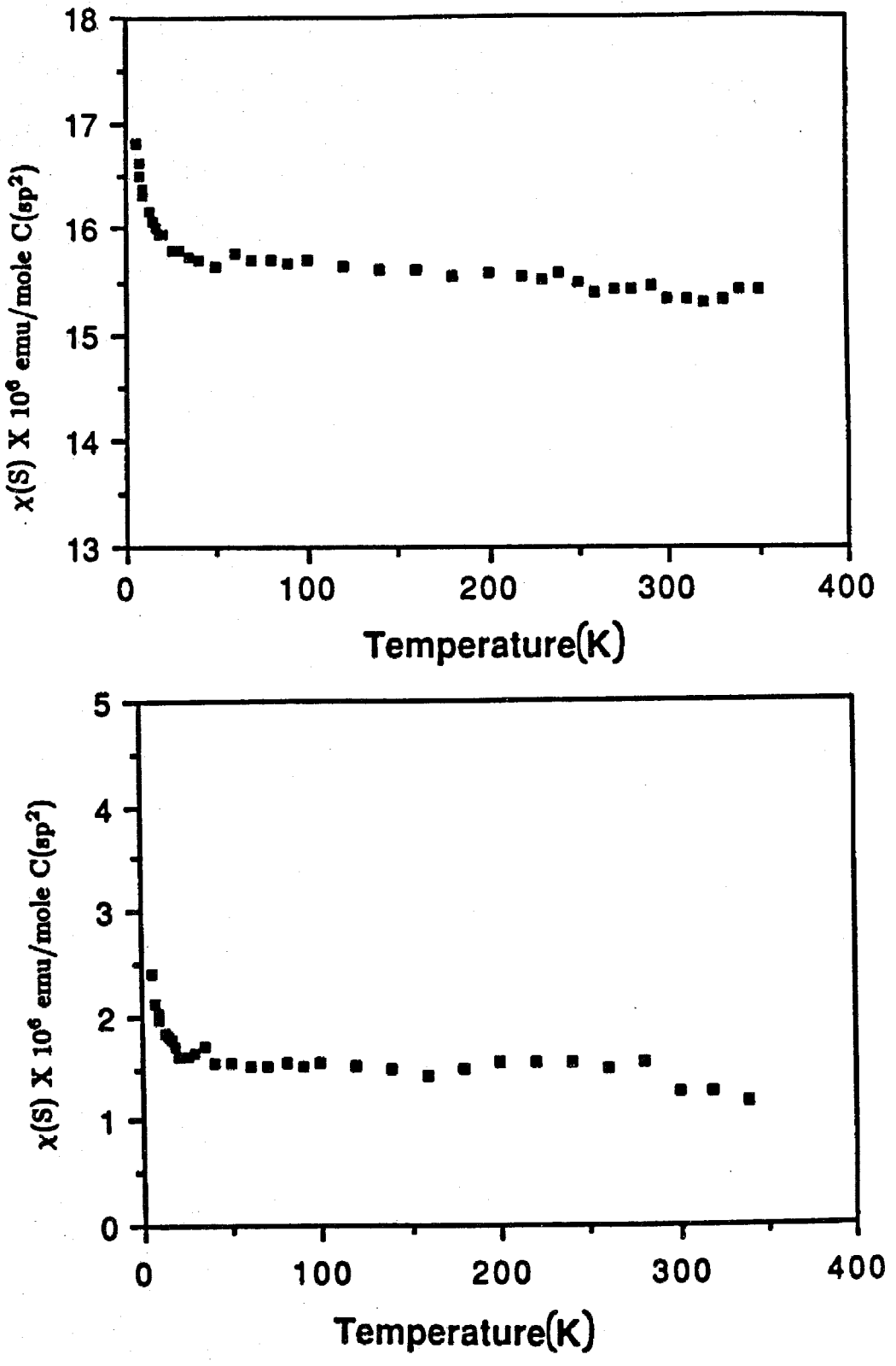

Figure 3.25. Temperature dependence of the spin only magnetic susceptibility (χ_S) of PDICB doped with 66% AsF_5 (a) and 64% I_2 (b).

At low temperature both the I_2 doped and AsF_5 doped materials exhibit χ_C with its characteristic 1/T(K) dependence. The magnitude of χ_C is determined by plotting χ_S against 1/T(K) as shown in Figure 3.26. The χ_C is less for the I_2 doped material than for the AsF_5 doped material. With this plot one can calculate the χ_C at 298 K and obtain χ_P at that temperature. With χ_P the density of states at the Fermi level is calculated, and these results and others from the literature are shown in Table 3.1.

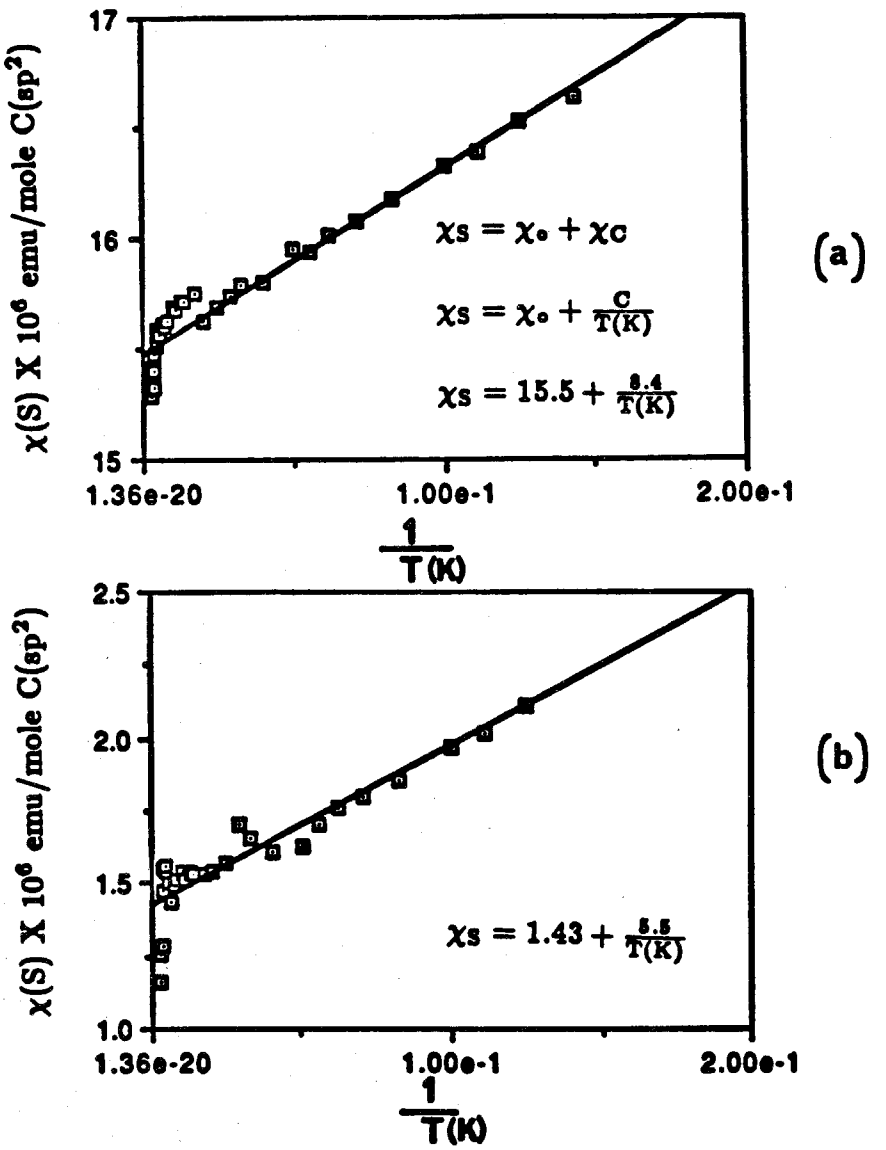

Figure 3.26. Determination of the Curie constant (C) for the calculation of χ_C: **PDICB** doped with 66% AsF_5 (a); and 64% I_2 (b).

Table 3.1. Comparison of density of states at the Fermi level of PDICB with other conductive polymers.

MATERIAL	$N(S)_F$	REFERENCE
$PDICB(AsF_5)_{1.5}$	.45 States/eV mole $C(sp^2)$	This Work
$PDICB(I)_{1.9}$	.044 States/eV mole $C(sp^2)$	This Work
$PA(I)_{.26}$	.10 States/eV mole C	43e
$PA(AsF_5)_{.1}$	.23 States/eV C	43d
$PT(AsF_5)_{.24}$	.23 States/eV C	43b
$PAN(HCl)_1$	.23 States/eV C+N	43a
†$PPP(SbF_5)_{0-.77}$	$\leq$ .01 States/eV C	43g

PA= polyacetylene; **PT**= polythiophene; **PAN**= polyaniline; **PPP**= poly-paraphenylene

†The absence of Pauli paramagnetism in PPP indicates that the conducting state is comprised of bipolarons.

Solid State ^{13}C NMR of Doped PDICB:

Once doped, **PDICB** becomes insoluble in all solvents and hence must be studied in the solid state. ^{13}C NMR yields valuable structural information about the nature of the structure of the materials that are formed. Hence, doped **PDICB** was studied with solid state cross polarization magic angle spinning (CPMAS) ^{13}C NMR.[14] **PDICB** exhibits a solid state spectra that is very similar to the solution spectra with two inequivalent methyl groups at 19 and 22 ppm and three olefinic carbon signals at 125, 129, and 135 ppm. Dipolar dephasing experiments indicated that the 125 ppm peak is the proton bearing olefinic carbon. In addition, dipolar dephasing indicates that the relaxation of the methyl groups is modulated indicating that they are capable of rotation.[15] Samples were prepared at a variety of I_2 concentrations and the spectra of these samples are shown in Figure 3.27. At low (13%) and intermediate (35%) doping levels two distinct new peaks at 146 and 156 ppm are observed. At high doping levels the spectrum becomes broad as a result of the presence of paramagnetic species in the material. The olefinic region undergoes a shift downfield as a result of the deshielding which results by the removal of electron density from the polymer's π system. The methyls are also shifted but to a lesser degree. Downfield shifts in carbocation species are well known and have been used as a means to characterize the degree of delocalization of the carbocations.[44] It can be seen that even at the highest doping levels, the spectral density extends to only 230 ppm. Figure 3.28 gives some representive shifts of carbocations with a variety of degrees of delocalization.[16] Thus, it can be concluded that I_2 doping results in the formation of fairly delocalized carbocations in **PDICB** .

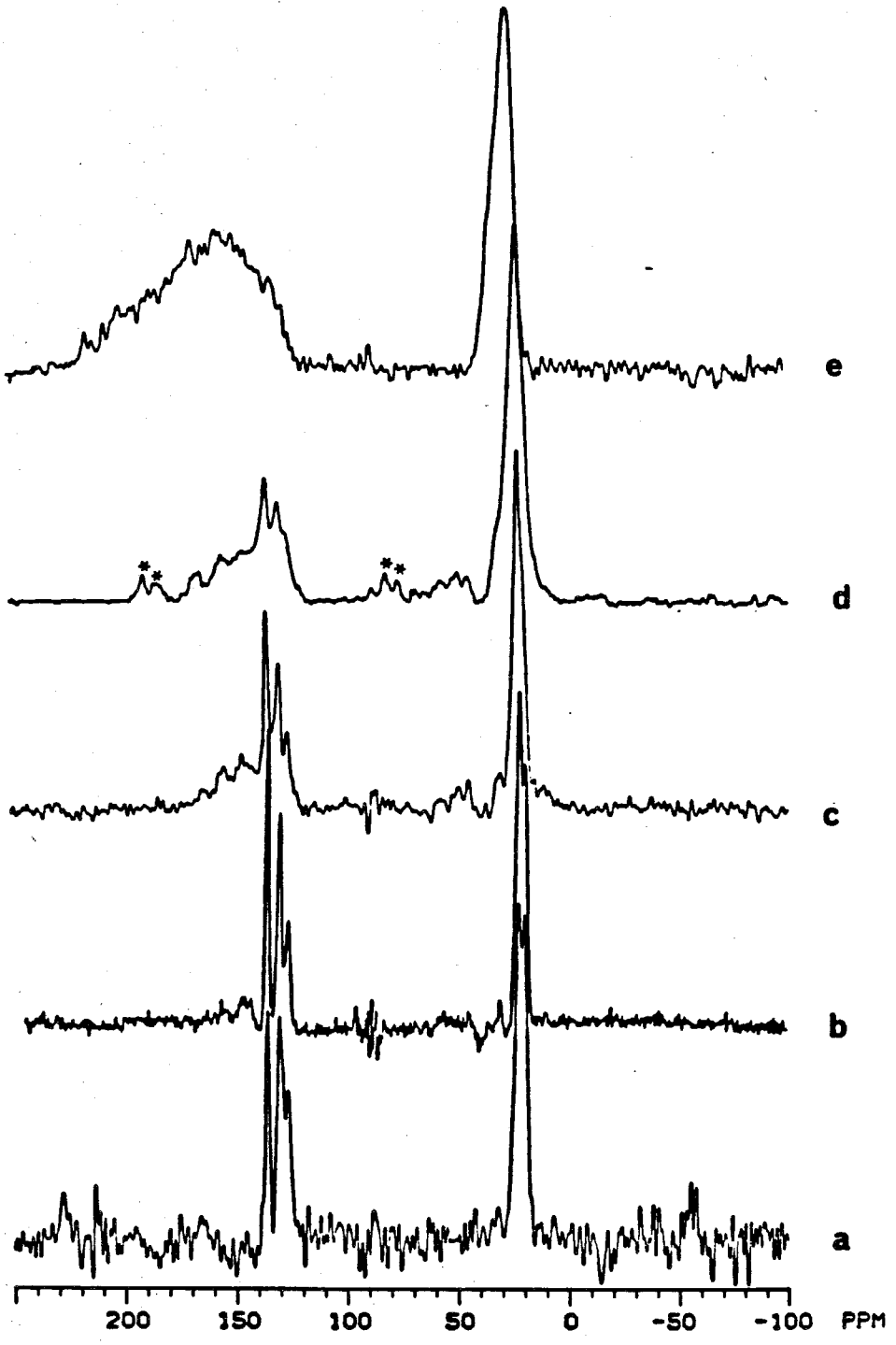

Figure 3.27. Solid state CPMAS ^{13}C NMR spectra of **PDICB** doped with I_2. Percentages of I_2 by weight: (a) 0%; (b) 13%; (c) 35%; (d) 45%; (e) 60%. (*)'s indicate spinning side bands.

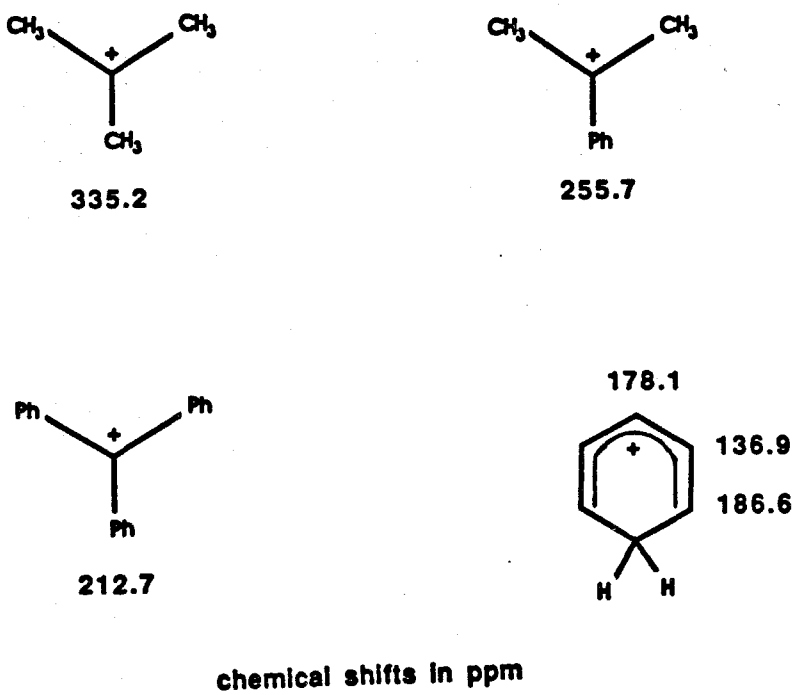

Figure 3.28. Some representative ^{13}C chemical shifts of carbocations.

Materials doped with Br_2 and AsF_5 were also investigated by CPMAS ^{13}C NMR. Representative spectra are shown in Figure 3.29. Again these materials displayed signals in the regions downfield of the olefinic region indicating the presence of delocalized carbocations. For heavily doped AsF_5 samples (Figure 3.29a), these signals extend further downfield than was observed for the I_2 doped materials. This indicates a more localized carbocation character where the deshielding is concentrated on fewer carbon centers. Another difference in the spectra of Figure 3.29 from those in Figure 3.27 is the presence of new signals at 55 and 50 ppm. In some of the spectra of Figure 3.27 there was a hint of a signal in this region but not as pronounced as is observed in Figure 3.29. These peaks are suggestive of chemical addition reactions to the polymer. For Br_2 this may involve the formation of an alkyl-bromide group such as is shown in Scheme 3.6. For a species

such as 15, the methyl groups next to the bromide group would be expected to have resonances in the region of 45 to 55 ppm.[16,13] The carbon directly bound to the bromine would have a very broad signal as a result of bromine's quadrupolar magnetic moment. Hence, carbons substituted with bromines are usually not observed in solid state ^{13}C NMR.[44] The peaks at 55 and 50 ppm region may also be the result of crosslinking or other chemical processes. The exact nature of this resonance can notbe assigned with the available data.

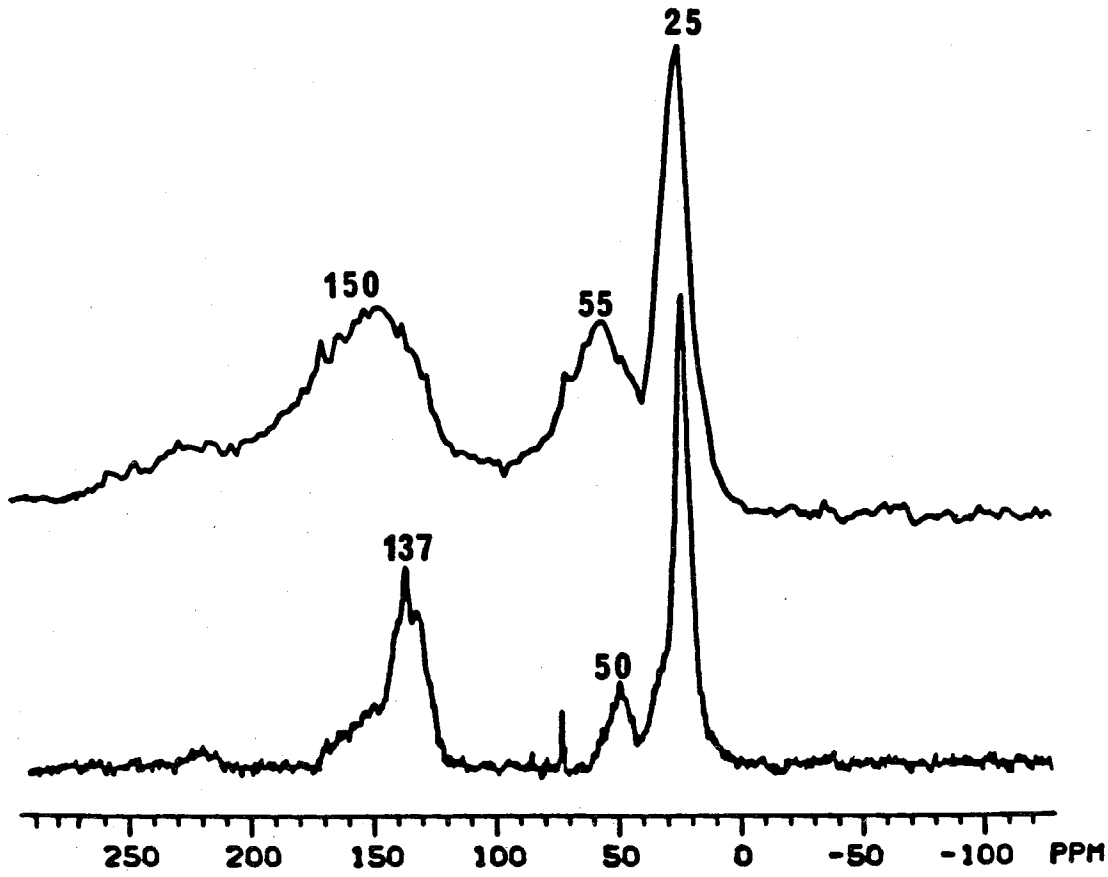

Figure 3.29. CPMAS ^{13}C NMR of **PDICB** doped with AsF_5 42% (a); and Br_2 60% (b).

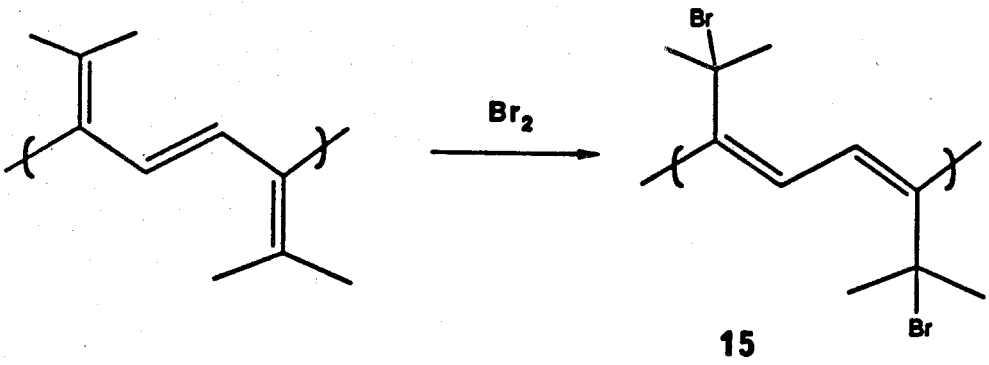

15

Scheme 3.6

Compensation of Doped PDICB:

The degree of chemical modification with doping is of interest in determining the structure of the conductive state of **PDICB**. This aspect can be addressed by compensation of the polymer with a reducing agent back to its neutral state. I_2 doping appears to give the least evidence for chemical modification of the polymer with doping. Thus, compensation of materials saturated with iodine was attempted with sodium naphthalinide. After treatment of the doped polymer with sodium naphthalinide, the polymer was rinsed with THF to give a tan material. Compensated films had a UV-vis maximum at 290 nm which was approximately the same as **PDICB** before doping (Figure 3.12). These spectra were broadened and exhibited tailing to longer wavelengths. CPMAS ^{13}C NMR spectra of the compensated materials were somewhat broadened and the olefinic carbon signals exhibited intensity from 130 to 170 ppm as shown in Figure 3.30. The broadened nature of these spectra indicates that some chemical modification has taken place, which is not surprising considering the conditions that the polymer has been subjected to. However, the gross structure of the polymer is preserved as evidenced by the fact that the compensated materials exhibit similar UV-vis and ^{13}C NMR spectra with some broadening (Figure 3.30).

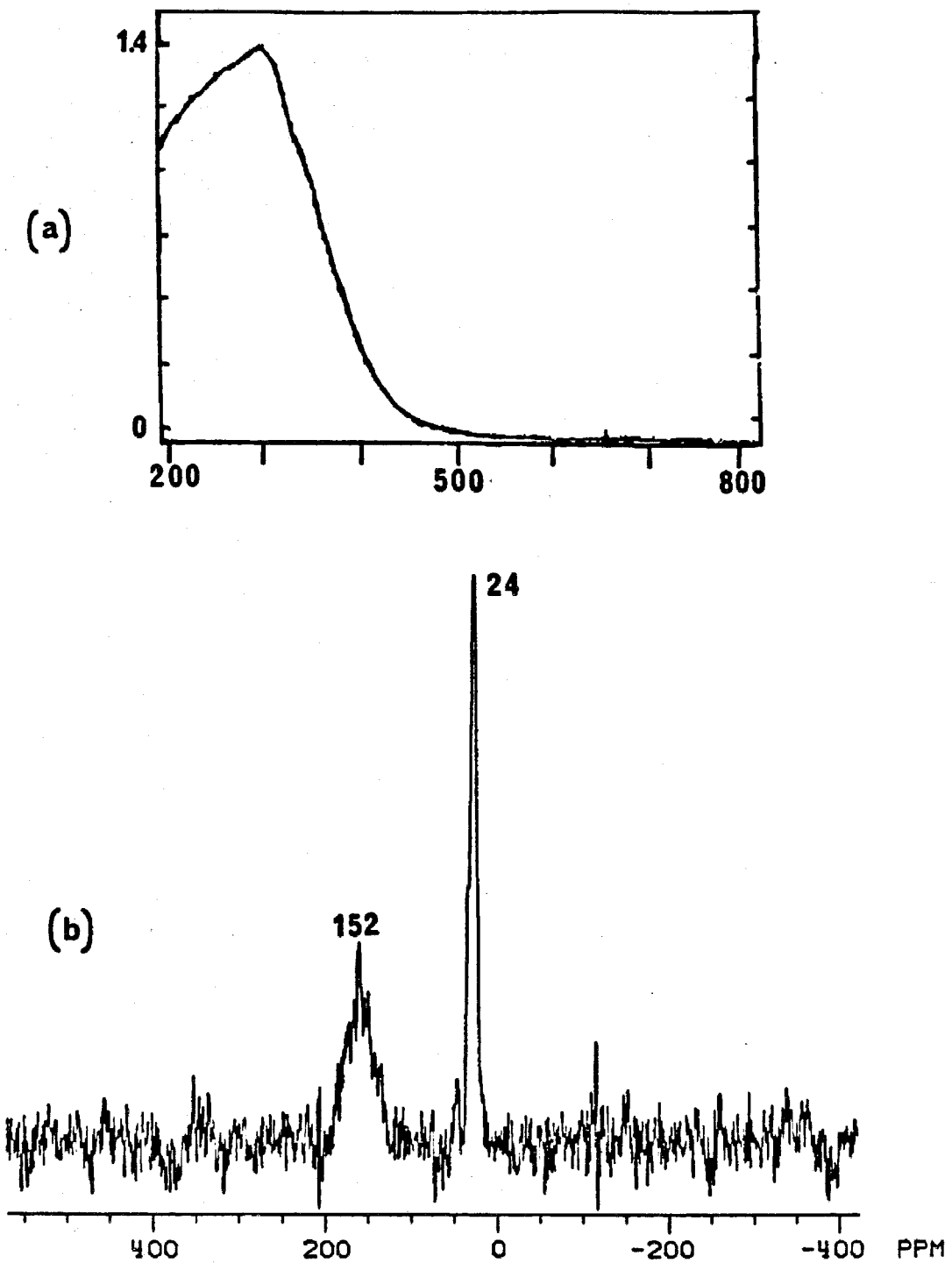

Figure 3.30. UV-Vis spectra (a) and CPMAS ^{13}C NMR (b) of PDICB which had been doped to 60% I_2 and then compensated with sodium naphthalinide.

CONCLUSIONS:

DICB can be **ROMP**ed to give **PDICB** with a variety of molecular weights. The properties of this material may be modified by synthesizing block copolymers with elastomers. **PDICB** is a sensitive material that is prone to crosslinking and is unstable towards ambient atmosphere. The conformation of **PDICB** is unique and forms segregated triene units which are orthogonal. Despite this localization, **PDICB** supports delocalized carbocation carriers and modest conductivities of $10^{-6}\ \Omega^{-1}cm^{-1}$ to $10^{-3}\ \Omega^{-1}cm^{-1}$. I_2 doping appears to result in the introduction of charge into the polymer backbone without major chemical modification. Doping with Br_2 and AsF_5 results in more chemical degradation of the polymer backbone. **PDICB** is fundamentally a different conductive polymer than others due to the fact that facile intrachain conduction is not possible as a result of the abrupt twisting of the polymer backbone. **PDICB** is not a metal by any stretch of the imagination. However, **PDICB** exhibits a temperature independent contribution to the magnetic susceptibility. Thus, this result casts doubt on the validity of the observation of Pauli susceptibility as an indication of a metallic state in a conductive polymer.

FUTURE OUTLOOK OF THE POLYMERIZATION OF DERIVATIVES OF DIMETHYLENECYCLOBUTENE

Tetraphenyl-dimethylenecyclobutene (**TPDMCB**) is a known compound[46] that is readily available by the synthetic route shown below in Figure 3.31. **16** is made by the literature method[47] in modest yields and is isolated by recrystallization from acetone. The zinc reduction of **16** proceeds to **TPDMCB** in a nearly quantitative yield and is easily purified by recrystallization. **TPDMCB** is a snow white low density solid which is slightly soluble in benzene or toluene. Catalysts **6**, **7**, **4**, **5** and **3** were unreactive toward **TPDMCB**; **6** and **7** did not react at temperatures as high as 75°C . Other catalysts such as $OsCl_3$, $RuCl_3$, $IrCl_3$, $ReCl_5$, (2,6-disopropylphenoxy)$_3$Ta=CH(t-butyl), WCl_6:Sn(Me)$_4$, and $WOCl_4$:$EtAlCl_2$ were investigated but none were successful at producing significant amounts of polymer. However, some low molecular weight yellow material was obtained for some of the catalysts which was soluble in acetone. The reason for the unreactivity of this monomer is not certain, but it is most likely the result of the steric bulk presented by the phenyl groups.

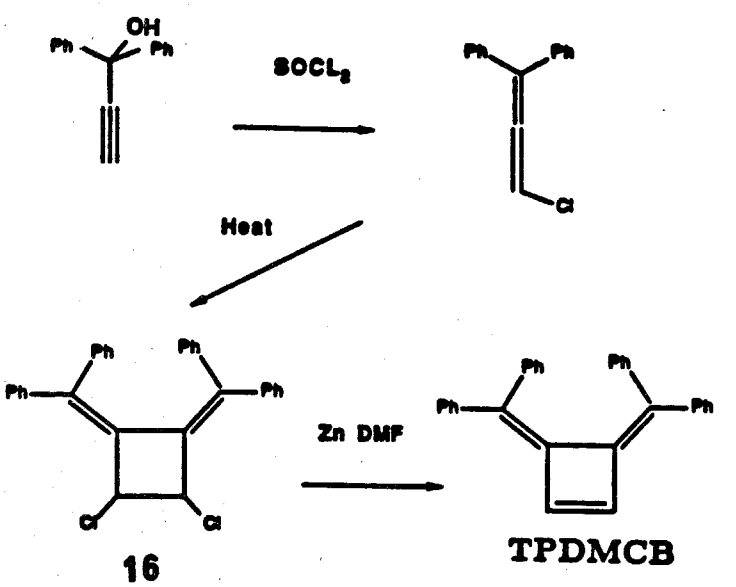

Figure 3.31. Synthesis of **TPDMCB**.

Other monomers that are worth pursuing are shown below in Figure 3.32. Monomer **17** may be the best candidate for the realization of the chemistry proposed in Scheme 3.1. Monomers **18** and **19** would be very interesting systems to study from the standpoint of generating functionality that will allow for facile intermolecular conduction. The dichloride precursor compound for **18** is known. Hence, the synthesis shown in Figure 3.31 will yield a facile route to this potential monomer.

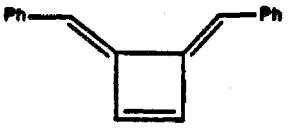

17

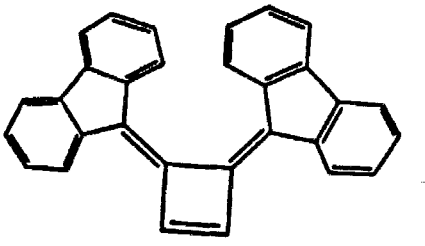

18

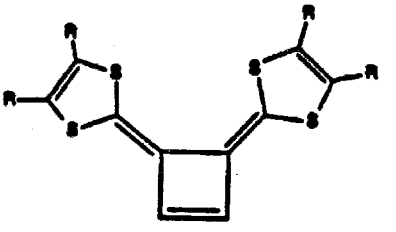

19

Figure 3.32. Potential monomers for the extension of this work. Only **15** is presently a known compound.

Experimental Section:

General Procedures: All manipulations of air- and/or moisture-sensitive compounds were carried out using standard Schlenk or vacuum line techniques. The flush gas (argon) was purified by passage through columns of activated BASF RS-11 (Chemalog^{TM}) oxygen scavenger and Linde 4 Å molecular sieves. Manipulation of solids and film casting was performed in a Vacuum Atmospheres glove box equipped with a MO-40-1 purification train. The purification train was charged with activated Ridox^{TM} oxygen scavenger and Linde 11 Å molecular sieves. When dealing with moisture sensitive materials, all glassware was rinsed with base, dried in a 140°C oven, and subjected to vacuum while hot.

^{1}H and ^{13}C NMR were recorded on a Joel FX-90Q spectrometer (89.6 MHz ^{1}H, 23.53 MHz ^{13}C). Chemical shifts were referenced to the solvent (^{13}C NMR) and to residual protons in the solvent (^{1}H NMR). Infrared spectra were acquired on a Shimadzu IR-435 spectrometer. Infrared samples were ground and pressed into KBr pellets, cast films on KBr windows, or free standing films. Infrared studies with doping were performed by casting films on the windows of a gas cell and exposing the film to the dopant vapor under vacuum. UV-vis spectra were taken with a HP-8451A diode array spectrometer.

ESR spectra were taken on a Varian E-line Century Series EPR spectrometer with a Varian E-102 microwave bridge. Low temperature measurements were obtained with an Oxford Instruments kryostat and a 3120 temperature controller. Single and double integrals were obtained by using a home-built data station which was interfaced with the spectrometer. The integrations and reported g values were referenced to a 2,2-diphenyl-1-picrylhydrazyl hydrate standard sample. Magnetic susceptibility measurements were performed on a commercial SHE SQUID susceptometer at the Southwestern Regional Facility at the University of Southern

California. Sample holder calibration was performed and its susceptibility was subtracted.

X-ray diffraction measurements were made under vacuum with a home-built Guinier camera using monochromatic Cu Kα radiation. The conductivity measurements were made with a home-built probe similar to that described in reference 33 and appendix B, or with a commercial Sigmatone probe sheet resistivity probe. In the four point conductivity measurements,[48] current was supplied by a Power Designs 605 precision power source (.1-6 V), current was measured with a Keithley 160B digital multimeter (.1 to 10^{-10} amps.), and the voltage was measured with a Fluke 895A differential voltmeter.

Gel permeation chromatographic (GPC) analyses were performed utilizing Shodex KF-803, 804, 805, and 805.4 columns with toluene as a solvent. The polymer was detected with a Spectroflow 757 variable wavelength absorbance detector and a Knauer differential refractometer. Samples were prepared with .2% by weight polymer in toluene. Injection volumes of .10 ml were used with a flow rate of 1.5 ml/min. The molecular weights were referenced to narrow dispersity polystyrene samples (Polysciences) ranging from MW= 3550 to 1,300,000. The detection of the polystyrene was only possible with the refractive index detector (because of overlap of the absorbance with the solvent), and the polymers could only be detected with UV at 300 nm (the polymers gave only a weak refractive index change). The GPC traces were corrected for the small difference in the retention volume caused by the different detectors. The molecular weight averages were calculated by the standard procedures.[24]

CPMAS ^{13}C NMR were obtained on a home built spectrometer at a carbon frequency of 35.36 Hz. A commercial Doty Scientific CPMAS probe was used. The samples were ground in Na_2SO_4 in a drybox into a homogenous mixture and packed tightly in a 7 mm o.d. sapphire rotor (Doty Scientific) with Kelef end caps.

Sample sizes were 100-200 mg and the balance was Na_2SO_4. A Doty Scientific CPMAS probe was employed and spinning speeds of 3.5 to 5 KHz were obtained. Data collection was performed with a Nicolet 1280 computer and Nicolet NMC software. Chemical shifts were referenced to an external adamantane standard. The adamantane standard was used for setting the Hartmann-Hahn matching condition and the 90°C ^1H pulse which was typically $\approx 5\mu s$. Cross-polarization contact times were 2 or 3 ms. A "rolling baseline" in some samples was eliminated by leftshifting the free-induction decay by 0-100μs, or by using a baseline fit routine in the software.

Materials: Solvents were dried and deoxygenated. Ether, THF, benzene, toluene, and pentane were dried with sodium benzophenone ketyl. CH_2Cl_2 and chlorobenzene were dried with P_2O_5. **DMCB** was made by the literature route[8] from 1,5-hexadiyne which was dried over activated sieves. **DMCB** was then purified by vacuum transfer from dry oil free NaH. **DICB** was primarily made by the method of Skattebol,[22] with purification by multiple recrystallization at the cyclopropane step. Purification of **DICB** at the final step was accomplished by vacuum transfer of the volatile product of the last step of the reaction. The titanocene metallacyle catalysts were prepared by the literature methods[49]. Catalysts **6** and **7** were made by the published procedure, catalyst **4** was made by the method of Kress and Osborn. A detailed experimental procedure for catalyst **4** is not available in the literature, and a detailed procedure is included in Appendix A. Catalyst **5** was synthesized by the method of Fischer.[50] The methanol or acetone that the polymer is precipitated into was not dried, but was deoxygenated by pulling vacuum on the solution multiple times and then bubbling argon through the solvent for a half an hour or more.

Polymerization of DMCB with $WOCl_4$:$Sn(CH_3)_4$: A Schlenk tube is charged with 44 mg (.128 mmole) of $WOCl_4$ in a drybox. $Sn(CH_3)_4$ (30 mg .167

mmole) is added in 2 ml chlorobenzene and allowed to react for 2 minutes. 6 ml more chlorobenzene is added and **DMCB** 200 mg (2.56 mmole) is added via a gas tight syringe. The reaction was allowed to proceed for 10 minutes and there was visible insoluble polymer in the polymerization mixture. The polymerization was then added to 300 ml MeOH, filtered, and dried. The polymer was isolated as a totally insoluble grey solid that was not swellable in solvent. The infrared is shown in Figure 3.1.

Polymerization of DMCB with $WOCl_4$:$EtAlCl_2$: Two Schlenk tubes were prepared in a glove box. One was loaded with $WOCl_4$ (30 mg .088 mmole), and the other was charged with $EtAlCl_2$ (11 mg .088 mmole). The $EtAlCl_2$ is dissolved in 10 ml of benzene and added to the catalyst. The catalyst is then stirred for 10 minutes at room temperature and the solution becomes progressively darker. **DMCB** .200 gr (2.56 mmole) is then added to the catalyst with a gas tight syringe. The polymerization is allowed to proceed for 10 minutes with the formation of polymer precipitate in the reaction vessel. The reaction mixture is then added to methanol, and the polymer is filtered and dried. The polymer was isolated as a grey intractable powder. The infrared is shown in Figure 3.1.

Polymerization of DMCB with 4 (NMR experiment): A 5 mm NMR tube was loaded with .500 ml of a stock solution of **4** (36 mg .061 mmole) in C_6D_6 in a glove box. The NMR tube was fitted with a septum, and the catalyst's purity was checked by recording its NMR spectra. 47 mg of **DMCB** (.61 mmole) was then added at RT with a gas tight syringe, and the solution was observed to turn from light orange brown to brown. The NMR spectra was recorded immediately and revealed the appearance of a peak at 5.09 ppm and the slow decline of the metalalkylidene signal. The amount of monomer was found to decrease by integration of its signal with respect to residual C_6D_5H in the solvent. A broad peak at 2.7 ppm was observed to appear at 5 minutes. This new peak was very small

with respect to the 5.09 ppm peak. After 70 minutes, these peaks had grown but still were less than 10% the area of the 5.09 ppm signal. The reaction was found to be 75% complete at 70 minutes. After 8 hours, no monomer was observed in the proton NMR spectrum.

Polymerization of DMCB with $(Me_3CCH_2O)_2WCl_2$:$EtAlCl_2$: Free standing films were prepared by the following procedure. $(Me_3CCH_2O)_2WCl_2$ (.113 g .25 mmole) and $EtAlCl_2$ (.063 g .50 mmole) were mixed in 2.5 ml of chlorobenzene. The Schlenk tube (3 cm by 10 cm) walls were coated with the catalyst. The Schlenk was fitted with a side arm with a reservoir of **DMCB** (.975 g 12.5 mmole). The apparatus was then put under static vacuum and the valve to the **DMCB** was opened. The initial reaction gave a purple color on the walls of the Schlenk tube but turned to brown quickly. The reaction was conducted for 1 hr and then MeOH was added. The films were rinsed with methanol and dried to give a clear film that was slightly yellowed. The film thickness was varied and ranged from .007 to less than .001. The infrared spectra is identical to the spectra for $WOCl_4$:$EtAlCl_2$ shown in Figure 3.1. The ^{13}C NMR of this material is shown in Figure 3.2.

Polymerization of DMCB with 4 (preparative): A Schlenk tube was charged with .188 g (.320 mmole) of **4** in 8 ml of toluene, and **DMCB** 2.00 g (25.6 mmole) in 1.5 ml of toluene was then added to the reaction mixture. The solution turned to a darker shade of orange-brown and was stirred at room temperature for 5 hours. At this time, small amounts of insoluble polymer were visible in the polymerization mixture. The reaction mixture was then transferred via cannula into 200 ml of acetone. A tan solid was produced upon precipitation, and the solid became dark red with further washing with acetone and drying. The polymerization gave an isolated yield of 45%. The isolated polymer was not soluble or swellable in solvent. The infrared spectra were very similar to those

in Figure 3.1 with some small variations in intensities. The ^{13}C NMR of this material is shown in Figure 3.3. Elemental analysis calculated: (C_6H_6) C, 92.3; H, 7.7; found: C, 62.0; H, 6.0; Br 9.1 (residual ash 8%).

Polymerization of DMCB with 5: 71 mg of **5** (.16 mmole), .5 g **DMCB** (6.4 mmole) and 32 mg (32 mmole) of phenylacetylene were dissolved in 4 ml of benzene in the drybox. The reaction flask was then subjected to three freeze pump thaw cycles and kept under vacuum. The reaction mixture was then heated at 60°C for 6 days. The reaction was considerably darker at this time and polymer precipitate was observed. The mixture was added to acetone to form a mixture of tan swollen polymer and dark red polymer chunks. The tan material became dark red upon drying. Considerable polymeric film was left on the walls of the reaction vessel which was not isolated. The isolated material gave a yield of 40%. The infrared spectra are again basically the same as those shown in Figure 3.1. Elemental analysis calculated: C, 92.3; H, 7.7; observed: C, 69.5; H, 5.74 (5.3 % ash) C/H = 1.01.

Polymerization of DMCB with 6 (solution): A 5 mm NMR tube was charged with 30 mg (.038 mmole) of **6** and .500 ml of C_6D_6 and fitted with a septum. A ^1H NMR spectrum of the catalyst was taken for reference, and then 60 mg (.76 mmole) of **DMCB** was added with a gas tight syringe. The solution turned from yellow to orange. New signals at 5.06 ppm and the region of 2.2 to 3.7 ppm were observed. The characteristic down field peak of the metal alkylidene was not observed at this time. After the initial consumption of approximately 5 equivalents of **DMCB** the reaction appeared to stop. Integration of the **DMCB** resonances with respect to residual protio solvent indicated no further reaction even when heated to 60°C .

Bulk Polymerization of DMCB with 6 and 7: Bulk polymerization was carried out in a drybox by first evaporating a .25 ml pentane solution of 30 mg

(.038 mmole) of **6** over a 4 cm^2 area of a glass microscope slide. **DMCB** .300 g (3.8 mmole) was then pipeted on to the slide. Immediate reaction takes place, and a homogenous orange-brown solution was formed which is observed to be viscous after one minute. The solution forms polymer film after 3-5 minutes, and after 10 minutes the films were removed from the glass slide with a razor blade. Film thicknesses were approximately .005 cm. The films were flexible and strong but could not be stretched. The films were rinsed with acetone and were yellow in appearance. Yields were variable as a result of the volatility of **DMCB**. Typical yields were 30%, and infrared spectra were similar to those obtained with other catalysts with the added presence of sharp bands at 1220, 1169, and 1078 cm^{-1}. These bands are attributed to catalyst residues in the films. A similar procedure was employed for catalyst 7. However, a yellow precipitated powder was formed rather than a film.

Polymerization of DICB with Titanocene Metallacycles: A variety of conditions were employed which led to polymers with a range of molecular weights. The purity of the monomer was found to vary slightly between preparations, and this factor led to varied results at high monomer to catalyst ratios. Some typical experiments are described below. All the reactions were quenched by slow cannula transfer into methanol. The methanol had been deoxygenated by initially pumping on the solvent while stirring and then bubbling argon through the solution. In most procedures, the reaction mixtures are diluted before precipitation. Dilution is necessary to avoid the formation of fibrous material with precipitation. The catalyst is more efficiently removed from polymer which precipitates in a slower manner. Too much dilution may lead to emulsions. A general procedure is given, as well as more specific procedures for samples of varied molecular weight distributions.

General Procedure: A very general procedure which has been found to produce reliable yields of 70-80% follows. The polymerization is run at room temperature in benzene with .01 M catalyst and .5 M monomer for 40 minutes. The reaction mixture is then diluted by a factor of 2 with benzene, and added to rapidly stirred methanol the volume of which is at least 10 times that of the reaction mixture. The resulting polymer precipitate is then filtered and dried. Further purification of the polymer can be accomplished by redissolving the polymer in $CHCl_3$ and precipitation in methanol. ^1H NMR (C_6D_6): 6.72 (2H br. s.), 1.93 (6H br. s.), 1.77 (6H br. s.) ppm. ^1H NMR ($CDCl_3$): 6.25 (2H br. s.), 1.77 (6H br. s.), 1.50 (6H br. s.) ppm. ^{13}C NMR ($CDCl_3$): 134.7, 129.4, 125.7, 22.2, 19.23 ppm. Infrared 2850 cm^{-1} (s), 1615 cm^{-1} (m), 1436 cm^{-1} (s), 1383 cm^{-1} (s), 1273 cm^{-1} (s), 1240 cm^{-1} (w), 1035 cm^{-1} (m), 941 cm^{-1} (s), 885 cm^{-1}, 705 cm^{-1} (w), 678 cm^{-1} (m).

Preparation of PDICB (MW = 65,000): A Schlenk tube was charged with the isobutylene metallacycle $Cp_2TiCH_2C(Me)_2CH_2$ 19.8 mg (.0798 mmole) in the glove box. This catalyst was dissolved in 6 ml of benzene at RT and stirred for 2 minutes. At this time 1.074 g (8.00 mmole) of **DICB** was added in 2 ml of benzene. The reaction heated up noticeably initially and was allowed to stir for 25 minutes while cooling to RT. At this time, 15 ml of benzene was added to the reaction and the reaction mixture was slowly added to 400 ml of a vigorously stirred methanol solution. **PDICB** precipitates as a white fluffy powder from the methanol solution. The methanol is removed by filtration and the polymer is pumped down at 10^{-6} torr overnight and stored in the glove box at RT. A yield of 83% is obtained, and ^1H NMR and ^{13}C NMR were identical to those given above. A polydispersity index of 2.1 is calculated for this material. Elemental analysis calculated: C, 89.4; H, 10.6; found: C, 89.01; H, 10.43. The reaction with **12** when done under the same conditions yielded a polydispersity index of 2.5 (Figure 3.8a), MW = 45,000, and a yield of 60% .

Preparation of PDICB (MW = 12,700): $Cp_2TiCH_2C(Me)_2CH_2$ (74 mg .30 mmole) is loaded into a Schlenk flask in the glove box. The catalyst is dissolved in 7 ml benzene and allowed to stir for 2 minutes. 1.0 g (7.5 mmole) of **DICB** in 3 ml of benzene is then added to the catalyst solution. The reaction warms up and is allowed to proceed for 15 minutes. The reaction is diluted with 10 ml of benzene and then precipitated in 300 ml of methanol. The polymer is obtained as a white fluffy polymer (.85 g) that is noticeably more soluble than the higher molecular weight polymer from the last procedure. A polydispersity index of 4.7 and an average molecular weight of 12,700 is calculated for this material. Elemental analysis calculated: C, 89.4; H, 10.6; found: C, 88.39; H, 10.10.

Low Temperature Polymerization of DICB with 3: The "Tebbe reagant" ($Cp_2TiCH_2Al(Me)_2Cl$) and a Lewis base constitute a low temperature source of titanocene methylidene. In the ^1H NMR of a mixture of the Tebbe reagent and **DICB** at RT, no reaction occurs. Cooling the sample to -80°C , adding pyridine-d^5, and slowly raising the temperature while monitoring the NMR signals of **DICB** revealed that polymerization occurs between -40 and -30 °C . Thus, for the low temperature polymerization, 42 mg (.15 mmole) of the Tebbe reagent, 23 mg (.19 mmole) of DMAP, and 2.0 g (1.5 mmole) of **DICB** were mixed together at -80°C in 10 ml of toluene. The reaction is first warmed to -30°C rapidly and allowed to warm to -20°C over the course of half an hour. The reaction was stirred at -20°C for half an hour and presented a very viscous mixture. The mixture was then diluted with 10 ml toluene and precipitated in 350 ml of methanol. The isolated yield was 35% and the polydispersity index was 5.37. The average molecular weight is 25,300 for this polymerization (see Figure 3.8a).

Polymerization of DICB with WCl_6:$Sn(CH_3)_4$: A Schlenk tube is charged with 22 mg (.052 mmole) of WCl_6, and 19 mg (.104 mmole) of $Sn(CH_3)_4$ in 5 ml of chlorobenzene and stirred for 4 minutes at RT. The reaction is cooled

to 10°C , and .53 g (3.9 mmole) of **DICB** is added in 5 ml of chlorobenzene. The reaction is allowed to proceed for 15 minutes at 10°C and then terminated by the addition of the reaction mixture to methanol.

Preparation of PDICB:polynorbornene (1:1.5) block copolymers: The norbornene block was prepared with catalyst **12** 20 mg (.077 mmole) in a 4 ml stock solution of norbornene (1.75 M). The reaction was heated at 65°C for 12 hours then cooled to RT and pumped down to a vacuum of 10^{-6} torr overnight. The rubbery polymer was then dissolved in 3 ml of benzene and heated in the oil bath for 5 minutes. .41 g (3.1 mmole) of **DICB** was then added to the reaction, and the reaction was further heated for 10 minutes at 65°C . The mixture was then removed from the oil bath and diluted with 10 ml benzene. The reaction was then slowly added to a vigorously stirred methanol solution to give .65 g of the block copolymer. ^{1}H NMR of the block copolymer was a composite of that of polynorbornene and **PDICB**, and integration of the olefin peaks gave the ratio of the monomers in the polymer (Figure 3.10).

Preparation of PDICB:polynorbornene (1:0.8) block copolymer: Catalyst **12** 20 mg (.077 mmole) was dissolved in 4 ml of a 1.75 M norbornene solution in benzene. The reaction was heated to 65°C for 6 hours and then cooled to RT and pumped to dryness overnight at 10^{-6} torr. The reaction was then dissolved in 3 ml of benzene and heated for 5 minutes in the 65°C oil bath. **DICB** (.41 g 3.1 mmole) was then added to the reaction, and allowed to polymerize for 10 minutes. The reaction mixture was then cooled and diluted with 5 ml benzene. The mixture was then precipitated in oxygen free methanol to give .45 g of the block copolymer with the above stated composition.

Preparation of PDICB:polynorbornene(1:6.5) block copolymer: Catalyst **12** (40 mg .15 mmole) was dissolved in 8 ml of a 1.75 M norbornene solution in benzene. The reaction was heated for 10 hours and cooled and pumped

at 10^{-6} torr overnight. The living polymer was then dissolved in 3 ml benzene and put in the 65°C bath for 5 minutes. The **DICB** (.20 g 1.5 mmole) was then added and the reaction was heated for 10 minutes and then cooled, diluted with 5 ml benzene, and precipitated in oxygen free methanol. The integration of the ^{1}H NMR showed the **PDICB** to polynorbornene ratio to be 1 to 6.5.

Preparation of TPDMCB: Compound **15** 7.8 g (17 mmole) was dissolved in dry DMF (150 ml) with Zn dust 3.4 g (52 mmole) and stirred for 14 hours. The bright yellow color of **15** disappeared and a white precipitate was observed. The precipitate was filtered from the DMF and further rinsed with 5 portions of DMF to get rid of a slight yellow color in the solid. The organic material was then dissolved in a minimum amount of benzene ($\approx$ 80 ml 35°C) and filtered away. Crystals deposited out of the filtered benzene solution. These crystals were collected and washed with 10°C benzene. The benzene solution was diluted by the addition of an equal volume of methanol and put in a -20 freezer to give a second crop of crystals. The compound was air sensitive and turned yellow with air exposure. The NMR data was consistent with that reported in the literature.[46] Mass spectra gave a parent ion of 382. Elemental analysis calculated: C, 94.24; H, 5.76; found: C, 93.67; H, 5.40.

Preparation of polyisopropylacetylene (14): Isopropylacetylene (Farchan) 1.02 g (15.0 mmole) which had been stored over activated sieves was added via syringe to $MoCl_5$ 82 mg (.020 mmole) in 13.5 ml of toluene. The reaction was stirred at RT for 24 hours and then precipitated in methanol to give the polymer powder ($\approx$1g). The polymer is not air sensitive, and hence workup was not performed under inert atmosphere. ^{1}H NMR (C_6D_6): 5.80 (br. s. .9 H), 4.94 (br. s. .1 H), 1.65 (br. s. 1H), 1.05 (br. s. 6H). ^{13}C NMR 144.7 (br.), 124(vbr.), 30.0(br), 21.43 (br.).

References and Notes:

1. (a) Ivin, K. J. *Olefin Metathesis*; Academic Press, 1983. (b) Draguton, V.; Balabon, A. T.; Dimonie, M.; *Olefin Metathesis and Ring Opening Metathesis and Polymerization of Cyclo Olefins*; John Wiley and Sons, 1985.

2. *Handbook of Conducting Polymers*; Skotheim, T. J. (ed.); Dekker: New York, 1986.

3. (a) Chien, J. C. W.; Babu, G. N.; Hirch, J. A. *Nature (London)* **1985**, 314, 723-724. (b) Chien, J. C. W.; Babu, G. N.; *Macromolecules* **1985**, 18, 622. (c) Chien, J. C. W.; Babu, G. N. *J. Chem. Phys.* **1985**, **82**, 441-456.

4. See letters to *Nature* **1986**, 319, 697-699.

5. Roberts, J. D. *Notes on Molecular Orbital Calculations*; W. A. Benjamin: New York, 1961.

6. March, J. *Advanced Organic Chemistry* 3rd ed. Mcgraw Hill Pub., 1985.

7. Ballard, D. G.; Couris, A.; Shirley, I. M.; Taylor, S. C. *J. Chem. Soc., Chem. Commun.* **1983**, 954.

8. (a) Huntsman, W. D.; Wristers, H. J. *J. Am. Chem. Soc.* **1963**, 85, 3308. (b) Huntsman, W. D.; Wristers, H. J. *J. Am. Chem. Soc.* **1967**, 89, 342-347.

9. (a) Hopf, H. *Angew. Chem., Int. Ed. Engl.* **1970**, 9, 723. (b) Blomquist, A. T., Maitlis, P. M. *Proc. Chem. Soc.*, **1961**, Sept., 332. (c) Martin, H. D.; Kagabu, S.; Schiwek, H. J. *Tet. Lett.* **1975**, 38, 3311-3314.

10. Gilliom, L. R., Grubbs. R. H.*J. Am. Chem. Soc.* **1986**, 108, 733.

11. Mienhart, J. D.; Thesis California Institute of Technology, 1986.

12. (a) Katz, T. J.; Lee, S. J. *J. Am. Chem. Soc.* **1980**, 102, 442. (b) Masuda, T.; Higashimura, T. *Acc. Chem. Res* **1984**, 17, 51.

13. Silverstein, R. M.; Bassler, G. C.; Morrell, T. C. *Spectroscopic Identification of Organic Compounds*; Wiley: New York, 1981.

14. Yannoni, C. S. *Acc. Chem. Res.* **1982**, 15, 201-208.

15. In the dipolar dephasing experiment a delay of 60 μs (without decoupling) is inserted between the cross polarization and data collection. Carbons with protons exhibit facile dipolar relaxation before the data is collected unless the relaxation is modulated by motion. Hence, the signals of stationary centers with protons are not observed. See, Alla, M.; Lippmaa, E. *Chem. Phys. Lett.* **1976**, 37, 260.

16. Levy, G. C.; Lichter, R. L.; Nelson, G. L. *Carbon-13 Nuclear Magnetic Resonance Spectroscopy*; Wiley-Interscience, 1980.

17. (a) Kress, J.; Osborn, J. A. *J. Am. Chem. Soc.* **1983**, 105, 6346. (b); Aguero, A.; Kress, J.; Osborn, J. A. Green, R. M. E.; Ivin, K. J.; Rooney, J. J. *J. Chem. Soc., Chem. Comm.* **1985**, 874. (c) Aguero, A.; Kress, J.; Osborn, J. A. *J. Chem. Soc., Chem. Comm.* **1985**, 793. (d) Kress, J.; Osborn, J. A. Green, R. M. E.; Ivin, K. J.; Rooney, J. J. *J. Am. Chem. Soc.* **1987**, 109, 899. (e) Kress, J.; Aguero, A.; Osborn, J. A. *J. Mol. Cat.* **1986**, 36, 1.

18. (a) Schrock, R. R.; Feldman, J.; Cannizzo, L. F.; Grubbs, R. H. *Macromolecules* **1987**, 20, 1169. (b) Schaverin, C. J.; Dewan, J. C.; Schrock, R. R. *J. Am. Chem. Soc.* **1986**, 108, 2771. (c) Schrock, R. R.; Depue, R. T.; Feldman, J.; Schaverien, C. J.; Dewan, J. C.; Liu, A. H. *J. Am. Chem. Soc* **1988**, 110, 1423.

19. Katz, T. J.; Lee, S. J.; Nair, M.; Savage, E. B. *J. Am. Chem. Soc.* **1980**, 102, 7940-7942.

20. Pouchert, C. J. *The Aldrich Library of FT-IR Spectra*; Vol. 1, 43D, Aldrich Chem. Co., 1985.

21. See Elsenbaumer, R. L.; Shacklette, L. W. in reference 2.

22. Skattebol, L.; Solomon, S. *J. Am. Chem. Soc.* **1965**, 87, 4506-4513.

23. Pasto, D. J.; Mitra, D. K.; *J. Org. Chem.* **1982**, 47, 1381-1382.

24. Yau, W. W.; Kirkland, J. J.; Bly, D. D. *Modern Size-Exclusion Chromatography*; Wiley: New York, 1979.

25. Polydispersity Index was calculated for the GPC peaks corrected for crosslinking. The corrected curves in Figure 3.8 are shown with a broken line.

26. Wallace, K. C.; Schrock, R. R. *Macromolecules* **1987**, 20, 448.

27. Cannizzo, L. F.; Grubbs, R. H. *Macromolecules* in press.

28. Gilliom, L. R. Thesis, California Institute of Technology 1985.

29. Odian, G. G. *Principals of Polymerization* 2nd ed., Wiley: New York, 1981.

30. Masuda, T.; Kawasaki, M.; Okana, Y.; Higashimura, T. *Polymer J.* **1982**, 14(5), 371-377.

31. Pranata, J.; Dougherty, D. A. *Synthetic Metals*, **1987**, 22, 171-178.

32. Bredas, J. L.; Chance, R. R.; Baughman, R. H.; Silbey, R. *J. Chem. Phy.* **1982**, 76, 3673-3678.

33. Chien, J. C. W. *Polyacetylene: Chemistry, Physics, and Materials Science*; Academic Press, 1984.

34. Kim, S. S.; Cebe, P.; Swager, T. M. manuscript in preparation.

35. Petit, M. A.; Soum, A. H.; Leclerc, M.; Prud'homme, R. E. *J. Polym. Sci., Chem. Ed.* **1987**, 25, 423-433.

36. Rabolt, J. F.; Clarke, T. C.; Street, G. B. *J. Chem. Phys.* **1979**, 71, 4614-4619.

37. Wertz, J. E.; Bolton, J. R. *Electron Spin Resonance: Elementary Theory and Practical Applications* Chapman and Hall, 1986.

38. See Gibson, H. W. in reference 2.

39. Weinberger, B. R.; Ehrenfreund, E.; Pron, A.; Heeger, A. J.; MacDiarmid, A. G. *J. Chem. Phys.* **1980**, 72, 4749-4755.

40. A widening of the ESR resonance has been observed with decreasing temperature in polyacetylene and was taken as evidence for motional narrowing. See reference 39.

41. Poole, C. P.; Farach, H. A. *Relaxation Processes in Magnetic Resonance*; Academic Press: New York, 1971.

42. Chien, J. C. W.; Wnek, G. E.; Karasz, F. E.; Warakomski, J. M.; Dickinson, L. C.; Heeger, A. J.; MacDiarmid, A. G. *J. Am. Chem. Soc.* **1982**, 15, 614-621.

43. (a) Epstein, A. J.; Ginder, J. M.; Zuo, F.; Bigelow, R. W.; Woo, H. S.; Tanner, D. B.; Richter, A. F.; Huang, W. S.; MacDiarmid, A.G. *Synthetic Metals* **1987**, 18, 303. (b) Moraes, F.; Davidov, D.; Kobayashi, M.; Chung, T. C.; Chen, J.; Heeger, A. J.; Wudl, F. *Synthetic Metals* **1985**, 10, (c) Chung, T. C.; Moraes, F.; Flood, J. D.; Heeger, A. J. *Phys. Rev. B* **1984**, 29, 2341. (d) Ikehata, S.; Kaufer, J.; Woerner, T.; Pron, A.; Pron, A.; Dury, M.; Sivak, A.; Heeger, A. J.; MacDiarmid, A. G. *Phys. Rev. Lett.* **1980**, 45, 1123. (e) Epstein, A. J.; Rommelmann, H.; Dury, M. A.; Heeger, A. J.; MacDiarmid, A. G. *Solid State Comm.* **1981**, 38, 683-687. (f) Weinberger, B. R.; Kaufer, J.; Heeger, A. J.; Pron, A.; MacDiarmid, A. G. *Phys. Rev. B* **1979**, 20,

223-230. (g) Peo, M.; Roth, S.; Dransfeld, K.; Tieke, B.; Hocker, J.; Gross, H.: Grupp, A.; Sixl, H. *Solid State Comm.* **1980**, 119-122.

44. Kittel *Introduction to Solid State Phys.*; 5th ed., John Wiley and Sons, 1975.

45. Eckert, H.; Yesinowski, J. P; Sandman, D. J.; Velazquez, C. S. *J. Am. Chem. Soc.* **1987**, 109, 761.

46. Toda, F.; Kumada, K.; Ishiguro, N.; Akagi, K. *Bull. Chem. Soc. Japan* **1970**, 43, 3535-3539.

47. (a) Landor, P. D.; Landor, S. R. *J. Chem. Soc.* **1963**, 2707-2711. (b) Byrn, S. R.; Maverick, E.; Muscio, O. J.; Trueblood, K. N.; Jacobs, T. L *J. Am. Chem. Soc.* **1971**, 93, 6680-6683.

48. Weider, H. H. *Laboratory Notes on Electrical and Galvanomagnetic Measurements*; Elsevier Scientific Pub., 1979.

49. Lee, J. B.; Ott, K. C.; Grubbs, R. H. *J. Am. Chem. Soc.* **1982**, 104, 7491.

50. Fischer, E. O.; Shubert, V.; Kleine, W.; Fischer, H. *Inorg. Synth.* **1979**, 19, 164.

Chapter 4

SYNTHESIS AND PROPERTIES OF POLYBENZVALENE: A SOLUBLE POLYACETYLENE PRECURSOR AND HIGH ENERGY POLYMER

INTRODUCTION:

Conductive polymers represent an active area of research in polymer science.[1] Polyacetylene (**PA**) is the simplest conductive polymer and has received extensive study.[2] Recently, **PA** has been shown to display conductivities that rival copper.[3] This deceptively simple material is a fundamental cornerstone in the field of conductive polymers. Hence, new synthetic routes to this material which can generate new morphologies should be pursued. In general, **PA** and many other conductive polymers are insoluble and infusible materials with low tensile strength. Thus, the manipulation of these materials into useful shapes and morphologies is limited. The morphology of many conductive polymers is fixed in the polymerization and is not easily modified. One solution to the processing problems encountered in conductive polymers has been to use a processable precursor polymer which can be transformed into a conductive polymer. Precursor routes to conductive polymers have been successful in producing high molecular weight materials with high conductivities and oriented morphologies.[4] The most relevant precursor method to this work is the synthesis of **PA** by the method of Feast (see Chapter 1).[4a] **PA** so synthesized has been called "Durham **PA**" and has seen considerable study. However, known precursor methods have been limited to processes which involve the extrusion of molecular fragments. In some cases, the extrusion involves over half the mass of the precursor polymer. Extrusions such as these restrict the processing of these materials into large shapes and prohibit processing by methods such as mold injection. In addition, materials produced by extrusion processes often have a porous structure which for some applications is undesirable. Thus, the development of precursor methodology for the synthesis of conductive polymers that is non-extrusive is desirable.

A strategy based on an intramolecular electrocyclic rearrangement may be successful at meeting this criteria.[5] In this scheme, olefins are masked by incorporating them into ring systems. The resulting saturated centers in the ring act

to make the polymer backbone non-planar and more flexible, which will impart greater solubility to the polymer. Well known electrocyclic reactions[5] that may be of use are shown in Figure 4.1.

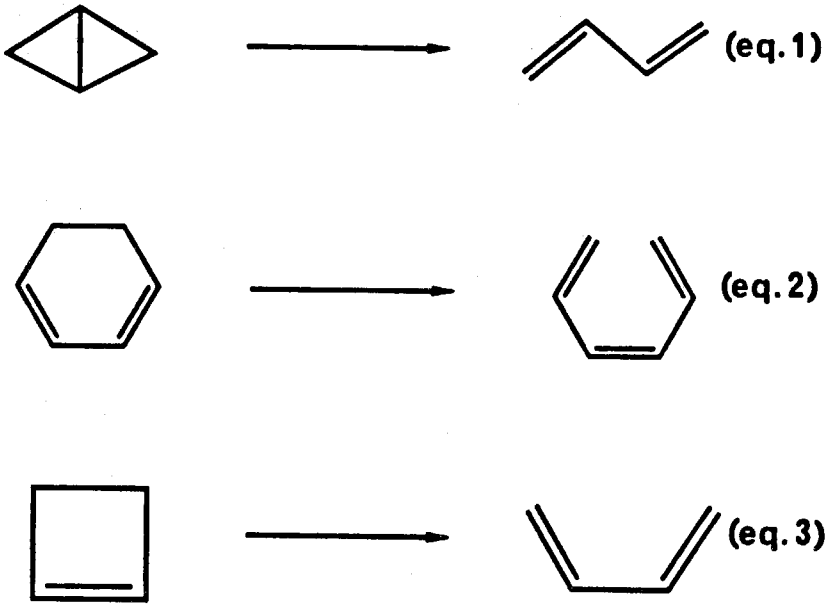

Figure 4.1. Electrocyclic reactions that may be useful in a non-extrusive precursor route to conductive polymers.

In Chapter 3, the electrocyclic ring closure of 1,3,5-trienes was proposed. However, the reverse reaction (equation 2, Figure 4.1) may also be thermodynamically favored by the substitution pattern. The use of this reaction as a precursor method has seen initial investigation by F. L. Klavetter in this group.[6] The conversion of bicyclobutanes to 1,3-dienes (equation 1, Figure 4.1) is a particularly attractive route as a result of the readily available monomer benzvalene (**BV**).[7] This isomerization has been promoted thermally,[8] photochemically,[9] and with a variety of transition metal catalysts.[10] As is shown in Scheme 4.1, it was envisioned that ring opening metathesis polymerization (**ROMP**) of **BV** would lead

to polybenzvalene (**PBV**), which would in turn be a soluble precursor polymer to **PA**. **ROMP** has been demonstrated to be a highly selective and well-behaved polymerization method.[11,12,13] The sigma bond in the bridging position of the bicyclobutane ring is a highly reactive bond and sometimes yields reaction chemistry reminiscent of an olefin. Hence, **BV** represents a test of the selectivity of **ROMP** .

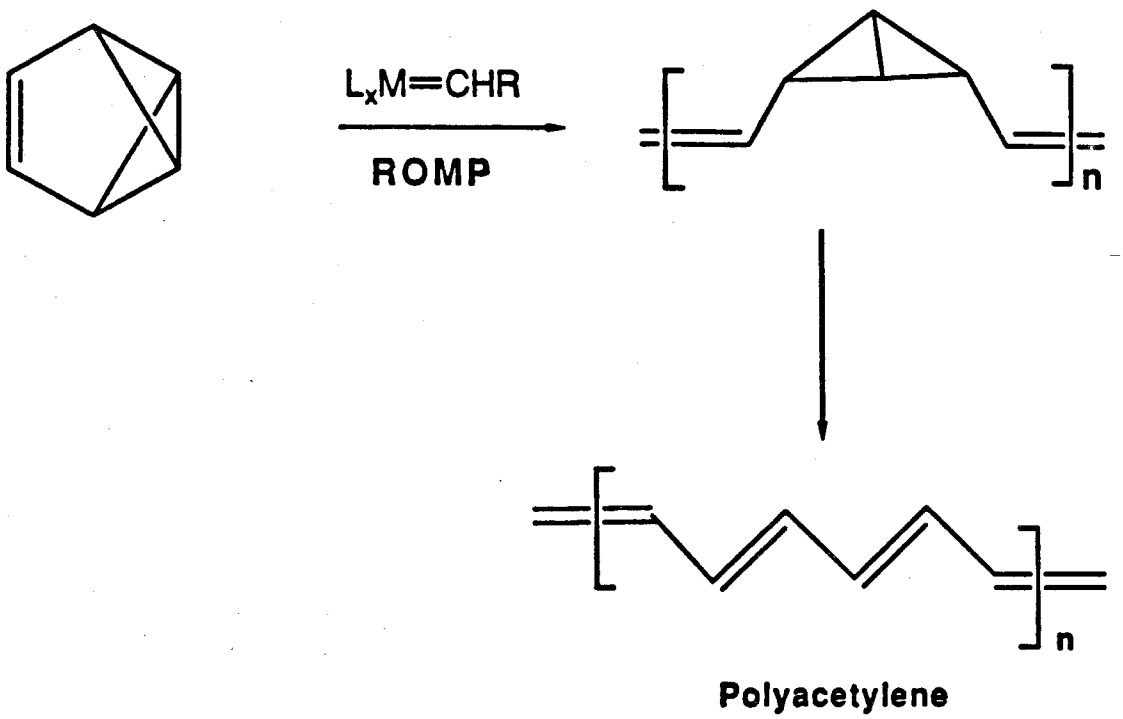

Scheme 4.1

An added feature provided by **PBV** is the fact that the polymer contains a considerable amount of strain energy. The bicyclobutane moiety has approximately 64 kcal/mol of strain energy,[14] and hence **PBV** has approximately 11 kcal/mol of strain energy per carbon atom. High energy polymers such as these have applications as a component of solid rocket fuel.[15]

BV is a valuable starting material in the synthesis of a vast number of

compounds.[16] Recent examples include the use of **BV** as starting material for the synthesis of new diradical precursors[17] and the fundamentally important yet elusive molecule tetrahedrane.[18] The availability of **BV** is a result of the synthesis developed by Katz.[7] This synthesis shown, in Scheme 4.2, is a one-pot procedure and yields 15 to 30 gram quantities of **BV**. Pure **BV** is a hazardous material and is only safely handled in solution.[19] The Katz procedure leads to the isolation of solutions of **BV**. The solvent in which the **BV** is isolated has its origin from the second equivalent of alkyl lithium. The major solvent in the reaction is dimethyl ether which is allowed to boil off during the product isolation. The concentration of the **BV** solution is determined by the concentration of the second alkyl lithium equivalent. Since ether will decrease the rate of **ROMP**,[20] the second alkyl lithium equivalent was butyl lithium in hexane rather than methyl lithium in ether as is often used.[7] **BV** solutions of 1 to 1.5 M were prepared and these solutions were diluted with benzene or toluene before polymerization. The addition of benzene or toluene is necessary as a result of the fact that hexane is not typically a good solvent for a polymers such as **PBV**.

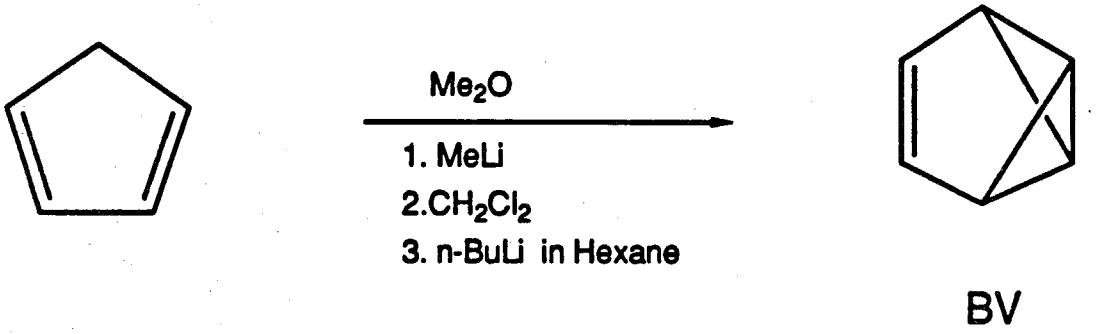

Scheme 4.2

RESULTS AND DISCUSSION:

Polymerization of BV:

Initial attempts at the **ROMP** of **BV** were with the titanocene metallacycles **1** and **2**.[21] The reaction of **BV** with these metallacycles is shown below in Scheme 4.3. The resulting metallacycles **3** and **4**) were thermally quite stable. Metallacycle **3** was observed to be stable by ^{1}H NMR spectroscopy up to 80°C at which point it gives unidentifiable products. Metallacycle **4** was prepared since trisubstituted metallacycles are less stable and more readily undergo **ROMP**.[11] **4** decomposed to a complex mixture of products at 65°C. Polymerizations at elevated temperatures are not acceptable as a result of the thermal instability of **BV** which is converted thermally to benzene.[16]

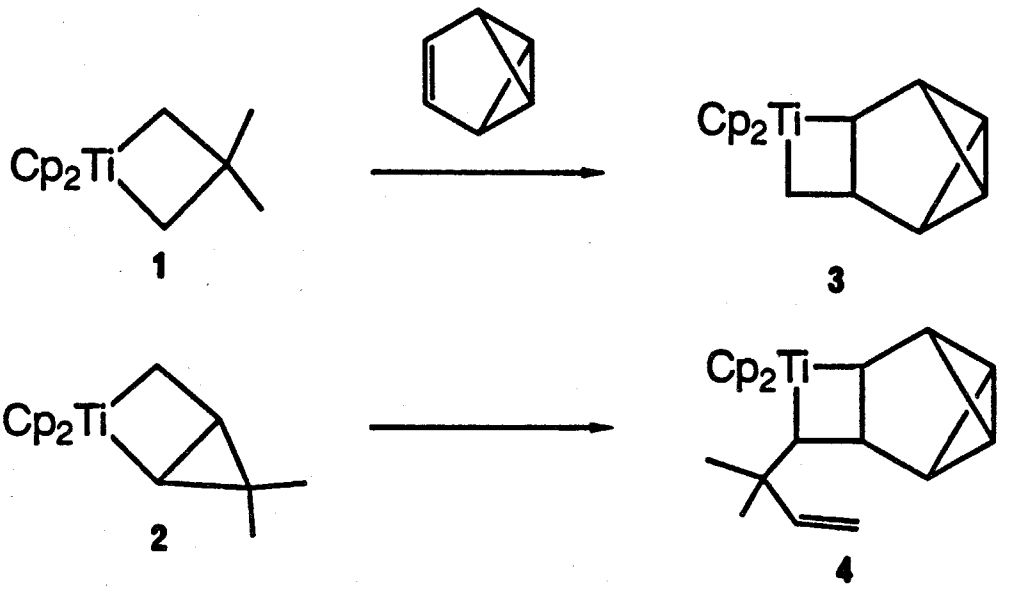

Scheme 4.3

The lack of productive metathesis for the titanocene catalysts may be due to a combination of factors. The heat of formation of **BV** is 87.3 kcal/mol,[16]

which yields a strain energy of ≈72 kcal/mol.[14] Subtracting the strain energy of the bicyclobutane group leaves 8 kcal/mol of strain energy to the ring bearing the olefin. Formation of the metallacycle further reduces the strain energy, and decreases the driving force for the ring opening. Sterics are likely not a problem since this monomer presents less steric bulk than norbornene. However, the need for the metallacycle to open via an olefin complex[22] on the reaction trajectory as described in Chapter 2 may present a problem. The rigidity of the bicyclobutane ring system may impede torsions about bonds that are necessary to allow the metallacycle to distort to the olefin complex (**5**).

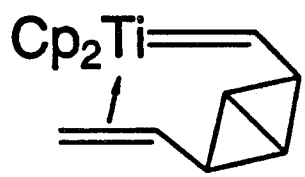

5

Attempts at **ROMP** of **BV** with Lewis acidic catalysts were also unsuccessful. The Lewis acidic catalysts investigated were WCl_4:$Sn(Me)_4$, $WOCl_4$:$Sn(Me)_4$, and $((Me)_3CCH_2O)_2W(Br)_2CHC(Me)_3$:$GaBr_3$. These catalysts reacted with **BV** exothermically to give a dark brown intractable material. The Fischer carbenes which are **ROMP** catalyst precursors[23] were also ineffective at producing polymer.[24]

The catalysts recently reported by Schrock (**6** and **7**)[20] and Osborn (**8**)[24] were effective at the polymerization of **BV**. The resulting polymer polybenzvalene (**PBV**) is a soluble polymer which displays properties as follows. Solutions of **PBV** may be precipitated as powders by slowly adding the polymerization mixture to a large volume of acetone. These powders were white to tan in color and would not redissolve after precipitation. Thus **PBV** must be handled in solution

and the film casting will need to be done directly from the polymerization reaction mixture. Films are initially soft, swellable, and display viscoelastic properties. Films a few days old are noticeably more brittle and not swellable. As a result of its high strain energy, **PBV** is a sensitive material that will undergo spontaneous exothermic decomposition (detonation) with the application of severe mechanical stress or with rapid heating. Solid samples of **PBV** must be handled carefully and quantities of the material were kept below a gram. However, in the numerous occasions that the material was detonated (both accidentally and intentionally) it seldom produced violent explosions. The spontaneous decomposition of freshly prepared samples is extremely exothermic. Powders were found to be particularly prone to detonation. Detonation of fresh samples produces orange smoke and an orange brown oily residue. The heat released in this decomposition is substantial. On one occasion, a 200 mg sample produced enough heat to melt the rubber gloves that the author was wearing when handling the material. Older samples (2 months) may still be detonated with heating, and these materials give off black smoke and ash.

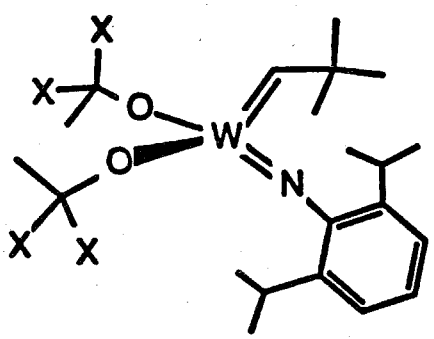

6 X= CF_3
7 X= CH_3
SCHROCK

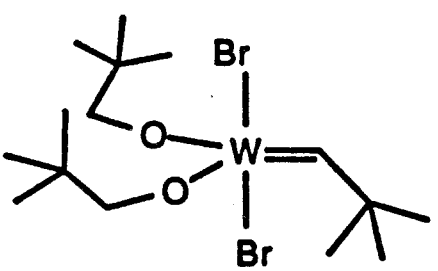

8
OSBORN

Gels are readily formed of **PBV** and were produced when the polymerization was run at too high a concentration. Concentrated solutions of **PBV** also gel in a matter of hours. Gels that were washed with a non-solvent such as methanol, acetone, or acetonitrile were extremely stretchable. Comparable materials could also be prepared by rinsing an evaporated film that was still swollen with non-solvent. These materials could be stretched more than 30 times their original length. These materials often detonated at these elongations.

Solution NMR spectra were obtained by subjecting solutions of **PBV** to cycles of partial evaporation and addition of C_6D_6. Catalyst **6** exhibits a high selectivity for *cis*-olefins in the polymerization of norbornene.[12] Polymerization of **BV** with catalyst **6** must be performed at subambient temperature. Reaction of **6** with **BV** at RT produced a red solution and only a very small amount of polymer. **6** was found to smoothly produce **PBV** at temperatures between -20°C and 0°C. When the polymerization temperature is raised to 0°C , the solution slowly turns from yellow to orange. **6** is effective in producing only one detectable olefin isomer of **PBV** as evidenced by ^{13}C NMR (Figure 4.2). Infrared spectroscopy of this material (Figure 4.6) reveals a *cis*-olefin C-H out of plane bending vibration at 750 cm^{-1} which suggests that this **PBV** produced with **6** is nearly exclusively *cis*-olefins. There are also infrared bands at 1000 cm^{-1} which are in the range of frequencies that *trans*-olefins C-H bending modes may exhibit. However, there is no reason to believe that the *cis* preference of **6** should not be exhibited in the **ROMP** of **BV**. The ^{13}C NMR chemical shifts of **PBV** can be compared with those of the **BV**, **9**, and bicyclobutane shown below.[25]

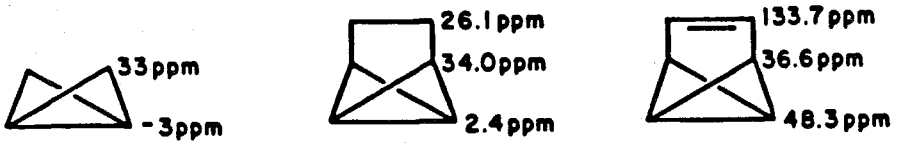

Bicyclobutane **9** **BV**

The carbon at the bridgehead of the bicyclobutane group is shifted upfield upon relieving ring strain.[25] This position's resonance ranges from 48.3 ppm in **BV** to -3.0 in bicyclobutane. Thus, the signal upfield at 12.8 ppm in the ^{13}C NMR of **PBV** is most likely the bridgehead carbon of the bicyclobutane group. The 47.8 ppm signal corresponds to the 33.7 ppm signal observed in **BV**. The large downfield shift in this resonance is not surprising considering the large change in environment experienced by this center upon polymerization.

The ^{1}H NMR of **PBV** synthesized with **6** is shown in Figure 4.3. This spectrum is complicated by residual hexane which is difficult to totally remove from the sample. The sample used for the NMR spectra shown in Figures 4.1 and 4.2 had been subjected to nine cycles of partial evaporation and addition of C_6D_6. The ^{1}H NMR spectra of **PBV** produced with **6** are very similar to that obtained for **BV**, which has peaks at 5.95, 3.53, and 1.84 ppm in benzene.

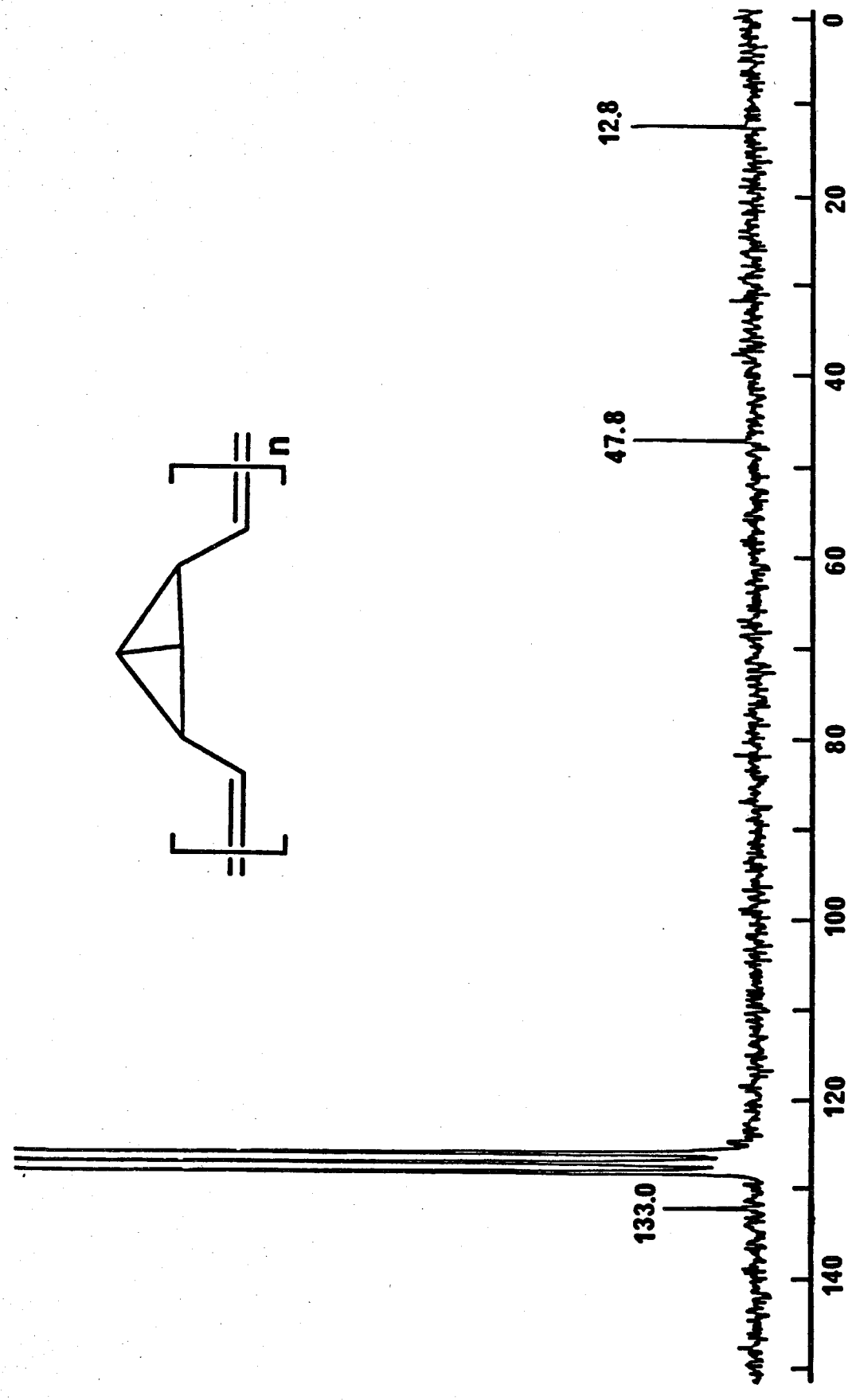

Figure 4.2. ^{13}C NMR (C_6D_6) of PBV synthesized with 6.

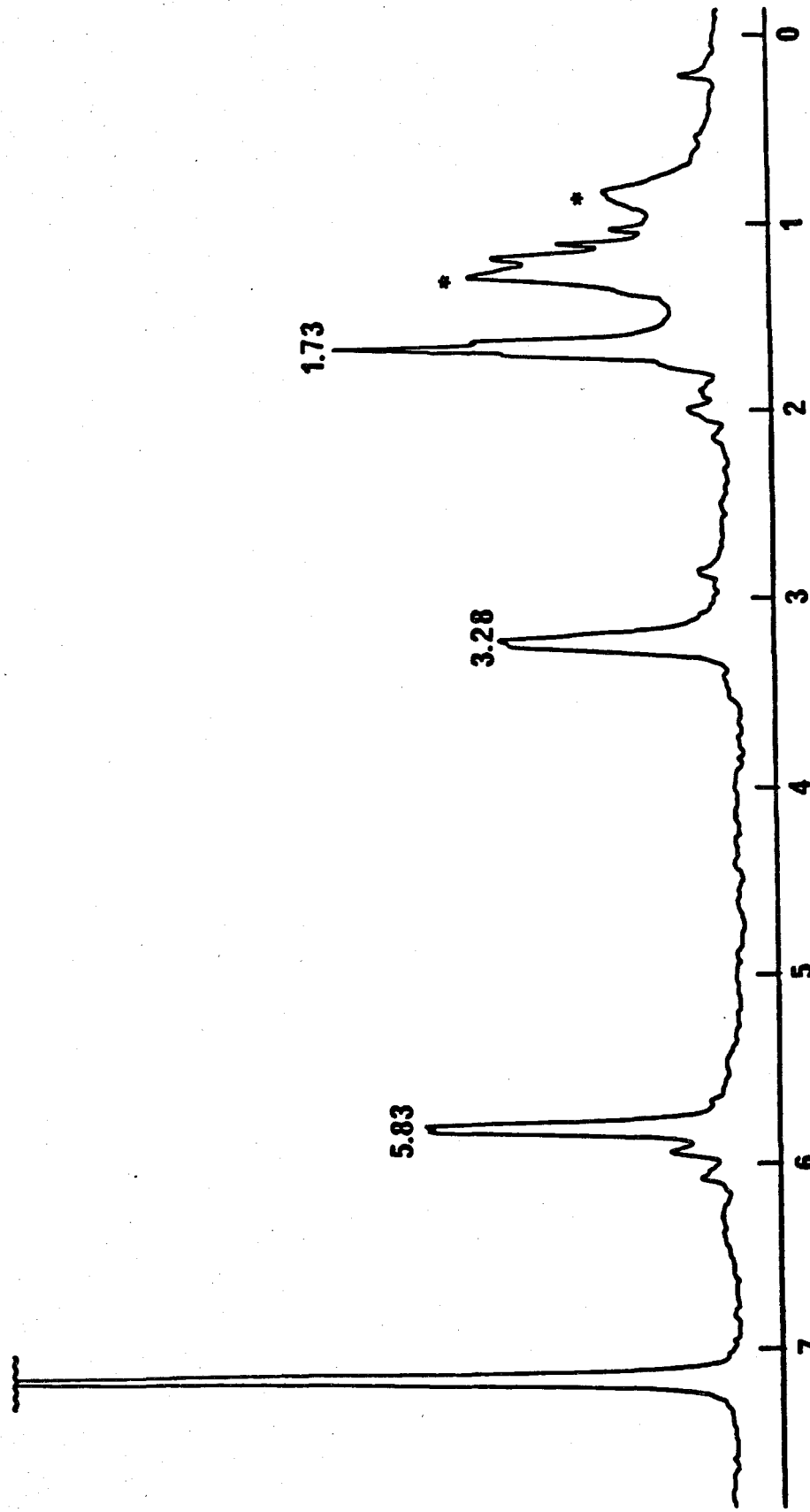

Figure 4.3. ^{1}H NMR (C_6D_6) of PBV synthesized with 6. Peaks marked with a * are the result of residual hexanes.

Both **7** and **8** produce polynorbornene with an excess of *trans* olefins.[12,24] NMR reveals that catalyst **7** produces mainly *cis*-**PBV** that is very similar to **PBV** obtained with **6**. However, there are minor peaks observed which may be the result of a small amount of *trans*-**PBV** synthesized with **7**. The material produced with **8** has similar physical properties to **PBV** produced with **6** and **7**, but the NMR data for this material is quite different. The ^{13}C NMR and ^{1}H NMR of **PBV** polymerized with **7** and **8** are shown in Figures 4.4 and 4.5 respectively. The ^{13}C NMR of **PBV** from polymerization with **7** exhibits the same signals as were observed for **6** with a hint of some additional olefin signals and numerous minor signals in the region of 20 to 40 ppm. **PBV** synthesized with **8** has a complex ^{13}C NMR and exhibits a second olefinic peak at 124.9 which may be from *trans*-olefins. It is interesting to note that all of the peaks observed in the ^{13}C NMR of **PBV** produced with **8** are also exhibited by **PBV** polymerized with **7**. Examination of the ^{1}H NMR also shows the same correlation of signals between the materials produced with these catalysts. This large dispersion in the ^{13}C chemical shifts may be a result of *cis-trans* olefin content, the conformational rigidity of the **PBV** backbone, and the sensitivity of the bicyclobutane resonances to their environment. As was discussed above the bridgehead carbon of bicyclobutane groups may display chemical shifts from -3 to 48 ppm depending on ring strain. The -2.2 ppm peak shown in Figure 4.4 would thus correspond to a bicyclobutane group which contains no extra strain due to the polymer conformation. Different olefin isomers that may be present in **PBV** synthesized with **7** and **8** are shown in Scheme 4.4. However, as a result of the NMR's complexity of **PBV** produced with **8**, its structure cannot be undisputably established with the data at hand, and the possibility of a different structure for this material must be considered.

cis-cis-cis

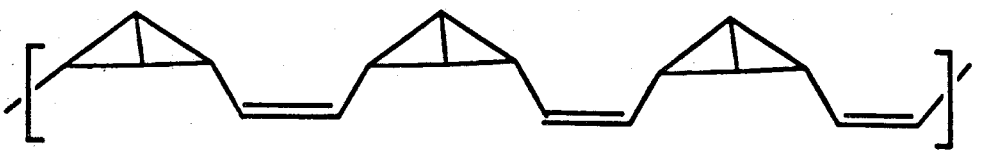

trans-trans-cis

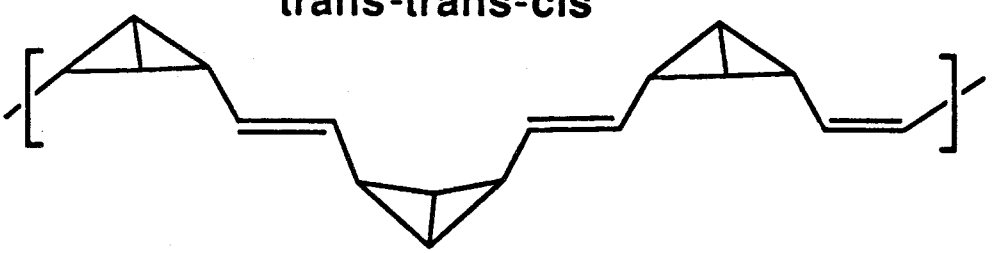

cis-trans-cis

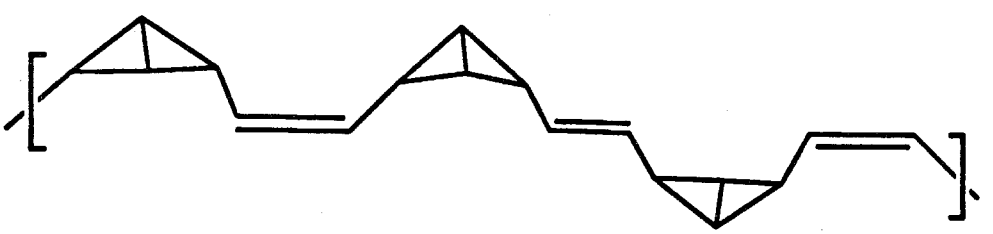

trans-trans-trans

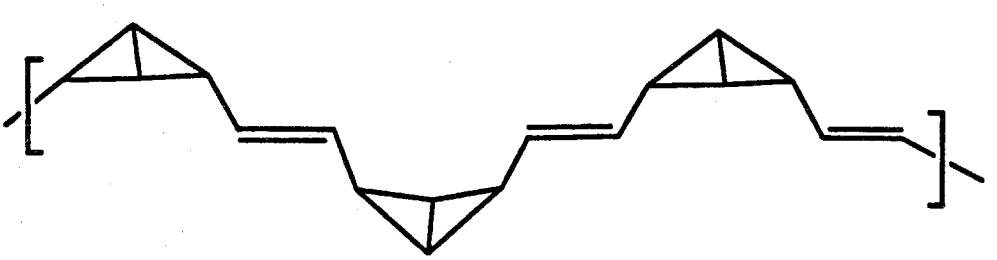

Scheme 4.4

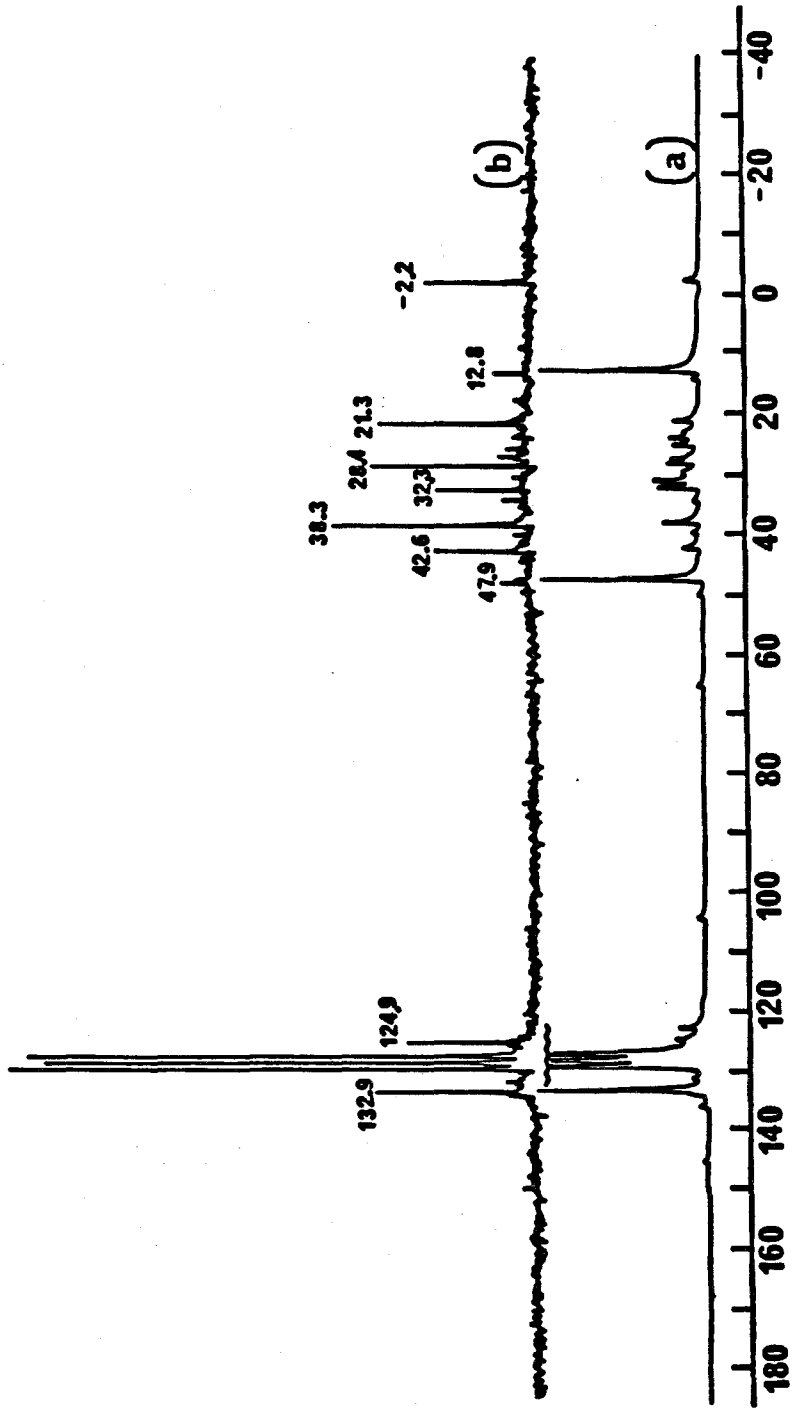

Figure 4.4 ^{13}C NMR (C_6D_6) of PBV polymerized with 7 (a); and with 8 (b).

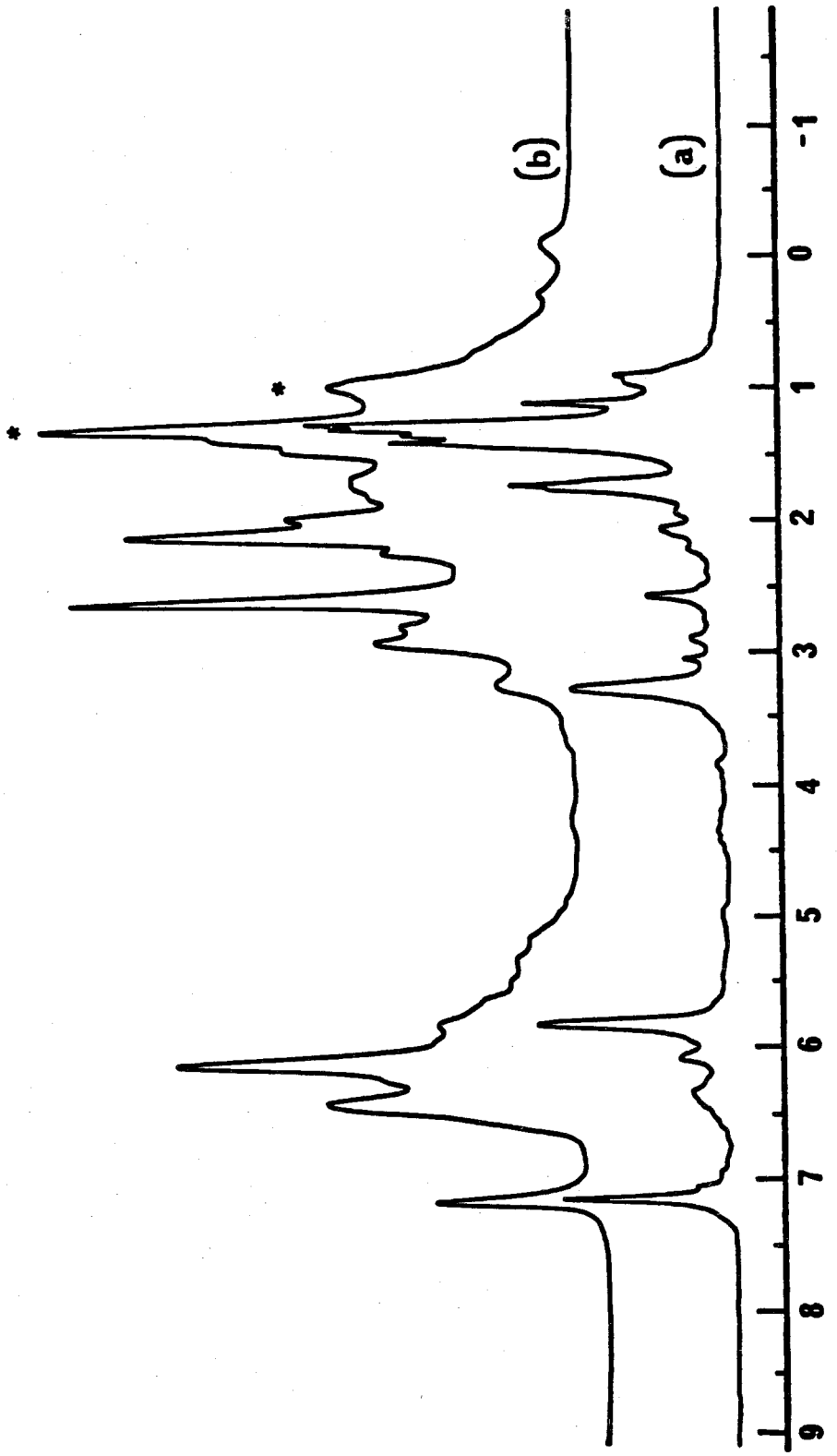

Figure 4.5 ^{1}H NMR (C_6D_6) of PBV polymerized with **7** (a); and with **8** (b). Peaks marked with a * are the result of residual hexane.

Infrared spectroscopy (Figure 4.6) also indicates similarities in the polymers obtained with all the catalysts. The bicyclobutane moiety gives rise to considerable mixing in the vibrational modes of **PBV**. Notably the strong and broad C=C stretching band is particularly unusual. This strong mixing of the vibrational modes is also observed for **BV** ,[26] and precludes a detailed analysis of these spectra. However, examination of these spectra suggests that the **PBV** produced by the three catalysts is very similar in structure. Throughout the studies reported hereafter, **PBV** produced with **6** and **7** were periodically compared and found to exhibit identical results. Polymerization with **7** is most convenient as a result of the fact that it proceeds smoothly at RT. Hence, unless otherwise stated the results reported henceforth are for **PBV** produced with **7**.

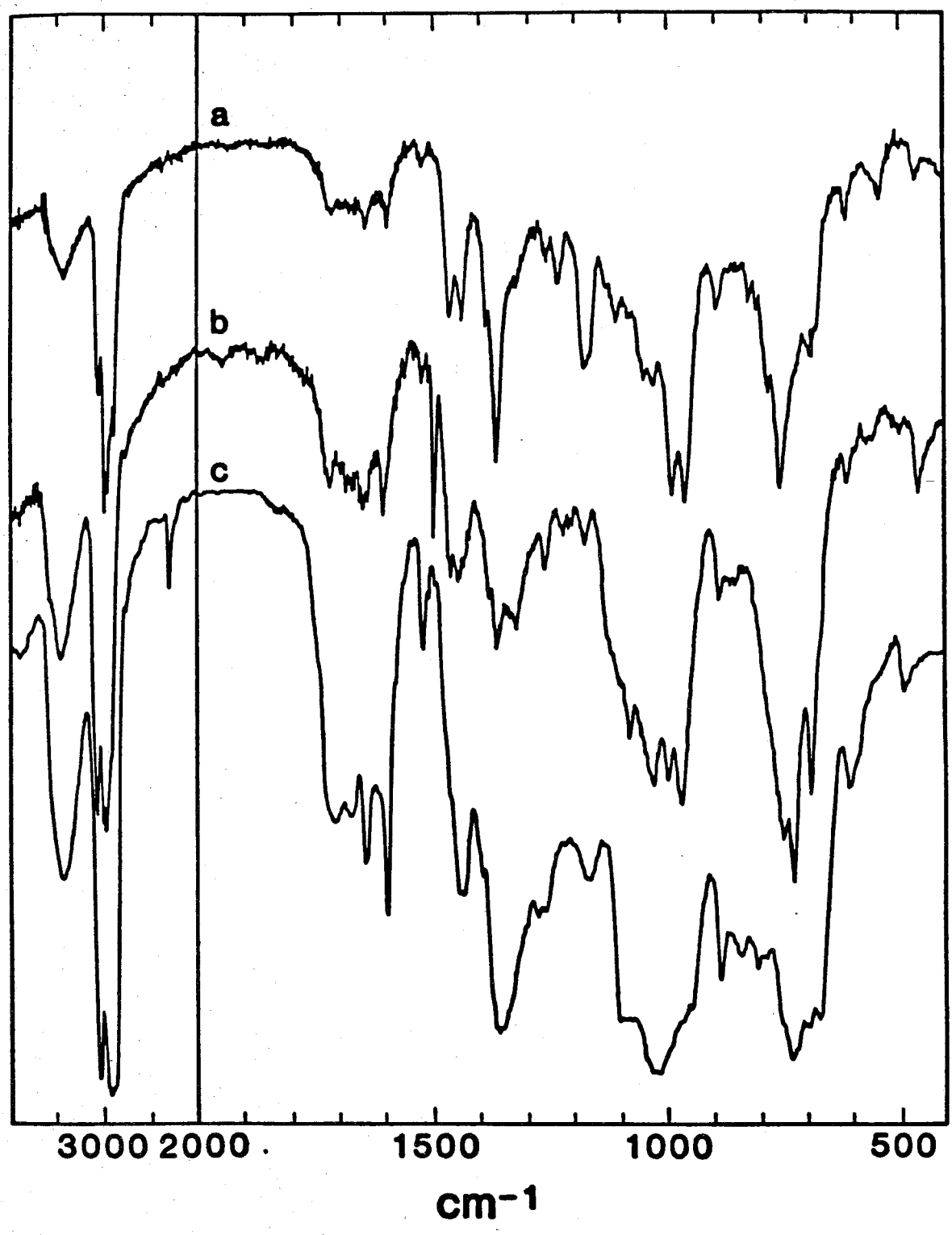

Figure 4.6. Infrared spectra of PBV produced with 7 (a); 6 (b); and 8(c).

As was discussed above, **PBV** is relatively unstable and cannot be redissolved after precipitation or casting into a film. As a consequence, the nature of the decomposition cannot be addressed with solution NMR. Hence, **PBV** was studied with solid state ^{13}C NMR with cross-polarization and magic angle spinning (CPMAS).[27] In general, the signals obtained were broad with linewidths of 1500 to 2500 Hz. In addition, integration revealed the olefinic region was approximately 40 to 45% of the total carbon signal, which is larger than the 33% that would be expected for the structure of **PBV**. A CPMAS ^{13}C NMR spectrum of **PBV** synthesized with **8**, which had been stored as a powder at room temperature for 2 weeks, is shown in Figure 4.7.

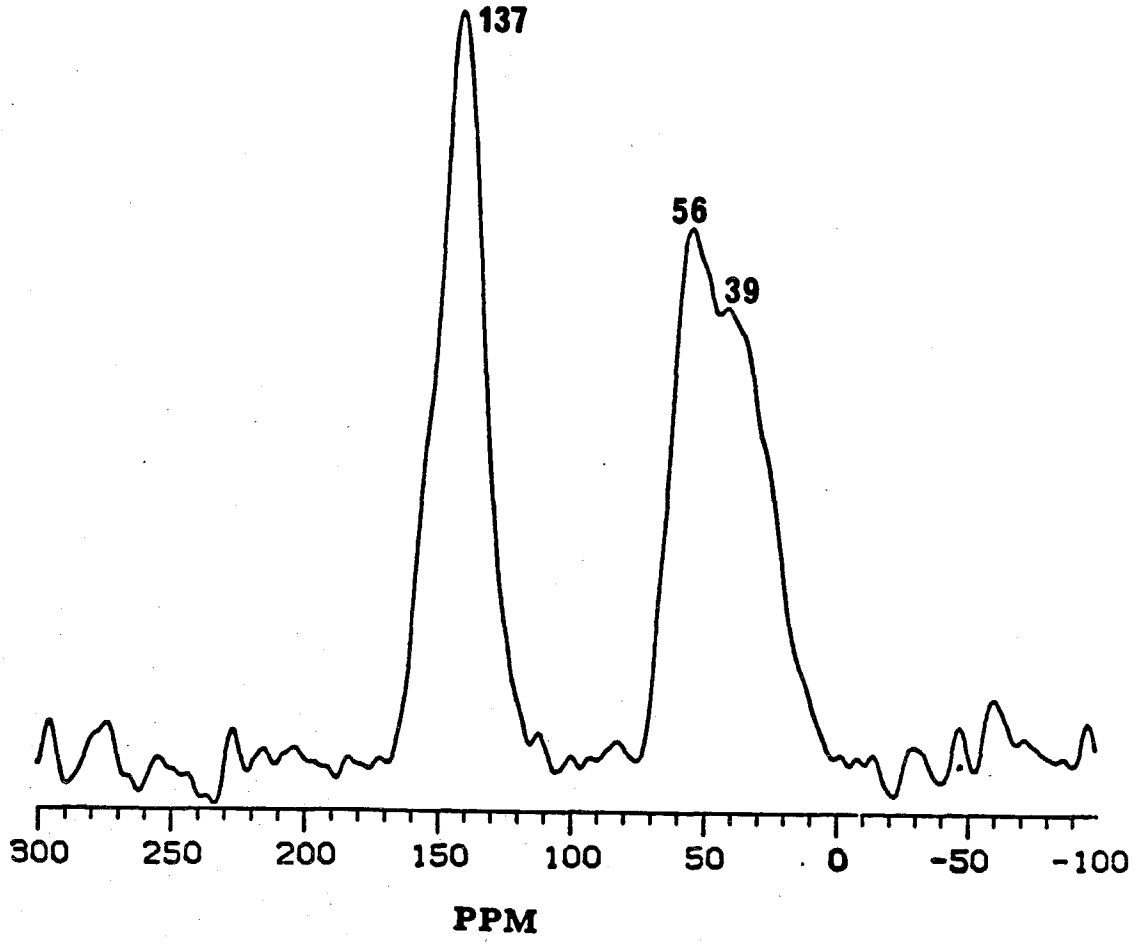

Figure 4.7. CPMAS ^{13}C NMR spectra of **PBV** produced with **8** after two weeks at room temperature.

Block Copolymers of PBV:

7 has been demonstrated to provide a living polymerization of norbornene.[12] Hence, as shown in Scheme 4.5 block copolymers of polynorbornene and **PBV** are readily produced. The living polymer **10** was prepared by the method described in the literature,[12] and then the **BV** was added to the mixture and polymerized. ^{1}H NMR, shown in Figure 4.8, confirms the presence of both polynorbornene and **PBV**. The ratio of the two materials is readily determined by integration of the olefinic signals and was found to be 1:1.2 (**PBV** to polynorbornene). The **PBV** block copolymer has less of a tendency to gel and is more soluble than the **PBV** homopolymer. Films of the block copolymer maintain a soft rubbery nature which is retained after a month of storage at room temperature. Thus, it appears that the block copolymers have an improved stability.

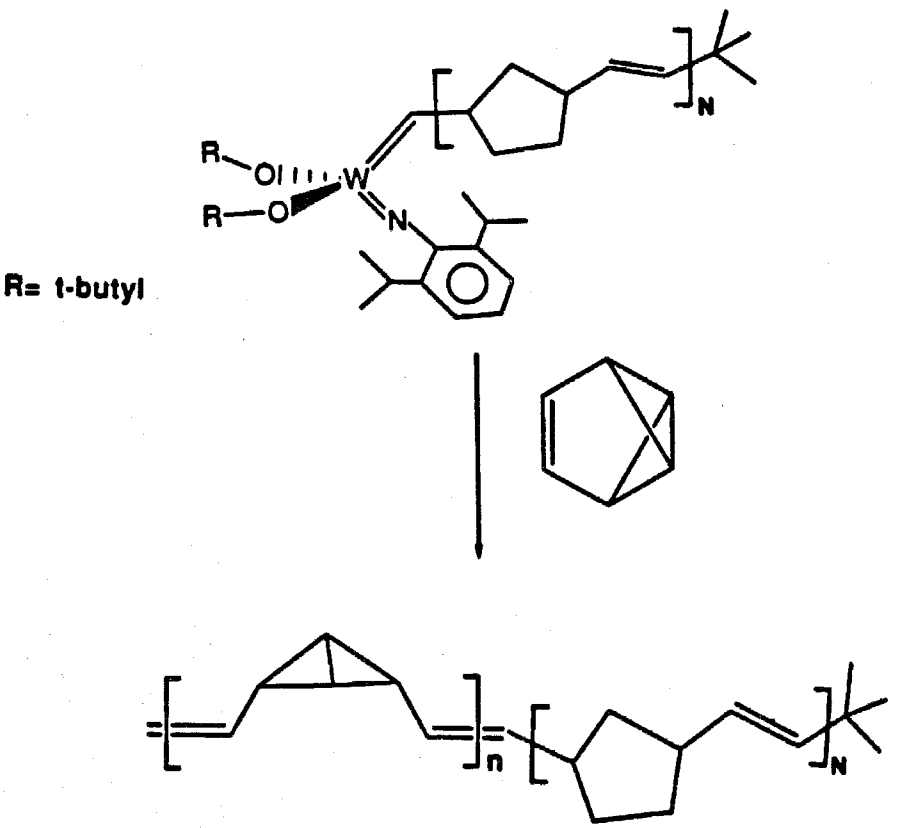

Scheme 4.5

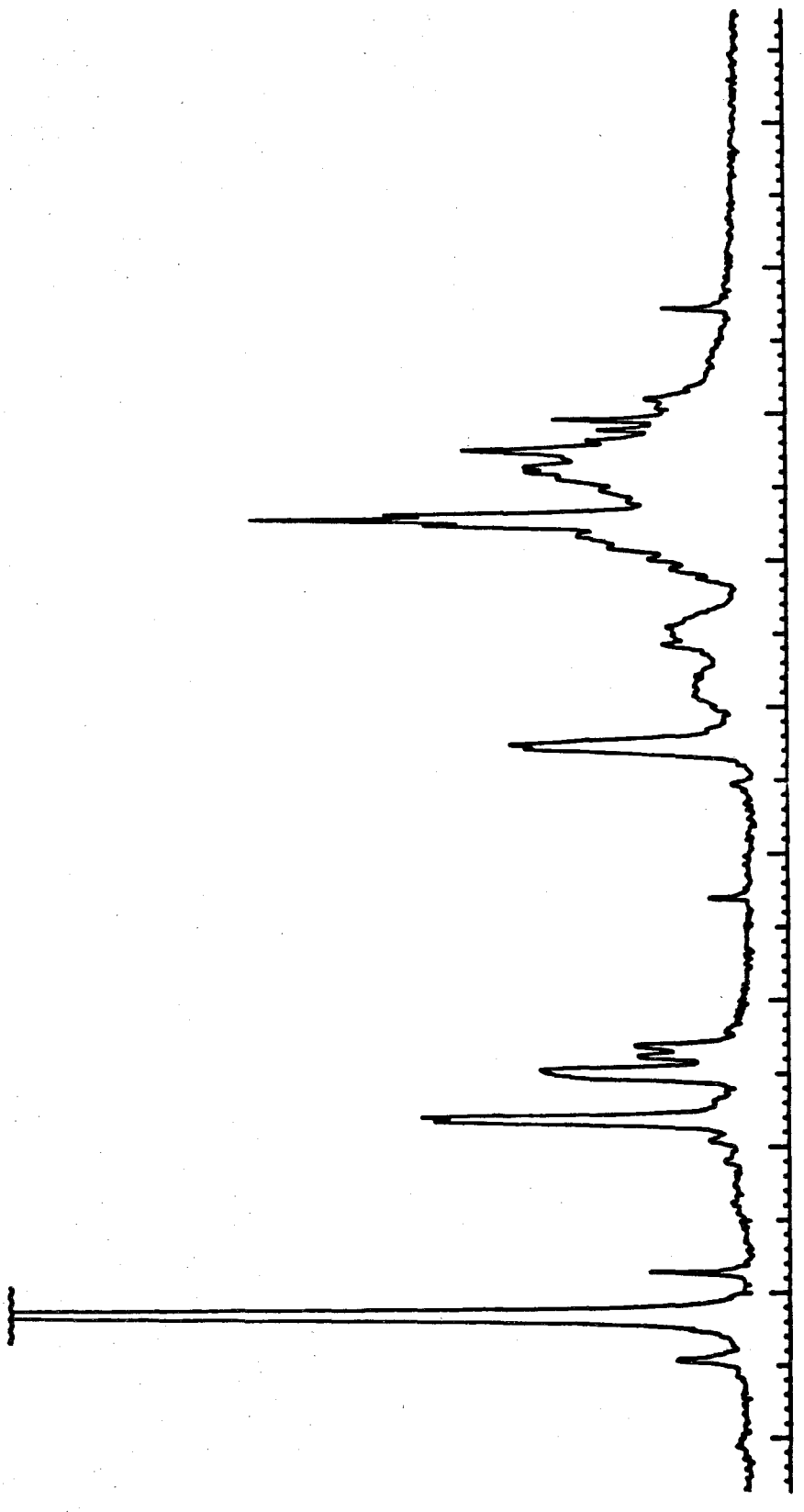

Figure 4.8. ^{1}H NMR of a PBV:polynorbornene (1:1.2) block copolymer in C_6D_6. Some of the signals from 1.2 to .9 ppm are the result of residual hexane.

Thermochemical Properties of PBV:

As mentioned earlier, **PBV** has interesting properties as a result of its high strain energy. The amount of strain energy can be measured by experimentally determining the heat of formation of **PBV**. The strain energy is defined as the difference in the heat of formation of the material of interest and that expected for a strainless molecule with the same atoms and chemical bonds.[14] By the use of Franklin's constants, the heat of formation of a hypothetical strainless repeating unit is calculated to be 14.5 kcal/mole.[14] The heat of formation was experimentally determined with bomb calorimetry to be 65 kcal/mole on a sample of **PBV** synthesized with **6** after storage for approximately one week at RT. Hence, the measured strain energy is calculated to be 51 kcal/mole. This measurement is compared with the strain energy of the bicyclobutane unit which is 64 kcal/mole. The lower than expected heat of formation is the result of partial decomposition of the sample.

The thermal transformation of **PBV** into **PA** is an attractive goal. Bicyclobutanes rearrange to 1,3-dienes at approximately 150°C to 200° C.[8] Hence, it was hoped that this process would constitute a mild thermal conversion of **PBV** to **PA**. Differential scanning calorimetry (DSC) of **PBV** reveals major exothermic processes at 153°C and 308°C as is shown in Figure 4.9. Reheating of the same sample after one run indicates an approximate position for the baseline. Integration of freshly prepared **PBV** from 50°C to 420°C reveals the liberation of 59 kcal/mole per repeating unit. **PBV** synthesized with all three catalysts showed the same behavior. However, **PBV** produced with **8** displayed a broader thermogram with a slightly lower integration of 51 kcal/mol per repeating unit. The exotherm at 153°C is in the right thermal range for the desired chemistry.

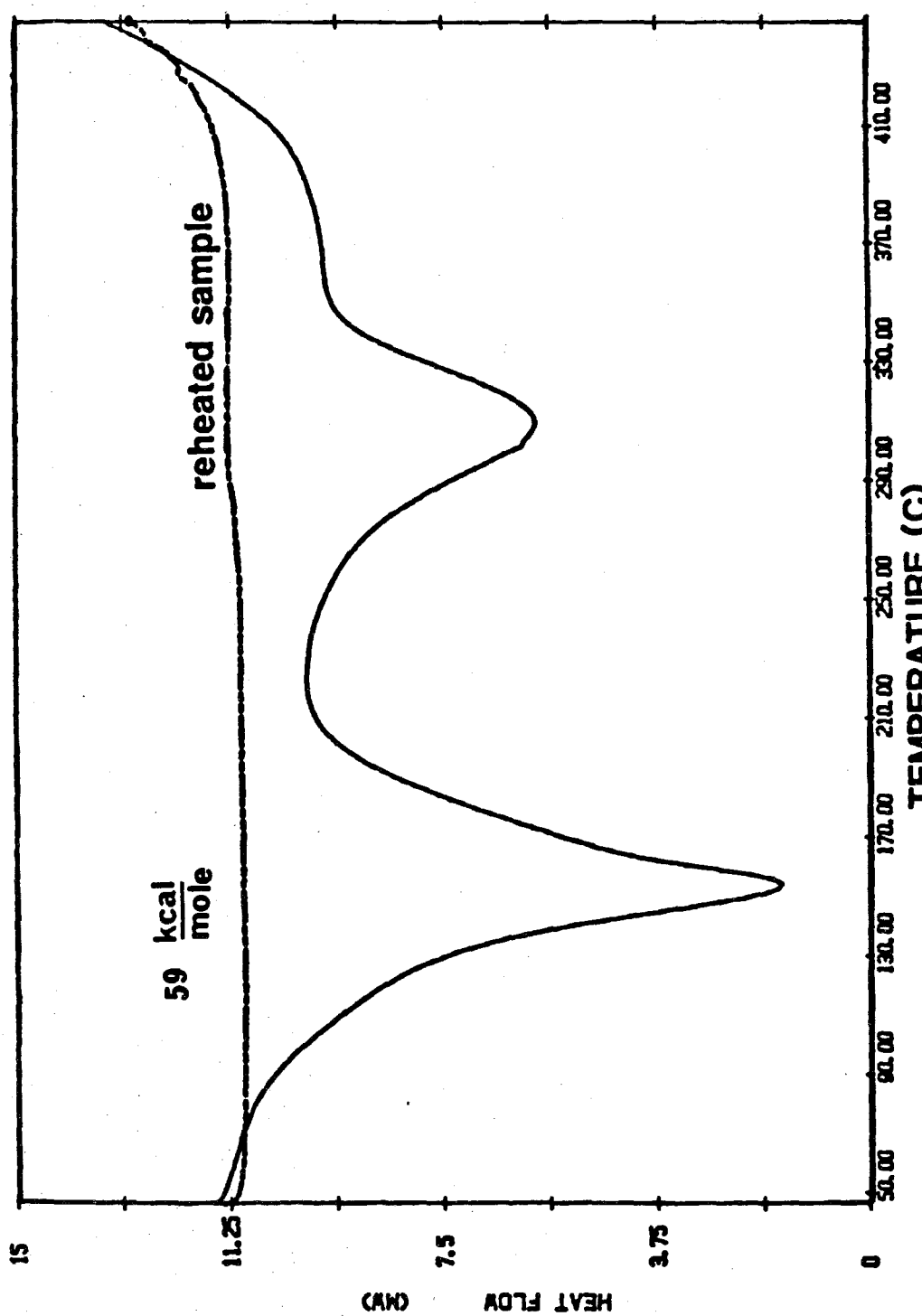

Figure 4.9. DSC thermogram of PBV at a scanning rate of 10°C per minute.

Samples that had been stored for two months at room temperature displayed a similar DSC trace to that which is shown in Figure 4.8. The exotherms of these materials were considerably broader and the 153°C peak is shifted to 174°C. Integration from 50°C to 380°C reveals approximately 75% of the chemical energy is retained.

Thermogravimetric analysis of **PBV** as shown in Figure 4.10 indicates that minor weight loss begins with the second exotherm and that major weight loss occurs at approximately 400°C. Thermomechanical analysis (Figure 4.11) revealed an expansion of the material at 150°C. The postulated ring opening of the bicyclobutanes is consistent with an expansion of the material since the ring opening produces a longer linkage of carbon atoms in the polymer backbone. Thermomechanical analysis also shows a contraction of the sample with the 308°C exotherm. Thus, the thermal analysis suggests that the desired chemistry may be occurring to some degree in the 153°C exotherm, but the 308°C exotherm is due to decomposition.

Samples of **PBV** that were thermally treated at 150 to 200°C resulted in dark brown materials which did not absorb iodine. It was noticed that a small amount of oxygen present in the thermolysis produced black and shiny materials. However, these materials could not be made to conduct with I_2 or AsF_5 doping. Solid state CPMAS ^{13}C NMR of thermalized samples reveals extremely broad signals. A CPMAS ^{13}C NMR of **PBV** after thermolysis at 300°C for 3 hours is shown in Figure 4.12. The extremely broad nature of this peak indicates that the thermal chemistry is extremely unselective and gives rise to a range of carbon centers with different environments.

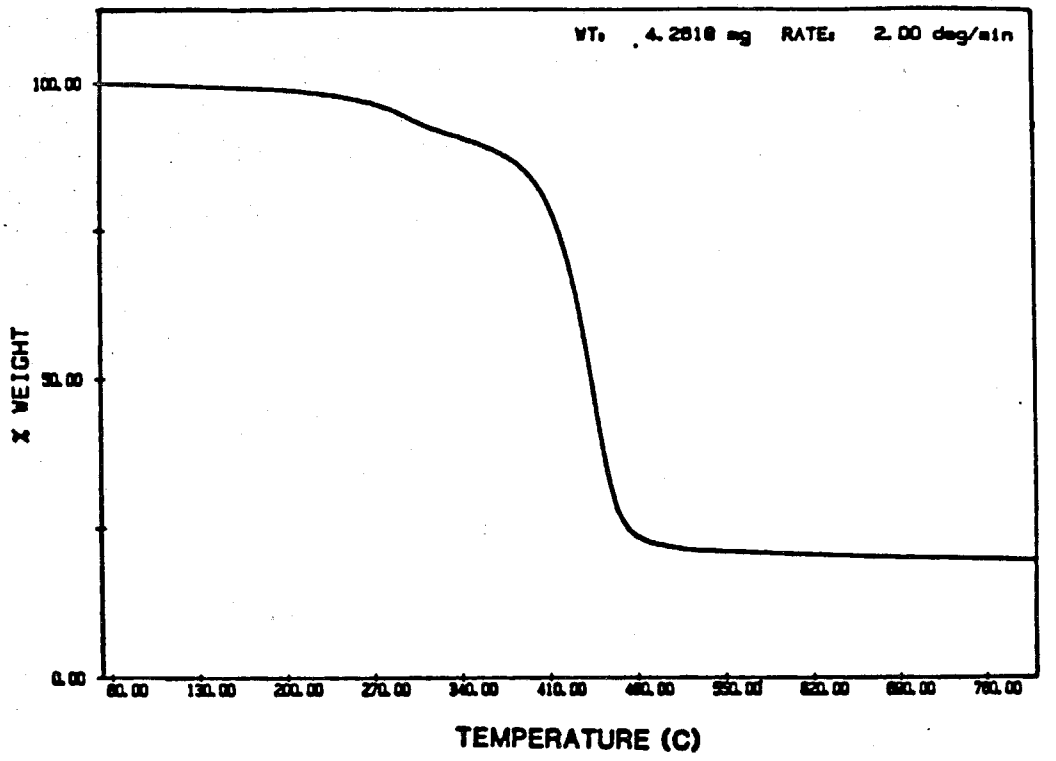

Figure 4.10. Thermogravimetric analysis of PBV .

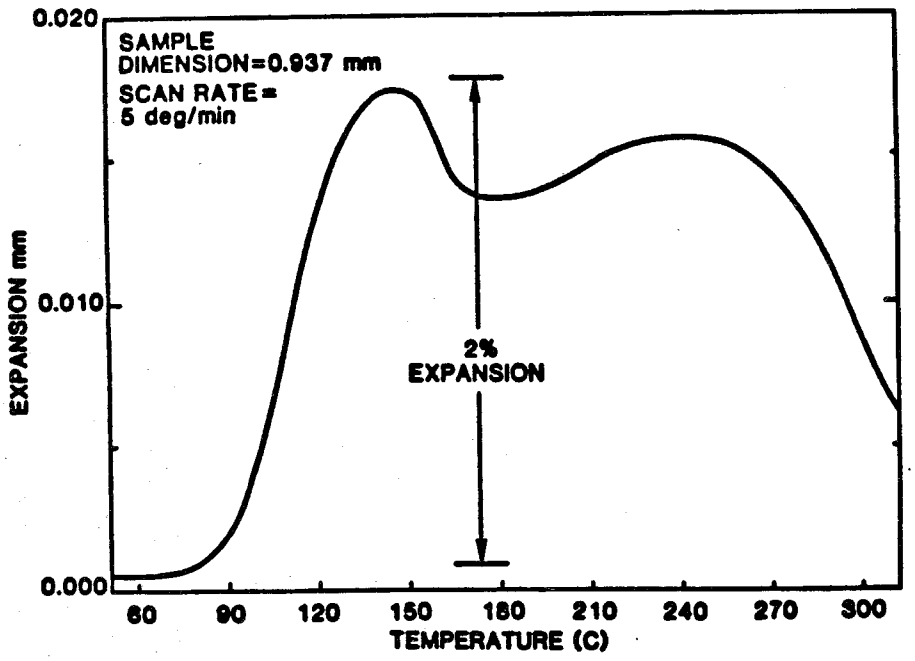

Figure 4.11 Thermomechanical analysis of PBV with approximately a 2.5 gram/cm^2 load.

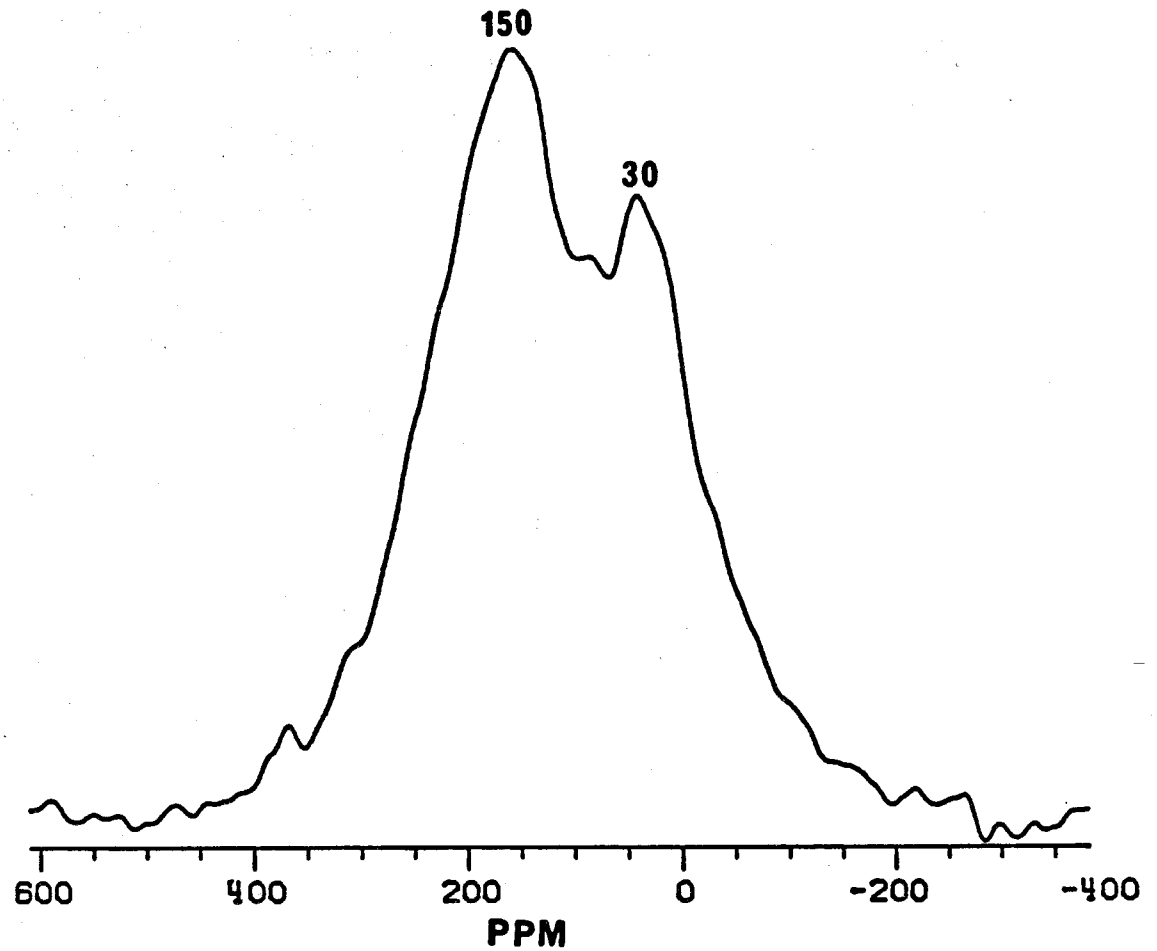

Figure 4.12. CPMAS ^{13}C NMR of **PBV** heated to 300°C for 3 hr.

Although photochemical ring-openings of bicyclobutanes are known, attempts at photochemically promoting the isomerization of **PBV** to **PA** were also unsuccessful. **PBV** was photolyzed with a mercury arc lamp (350 watts) in a quartz tube with and without triplet sensitizers with no observable change. Illumination with a 193 nm laser light (ArF excimer laser) with a peak power of 30 megawatts was also performed. This also produced no visible change other a tearing of the film due to the impact of the laser pulse. Hence, photochemical methods do not appear to be efficient at opening the bicyclobutane rings.

Chemical Isomerization of PBV:

With the difficulties encountered in the thermal chemistry, chemical methods of opening the bicyclobutane rings were pursued. The conversion of bicyclobutanes into 1,3-dienes with silver ion has seen considerable investigation.[10] Silver ion is a highly selective catalyst for this transformation. The preservation of stereochemistry during this isomerization has led to the suggestion that it may be a conserted reaction.[10] Treatment with Ag^+ ion in THF transforms the **PBV** film into a dull slivery-black film that resembles **PA** in appearance. CPMAS ^{13}C NMR (Figure 4.13) confirms that **PA** has been formed with the Ag^+ treatment (Scheme 4.5). The 135 ppm peak corresponds to *trans* olefins and the 127 ppm indicates the presence of *cis* olefins.[28] Ag^+ salts have been demonstrated to oxidatively dope **PA**.[29] Hence, as **PA** is produced, Ag° is also deposited in the material. This material exhibits a conductivity before doping of $\approx 10^{-8}\ \Omega^{-1}cm^{-1}$. I_2 doping produced materials with low conductivities of $\approx 10^{-4}$-$10^{-6}\ \Omega^{-1}cm^{-1}$. There was a noticeable amount of white AgI formed with the I_2 treatment. The deposition of silver into the **PA** is a problem and may be the cause of the low conductivities observed in this material.

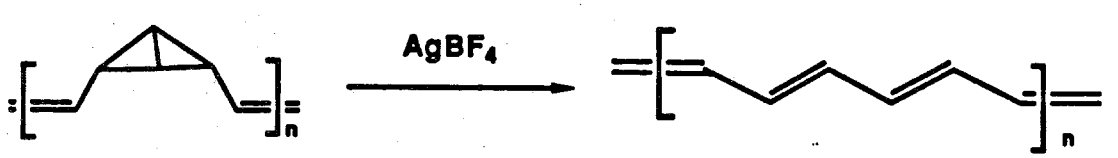

Scheme 4.5

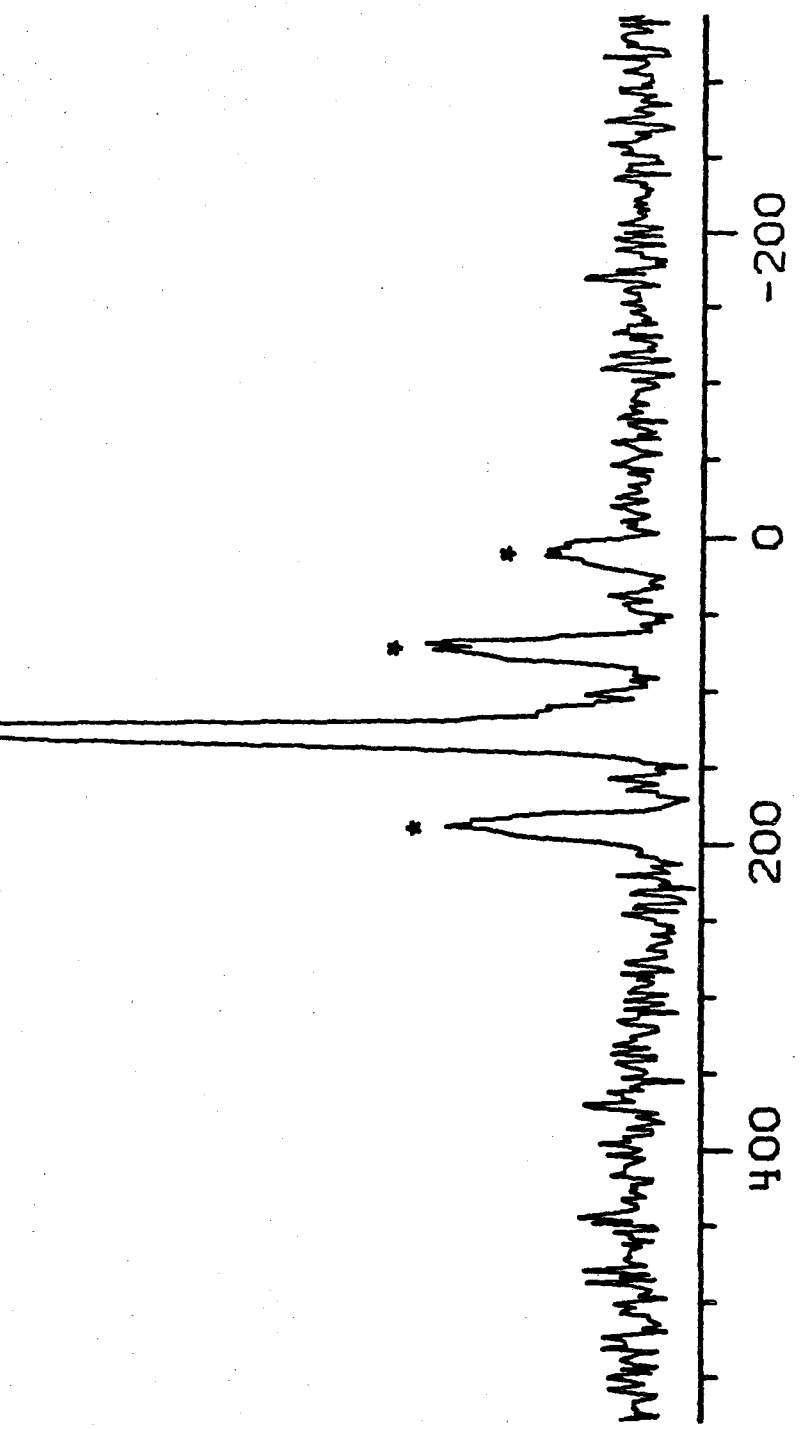

Figure 4.13. CPMAS ^{13}C NMR of PA produced from treatment of PBV with $AgBF_4$. (*)'s indicate spinning sidebands.

Gassman reported the isomerization of tricyclo[4.1.0.0^{2,7}]heptane by a variety of Lewis acidic catalysts.[10b] The results of interest are summarized below in Table 4.1. Again, the most selective catalyst was the silver ion. However, some of the other catalysts also gave the 1,3-diene as the major product. Thus, the isomerization of **PBV** by the catalysts shown in Table 4.1 was investigated.

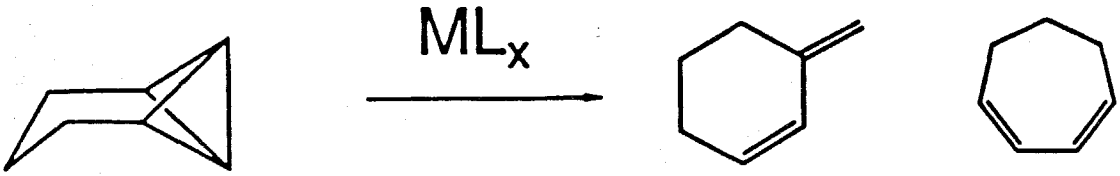

10 **11**

TABLE 4.1

From Gassman reference 10b

CATALYST	% YIELD OF PRODUCTS	
	10	**11**
$AgBF_4$	0	100
ZnI_2	11	88
$HgBr_2$	8	85
$[Rh(CO)_2Cl]_2$	98	0

PBV was isomerized with catalysts similar to those used by Gassman and the results are summarized in Table 4.2. These transformations were performed by soaking freshly cast films of PBV in a THF solution of the catalyst. The catalyst is then washed from the films. As would have been predicted based on Gassman's results, it appears that $AgBF_4$, $HgBr_2$, $HgCl_2$ and ZnI_2 give a high yield of olefins. Isomerization with $HgCl_2$ in addition to yielding materials exhibiting the highest conductivity gave materials with excellent mechanical properties. This material is extremely durable and has a qualitatively high tensile strength. As a result of the superior properties exhibited by the material produced with $HgCl_2$, studies were focused on this material.

TABLE 4.2

Isomerization of PBV

Catalyst	Appearance	Conductivity† undoped	Conductivity† Saturated with I_2
$AgBF_4$	Silvery-black dull	$\sigma=10^{-8}$	$\sigma=10^{-4}$
ZnI_2	Black shiny	$\sigma=10^{-6}$	$\sigma=.2$
$HgBr_2$	Black shiny	$\sigma=10^{-7}$	$\sigma=.1$
$HgCl_2$	Silvery-black shiny	$\sigma=10^{-5}$	$\sigma=1.0$
$[Rh(COD)Cl]_2$	Burgundy-red	-	$\sigma=10^{-6}$

† in $\Omega^{-1}cm^{-1}$

Further study of the $HgCl_2$ isomerized material demonstrates that it does indeed produce **PA**. To distinguish the material from $HgCl_2$ isomerization of **PBV** from other forms of **PA**, this material will be called "Pasadena polyacetylene" (**PPA**). UV-vis spectroscopy of **PPA** shows an absorption onset of 1.9 eV and a peak maxima of 2.8 eV. The absorption onset yields a band gap of 1.9 eV for this material. These values are compared with "Shirakawa **PA**" which has a band gap of 1.4 eV.[2] "Durham **PA**" in its *trans* unoriented form has a bandgap of 1.5 eV and an absorption maxima of 2.3 eV.[30] The higher energy band gap indicates that the conjugation lengths are shorter in **PPA** than these other forms of **PA**. Infrared spectroscopy of this material is shown in Figure 4.14. Broad major absorptions for *cis* and *trans* olefins are observed at 740 cm^{-1} and 1005 cm^{-1} respectively. The infrared spectra also reveal residual saturation as evidenced by the saturated C-H stretching band at 2800 cm^{-1}. Materials produced with $HgBr_2$ and ZnI_2 display similar spectra. The absorption bands are wide in comparison with Shirakawa **PA** as a result of a more disordered structure.[2] An infrared spectrum of **PPA** after thermal isomerization to *trans*-**PPA** is also shown in Figure 4.14. The broad nature of these spectra preclude a quantitative determination of the *cis* to *trans* content. However, a *cis:trans* ratio is estimated to be approximately 40:60. As described earlier, **PBV** is nearly exclusively *cis* before isomerization to **PPA**. Therefore, the bicyclobutane ring opening produces mainly *trans* olefins. A *Trans* preference is observed for the catalytic opening of other bicyclobutanes to acyclic dienes.[10]

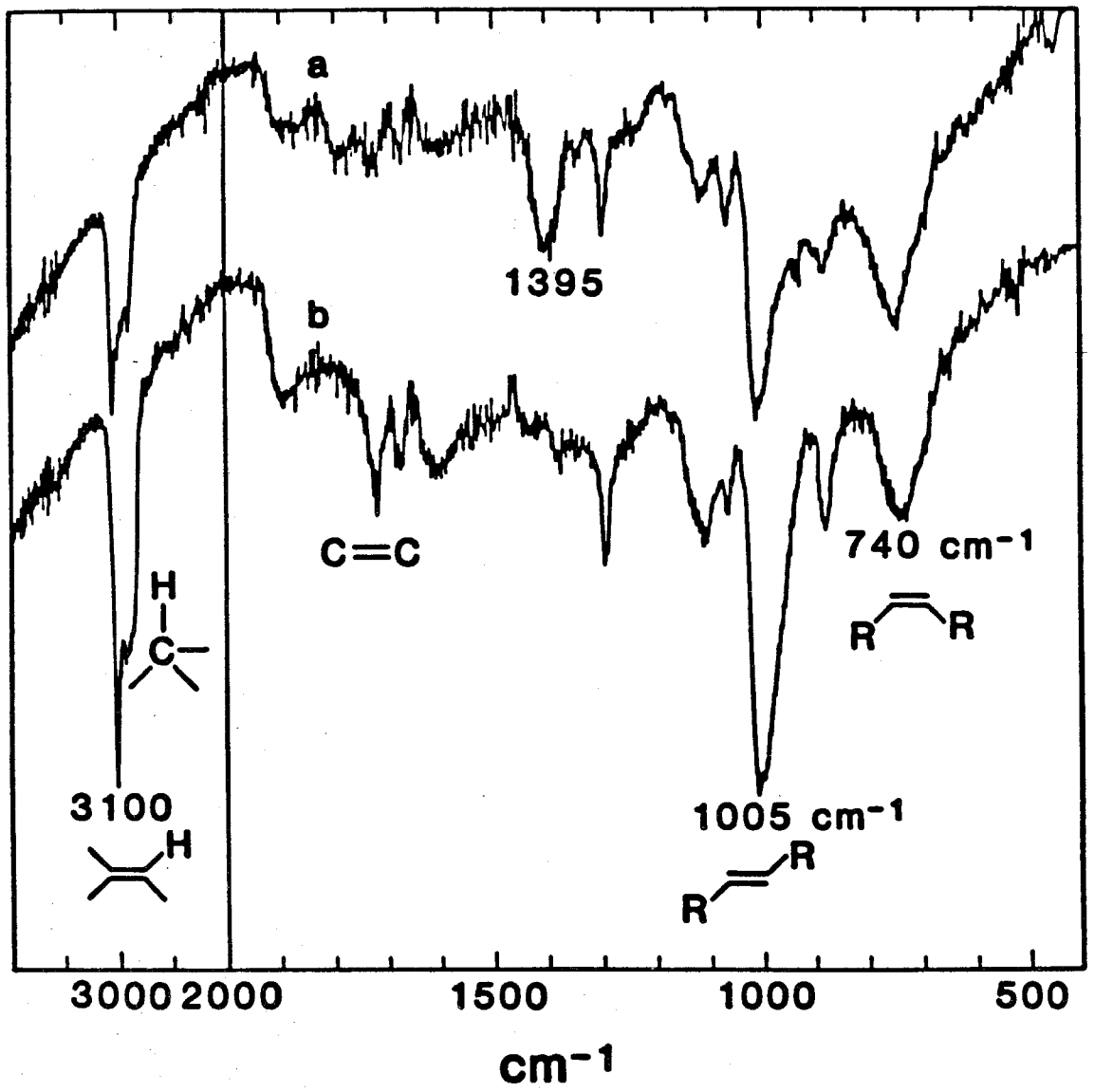

Figure 4.14 Infrared spectra of PPA as produced (a); and after thermal isomerization at 140°C for 6 hours (b).

CPMAS ^{13}C NMR also supports the conclusion that the $HgCl_2$ isomerization of **PBV** produces **PA**. **PPA** as produced is ductile and cannot be ground into a homogenous sample. A homogenous tightly packed sample is necessary to achieve the 3.5-5 kHz spinning rates required to achieve narrow lines and small spinning sidebands. *Trans*-**PA** is considerably more brittle than *cis*-**PA**,[2] and thus the samples were first isomerized at 150°C for 6 hours. The resulting materials were readily ground and the ^{13}C NMR spectrum is shown in Figure 4.15. The peak at 135.5 ppm is in agreement with *trans*-**PA** produced by other routes.[28] There is also an additional peak at 40 ppm which is indicative of saturated carbon centers.[25] At longer cross-polarization contact times this peak is diminished. At a contact time of 10 ms, only the 135 ppm peak is observed. This relaxation behavior indicates that the carbons responsible for the 40 ppm resonance are in a more rigid environment and hence have a shorter $T_1\rho$ than the 135.5 ppm signal.[31] A more rigid environment is consistent with these carbon centers resulting from crosslinking. Quantitative measurements of the amount of saturated material in **PPA** were performed at a cross-polarization contact time of 2 ms. Integration determined the **PPA** to contain 10 - 19% of saturated material.

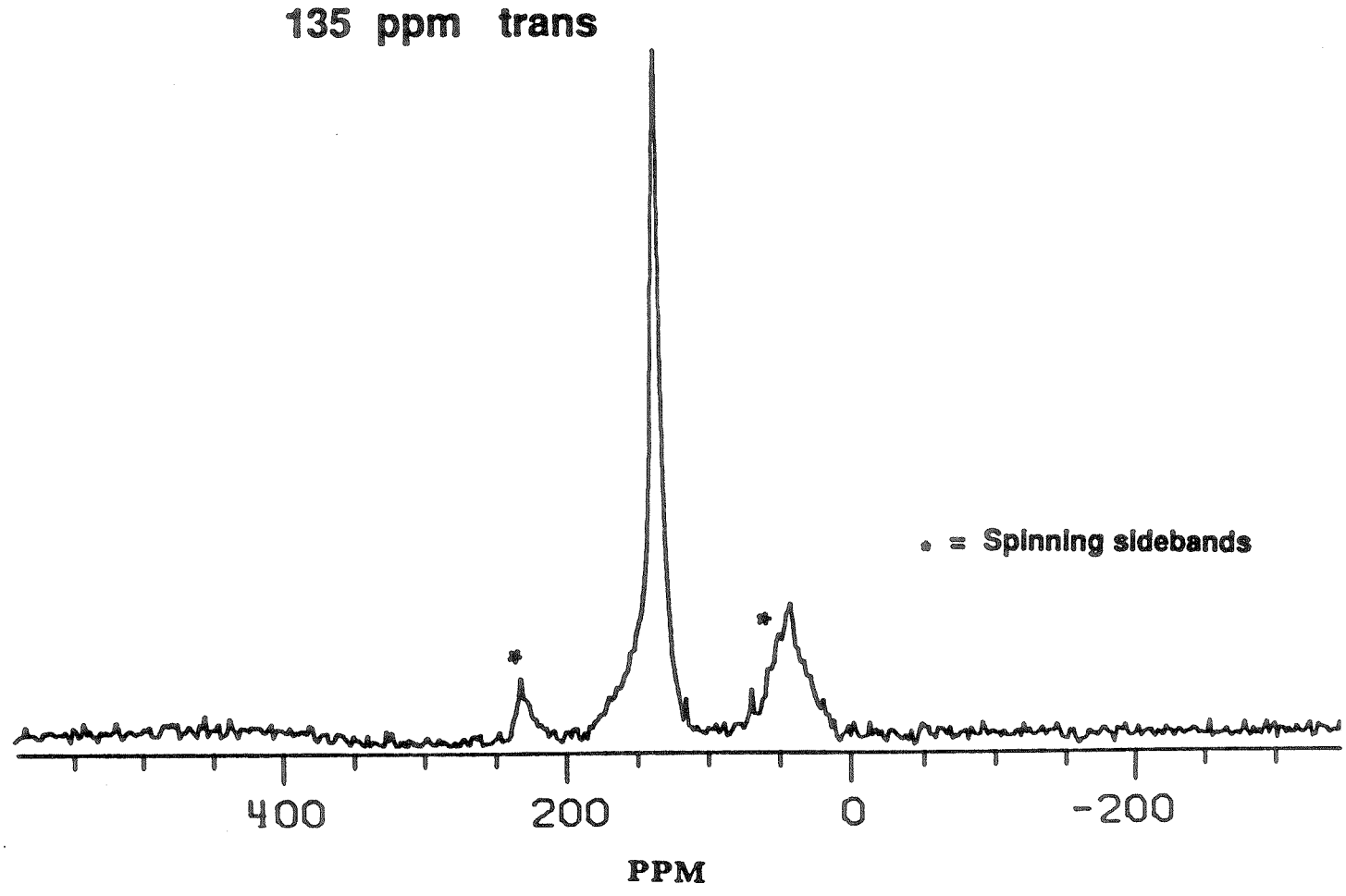

Figure 4.15 CPMAS ^{13}C NMR of *trans*-PPA after thermal isomerization at 150°C for 6 hours.

Other chemical isomerizations of PBV were attempted. Treatment with H_2SO_4 produced shiny black materials, but these materials could not be made conductive. Br_2 treatment caused the films to swell in size, indicating chemical addition to the polymer. These materials were light brown in color and are insulators. I_2 doping changes PBV into a black shiny material which displayed conductivities of $\approx 10^{-4}\Omega^{-1}cm^{-1}$. These materials were brittle and easily broken. A CPMAS ^{13}C NMR spectrum of I_2 treated material is shown in Figure 4.16. This spectrumeveals that approximately 60% of the carbon atoms of this material are sp^2 carbons. As was seen in Chapter 1, I_2 doping produces delocalized carbocations. These species are characterized by the olefinic peak which extends to 230 ppm.

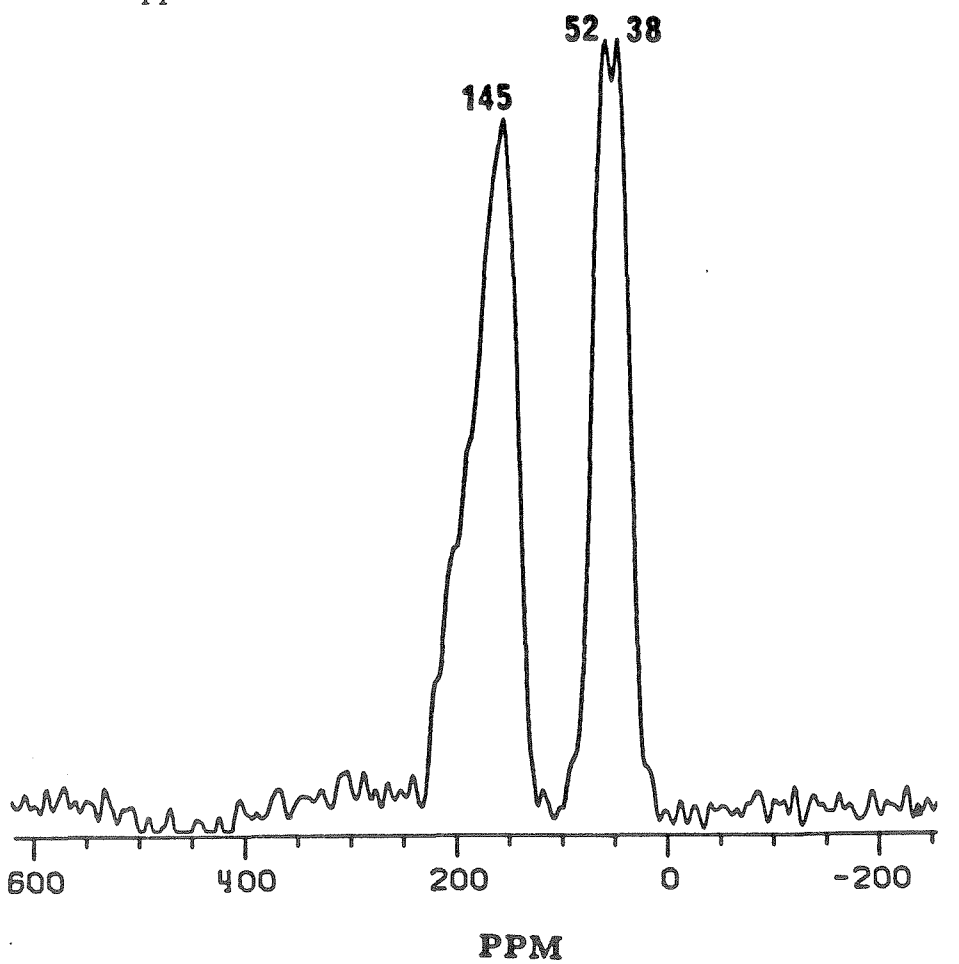

Figure 4.16. CPMAS ^{13}C NMR of PBV after treatment with I_2 vapor.

Morphology of PPA:

The conductivity of conductive polymers is known to increase with increasing crystallinity.[1] This is a consequence of an number of factors which include greater carrier mobility in a more rigid lattice, higher conjugation lengths, and better interchain overlap. An advantage of a percursor route is the fact that a variety of morphologies can be produced depending on the processing. Hence, the morphology of **PPA** was studied.

Scanning electron microscopy (SEM) indicates a smooth totally featureless morphology for **PBV**. After isomerization to **PPA** , the surface is still smooth and devoid of the fibular morphology observed in Shirakawa **PA**. However, as shown in Figure 4.17 SEM shows the surface to have stress lines. Hence, the isomerization of **PBV** to **PPA** produces stress as a result of the volume changes that occur with isomerization.

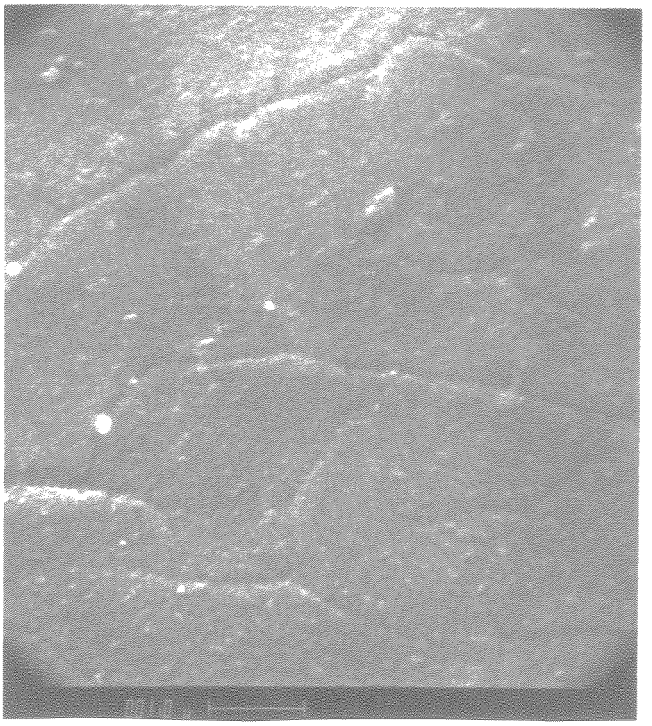

Figure 4.17 Scanning electron micrograph of **PPA** at a magnification of 12,000.

X-ray diffraction indicates a low level of crystallinity in these materials. A plot of X-ray (CuKα) diffraction intensity of **PBV**, and the **PPA** as produced before and after thermal isomerization, is shown in Figure 4.18. **PBV** exhibits a maxima at $2\theta = 17.6°$ which corresponds to a d-spacing of 5.21 Å.[32] This peak is superimposed with a very broad and asymmetric peak. **PPA** exhibits a characteristic **PA** diffraction peak at $2\theta = 23°$, which corresponds to a d-spacing of 3.80Å. The full width at half height ($w_{\frac{1}{2}}$) of **PPA** is $2\theta = 9.8°$, which is considerably broader than **PA** produced by other methods. For example, Shirakawa *cis*-**PA** has a $w_{\frac{1}{2}}$ of $2\theta = 1.5°$,[2] and unoriented Durham *cis*-**PA** has a $w_{\frac{1}{2}}$ of $2\theta = 4.0°$.[33] There is no noticeable change in **PPA** upon isomerization and annealing at 120°C (Figure 17b). The peak width of unoriented Durham **PA** was observed to narrow with thermal annealing to widths of $2\theta = 2.0°$.[33] The $2\theta = 23.4°$ peak of **PPA** is noticeably asymmetric with a shoulder at lower angles. This shoulder at higher d-spacing may be the result of crosslinks which cause the chains to distort from tight crystalline packing. Durham **PA** exhibits a nearly symmetric peak at 23°.[33] The tail of an intense amorphous halo is also observed. This scattering gives rise to the sloping baseline and overlaps the $2\theta = 23.4°$ peak. At larger angles there is a hint of a $2\theta = 43°$ reflection which corresponds to d = 2.1 Å. These results demonstrate that the morphology of **PPA** is considerably more amorphous than Durham **PA**.

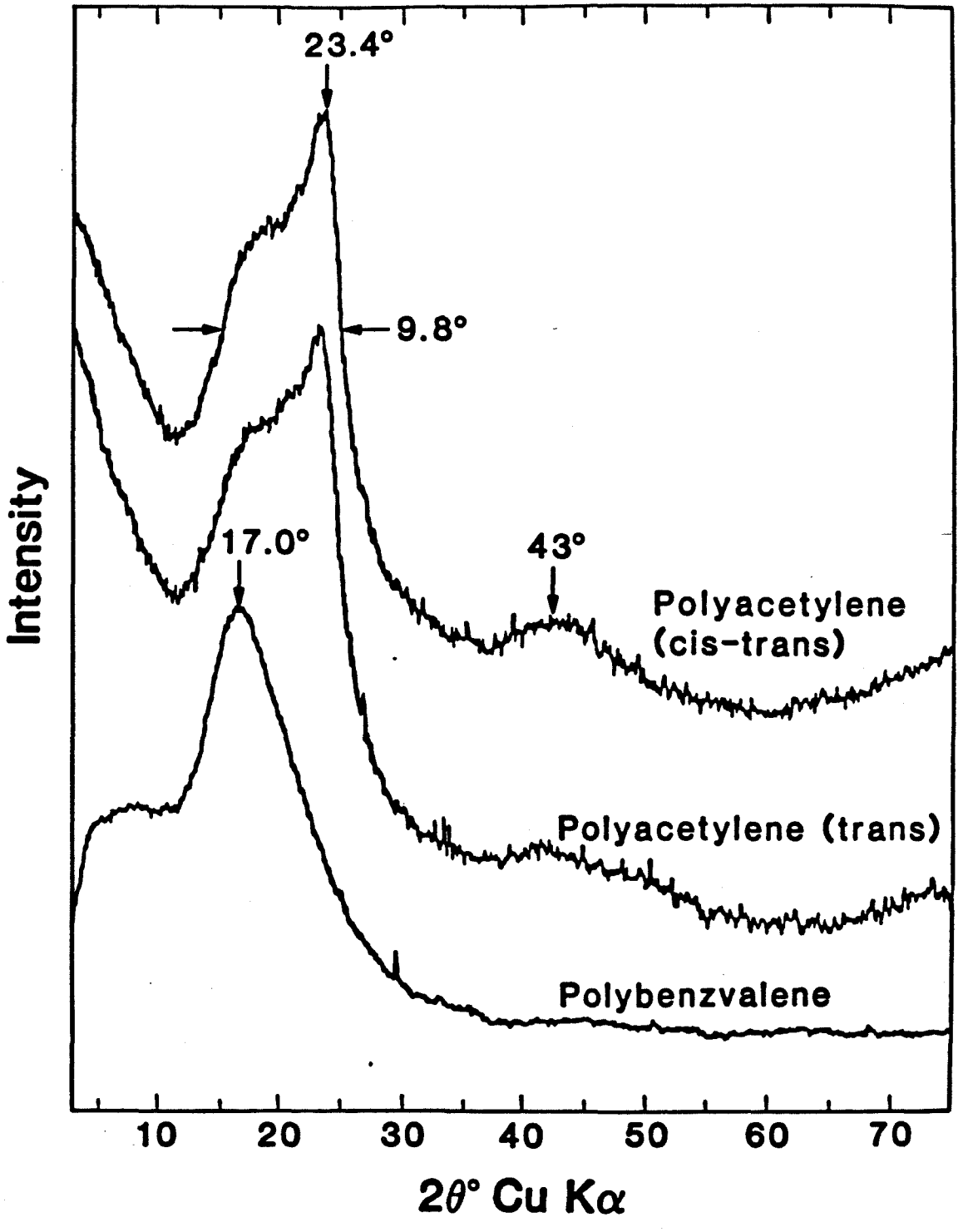

Figure 4.18. X-ray diffraction from films of PBV ; *cis-trans* PPA as produced; and *trans*-PPA after thermal isomerization at 120°C 48 hours.

PBV is a soft rubbery material and is readily stretched. Oriented **PPA** was produced by evaporating **PBV** films on polyethylene sheeting and then stretching. The polyethylene support held the **PBV** in an extended form and then both materials were immersed in a THF solution of $HgCl_2$. The **PPA** was then removed from the polyethylene backing as a strong flexible ribbon. Two different polyethylene sources were used (see experimental section). One support allowed the material to be stretched 2.3 times its length and the other 6.0 times the initial length. The conductivity of oriented **PPA** is higher, as was expected. The elongated **PPA** l/l_o= 2.3 and l/l_o= 6.0 displayed conductivities of 13 $\Omega^{-1}cm^{-1}$ and 49 $\Omega^{-1}cm^{-1}$ respectively when saturated with I_2 vapor.

SEM as shown in Figure 4.19 reveals a highly textured appearance for the elongated **PPA** . The material develops small troughs that are $\approx$ .5 microns apart. Higher magnification reveals that these materials have fibrils which are $\approx$200Å in diameter as shown in Figure 4.20.

Stretching polymers is well-known to induce crystallinity, and thus the oriented **PPA** above was studied by X-ray diffraction. X-ray diffraction intensity of oriented **PPA** $l/l_o = 6$ is shown in Figure 4.21. The X-ray diffraction was measured at two different orientations of the **PPA** with respect to the X-ray detection. The interchain diffraction is strong when the X-ray intensity is monitored perpendicular to the direction of orientation. The dramatic difference in intensity for the diffraction parallel confirms that the chains are indeed aligned in the stretching direction. The $2\theta = 23.4°$ peak is qualitatively the same for both elongations. However, the $l/l_o = 2.3$ material still exhibits some tailing at low angles ($\leq$10°) from an amorphous halo which is still present.

Figure 4.19 SEM of orientated **PPA** (l/l_0=6) at 2,000 magnification.

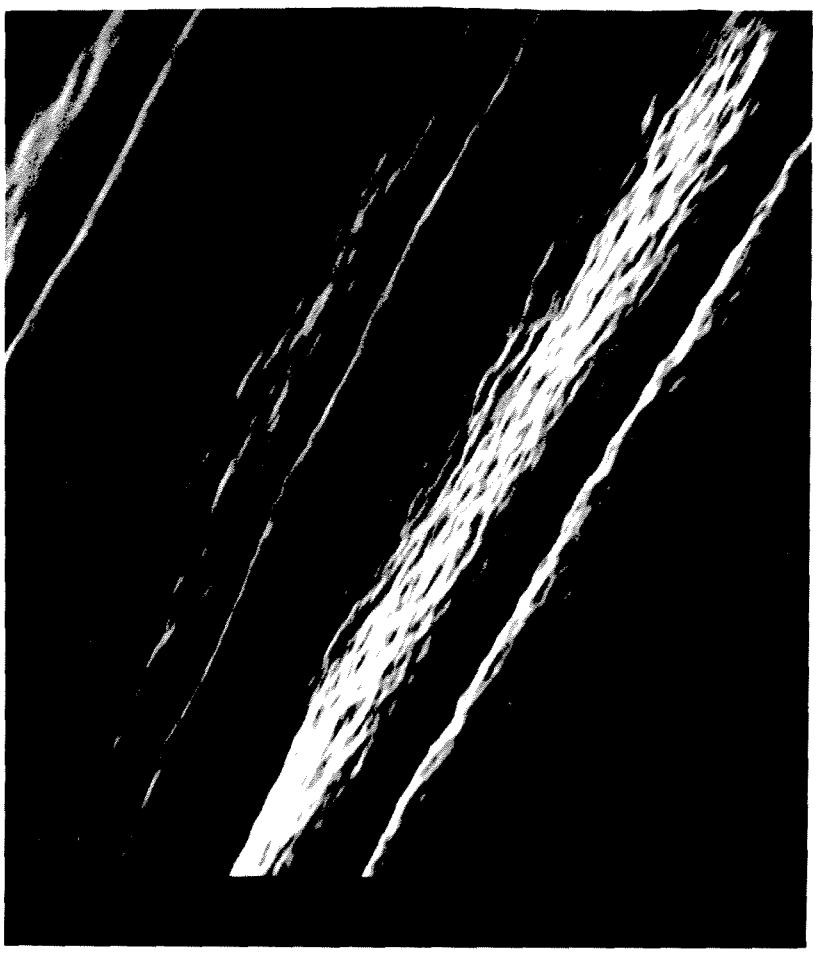

Figure 4.20 SEM of orientated **PPA** (l/l_0=6) at 30,000 magnification.

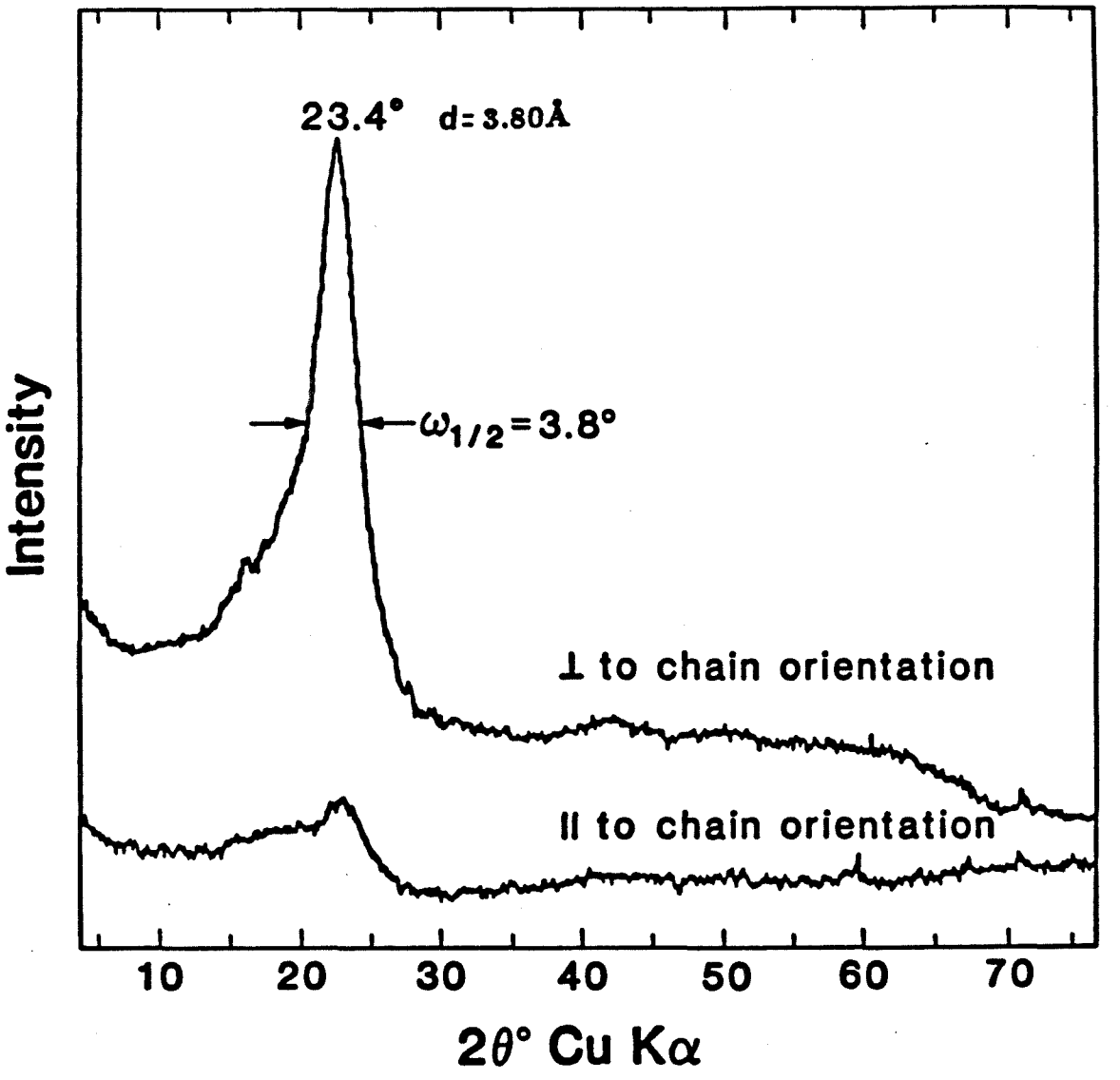

Figure 4.21 X-ray diffraction intensity of PPA (l/l_0=6). The interchain diffraction is strongest perpendicular to the direction of chain orientation and much weaker parallel to the direction of orientation.

Morphology of Block Copolymers:

Binary polymer blends usually phase separate even when the two materials are very similar in structure. This is a consequence of the fact that polymers exhibit a very low entropy of mixing, the thermodynamic driving force which is responsible for the mixing of simple fluids.[34] Block copolymers are well-known to compatibilize polymers which would phase separate as a blend and produce materials without phase separation.[35] The block copolymer of **PBV** and polynorbornene discussed earlier was shown to exist as a single phase. This conclusion is based on DSC, which showed no detectable glass transition for polynorbornene. The polynorbornene block should have a T_g in the range of 30°C to 40°C. However, the DSC thermogram displayed displays no phase transitions over the region of 20°C to 50°C. The molecular weight of each block should theoretically be approximately 50 repeating units. Shorter segments such as these will have less of a tendency to phase separate than higher molecular weight materials.[35] In addition the similarity in the structure of polynorbornene and **PBV** helps to produce a single phase. The isomerization of the **PBV** to **PPA** in the block copolymer may provide a unique morphology in which the **PPA** is intimately dispersed with the polynorbornene. However, once the **PBV** is isomerized to **PPA** DSC reveals a polynorbornene glass transition at 38°C which indicates that some phase separation has occurred.

The morphology of the block copolymers was manipulated by stretching the **PPA**:polynorbornene block copolymers to 6 times their original length and then isomerizing the **PBV** to **PPA** with $HgCl_2$ in acetone. A block copolymer of **PBV**:polynorbornene (1:1.2) was so treated, and oriented (l/l_0=6) ribbons of **PPA**:polynorbornene were produced. This oriented material exhibited a conductivity of .37 $\Omega^{-1}cm^{-1}$ when saturated with I_2. The decrease by a factor of 10^2 from that of the **PA** homopolymer (l/l_0=6) is more than a dilution effect. SEM as

shown in Figure 4.22 reveals that the material has a much smoother appearance than the **PA** homopolymer. Also, it appears that the polynorbornene has the effect of allowing the material to relax (flow) to relieve stress. This is more clearly seen in the SEM shown in Figure 4.23a. There is only a hint of any fibrillation in this material when viewed at high magnification (Figure 4.23b).

X-ray diffraction results of the oriented **PPA**:polyorbornene block copolymer discussed above is shown in Figure 4.24. The diffraction is dominated by a large intensity 2θ=19.6° peak which corresponds to a d-spacing of 4.67Å. This diffraction is isotropic since it displays approximately the same intensity at both orientations. The diffraction perpendicular shows only a hint of the 23.4° interchain polyacetylene diffraction. The 23.4° peak is a result of **PPA** which has phase separated from the polynorbornene. Thus, it appears that the polynorbornene has the effect of increasing the interplane spacing of the **PPA** chains. These results suggest that the **PPA**:polynorbornene block copolymer may mainly exist as a single phase.

Figure 4.22 SEM of the unoriented **PPA**:polynorbornene (1:1.2) block copolymer at 20,000 magnification (a); and the oriented block copolymer (l/l_o=6) at 3000 magnification (b).

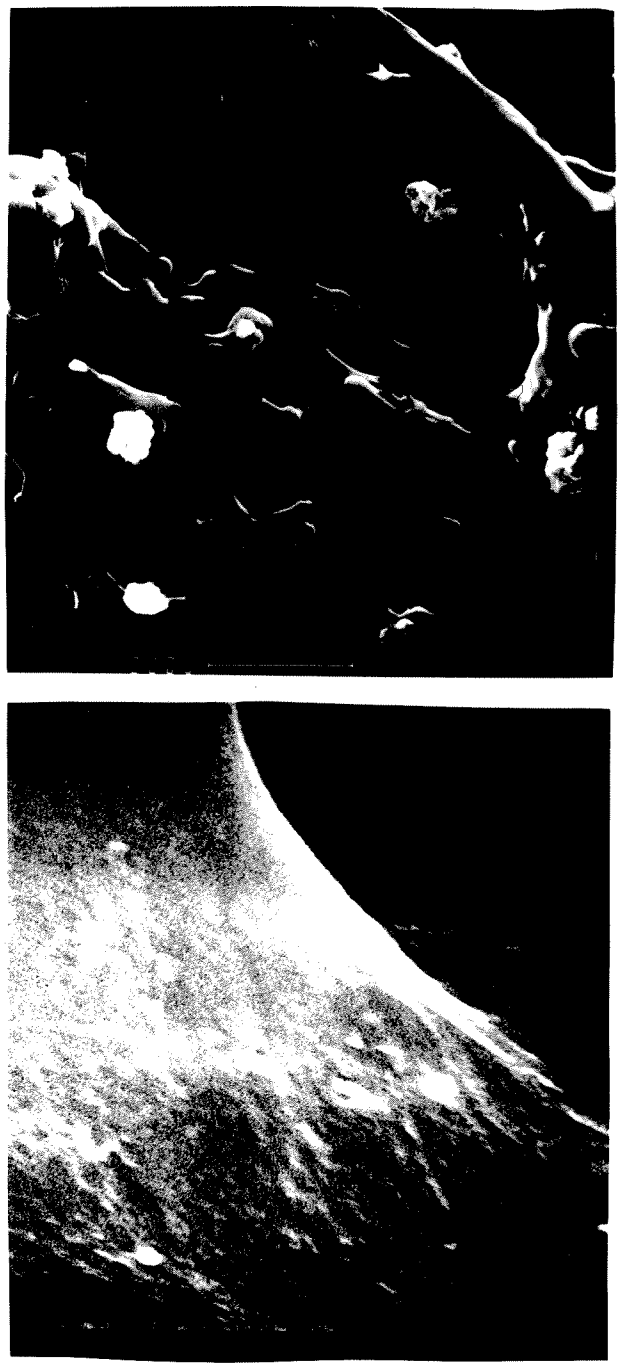

Figure 4.23 SEM of the oriented (l/l_o=6) **PPA**:polynorbornene block copolymer at 2,000 (a); and 30,000 (b) magnification.

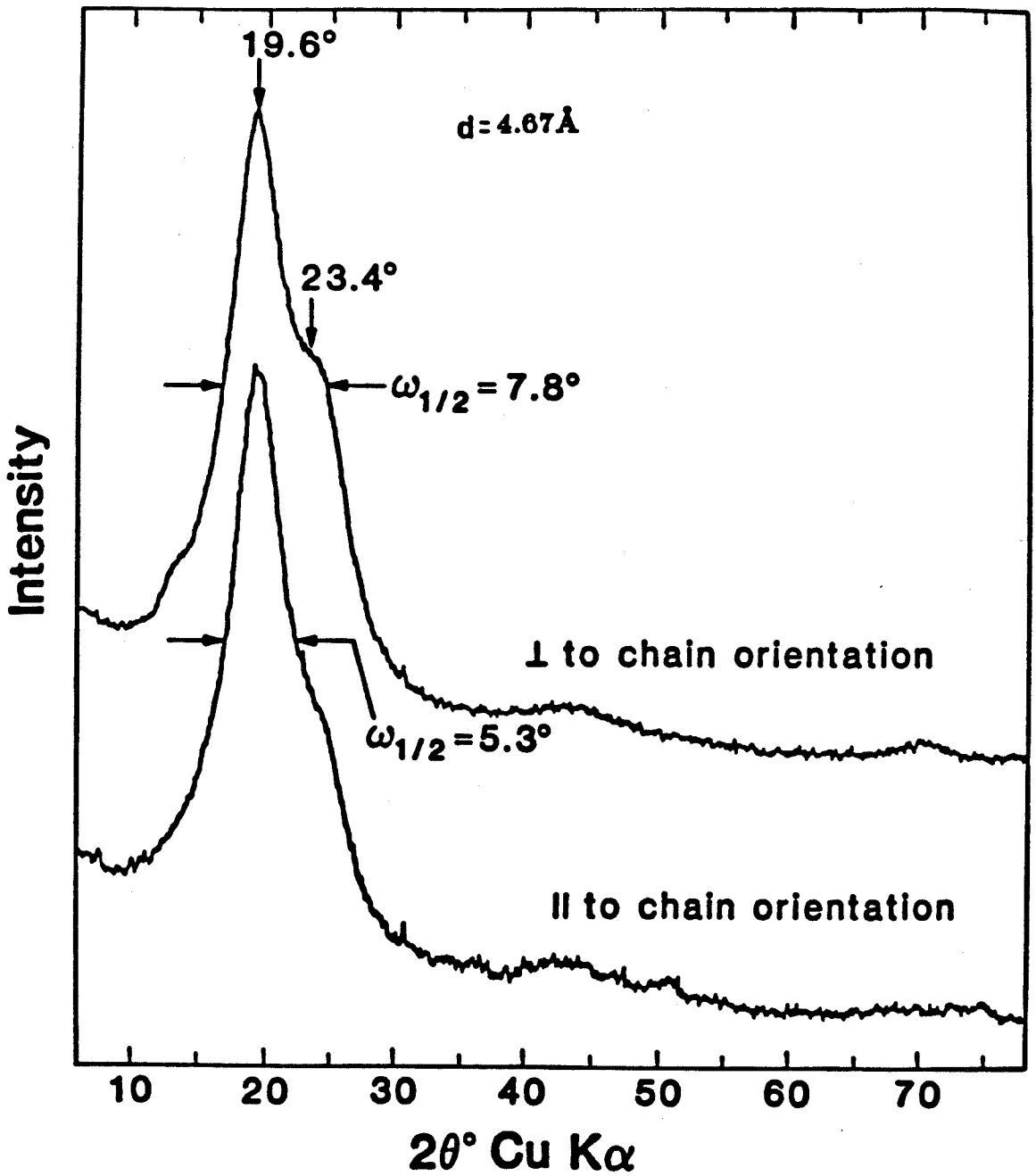

Figure 4.24 X-ray diffraction of the **PPA**:polynorbornene (1:1.2) block copolymer stretched to 6 times its length. The 19.6° peak is isotropic and the 23.4° peak is anisotropic, indicating partial orientation of some of the phase separated **PPA**.

Raman Spectroscopy:

Resonantly-enhanced Raman scattering has given insight to the conjugation lengths in **PA**.[30,36] The use of Raman dispersion to obtain quantitative information about conjugation lengths is controversial.[30] However, qualitative comparisons may be made by comparison with other forms of **PA**. The Raman bands of **PA** have a large dispersion with wavelength as a result of the distribution of bond orders arising from the distribution of conjugation lengths.[30] Preliminary studies of the Raman scattering from **PPA** are presented below. Two of the characteristic peaks for **PA** were observed and the spectra for the oriented and unoriented **PA** are shown in Figure 4.25. These peaks are at approximately 1200 cm^{-1} and 1500 cm^{-1} and correspond to the C-C and C=C stretching modes respectively. Higher conjugation lengths result in lower energy Raman bands. This effect is seen in the shift of the resonances from 1230 cm^{-1} to 1225 cm^{-1} and 1528 cm^{-1} to 1517 cm^{-1} with orientation (l/l_0=6). The C=C mode of Shirakawa **PA** has been found to be 1518 cm^{-1} at the same excitation frequency (488 nm). Hence, the unoriented **PPA** has a Raman band that is lower than Shirakawa **PA**, but the oriented material displays a band at the same frequency. Hence, the conjugation length of **PPA** is increased with orientation. The Raman spectrum for the **PPA**:polynorbornene block copolymer is shown in Figure 4.26. This material curiously displays peaks at 1225 cm^{-1} and 1511 cm^{-1}, indicating that the **PPA** block copolymer actually has a longer conjugation length than the **PPA** homopolymer. This may be the result of less crosslinking in the block copolymer than the homopolymer.

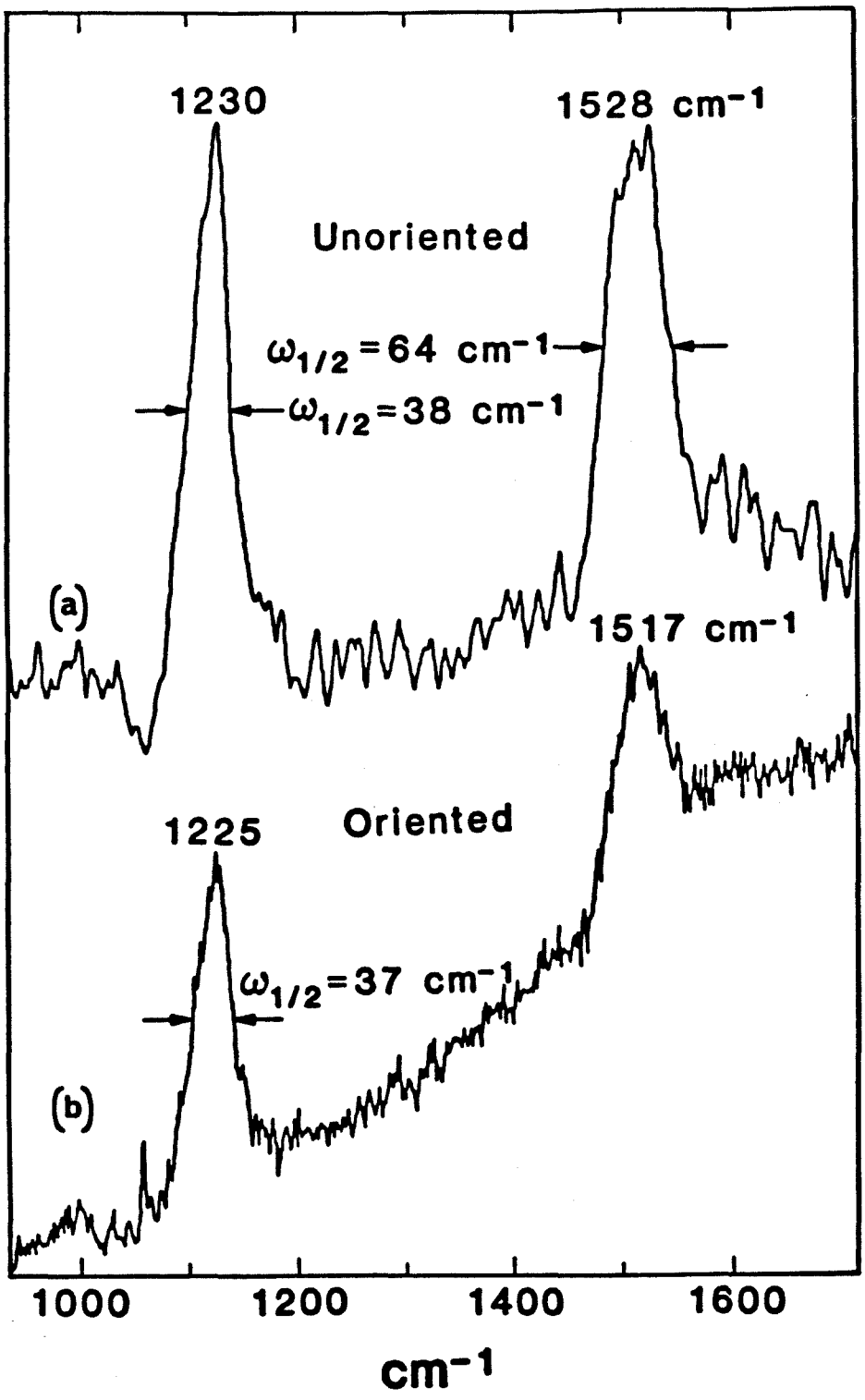

Figure 4.25 Raman spectra obtained with 488 nm laser light of the unoriented PPA (a) and the PPA stretched 6 times its length (b). The sloping baseline for b is an artifact of the experiment.

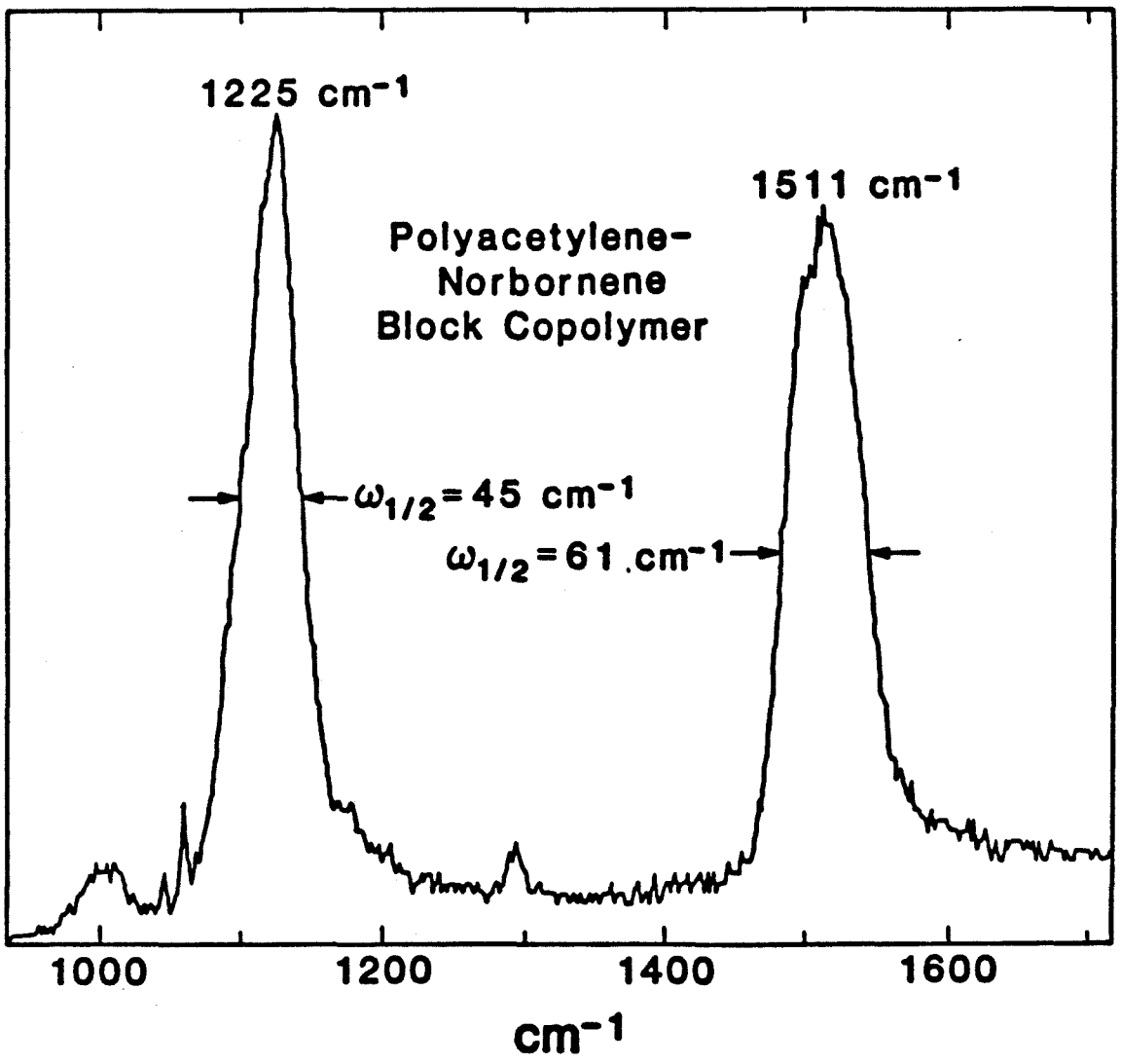

Figure 4.26 Raman scattering for the unoriented PPA:polynorbornene (1:1.2) block copolymer with 488 nm laser light.

FUTURE OUTLOOK:

The synthesis of **PBV** by **ROMP** is an accomplishment in itself and demonstrates the high selectivity of the currently available metathesis catalysts. Transition metals are well known to insert into strained bonds, and the center bond of the bicyclobutane group is one of the most strained single bonds known. Hence, this result is another indication of the extremely general nature of **ROMP** and that the future for this polymerization method is indeed bright.

The bicyclobutane is also one of the most energy rich carbon structures known with 16 kcal/mole C. By incorporating this and/or other strained structures into polymers, a wide range of high energy materials are available. This concept is being successfully exploited by E. J. Ginsburg in this group.

The use of cyclic structures to mask olefins represents a general concept in conductive polymer precursor methodology. While the limited stability of **PBV** presents technical problems, future systems may be designed that yield more slective chemistry and materials that are more easily handled. A straightforward extension of the work at hand is shown in Scheme 4.6. The dialdehyde (**11**) is made by reaction of **BV** with singlet oxygen.[37] Reaction of this molecule with **12** was investigated briefly by the author and found to cleanly produce the bis-Wittig product **13**. Hence, step growth polymerizations between **11** and bis-ylides should produce polymers. A polymer that could be synthesized by this method is shown in Scheme 4.7. Opening of the bicyclobutanes will produce **14**, which will likely be a good conductor. Other aromatic groups and heterocycles may also be applied in this scheme.

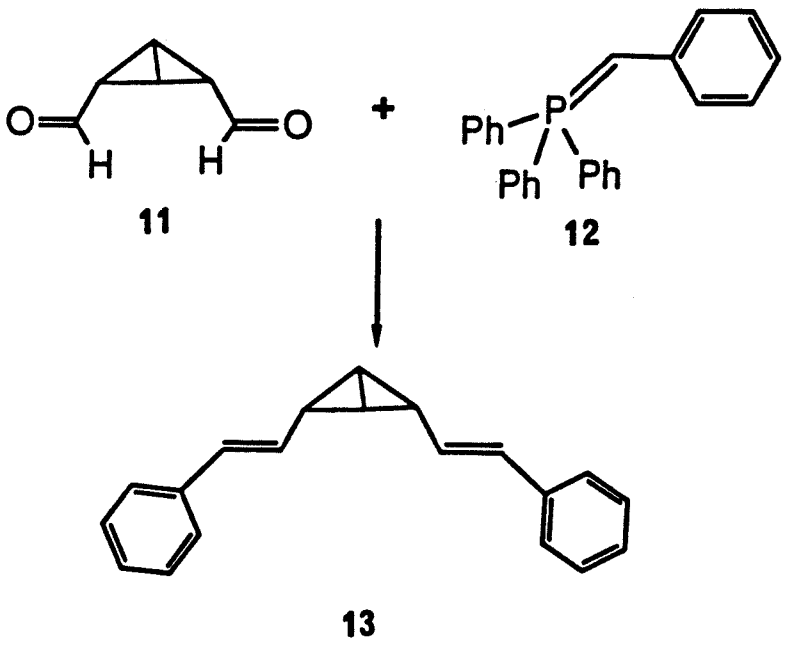

11 12 13

Scheme 4.6

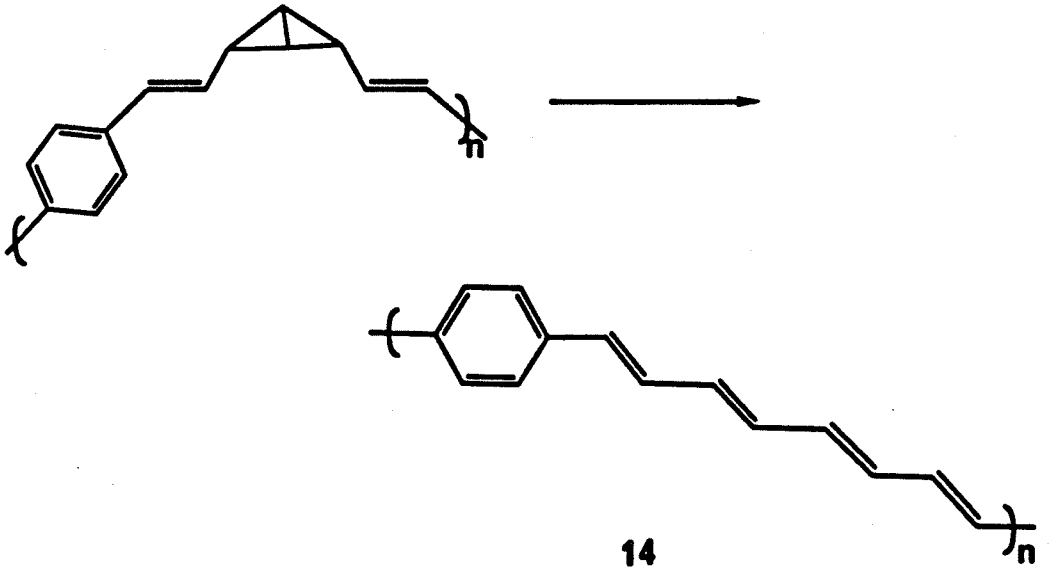

14

Scheme 4.7

Experimental Section:

General Procedures: All manipulations of air- and/or moisture-sensitive compounds were carried out using standard Schlenk or vacuum line techniques. The flush gas (argon) was purified by passage through columns of activated BASF RS-11 (Chemalog^{TM}) oxygen scavenger and Linde 4 Å molecular sieves. Manipulation of solids and film casting was performed in a Vacuum Atmospheres glove box equipped with a MO-40-1 purification train. The purification train was charged with activated Ridox^{TM} oxygen scavenger and Linde 11 Å molecular sieves. When dealing with moisture sensitive materials, all glassware was rinsed with base, dried in a 140°C oven, and subjected to vacuum while hot.

^{1}H and ^{13}C NMR were recorded on a Joel FX-90Q spectrometer (89.6 MHz ^{1}H, 23.53 MHz ^{13}C). Chemical shifts were referenced to the solvent (^{13}C NMR) or to residual protons in the solvent (^{1}H NMR). Infrared spectra were acquired on a Shimadzu IR-435 spectrometer. Infrared samples were free standing films of the polymer. UV-vis spectra were obtained on a HP-8451A diode array spectrometer. Samples for UV-vis analysis were films of $\approx$.1 micron thick.

The conductivity measurements were made with a home-built probe described in appendix B, or a commercial Sigmatone sheet resistivity probe. In the four point conductivity measurements,[38] current was supplied by a Power Designs 605 precision power source (.1-6 V), current was measured with a Keithley 160B digital multimeter (.1 to 10^{-10} amps.), and the voltage was measured with a Fluke 895A differential voltmeter.

Gel permeation chromatographic (GPC) analyses were performed utilizing a low resolution Alltech TSK-gel GMH6 column with toluene as a solvent. High resolution columns were not used as a result of residual catalyst in the polymer solution and the tendency for the polymer to decompose. Solutions directly from

the reaction mixtures were diluted and injected, and hence residual solvents were also present. Therefore, the GPC data is only a qualitative indication of the molecular weight. The polymer was detected with a Spectroflow 757 variable wavelength absorbance detector and a Knauer differential refractometer. Samples were prepared with .2% by weight polymer in toluene. Injection volumes of .10 ml were used with a flow rate of 1.5 ml/min. The molecular weights were referenced to narrow dispersity polystyrene samples (Polysciences) ranging from MW= 3550 to 1,300,000.

CPMAS ^{13}C NMR were obtained on a home-built spectrometer at a carbon frequency of 35.36 Hz. A commercial Doty Scientific CPMAS probe was used. The samples were ground in Na_2SO_4 in a drybox into a homogenous mixture and packed tightly in a 7 mm o.d. sapphire rotor (Doty Scientific) with Kelef end caps. Sample sizes were 100-200 mg and the balance was Na_2SO_4. A Doty Scientific CPMAS probe was employed and spinning speeds of 3.5 to 5 KHz were obtained. Data collection was performed with a Nicolet 1280 computer and Nicolet NMC software. Chemical shifts were referenced to an external adamantane standard. The adamantane standard was used for setting the Hartmann-Hahn matching condition and the 90°C ^1H pulse which was typically $\approx 5\mu s$. Cross-polarization contact times were 2 or 3 ms. A "rolling baseline" in some samples was eliminated by leftshifting the free-induction decay by 0-100μs, or by using a baseline fit routine in the software.

X-ray diffraction was measured with a home-built Guinier camera in a vacuum with mono-chromatic Cu Kα radiation. Plots of the X-ray data were obtained by scanning the developed film with a LKB Bromma Ultroscan XL laser densitometer. Within the stacked plots of X-ray diffraction shown in Figure 4.18 care was taken to insure that the film thickness was the same and that the exposure times were the same. X-ray photographs of the oriented films (Figures 4.21 and 4.24) were

obtained with one sample at different orientations and the same exposure time. The X-ray films from these experiments were developed simultaneously to further insure the correct relative intensities.

Thermal analysis was performed on a Perkin Elmer DSC-7, a TGS-2 thermogravimetric analyzer, a TMS-2 thermomechanical analyzer, and a 3600 data station. Scanning rates are specified in the figures. Scanning rates of less than 20°C per minute were used to avoid detonation of the **PBV** samples.

SEM photographs were obtained on an ETEC autoscan electron microscope. Samples were prepared by coating the materials with 100 Å of Au:Pd (80:20) with a Technics Hummer 5 sputter coater. The photographs shown were taken at an angle of 65° to the surface.

Raman spectra were obtained in a backscattering configuration with a Spex 1-m double monochromator instrument and photomultiplier tube operating in the photon counting mode. The excitation source was the 488 nm line of an Ar^+ laser with a nominal intensity less than 200 mwatts. The laser beam was focused to a spot $\approx 100\mu m$ in diameter. A Spec SCAMP computer was used to drive the monochromator and collect data. The spectra were obtained at room temperature and the spectra displayed are the result of 1-5 scans. Samples were prepared in a glove box and consisted of a film of **PPA** sandwiched between two microscope cover slides. The edges of the slides were sealed as well as possible with tape and the samples were kept in a sealed chamber under N_2 until the just before scanning the sample.

Thermolysis of **PBV** was conducted in a tube furnace under dynamic vacuum. The temperature was monitored with a thermocouple which was put in the furnace next to the tube.

Materials: Solvents were dried and deoxygenated. Ether, THF, benzene, toluene, and pentane were dried with sodium benzophenone ketyl. Pentane was

purified prior to drying and deoxygenation by treatment with H_2SO_4 for 3 weeks. CH_2Cl_2 and chlorobenzene were dried with P_2O_5. The titanocene metallacyle catalysts were prepared by the literature methods[21]. Catalysts **6** and **7** were made by the published procedure[20] and purified by recrystallization from pentane (20°C to -50°C). Catalyst **8** was made by the method of Kress and Osborn.[24] A detailed experimental procedure for catalyst **8** is not available in the literature. Hence, a detailed procedure is included in Appendix A. The methanol or acetone used to precipitate the polymer was not dried, but was deoxgenated by pulling vacuum on the solution multiple times and then bubbling argon through the solvent for a half an hour or more. $HgCl_2$ (Baker) was purified by sublimation under dynamic vacuum. ZnI_2 (Aldrich) was purified by heating at 100°C under vacuum for 12 hours. $AgBF_4$ (Alfa), $HgBr_2$ (Allied Chemical) and $(RhCl(COD))_2$ (Strem) were used without purification.

Polyethylene was used as a substrate for the stretching of films. One source of polyethylene was Handi Wrap™ which could be stretched to 2.3 times its length. The other source of polyethylene was the strapping which holds six-packs of beer or pop cans together. This material could be stretched to 6.0 times it's length. The stretching was found to be uniform by measuring the distance between marks on the substrate before and after elongation.

BV is explosive in pure form and must be handled in solution. Solutions of **BV** were prepared by the published procedure,[7] with the condition that the second equivalent of alkyl lithium is butyl lithium. By using a concentrated butyl lithium solution in hexanes, **BV** could be obtained as a 1.0-1.5 molar solution in hexanes (other residual solvents are also present). The concentration of **BV** was determined by NMR integration against an internal standard of mesitylene. Solutions of **BV** were degassed, placed under inert atmosphere, and stored over 4 Å molecular sieves at -50°C . The synthesis of **BV** may result in residual

dimethylether and diethylether in the solution of **BV** which will decrease the activity of the catalysts and hence, change reaction times. The polymerization procedure presented below is based on a concentration of diethylether of approximately 1 M with no residual dimethylether. Both **PBV** and **BV** are *potentially dangerous materials* and should be handled with caution.

General Synthesis of PBV: The polymerization of **PBV** is described below for catalysts **6**, **7**, and **8**. These catalysts are air and water sensitive, and all manipulations were carried out under inert atmosphere. Films of **PBV** were cast directly from the reaction mixture onto glass slides. **PBV** may also be precipitated as a white or slightly yellowed powder by slow addition of the polymerization mixture to a ten fold or greater volume of a non-solvent such as acetone or methanol. Approximate polymerization yields in the procedures below were determined by weighing precipitated powders. Precise yields of **PBV** were not obtained as a result of the sensitive nature of the material and the in situ procedures used. As a result of the tendency for **PBV** to undergo spontaneous exothermic decomposition, it is recommended that solid samples be limited to 1 gram or less. Powders of **PBV** seem to be most prone to decomposition, and were observed to decompose when scraped away from the walls of glassware. Films should be gently cut with a razor blade since tearing may also cause decomposition. Freshly prepared samples of **PBV** are most sensitive. However, samples that had been stored for 3 months at RT have also been observed to spontaneously decompose with rapid heating. NMR samples were prepared by removing an aliquot of the polymerization solution and subjecting it to repeated evaporation of the solvent and the addition of C_6D_6. Samples were evaporated to approximately one third the original volume with each cycle. As this procedure is repeated a greater portion of the polymer begins to gel. Hence, the best results were obtained by subjecting the sample to approximately 7-10 cycles and in the presence of residual hexane.

Synthesis of PBV with 6: The activity of the fluoronated catalyst (**6**) is considerably greater than that of the non-fluoronated catalyst (**7**).[20] Reaction of **6** with **BV** at RT results in a red solution and low yields of **PBV**, hence lower temperatures are required. A monomer concentration of .15 M is used (balance toluene) and a 50:1 monomer to catalyst ratio. The dilute conditions are necessary to avoid the formation of insoluble polymer in the reaction. For example: 1.9 ml of a 1 M solution of **BV** (1.9 mmole) is added to a 11 ml toluene solution of **6** (30 mg, .038 mmole) at -20°C . The reaction mixture is initially yellow in color. After .5 hr. at -20°C the reaction mixture is slowly allowed to warm to 0°C over the course of 1.5 hr. The reaction mixture is light orange and the presence of polymer is apparent from the increased viscosity. The catalyst is deactivated by the addition of 10 equivalents of acetone (based on the number of moles of catalyst). The reaction mixture is concentrated *in vacuo* to approximately one third the original volume and cast into light orange films in a glove box. These films are soft and rubbery and are ≈.03 mm thick. The reaction yield was found to be approximately 70%. ^{1}H NMR (C_6D_6) (Figure 4.3): 5.83 (2H, br. d.), 3.28 (2H, br. d.), 1.72 (2H, br. t.) ppm. ^{13}C NMR (C_6D_6) (Figure 4.2): 133.0, 47.8, 12.8 ppm. Infrared (Figure 4.6): 3450 (m. br.), 3025 (s.), 2970 (s.), 2920 (s.), 1590-1720 (w.), 1495 (m.), 1450 (m. br.), 1360 (m.), 1320 (m.), 1080 (s.), 1023 (s.), 995 (s.), 983 (s.), 750 (s.), 724 (s.), 693 (s.) cm^{-1}. GPC analysis on a low resolution column indicated a very broad molecular weight distribution ranging from 600,000 to 1,000. This distribution had three components: a low molecular weight peak at approximately 2000, a maxima at 50,000, and a shoulder at high molecular weight which extended to 600,000.

Synthesis of PBV with 7: Catalyst **7** is most conveniently used since the reaction proceeds smoothly at RT. This procedure is best accomplished by conducting the reaction in a glove box. Polymerization reaction conditions were

.5 M in **BV**, a 60:1 monomer to catalyst ratio, and a reaction time of 2.5 hrs.. For example: .75 ml of a 1.5 M solution of **BV** (1.13 mmole) is added to a 1.75 ml benzene solution of **7** (10.7 mg, .019 mmole). After 2.5 hrs the yellow homogeneous reaction mixture is viscous. At this time the reaction mixture is cast directly into films on glass microscope slides in a glove box. Once dry, the smooth films are light yellow in appearance, ≈.03mm thick, and soft and rubbery. The reaction yield was approximately 70%. ^{1}H NMR (C_6D_6) (Figure 4.5): 6.35 (br. s.), 6.06 (br. s.), 5.83 (2H, br. s.), 3.29 (2H, br. s.), 2.58 (br. s.) 1.72 (2H, br. t.) ppm. ^{13}C NMR (C_6D_6): 133.0, 47.8, 12.8 ppm and multiple smaller peaks in the region of 20-40 ppm (Figure 4.4). Infrared (Figure 4.6):3450 (m. br.), 3025 (s.), 2920 (s.), 1590-1720 (w.), 1460 (m. s.), 1440 (m. s.) 1360 (s. s.), 1075 (m . s.), 980 (s. br.), 965 (s. br.), 750 (s. br.) cm^{-1}. The UV-vis spectrum of a film ≈.0005 mm thick is shown below in Figure 4.27. The film had been washed with acetone multiple times and dried.

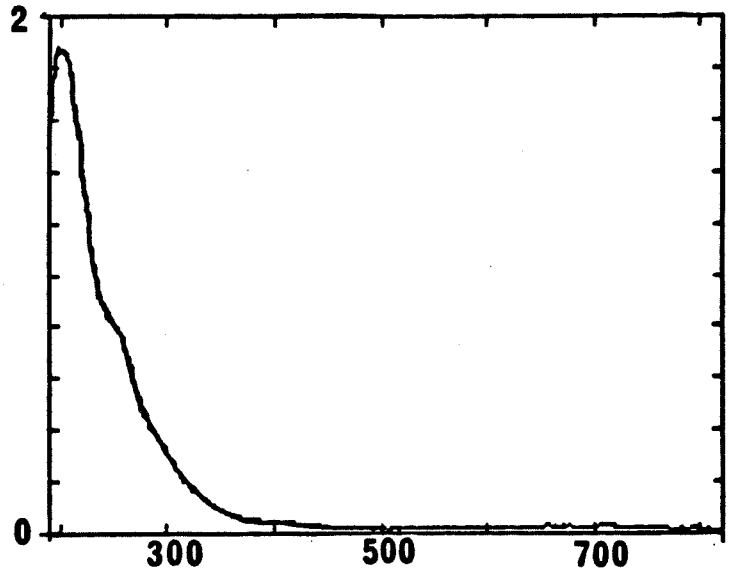

Figure 4.27. UV-vis spectrum of **PBV** film.

GPC analysis on a low resolution column indicated a very broad molecular weight distribution ranging from 600,000 to 3,500. The low molecular weight component is less for this catalyst than for **6**. The average molecular weight is estimated to be 30,000.

Synthesis of PBV with 8: Catalyst **8** is an oil which is not readily purified. The activity of this catalyst has been found to be greatly enhanced by Lewis acids. The last step in the synthesis of **8** involves reaction with $AlBr_3$ and hence, small amounts of Lewis acidic material may be present. As a result, this catalyst has in practice been found to have a varied activity. The activity of the catalyst when obtained in high purity was considerably lower than that which has slight impurities. The impurities were not detectable by ^1H NMR. If the catalyst impurity was too high, gels were produced in the polymerization. Hence, the best results were obtained with **8**, which was only slightly impure. Polymerization conditions were .50 M **BV** and .010 M **8** with a monomer to catalyst ratio of 50. A reaction time of 7 hours at RT produced a yield of 80% **PBV**. An example of a preparation is as follows. A solution of **8** (88 mg .15 mmole) in 5 ml of benzene is prepared. 5 ml of a 1.5 M solution of **BV** is diluted with 5 ml of benzene and then added to the solution of **8**. The reaction turns from a light orange-brown to a darker red-brown color in approximately 1 minute. This solution is stirred for 7 hours at RT and then cast into soft rubbery films which are orange brown in color. ^1H NMR (C_6D_6) (Figure 4.5): 6.48 (br. s.), 6.08 (br. s.), 6.83 (br. s.), 3.37 (br. s.), 2.93 (br. s.), 2.87 (br. s.), 2.13 (br. s.) 2.65 (br. s.), 2.03 (br. s.), 1.73 (vbr. s.) ppm. ^{13}C NMR (C_6D_6) (Figure 4.4): 132.9, 124.9, 47.9, 42.6, 38.3, 32.3, 28.4, 21.3, 12.8, -2.2 ppm. Infrared (Figure 4.6): 3450 (m. br.), 3025 (s.), 2930 (br.), 1699 (m. br.), 1675 (m. br.), 1635 (m. s.) 1595 (m. s.) 1510 (w. s.), 1435(m. br.) 1360 (s. vbr.), 1015 (s. vbr.), 890 (m. s.), 735 (s. vbr.), 615 (w. br.) cm^{-1}.

Synthesis of PBV:Polynorbornene block copolymers with 7: The synthesis of the polynorbornene living polymer is a procedure adapted from the literature[12] and was run in a glove box; .245 g (2.6 mmole) of norbornene in 1.5 ml of benzene was added to 30 mg (.052 mmole) of **7** in 2 ml of benzene. This reaction was stirred for 1 hour at RT. At this time, the reaction was diluted with 6 ml of benzene and then 2.6 ml of a 1 M solution of **BV** (2.6 mmole) was added. The reaction was stirred for 3 more hours and then cast into films. The films were slightly yellowed, ≈.06 mm thick, and soft and rubbery. The ^{1}H NMR shown in Figure 4.8 is a composite of polynorbornene[11] and **PBV**. From integration of the olefinic peaks in this spectra the ratio **PBV** to norbornene was determined to be 1 to 1.25. GPC analysis on a low resolution column indicated a broad, nearly isotropic distribution from approximately 300,000 to 4,000 with an average molecular weight of approximately 80,000.

General Isomerization of PBV: In general, due to the instability of **PBV**, efforts were made to isomerize the materials as soon as possible. Hence, as soon as the films were evaporated to a level at which they were tacky they were immersed in the solution of the catalyst. As a result, the films were still swollen with solvent. However, if the films were not evaporated thoroughly enough then the resulting materials had poor mechanical properties and were not as smooth in appearance. The isomerization of the **PBV** homopolymer was performed in a glove box. As a result of the solvent used for the isomerization of the block copolymers, these materials were isomerized in a Schlenk flask.

Isomerization of PBV with $HgCl_2$ and $HgBr_2$: A 5 % solution of $HgCl_2$ is prepared in THF. Freshly cast films of **II** on glass slides are immersed in this solution in a glove box at RT. The films turn red within seconds, to blue-green over the next thirty seconds, and finally to a black silvery shiny film within 2-3 minutes. Films are soaked in this solution for at least 1 hr and then removed from

the glass slide. The resulting free-standing films of **III** are washed with THF, and further purified by soxhlet extraction with THF. A similar procedure was carried out for $HgBr_2$ with similar results. The only observed difference was the fact that the rate of color changes is $\approx$ 10 times slower and that the films are not quite as silvery. The residual $HgCl_2$ was difficult to remove from the films. X-ray diffraction of films that were washed with THF multiple times displayed many sharp diffraction peaks. It is interesting to note that these peaks did not index with those of $HgCl_2$ with or without exposure to THF. Soxhlet extraction with THF for 48 hours resulted in the disappearance of these peaks. However, elemental analysis (Spang Microanalytical Laboratories) revealed the films to be 89.2% carbon and hydrogen (C/H=1.09). Further soxhlet extraction with acetone (24 hours), and then methanol (24 hours) gave analyses (Caltech Microanalytical Facility) with a carbon and hydrogen content of 91.55 (C/H = .955). CPMAS ^{13}C NMR of the thermally isomerized material (150°C 6 hours) is shown in Figure 4.15 and consists of peaks at 135.5 (s.) and 40 (br.) ppm. Infrared (Figure 14): 3100 (s. s.), 2900 (m. br.), 1497 (m. br.), 1395 (w. s.), 1005 (s. vbr.), 740 (s. vbr.) cm^{-1}. UV-vis spectra of a film $\approx$.0005 mm thick is shown in Figure 4.28.

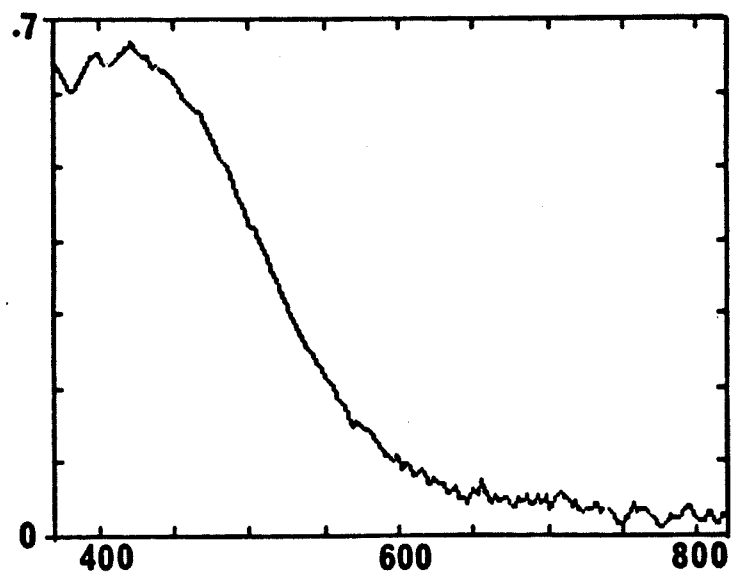

Figure 4.28. UV-vis spectra of **PPA** .

The **PBV**:polynorbornene block copolymer is isomerized in much the same fashion except acetone is used instead of THF. This is necessary because the block copolymer is soluble in THF, which results in poor quality films.

Isomerization of PBV with $AgBF_4$: The isomerization with $AgBF_4$ is much slower than was observed with $HgCl_2$. Films soaked in a 2% solution of $AgBF_4$ solution in THF turned red over the course of 5 minutes. The isomerization appeared at times to initiate in small areas of the film and then spread throughout the film. The films turned to a dark silvery dull material over the course of 30 minutes. CPMAS ^{13}C NMR : 135 and 127 ppm. Metallic silver deposited in the film precluded infrared analysis.

Isomerization of PBV with ZnI_2: ZnI_2 is not extremely soluble in THF, and hence a saturated solution was used with excess solid ZnI_2. This isomerization is slow and after 2 hours the **PBV** films were red in color. After soaking in the ZnI_2 solution for 24 hours, the films were black and shiny. These films were then rinsed multiple times with THF. The films were strong and flexable. Infrared: 3100 (s. s.), 2900 (m. br.), 1410 (s. vbr.), 1395 (w. s.), 1005 (s. vbr.), 760 (s. vbr.).

Isomerization of PBV with $(RhCl(COD))_2$: **PBV** films were soaked in a 1% solution of $(RhCl(COD))_2$ in THF for 5 days. The films slowly became red over this period and were brittle. These films were rinsed multiple times with THF. Infrared: 3090 (s. s.), 2900 (s. br.), 1715 (s. vbr.), 1650 (m. s.), broad absorbance bands 1480-660 (s.) cm^{-1}.

Treatment of PBV with I_2: Films of **PBV** were treated with I_2 vapor in vacuum. Weight uptake measurements indicated that the resulting material was 80% I_2 by weight. These films were extremely brittle. Conductivities of films saturated with I_2 were $\approx 10^{-4}\ \Omega^{-1}cm^{-1}$. CPMAS ^{13}C NMR : 145, 52, 38 ppm.

Preparation of Titanocene Metallacycles 3 and 4: Initial experiments consisted of NMR tube reactions between **BV** and **1** and **2**. The reaction stoichiometries were approximately 20:1 **BV** to metallacycle. New ^{1}H NMR (C_7D_8) cyclopentadiene resonances for the catalyst appeared at 5.59 and 5.27 ppm for **3** and 5.65 and 5.55 ppm for **4**. **3** was isolated as a red oily solid by removing all volatiles at RT. ^{1}H NMR (C_7D_8): 5.59 (5H s.), 5.27 (5H s.), 4.35 (1H d.), 2.80 (1H d.d.), 2.00 (1H m.), 1.88 (1H d.), 1.60 (1H d.), 1.24 (1H m.), .89 (1H m.), .28 (1H m.) ppm. These compounds are under further investigation by Dave R. Wheeler, and full characterization will be reported with those results.

References and Notes:

1. *Handbook of Conducting Polymers*; Skotheim, T. J. (ed.); Dekker: New York, 1986.

2. Chien, J. C. W. *Polyacetylene: Chemistry, Physics, and Material Science* Academic Press 1984.

3. Naarman, H.; Theophilou, N. *Synthetic Metals* **1987** 22, 1.

4. (a) Edwards, J. H.; Feast, W. J. *Polymer* **1980**, 21, 595. (b)Karasz, F. E.; Capistran, J. D.; Gagnon, D. R.; Lenz, R. W. *Molec. Cryst. Liq. Cryst.* **1982**, 118, 567. (c) Ballard, D. G.; Couris, A.; Shirley, I. M.; Taylor, S. C. *J. Chem. Soc. Chem. Commun.* **1983**, 954.

5. (a) Marvell, E. N. *Thermal Electrocyclic Reactions* Academic Press, 1980. (b) *Pericyclic Reactions* Marchand, A. P.; Lehr, R. E. (ed.); Academic Press 1977.

6. Klavetter, F. L. unpublished results.

7. (a) Katz, T. J.; Wang, E. J.; Acton, N. *J. Am. Chem. Soc.* **1971**, 93, 3783. (b) Katz, T. J.; Roth, J.; Acton, N.; Carnahan, E. *Org. Synth.* 1973, 53, 157.

8. (a) Weinstein, S.; Leftin, J. H.; Kerbs, J.; Gil-Av, E. *J. Chem. Soc. D.* **1971**, 1616. (b) Cristl, M.; Heinemann, U.; Kristof, W. *J. Am. Chem. Soc.* **1975**, 97, 2299. (c) Blanchard, E.P., Jr.: Cairncross, A. *J. Am. Chem. Soc.* **1966**, 88, 487-495. (d) Closs, G. L.; Pfeffer, P. E. *J. Am. Chem. Soc.* **1968**, 90, 2452-2453. (e) Wiberg, K. B.; Lavanish, J. M. *J. Am. Chem. Soc.* **1966**, 88, 5272-5275.

9. (a) Renner, C. A.; Katz, T. J.; Pouliquen, J.; Turro, N. J. *J. Am. Chem. Soc.* **1975**, 97, 2568. (b) Adam, W.; Oppenlander, T. *Angew. Chem., Int. Ed. Engl.* **1986**, 25, 661-672 and references therein. (c) Adam, W.; Oppenlander, T.; Zang, G. *J. Am. Chem. Soc.* **1985**, 107, 3921-3924. (d) Becknell, A. F.; Berson, J. A.; Srinivasan, R. *J. Am. Chem. Soc.* **1985**, 107, 1076-1078.

10. (a) Mango, F. D. *Coord. Chem. Rev.* **1975**, 15, 109 and references therein. (b) Gassman, P. G.; Atkins, T. J. *J. Am. Chem. Soc.* **1971**, 93, 4597.

11. (a) Gilliom, L. R.; Grubbs, R. H. *J. Am. Chem. Soc.* **1986**, 108, 733.

12. Schrock, R. R.; Feldman, J.; Cannizzo, L .F.; Grubbs, R. H. *Macromolecules* **1987**, 20, 1169.

13. Wallace, K. C.; Schrock, R. R. *Macromolecules* **1987**, 20, 448.

14. Wiberg, K. B. *Angew. Chem., Int. Ed. Engl.* **1986**, 25, 312.

15. Dr. R. B. Wardle personal communication.

16. Christl, M. *Angew. Chem., Int. Ed. Engl.* **1981**, 20, 529-546.

17. Snyder, G. J.; Dougherty, D. A. *J. Am. Chem. Soc.* **1985**, 107, 1774-1775.

18. Kaisaki, D. A.; Dougherty, D. A. *Tetrahedron Lett.* **1987**, 28, 5263-5266.

19. The authors of reference 7 report that detonation of samples of benzvalene of 254 mg were violent.

20. (a) Schaverien, C. J.; Dewan, J. C.; Schrock, R. R. *J. Am. Chem. Soc.* **1986**, 108, 2771. (b) Schrock, R.R.; Depue, R.T.; Feldman, J.; Schaverien, C. J.; Dewan, J. C.; Liu, A. H. *J. Am. Chem. Soc.* **1988**, 110, 1423.

21. (a) Lee, J. B.; Ott, K. C.; Grubbs, R. H. *J. Am. Chem. Soc.* **1982**, 104, 7491. (b) Gilliom, L. R.; Grubbs, R. H. *Organometallics* **1986**, 5, 721. (c) Strauss, D. A.; Grubbs, R. H. *J. Mol. Cat.* **1985**, 28, 9 and references therein.

22. (a) Anslyn, E. V.; Grubbs, R. H. *J. Am. Chem. Soc.* **1987**, 109, 4880. (b) Upton, T. H.; Rappe', A. K. *J. Am. Chem. Soc.* **1985**, 107, 1206.

23. Katz, T. J.; Savage, E. B.; Lee, S. J.; Nair, M. *J. Am. Chem. Soc.* **1980**, 102, 7940 and 7942 and references therein.

24. (a) Kress, J.; Osborn, J. A. *J. Am. Chem. Soc.* **1983**, 105, 6346. (b) Aguero, A.; Kress, J.; Osborn, J. A. *J. Chem. Soc., Chem. Commun.* **1985**, 793. (c) Kress, J.; Osborn, J. A.; Green, R. M. E.; Ivin, K. J.; Rooney, J. J. *J. Chem. Soc., Chem. Commun.* **1985**, 874. (d) Kress, J.; Aguero, A.; Osborn, J. A. *J. Mol. Cat.* **1986**, 36, 1. (e) Kress, J.; Osborn, J. A.; Green, R. M. E.; Ivin, K. J.; Rooney, J. J. *J. Am. Chem. Soc.* **1987**, 109, 899.

25. Levy, G. C.; Lichter, R. L.; Nelson, G. L. *Carbon-13 Nuclear Magnetic Resonance Spectroscopy;* Wiley-Interscience, 1980.

26. Griffith, D. W. T.; Kent, J. E.; Dwyer, F. O. *Aust. J. Chem.* **1975**, 28, 1397.

27. Yannoni, C. S. *Acc. Chem. Res.* **1982**, 15, 201-208.

28. See Clarke, T. C.; Scott, J. C. in reference 1 pages 1127-1156.

29. Clarke, T. C.; Geiss, R. H.; Kwak, J. F.; Street, G. B. *J. Chem. Soc., Chem. Comm.* **1978** 489-490.

30. (a) Bott, D. C. et al. *Synthetic Metals* **1986**, 14, 245 and references therein.

31. Eckert, H.; Yesinowski, J. P.; Sandman, D. J.; Velazquez, C. S. *J. Am. Chem. Soc.* **1987**, 109, 761.

32. Elias, H. *Macromolecules*; vol. 1, 2nd ed. page 155, Plenum Press, 1984.

33. Bott, D. C.; Brown, J. N.; Winter, J. N.; Barker, J. *Polymer J.* **1987**, 28, 601 and references therein.

34. Billmeyer, F. W. Jr. *Textbook of Polymer Science;* 3rd ed., John Wiley and Sons, 1984.

35. Noshay, A.; McGrath, J. E. *Block Copolymers: Overview and Critical Survey;* Academic Press: New York, 1977.

36. (a) Kuzmany, H. *Phys. Status Solidi; (B)* **1980**, 83, 521. (b) Fitchen, D. B. *Mol. Cryst. Liq. Cryst.* **1982**, 83, 95.

37. Leininger, H.; Christl, M.; Wendisch, D. *Chem. Ber.* **1983**, 116, 681-689.

38. Seeger, K. *Semiconductor Physics* Springer-Velag: New York, 1973.

Chapter 5

NEW PRECURSOR ROUTES TO CONDUCTIVE POLYMERS: HYDROLYSIS AND ELIMINATION REACTIONS OF KETALS

INTRODUCTION:

The majority of conductive polymer precursor methods studied to date have relied on elimination reactions to produce extended conjugation (see Chapter 1).[1] However, organic chemistry has a great deal more to offer to the field of conductive polymers than elimination reactions. In Chapter 4, the use of electrocyclic reactions as a precursor methodology were discussed, and a particular example was investigated. In this chapter, the use of tautomerism as well as elimination reactions are investigated as precursor routes to conductive polymers.

The most abundant tautomerism in organic chemistry is that of the keto-enol equilibrium.[2] Feast has explored this concept as shown in Scheme 5.1.[3] In this scheme, the soluble precursor polymer **1** is hydrolyzed and then enolized to create extended conjugation. The enolized material **2** displayed an intrinsic conductivity of 2.9 X $10^{-7}\Omega^{-1}cm^{-1}$, and oxidation gave a modest increase in conductivity to $10^{-5}\Omega^{-1}cm^{-1}$. The low conductivity of the doped polymer may be a result of oxidation producing diketone structures which would have the effect of interrupting the conjugation.

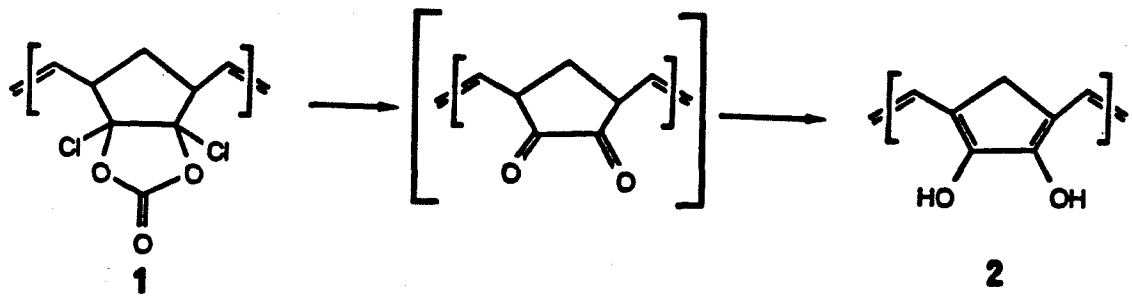

1 **2**

Scheme 5.1

Cyclic olefins of the [2.2.1] ring system are the most attractive monomers for ring-opening metathesis polymerization (**ROMP**). This class of monomers is readily available from Diels-Alder chemistry, and the **ROMP** of this ring system has seen extensive study.[4] One goal of the Grubbs group is to develop well-behaved living polymerizations of monomers which can yield conducting materials. Monomers derived from the [2.2.1] ring system have afforded living polymerizations with narrow dispersities.[5] With living polymerizations in hand, highly uniform block copolymers may be produced.[6] Such block copolymers may display a variety of phase separated supermolecular structures.[7] The development of conductive polymer precursors derived from the **ROMP** of the [2.2.1] class of monomers will be an effective means of attaining uniform block copolymers. Conductive polymer supermolecular structures could potentially have applications in the field of molecular electronics,[8] and would be the conductive polymer analogs of semiconductor superlattices.[9] In converting polymers derived from this monomer class into conductive polymers, methods for the removal of the saturated centers which interrupt the conjugation must be developed. The saturated carbon center that must be removed from the polymers of interest are the positions which were the bridgehead positions of the monomer. As was discussed above, Feast has investigated enolization as a means of removing this saturated center from the conductive polymer backbone.[3] The use of DDQ oxidation has been explored in this group,[10] but this process was limited to the production of powders. The usefulness of precursor methods in conductive polymer synthesis is the production of continuous samples with desirable mechanical properties and manipulatable morphologies.[11]

In pursuit of new precursor methodologies toward the transformation of polymers derived from **ROMP** of cyclic olefins of the [2.2.1] structural type into conductive polymers, routes to polybenzoquinonenorbornadiene (**PBQ**) were investigated. As is shown in Scheme 5.2, it was envisioned that **PBQ** could tautomerize

to the polybenzohydroquinone (**PBHQ**), and thus eliminate the saturated centers which interrupt extended conjugation.

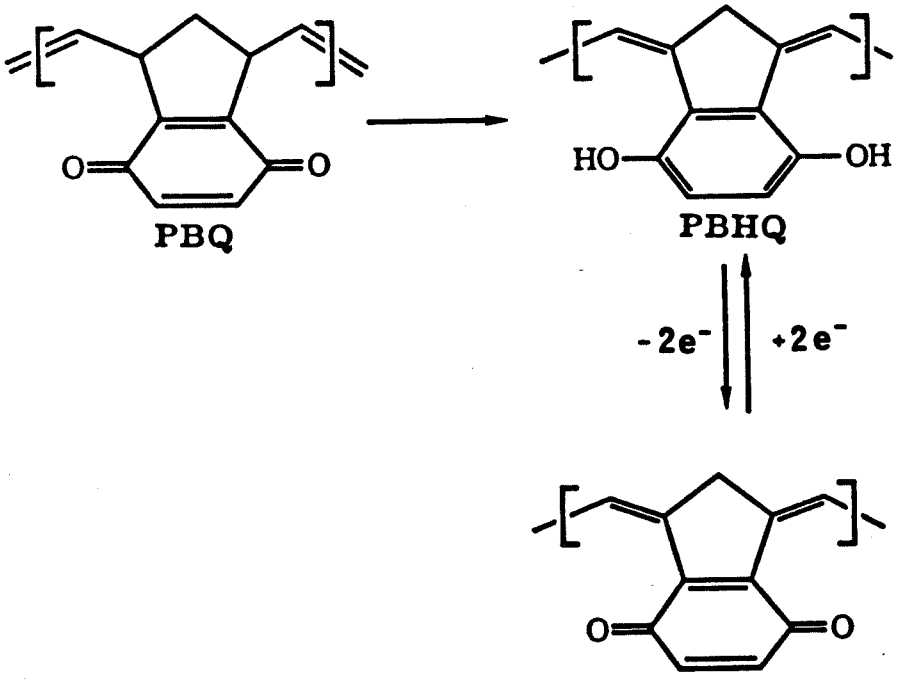

Scheme 5.2

A primary technological application of conductive polymers in the near future will be in lightweight rechargeable batteries.[12] Quinones are well-know for their reversible electrochemistry,[13] and hence materials such as **PBHQ** may be efficient battery materials. This electrochemical process is shown for **PBHQ** in Scheme 5.2. Quinones are also well-known to form charge transfer complexes with hydroquinones as well as other electron rich molecules.[14] The formation of hemiquinone structures in these materials may provide a mechanism for facile interchain conduction. Hydroquinones have been used as anti-oxidants, and therefore conductive polymers such as **PBHQ** have a built-in anti-oxidant. This feature is of practical utility, since the air sensitivity of conductive polymers has been a major obstacle to the commercial feasibility of these materials.

RESULTS AND DISCUSSION:

Synthesis of Monomers:

Attempts at straightforward synthesis of **PBQ** and derivatives of **PBQ** from the corresponding benzoquinonenorbornadienes (**3**) as shown in Equation 5.1 was unsuccessful. A number of catalysts were investigated in this transformation,[15] but only $OsCl_3$ gave a significant yield of polymer. However, the material obtained with $OsCl_3$ was a black intractable powder. It was not surprising that this polymerization was unsuccessful, since in general the quinone group is quite reactive. In addition, early transition metal **ROMP** catalysts are known for their facile Wittig type reactions with carbonyl groups,[16] and thus the presence of quinones is incompatible with these catalysts.

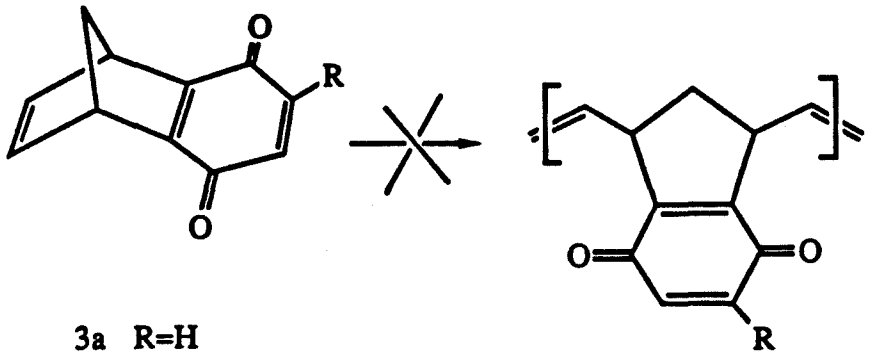

3a R=H
3b R=CH_3
3c R= Ph

Equation 5.1

Given the incompatibility of the quinone group with the currently available **ROMP** catalysts, protection of the carbonyls with ketal groups was pursued. Straightforward conversion of the quinones to ketals was unsuccessful under a variety of conditions. Thus, an alternative synthesis was pursued. Electrochemical oxidation of dimethoxybenzene derivatives provide a facile preparation of quinone bisketals.[17] A synthesis employing this electrochemical oxidation was developed

as shown below in Scheme 5.3. The electrochemical oxidation of **5** to **6** was found to be a facile transformation with only minor side products. This oxidation was performed simply by applying a 6 V potential between two platinum electrodes in the reaction mixture; **6** was isolated in a 70% yield from the electrolysis as an air sensitive material. If degraded by air, **6** could not be obtained in a high purity form. **6** was not easily recrystallized, and it decomposed with any attempted chromatography.[18] Purification of **6** was achieved by careful multiple sublimation (≈6-7 times). This synthesis is based on inexpensive starting materials and is readily employed to prepare large quantities of monomer. Preparations on a scale of 20 grams were performed without difficulty.

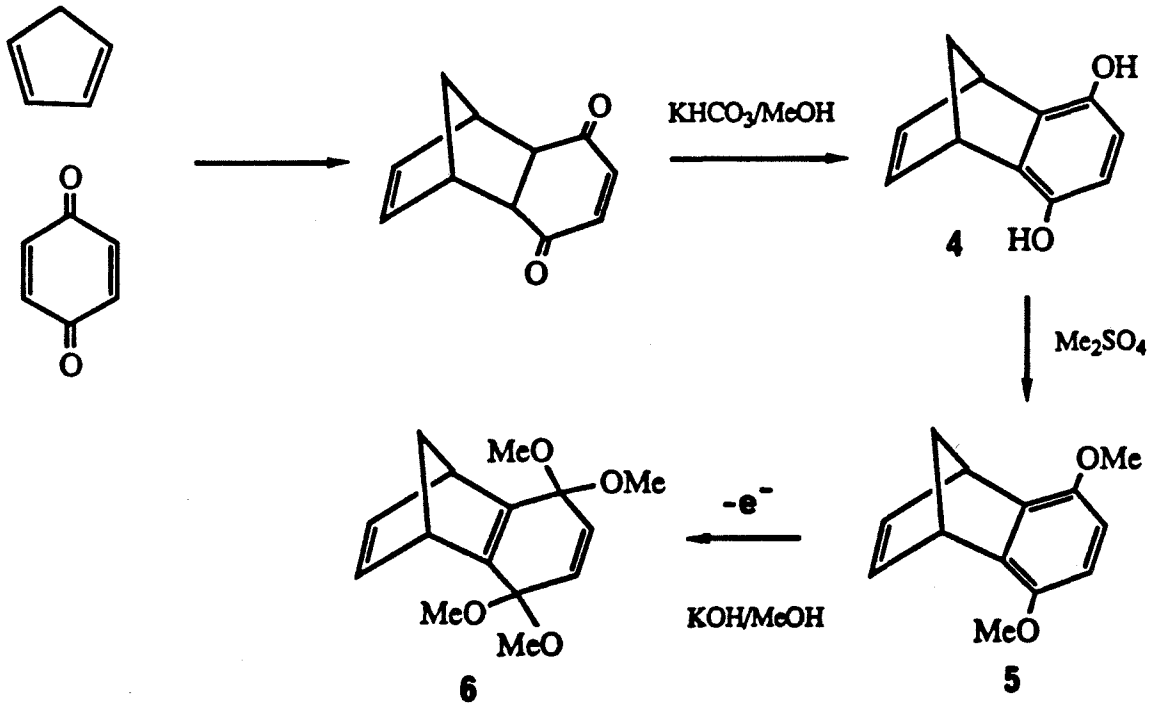

Scheme 5.3

The electrochemical oxidation of Scheme 5.3 was also found to be effective in the synthesis of monomers **7** and **8**. The precursor to **7** is more easily oxidized, and hence higher current efficiencies were obtained in the synthesis of this monomer. In addition, **7** is more readily purified as a result of the fact that crude reaction mixtures can be recrystallized. As obtained from the electrolysis, **8** could not be recrystallized. Initial sublimation gave a white material, but with repeated sublimation this material became slightly yellowed. The most effective purification for **8** will most likely be initial sublimation, and then fractional recrystallization.

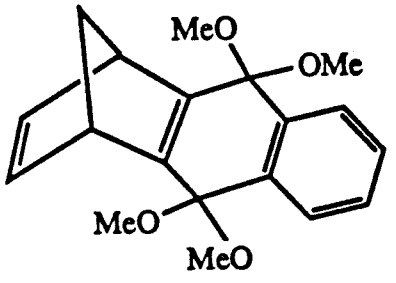

7

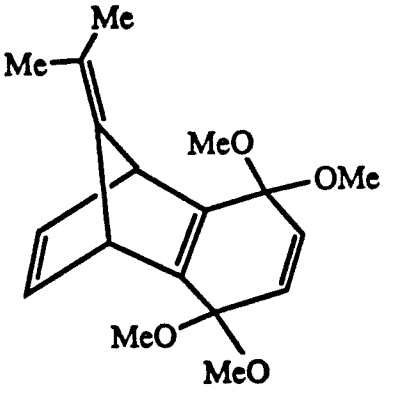

8

The structures of **6**, **7** and **8** were consistent with their NMR spectra. Diagnostic peaks in the ^{13}C NMR are the ketal resonances which are observed in the range of 95 - 100 ppm. The ^{1}H NMR displays the characteristic resonances of the [2.2.1] ring system with bridgehead protons at $\approx$4 ppm exhibiting coupling to the disubstituted olefin. Additionally, **6** was hydrolized with dilute HCl to benzoquinonenorbornadiene (**3a**) which displayed an ^{1}H NMR identical to material prepared by another route.

ROMP of Quinone Bisketals:

Initial investigation of the **ROMP** of the above mentioned bisketals indicated it was necessary to have monomers of high purity. For example, although the ^{1}H and ^{13}C NMR of **8** seem to be relatively clean, no polymer could be produced even at catalyst to monomer ratios of 1 to 10. The best indication of monomer purity was found to be the melting range. Melting ranges of as high as 12°C were obtained for impure samples, and melting ranges of 3°C or less were observed for high purity monomers. Catalysts that were found to be effective for the **ROMP** of **6** are shown below.

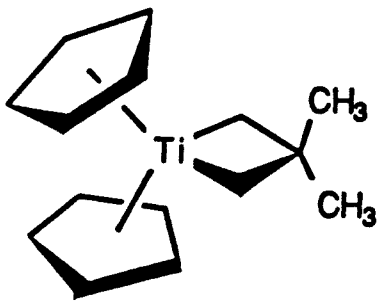

9

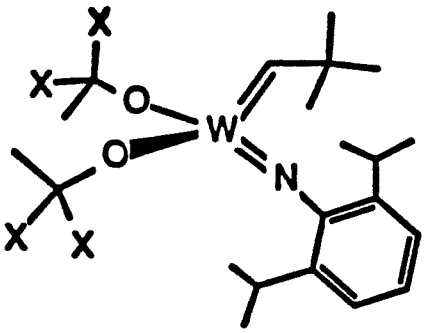

10 X= CF_3
11 X= CH_3

The titanocene metallacycle catalyst **9** was found to polymerize **6** slowly at 55°C. Catalysts **10** and **11** were found to polymerize **6** rapidly at RT. A living polymerization of norbornene has been demonstrated for **11**.[5b] In addition, **ROMP** of **6** with **11** proceeds at a convenient rate at RT. Thus, throughout the remainder of this chapter unless otherwise stated the materials discussed were produced with **11**. The polymerizations of **6** and **8** to produce the polybenzoquinone bisketal (**PBK**) and polynaphthoquinone bisketal (**PNK**) are shown in Scheme 5.4. When the monomers **6** and **7** are rigorously pure, quantitative yields of the polymer were obtained. Quantitative yields were observed even when monomer to

catalyst ratios as high as 225 were used. Polymerizations were monitored by thin layer chromatography and terminated at completion. No adverse effects were observed when polymerizations were allowed to stir for 10 hours after completion of the polymerization. Monomer **8** has yet to be obtained in pure enough form to be efficiently polymerized.

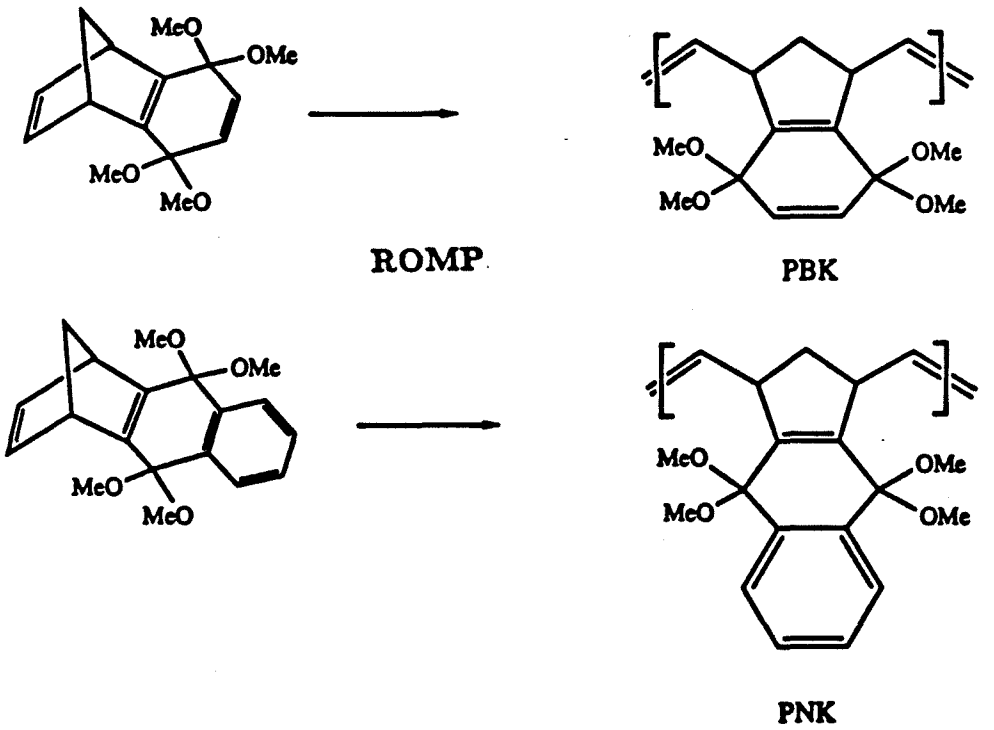

Scheme 5.4

PBK and **PNK** are extremely soluble polymers and readily dissolve in acetone, THF, methylene chloride, chloroform, benzene, and toluene. **PBK** is slightly soluble in ether, methanol, and acetonitrile. These polymers can be quantitatively precipitated as white powders by slow addition to a large volume of hexane. The solubility of these polymers is also reflected in the difficulty encountered in removing residual solvent from the polymers. Hence, even with pumping powders at 10^{-6} torr for 12 hours, solvent signals were often observed in ^{1}H NMR spectra. The ^{1}H NMR and ^{13}C NMR of **PBK** and **PNK** are compared in Figures 5.1 and 5.2. The spectral shifts of **PBK** and **PNK** are similar to those exhibited by

the monomers **6** and **7** (see experimental section). The notable exceptions to this are the methylene groups and metathesized olefin which experience considerable changes of environment with **ROMP**. The methylene resonances are observed to be sensitive to diad tacticity in the polymer.[4] Since both monomers have a plane of symmetry, there is no head to tail tacticity. However, there are **m** and **r** diads as shown in Figure 5.3 for **PBK**. Catalyst **11** has been observed to give atactic polymers with an equal amount of **m** and **r** diads.[19] Hence, two approximately equal intensity signals are observed in the ^{1}H NMR . The ^{1}H NMR shifts of these signals are at 1.55 and 2.25 for **PBK** and 1.87 and 2.45 for **PNK**. Similarly, the methylene group in **PBK** displays two signals in the ^{13}C NMR at 36.8 and 42.0 ppm. For **PNK** one methylene center is observed in the ^{13}C NMR at 35.8 ppm, and there is a hint of a second signal at 43.5 ppm.

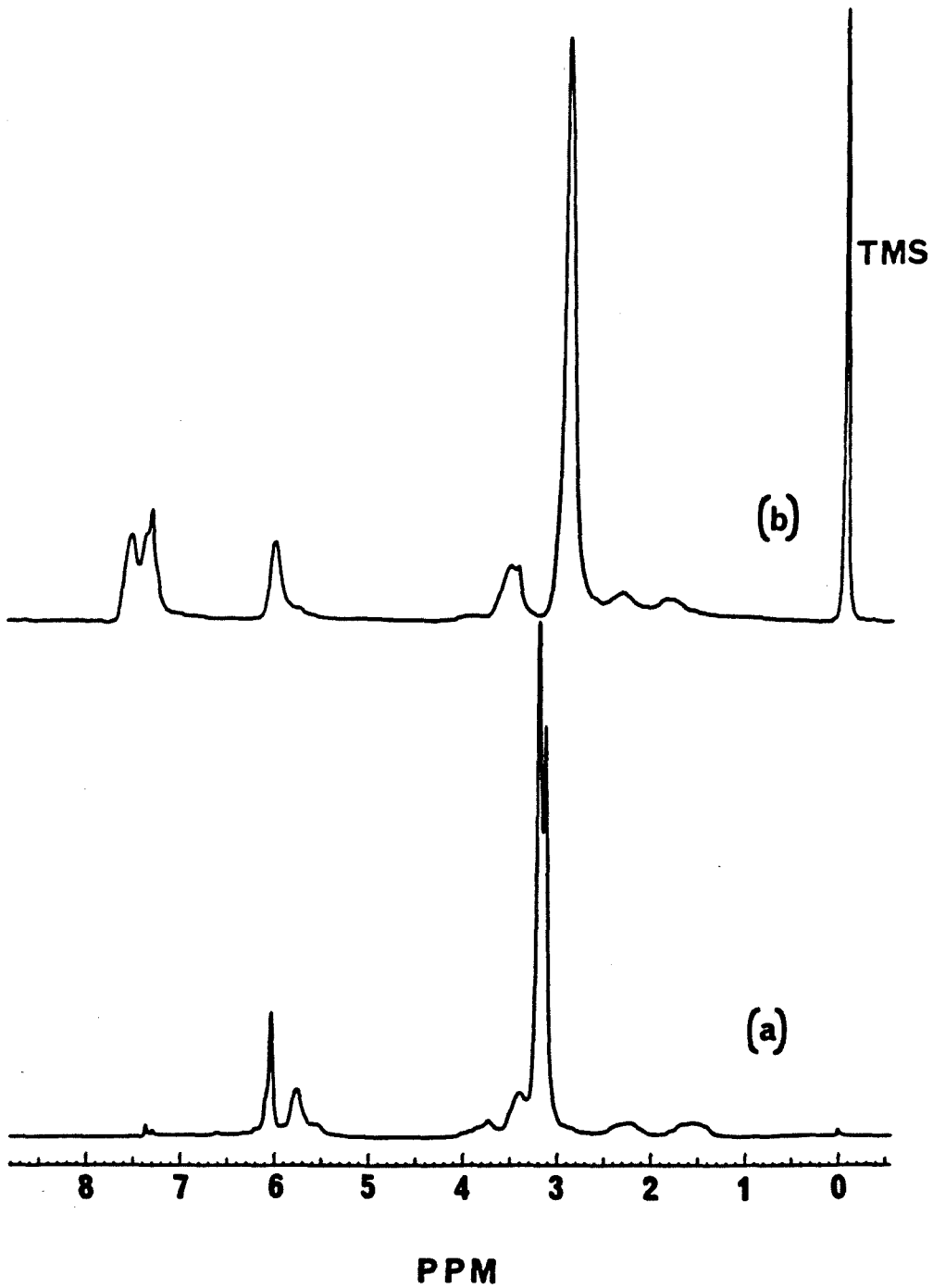

Figure 5.1. ^{1}H NMR ($CDCl_3$) of **PBK** (a); and **PNK** (b).

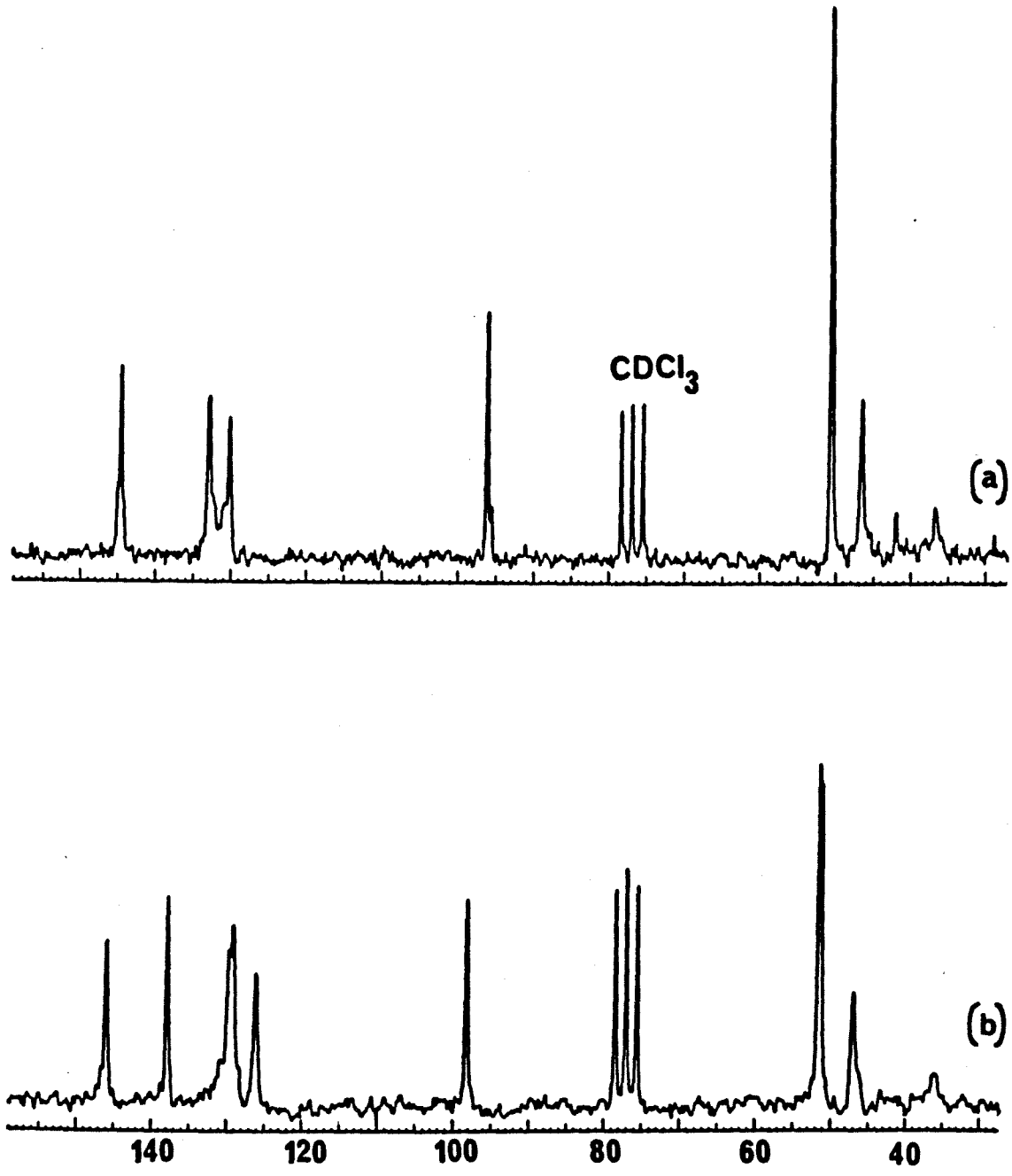

Figure 5.2. ^{13}C NMR ($CDCl_3$) of PBK (a); and PNK (b).

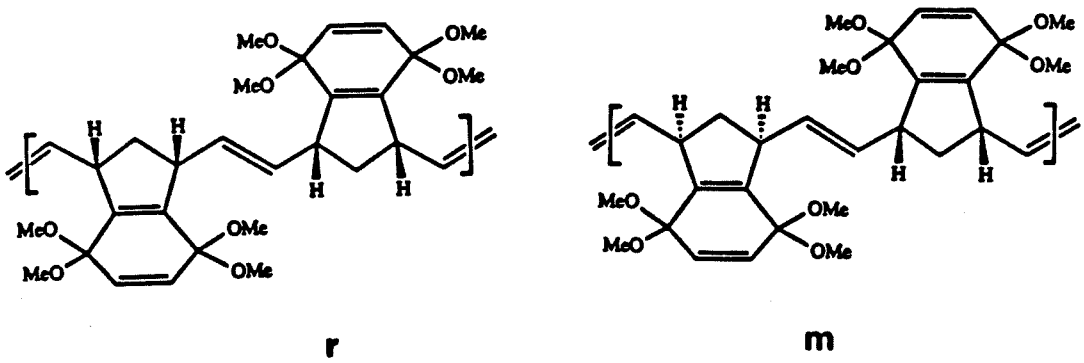

Figure 5.3 Tacticity of diads of **PBQ**.

In addition to diad tacticity, **PBK** and **PNK** may exhibit *cis* or *trans* double bonds. The ^{1}H and ^{13}C NMR suggest that mainly one isomer exists. This conclusion is based on the fact that the same number of ^{13}C NMR signals are in both **PBQ** and **PNQ** as were observed for **6** and **7** respectively. The bulky nature of the monomer is expected to have the effect of producing *trans* olefins as was discussed in Chapter 2. The infrared spectra of **PBK** is complicated (Figure 5.5), and peaks are in regions that could be assigned to both *trans* or *cis* olefins. However, it is known that **10** exhibits a high selectivity for *cis* olefins in the polymerization of norbornene,[5b] where **11** exhibits a *trans* preference. The ^{1}H NMR of **PBQ** produced with **10** and **11** are compared in Figure 5.4. For these spectra, it is deduced that **10** produces predominantly the opposite olefin isomer from **11**. This can be seen by examining the olefinic region in which both materials display a resonance at $\approx$6 ppm corresponding to the olefin of the quinone bisketal. However, the other olefinic signal, which is that of the metathesized olefin, is upfield of this signal for materials produced with **11** and downfield in polymer from **10**. Based on the *cis* preference of **10**, the metathesized double bond of **PBQ** produced with **10** is assigned to be *trans*.

Figure 5.4. ^{1}H NMR (C_6D_6) of PBQ produced with **11** (a); and with **10** (b).

PBK and **PNK** were observed to be slightly sensitive to ambient conditions. Samples became yellowed over the course of a matter of days when left open to the atmosphere. However, infrared spectra indicated only a very slight broadening after 2 weeks of exposure to ambient atmosphere. Hence, for long-term storage, samples were kept in a glove box. Materials were often stored in vials with polyethylene caps for a matter of weeks with no observable change in appearance. Samples that were slightly yellowed from atmospheric exposure exhibited ^{1}H NMR spectra that were identical to that of freshly prepared polymer. Strong freestanding films were readily produced from **PBK** and **PNK**. Films of both **PBK** and **PNK** were hard materials indicating that their glass transition temperatures are above ambient temperature.

Hydrolysis of PBK and PNK:

Investigation of the hydrolysis of **PBK** and **PNK** with dilute acid indicated that the desired polymers **PBQ** and **PNQ** are produced as shown in Scheme 5.5. Upon soaking films of **PBK** and **PNK** in 15% HCl for 2 - 6 days, the films were observed to become shiny black with reflected light and transmit an orange-brown color when held to a light. All of the hydrolysis reactions were done under ambient conditions. The films are somewhat flexible but break if bent too sharply. Films derived from **PBK** are more robust that those from **PNK**. Once hydrolyized, these films are totally insoluble. Infrared spectroscopy has proved to be a valuable tool in monitoring this hydrolysis reaction. As shown in Figure 5.5, **PBK** has a considerable number of strong ketal bands in the region of 1000 - 1200 cm^{-1} which are lost with hydrolysis. In addition, the sharp band at 2840 cm^{-1} which is indicative of methoxy groups is also removed upon hydrolysis. The strong band at 1655 cm^{-1} is assigned to the quinone carbonyl of **PBQ**. The O-H stretching band at 3500 cm^{-1} is mainly due to H_2O in the material, which was also observed in elemental analysis results (see experimental).

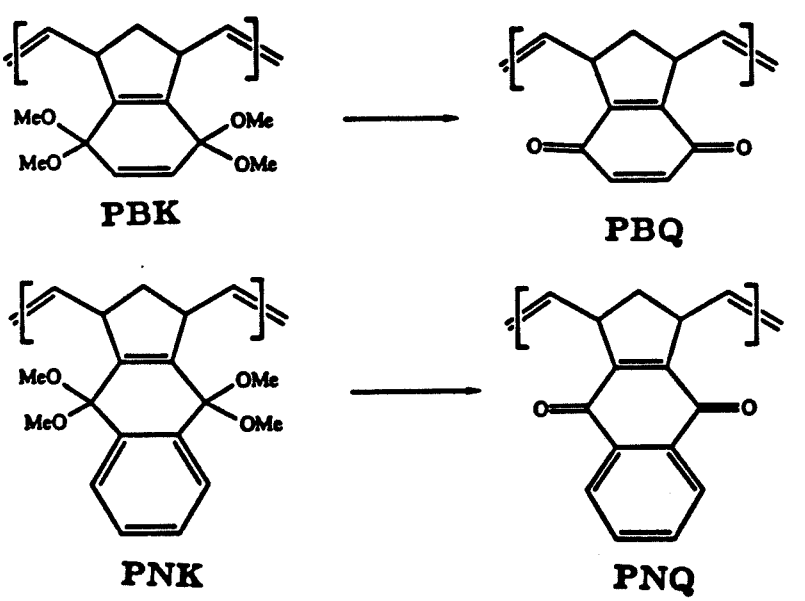

Scheme 5.5

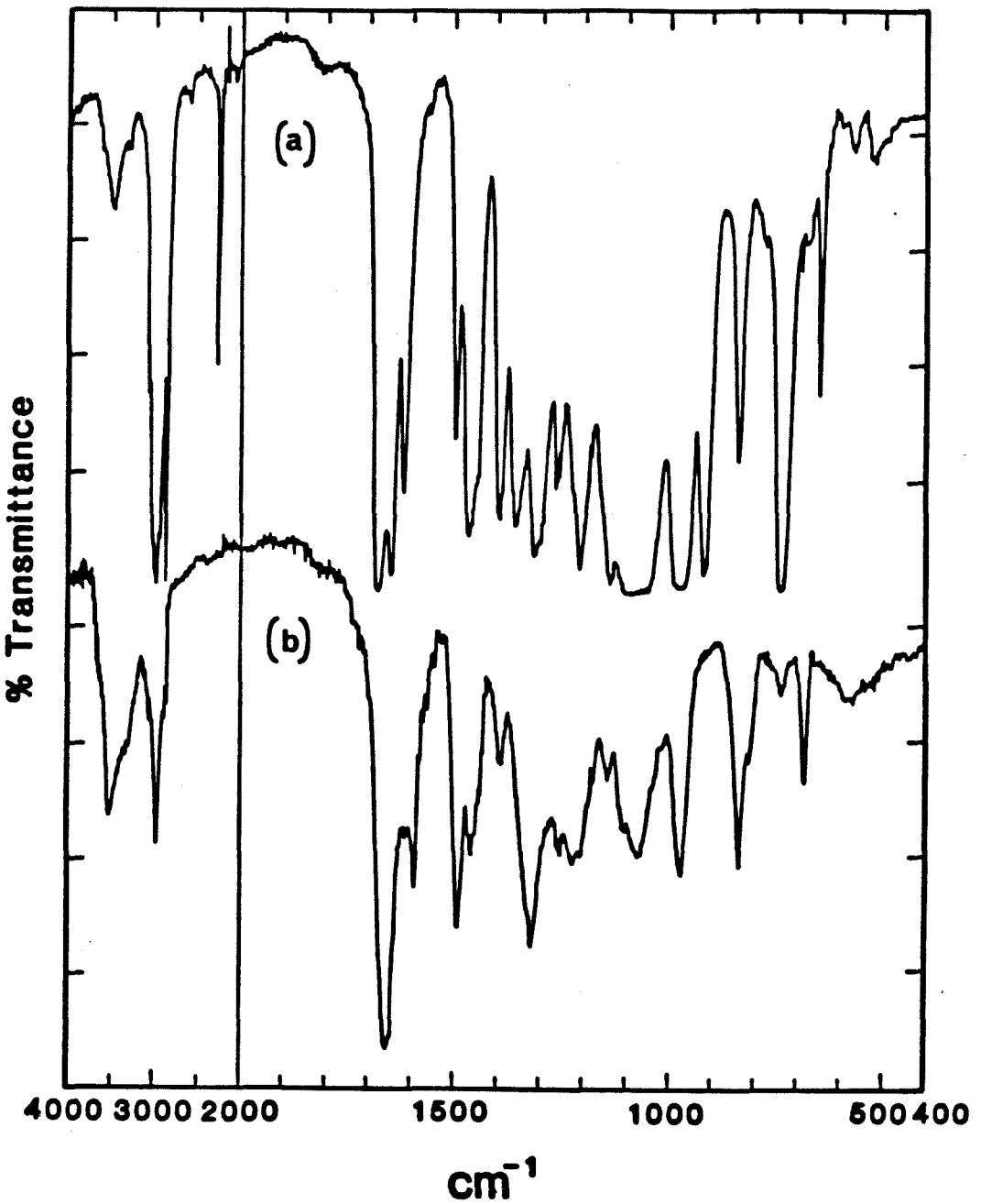

Figure 5.5. Infrared spectra of PBK (a) and PBQ (b).

The conversion of **PBK** and **PNK** to **PBQ** and **PNQ** is confirmed by solid state ^{13}C NMR spectroscopy.[20] CPMAS ^{13}C NMR spectra of **PBQ** and **PNQ** are shown in Figures 5.6 and 5.7 respectively. The ^{13}C NMR of **PBQ** is particularly informative since all of the carbon centers are resolved. The peak at 188 ppm is indicative of the quinone group and dipolar dephasing experiments[21] demonstrate that this peak and the resonance at 134 ppm are the non-proton bearing carbon atoms. Another notable feature of these spectra is the absence of a methoxide resonance which would be observed in the region of 50 - 60 ppm and a ketal carbon which would be observed at $\approx$95 ppm. For **PNQ**, the quinone carbonyl group is observed at 184 ppm. Dipolar dephasing experiments on **PNK** reveal that the resonances at 184, 152, and 135 ppm correspond to non-protonated carbon centers in **PNK**.

Scanning electron microscopy (SEM) was performed on films of **PBK** and **PBQ**. **PBK** has a totally featureless smooth appearance even under high magnification. However, **PBQ** exhibits a highly porous structure with some stress lines. The pores in **PBQ** are circular and approximately .1 to 1 microns in diameter. SEM photographs of these features are shown in Figure 5.8.

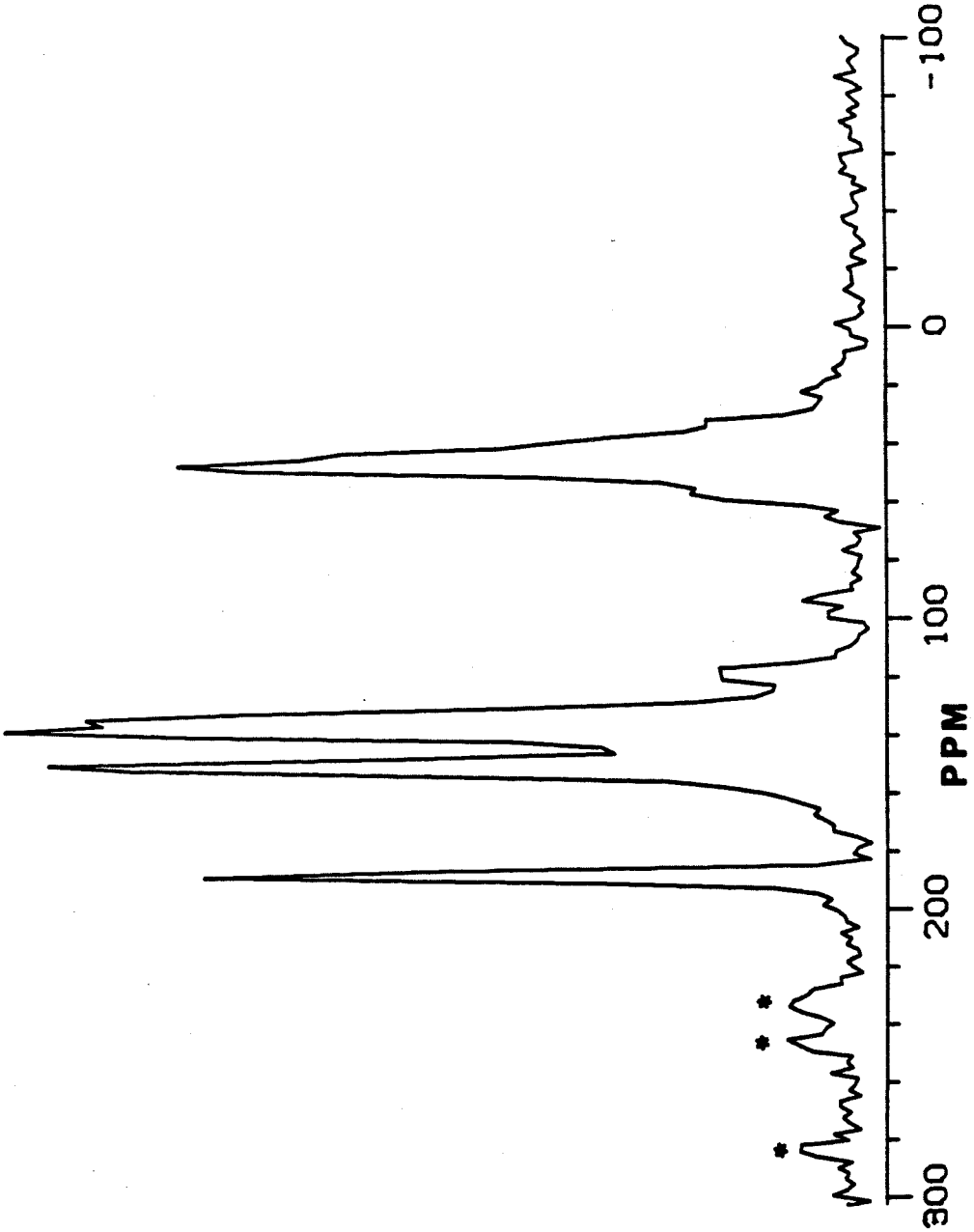

Figure 5.6. CPMAS ^{13}C NMR of PBQ produced by treatment of PBK with 15% HCl for 24 hours. *'s indicate spinning side bands.

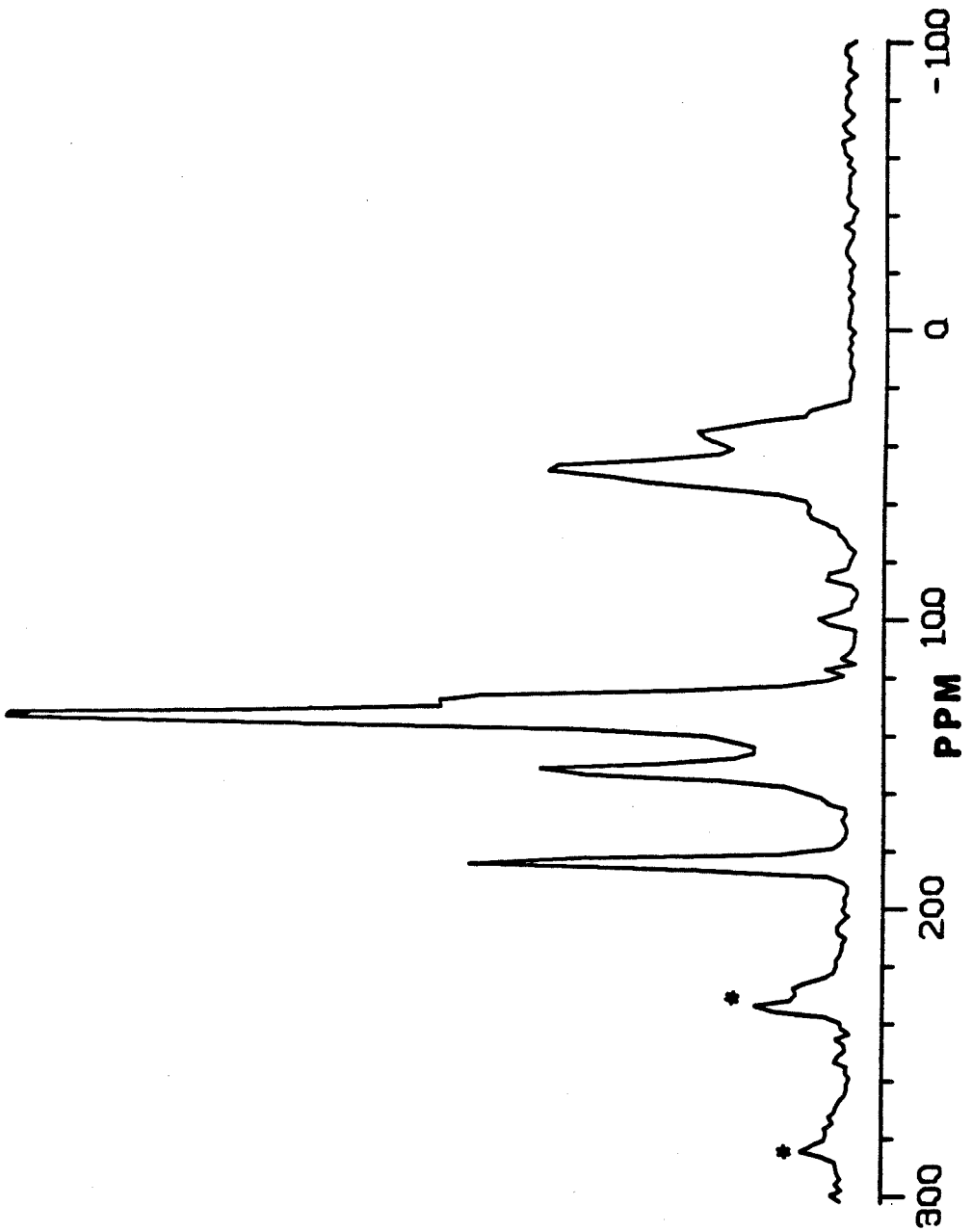

Figure 5.7. CPMAS ^{13}C NMR of PNQ produced by treatment of PNK with 15% HCl for 36 hours. *'s indicate spinning side bands.

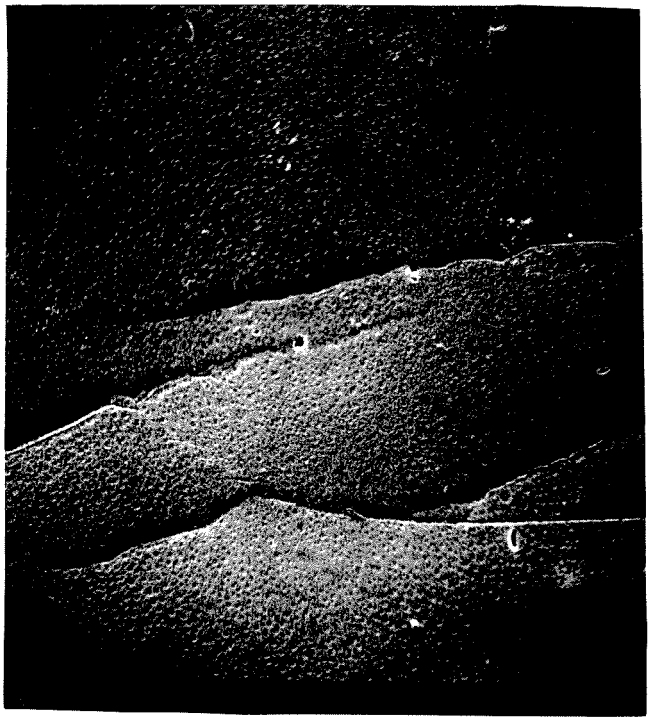

(a)

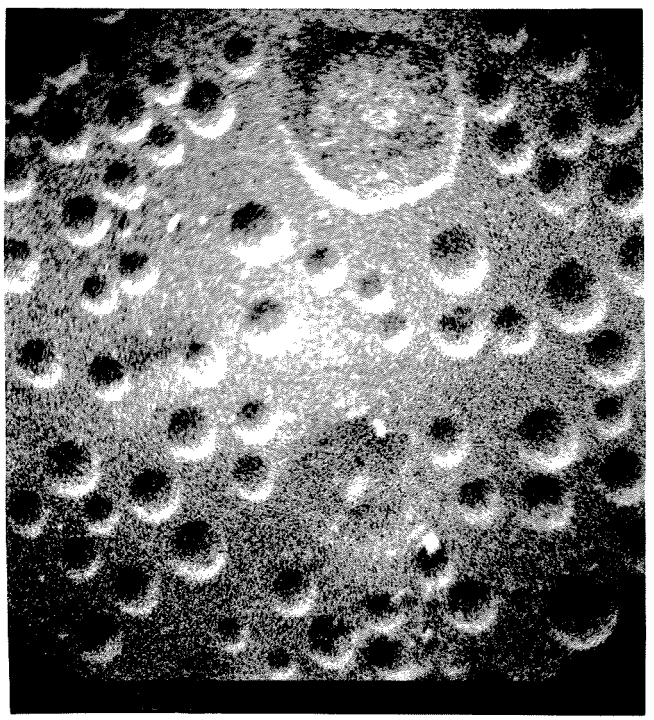

(b)

Figure 5.8. SEM photographs of **PBQ** produced by hydrolysis of **PBK** with 15% HCl for 5 days at a magnification of 2,000 (a); and 20,000 (b).

The fact that **PBQ** and **PNQ** do not tautomerize more readily to **PBHQ** and **PNHQ** may be a reflection of the fact that the aromatic stabilization of the hydroquinone structure is not immediately realized upon enolization. This can be readily seen by considering the mechanism of enolization as is shown for **PBQ** in Scheme 5.6. Tautomerization of a single quinone group does not lead to the aromatic hydroquinone structure as a result of the valence structure imposed on it by adjoining repeating units. Thus, multiple repeat units must all be simultaneously enolized to allow the aromaticity of the hydroquinone group to be realized. However, the exact details of this process may be complicated by redox reactions that may occur within these materials.

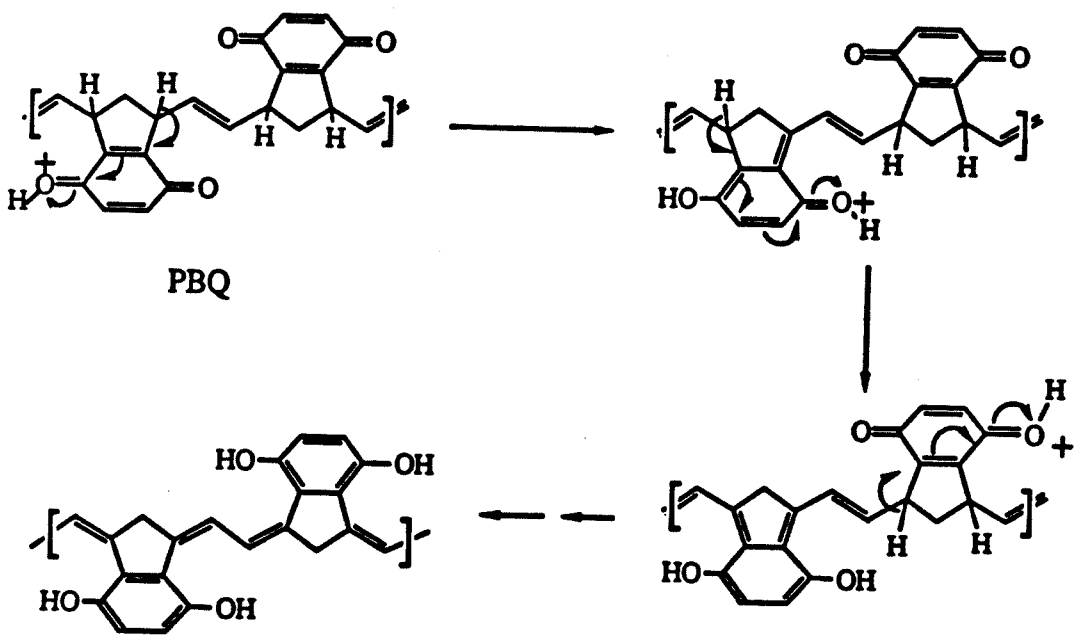

Scheme 5.6

In an attempt to accelerate the tautomerization to the hydroquinone polymers, **PBQ** and **PNQ** were treated with concentrated HCl. Infrared analysis shows the distinct absence of the quinone carbonyl stretching frequencies and a large O-H stretching band. However, CPMAS ^{13}C NMR of this material exhibits a peak at 56 ppm indicating the presence of residual methoxide groups. In addition, there are no residual ketal groups in this material since there were no signals in the region of 90 to 100 ppm. These results are consistent with methanol elimination being competitive with hydrolysis under these conditions as shown below in Scheme 5.7.

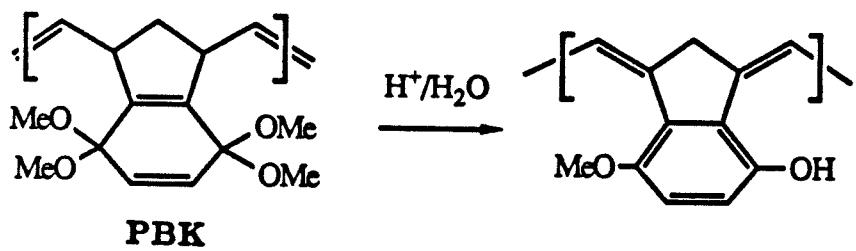

PBK

Scheme 5.7

The conversion of **PBK** to **PBQ** was also attempted with TsOH in acetone. Films immersed in a 5% TsOH:acetone solution became black and shiny over the course of 1 - 2 hours. These films transmitted no light even when held up to a high intensity lamp. Solid state ^{13}C NMR reveals that this procedure gave more of the elimination product than the concentrated HCl treatment.[22] However, it is interesting to note that the films so treated were extremely strong and durable materials with mechanical properties that are far superior to those produced with aqueous hydrolysis. Infrared spectroscopy of this material shows a C=O stretching resonance at 1655 cm^{-1}, but this band is much smaller than that obtained for **PBQ** . Films treated with a 5% TsOH/acetonitrile solution gave nearly identical infrared spectra to those obtained in acetone. However, in this case films became black and shiny in a matter of minutes.

Preliminary studies have indicated that the conversion of **PBQ** to **PBHQ** is possible. These studies have been limited to infrared investigations as a result of technical problems encountered with the solid state NMR spectrometer. The infrared spectra for different chemical treatments of **PBQ** are shown in Figure 5.9. Soaking films of **PBQ** in 15% HCl for 3 weeks results in an increase in the O-H stretching band and a decrease in the intensity of the C=O stretching band (Figure 5.9b). In addition, the C=O is broadened, as is the whole spectra, and is shifted to a lower frequency. These observations are consistent with partial enolization and hydrogen bonded structures in the material. Treatment of films with 5% KOH or pyridine continued this trend as shown in Figure 5.9c and 5.9d. Both of these samples were rinsed with 15% HCl before the spectra were taken. A large increase in the O-H stretching frequency and considerable broadening of the spectra was observed. The C=O stretching band continued its shift to lower frequencies and was at approximately 1595 cm^{-1} for the KOH treated film. These films were black and shiny and would not transmit light when viewed from behind with a high intensity lamp. It is interesting to note that after treatment with pyridine, the film was highly swollen and soft. Once this swollen film was rinsed 15% HCl, the film reduced in size and then became crisp and somewhat brittle. Films treated with 15% HCL for 3 weeks displayed a conductivity of $\approx 10^{-7}\Omega^{-1}cm^{-1}$ after drying.[23] The conductivity of **PBQ** was below the limits of detection. These results are promising yet inconclusive. Futher characterization with CPMAS ^{13}C NMR is necessary to establish the structure of the polymer with certainty. Treatment of films that had been soaked for one month in 15% HCl with $NaClO_3$:NH_4VO_3 in 2% H_2SO_4[24] changed the black and shiny films into yellow films. Quinone groups are yellow in color. However, these films were extremely fragile and broke into small pieces when removed from the solution.

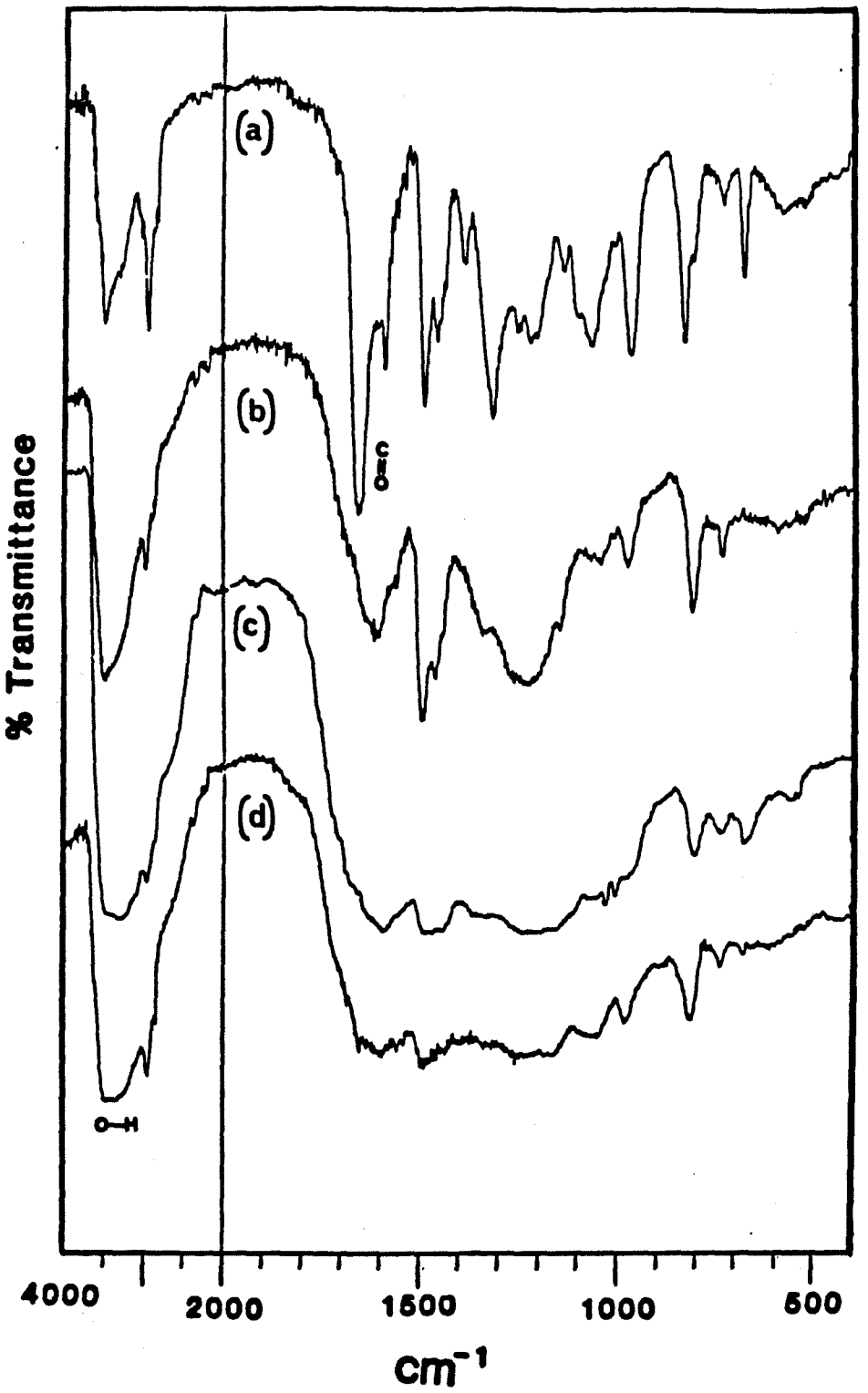

Figure 5.9 Infrared spectra of **PBQ** produced by soaking **PBK** in 15% HCl for 6 days (a); after soaking in 15% HCl for 3 weeks (b); after soaking in pyridene for 6 days (c); and after treatment with 5% KOH for 1 day (d).

Treatment of PBK with Anhydrous Acid:

The observation of methanol elimination reactions in the hydrolysis of **PBK** and **PNK** prompted efforts to selectively produce the elimination product (**12**) as shown in Scheme 5.8. This may be best accomplished by treating the films with anhydrous acid, thus eliminating the hydrolysis reaction pathway. Treatment of **PBK** with ether saturated with HCl produced a red material. A red color is consistent with **12**; however, elemental analysis showed this material to contain approximately 10% chlorine. Treatment of **PBK** with TsOH in benzene also produced a red material. CPMAS ^{13}C NMR of this material is shown in Figure 5.10. The peak at 56 ppm is indicative of methoxide groups and integration of this spectra indicates the ratio of sp^2 to sp^3 carbons to be 2.0. Theoretically, a sp^2 to sp^3 ratio of 2.66 is predicted for **11**. For reference, the ratio of sp^2 to sp^3 for **PBK** is 0.86. Hence, it appears the elimination reaction is proceeding, yet this transformation has not yet been made quantitative. Future studies in the optimization of this process will be pursued with non-nucleophilic conjugate bases in a variety of solvents.

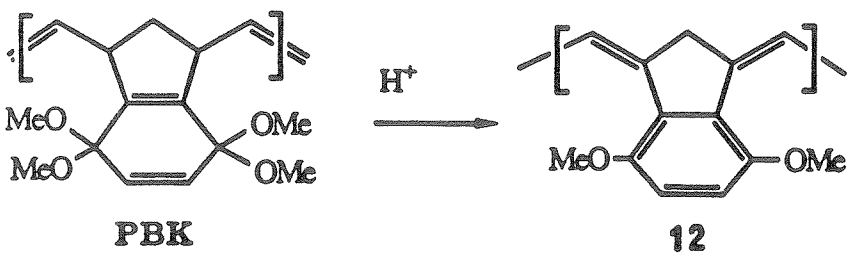

PBK **12**

Scheme 5.8

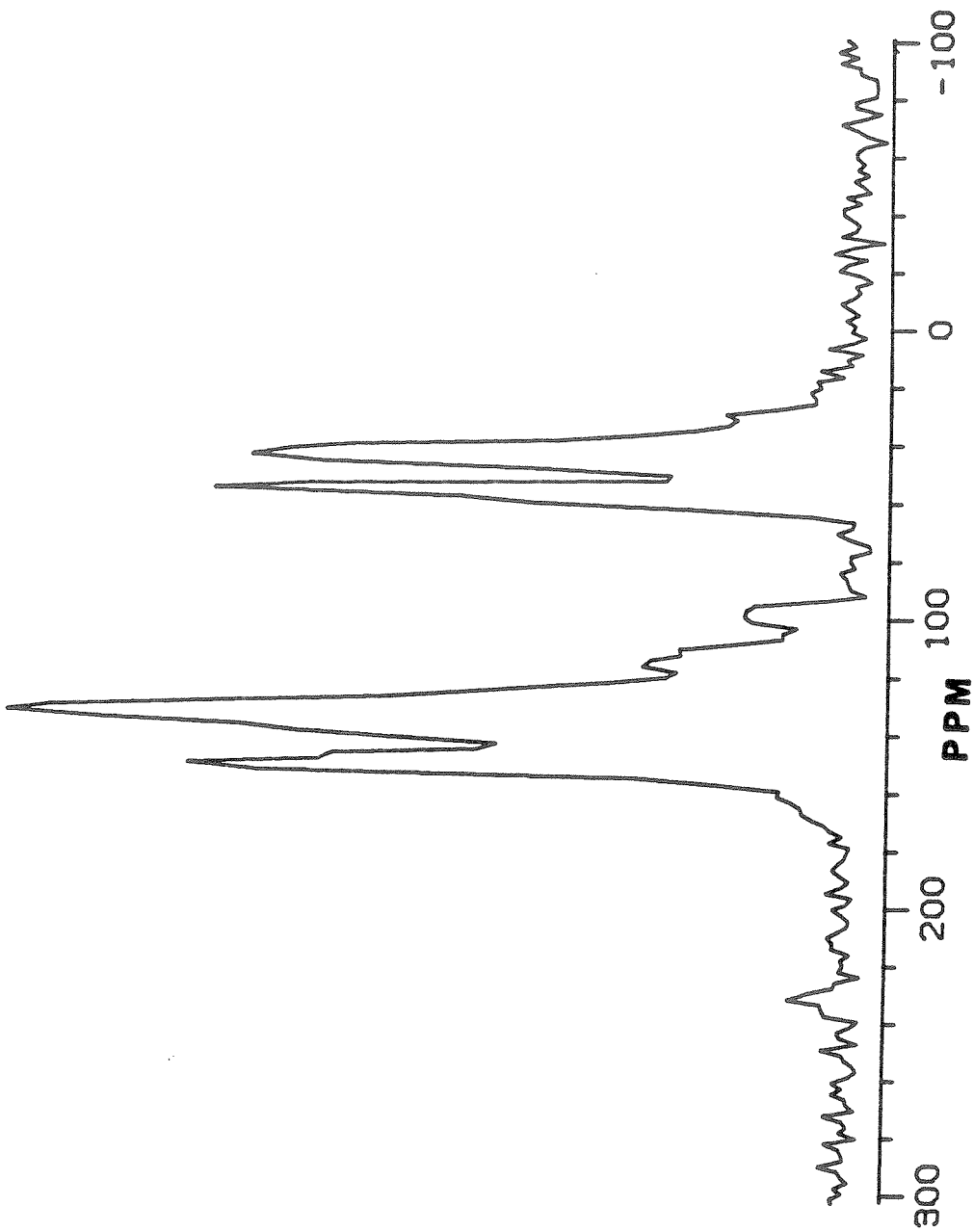

Figure 5.10 CPMAS ^{13}C NMR of PBK treated with 1% TsOH in benzene for 12 hours.

Thermochemistry of PBK and PNK:

Thermogravimetric analysis of **PBK** and **PNK** reveals a stepwise weight loss as shown in Figure 5.11. The weight % reductions of the first steps for **PBK** and **PNK** are both approximately 20%. This weight loss is approximately what would be predicted for the elimination of two equivalents of methanol per repeating unit (Scheme 5.7). Such an elimination for **PBK** would result in a 24% weight loss, and for **PNK** this process would correspond to a 20% weight loss. Thermolysis of **PBK** and **PNK** at 200°C produced a material that was burgundy-red in appearance. This color is again consistent with structure **12**. Once thermolized, these materials are totally insoluble in all solvents. During thermolysis at ≈180°C, samples were initially observed to be soft and to flow with physical manipulation. Hence, these materials apparently have an accessible glass transition temperature and can be melt processed. The UV-vis spectra of **PBK** thermolized at 200°C for 12 hours showed a very broad absorption with spectral intensity from 700 to 190 nm. The onset at 700 nm gives a band gap of this material of 1.8 eV. Thermolized samples of **PBK** maintained good material properties, but heat treated samples of **PNK** were more brittle. The nature of the extruded products were analyzed by ^{1}H NMR. This was accomplished by heating these samples in a hot tube in vacuum at 200°C for 12 hours and collecting the volatile products in a cold trap. The volatiles in the cold trap consisted of a clear colorless liquid for **PBK** and a slightly yellowed liquid for bf PNK. ^{1}H NMR revealed MeOH to be the sole extrusion product from **PBK**. However, the volatiles collected for **PNK** displayed minor signals in the olefinic region in addition to those of methanol. The weight loss steps in the thermolysis of **PNK** (Figure 5.11b) are less pronounced than those of **PBQ**, which also seems to suggest that **PNK**'s thermochemistry may not be as specific as that of **PBK**.

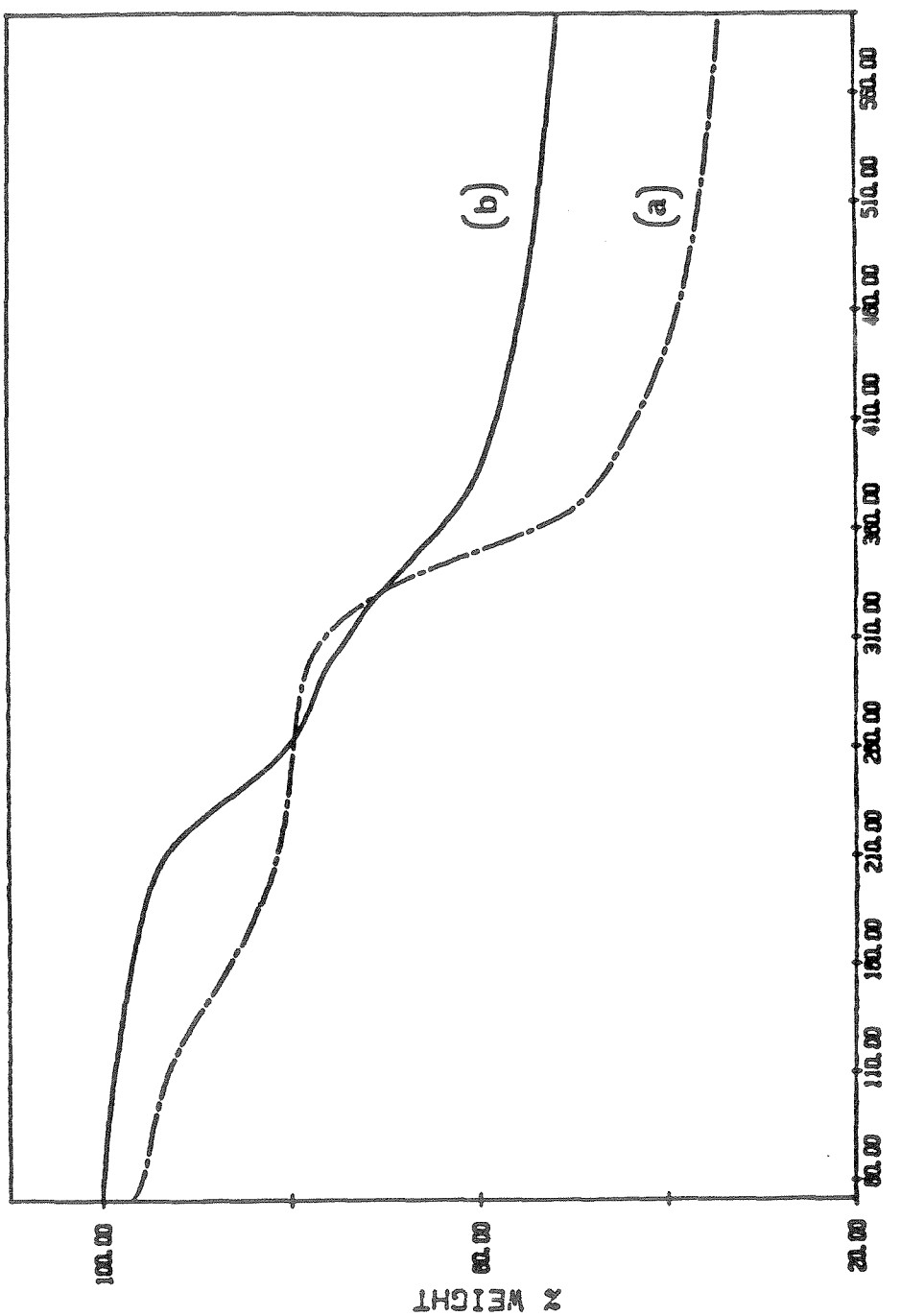

Figure 5.11 Thermogravimetric analysis of PBK (a); and PNK (b);.

Elemental analysis (C,H) of **PBK** treated at 200°C for 12 hours indicated that the elimination reaction had only proceeded to approximately 65% completion. CPMAS ^{13}C NMR also supports the conclusion that the methanol elimination only proceeded to partial completion. As shown in Figure 5.12, ^{13}C NMR of thermalized samples of **PBK** and **PNK** again show the 56 ppm resonance indicating the presence of the methoxy groups. Integration of these spectra reveal a sp^2 to sp^3 ratio of 1.7 and 3.3 for thermolized samples of **PBK** and **PNK**, respectively. These ratios also confirm that the elimination of methanol was incomplete. Theroretically, the sp^2 to sp^3 ratio of the desired materials should be 2.66 and 4.33 for **PBK** and **PNK**, respectively. In an effort to drive the elimination of methanol to completion, samples of **PBK** were heated to 300°C for 12 hours. In this experiment, an orange solid formed on the side of the tube just out of the hot zone of the furnace. Hence, additional unselective chemistry occurs under these conditions. Impregnation of **PBK** with the Lewis acid ZnI_2 was briefly investigated as a means of optimizing the elimination of methanol. Films of **PBK** were impregnated with .1 equivalent of ZnI_2 by co-dissolving the two materials in THF and then casting them into a film. Once dry, the films became red and thermogravimetric analysis revealed a weight loss of 20% in the first step with a slight shift of some of the weight loss to a lower temperature. Further investigation on the effect of impregnation with Lewis acids before thermolysis is in order.

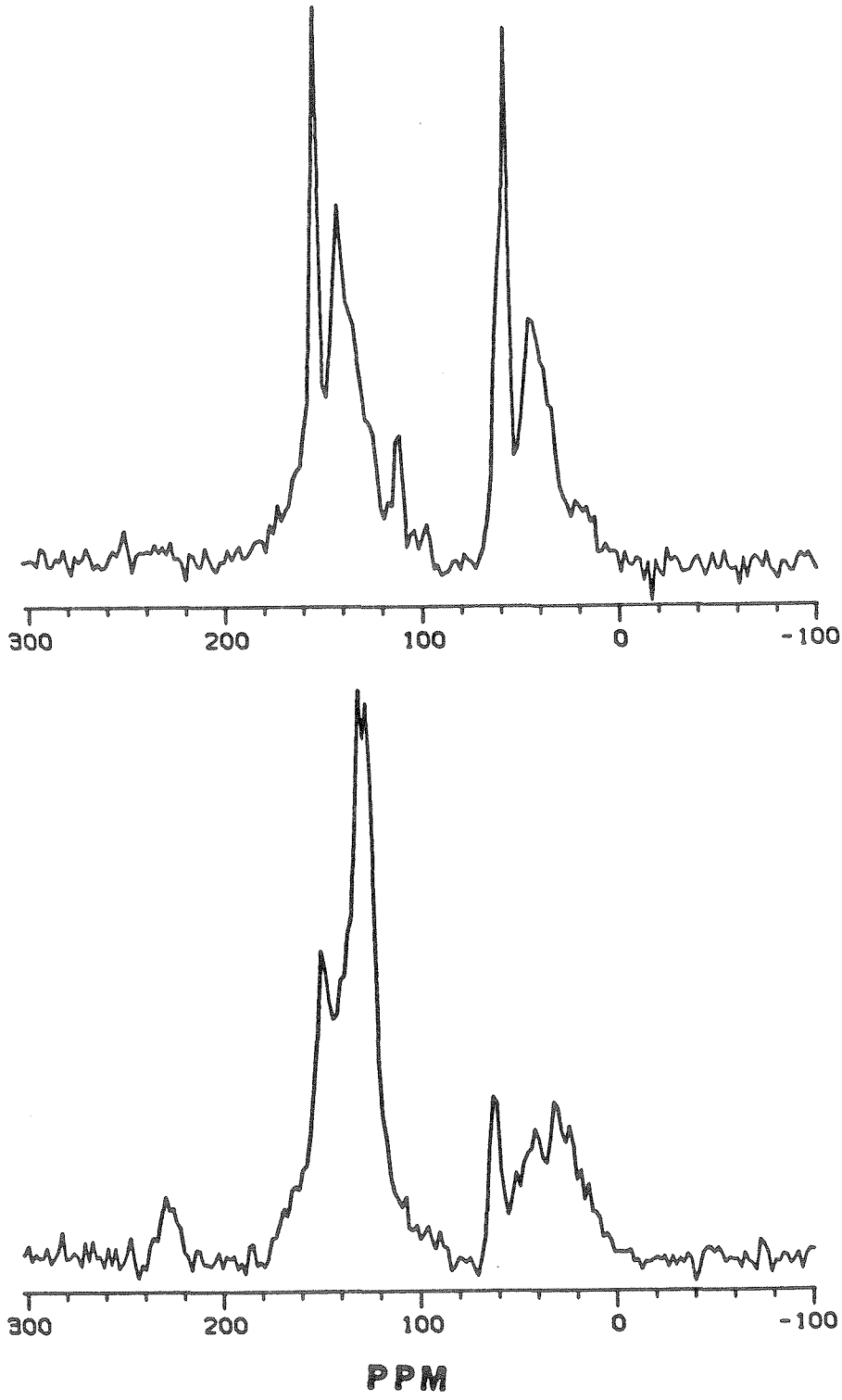

Figure 5.12. CPMAS ^{13}C NMR of material from the 200°C (12 hour) thermolysis of PBK (a); and and PNK (b). (*)'s indicate spinning side bands.

Resonant Raman spectroscopy on the material obtained from the thermolysis of **PBK** was performed to obtain additional information regarding its structure. The Raman spectrum from 1000 to 1700 cm^{-1} is shown below in Figure 5.13. This spectrum exhibits an intense signal at 1574 cm^{-1}, which is characteristic of a C-C stretching mode. There are other minor peaks at 1405 cm^{-1} and 1060 cm^{-1}. The peak at 1060 cm^{-1} is most likely a result of a mode of the methoxy group. Dimethoxy benzene exhibits C-C stretching modes at 1415, 1588, and 1610 cm^{-1}.[25] Extending conjugation is well-known to produce a shift of the C-C stretching bands to lower frequency,[26] hence the Raman spectrum is consistent with the proposed elimination chemistry and the formation of structures such as **12**.

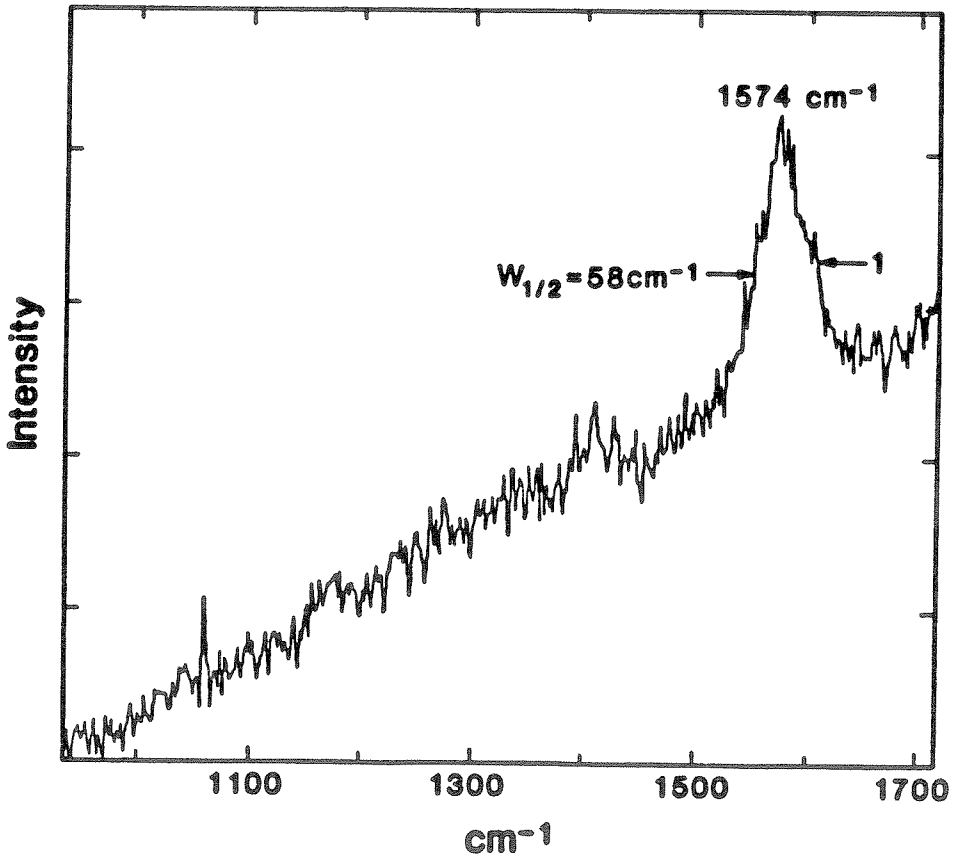

Figure 5.13. Raman scattering of a material produced from thermolysis of **PBK** at 200°C for 45 minutes.

Differential scanning calorimetry (DSC) of **PBK** is shown in Figure 5.14. This thermogram displays two exotherms at 130 and 210°C. Hence, it can be inferred that two different processes occur over the region of the first step in the weight loss. As is shown in Figure 5.14, reheating the samples shows only a smooth upward slope due to the heat capacity of the sample. Integration from 90 to 265°C indicates that the transformation liberates approximately 13 kcal/mole per repeat unit. The origin of the two exotherms cannot be determined at this point. However, the effect of Lewis acids on these processes warrants investigation.

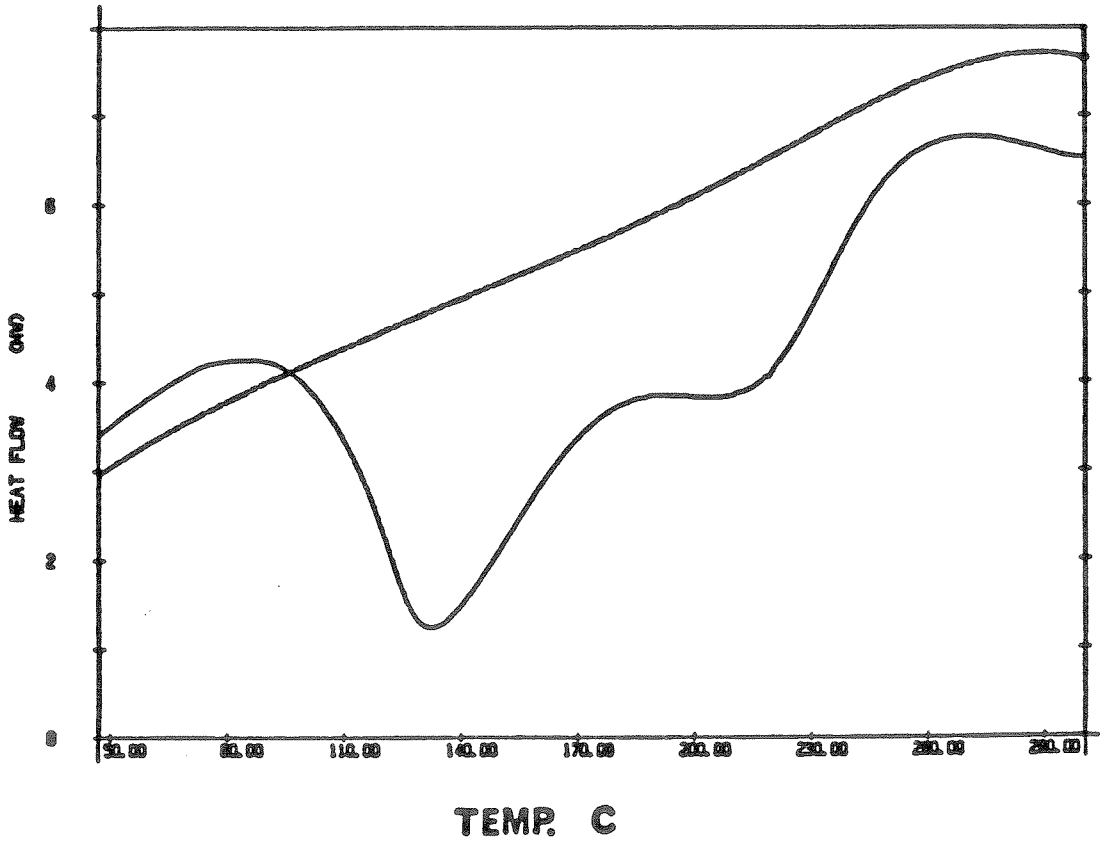

Figure 5.14 DSC thermogram of **PBK** at a scanning rate of 10°C per minute. The broken line is for the same sample when reheated.

Conductivity of Materials Derived from PBK:

The conductivities of some of the materials described in the previous section were monitored as a function of I_2 doping. The conductivities of samples produced by thermolysis of **PBK** and produced by treatment of **PBK** with concentrated HCl are shown in Figure 5.15. The rapid rise of the conductivity of the thermolized samples with I_2 exposure suggests that carriers are readily formed in this material. It additionally suggests that this material possesses extended conjugation which allows transport of carriers throughout the material. Peak conductivities of 4 X $10^{-3}\Omega^{-1}cm^{-1}$ were obtained for this material, and weight uptake measurements indicate the polymer to saturate at 35% I_2. If the dopant species is assumed to be I_3^-, this corresponds to approximately 1 charge per three repeat units. The conductivities of the material treated with concentrated HCl are observed to rise only very slowly, and this material requires 35 hours to attain a maximum conductivity of 5 X $10^{-4}\Omega^{-1}cm^{-1}$. A sample prepared from HCl/ether was observed to give a lower conductivity of 5 X $10^{-7}\Omega^{-1}cm^{-1}$ and samples treated with 15% HCl for three weeks gave a conductivity of $\approx 10^{-4}$ when saturated with I_2. These samples required multiple days of I_2 exposure to attain these conductivities.

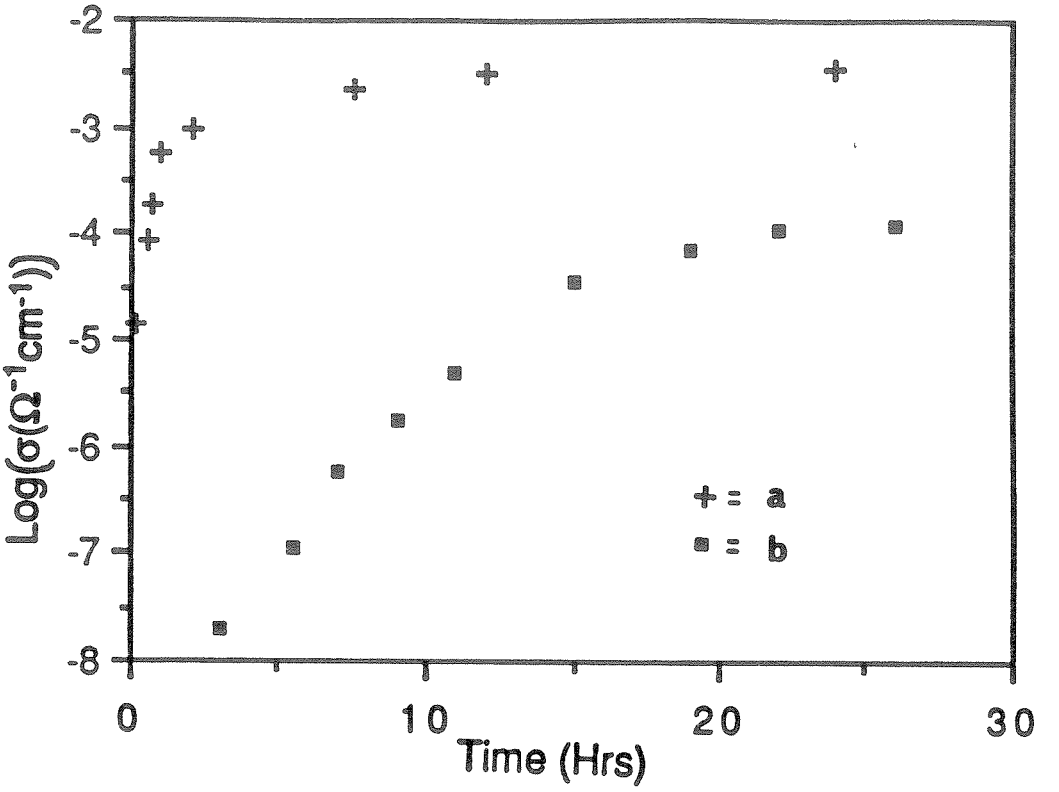

Figure 5.15 Conductivity of polymer samples as a function of exposure to I_2: material from the thermolysis of **PBK** at 200°C for 45 minutes (a); and from concentrated HCl hydrolysis of **PBK** (b).

Iodine doping of the material produced by the thermolysis of **PBK** was further investigated by infrared spectroscopy. The spectra obtained are shown in Figure 5.16. These spectra show a large increase in the region of 1600 to 1000 cm^{-1} with doping. This result is similar to that shown in Chapter 3, Figure 3.18, and may be interpreted similarly. Hence, the large increase in this region is the result of delocalized charge in the polymer backbone.

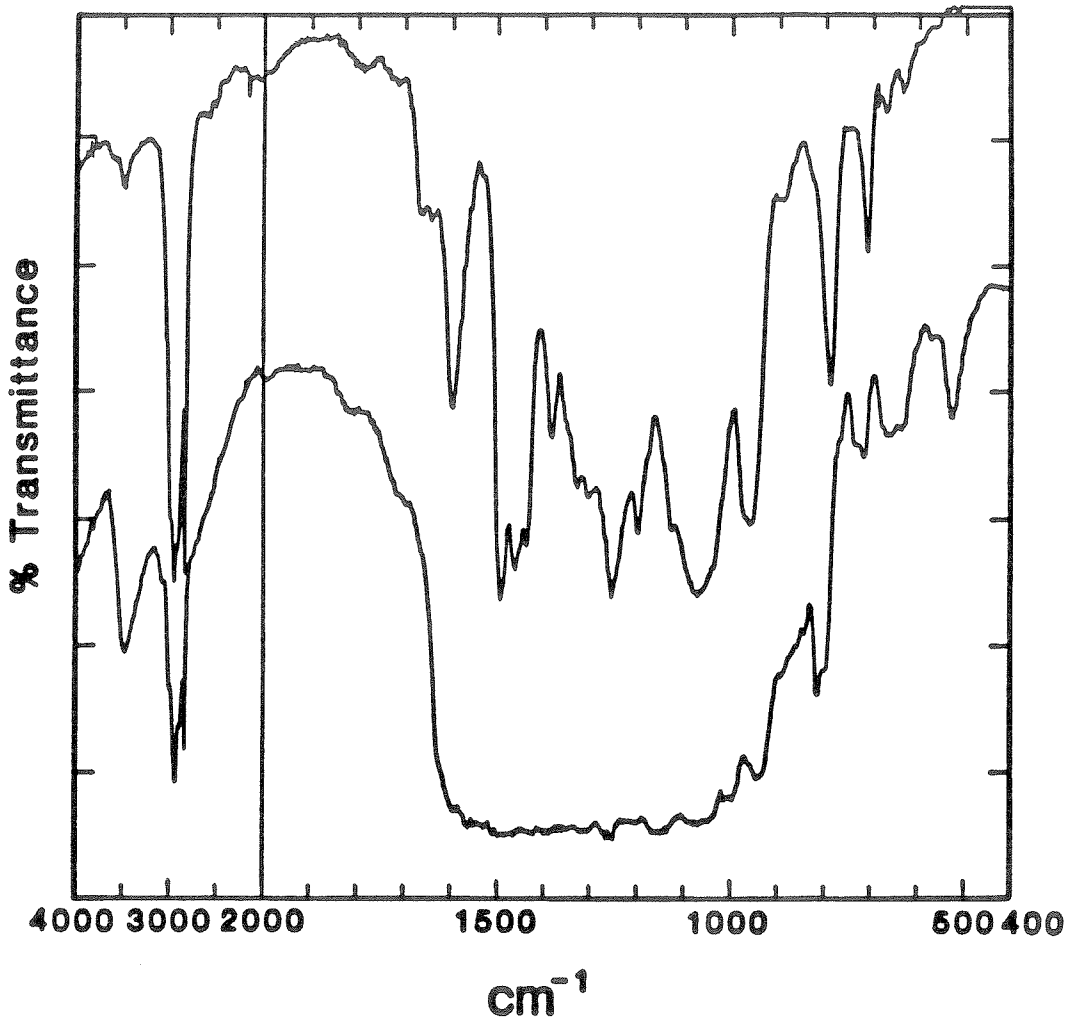

Figure 5.16 Infrared spectra of product from thermolysis of PBK at 200°C for 45 minutes (a); and after I_2 exposure in vacuum for half an hour (b).

FUTURE OUTLOOK:

The study presented herein is a preliminary one. This project is multifaceted and requires focus on some individual problems. The hydrolysis chemistry appears to be selective in dilute aqueous acid. However, the mechanical properties of materials produced in this manner are poor. The mechanical properties of materials produced by hydrolyses in acetone and acetonitrile on the other hand are excellent. Hence, a compromise is in order and hydrolyses in mixtures of water and these solvents or alcohol should be attempted. By improving the material properties of these samples, further investigation of enolization and oxidation will be facilitated. Samples that have been oxidized after enolization to date, have been too fragile to handle.

Of primary interest in the chemistry of **PBQ** and **PNQ** , is locating the most conductive state of these materials. I_2 doping has not yielded highly conductive materials. Perhaps the most attractive method to dope these materials would be to oxidize the enolized materials to quinones and then dope with a protic acid as shown below in Scheme 5.9. This process is very similar to the process in which polyanaline's most conductive state is produced. In addition, the attainment of a polyacetylene backbone in this process may be possible. This can be seen by considering another tautomerization of the doped polymer as shown in Scheme 5.10. The formation of the polyacetylene backbone is speculative. However, these processes are not unprecedented. Oxidation of the polymer may be most selectively done electrochemically.

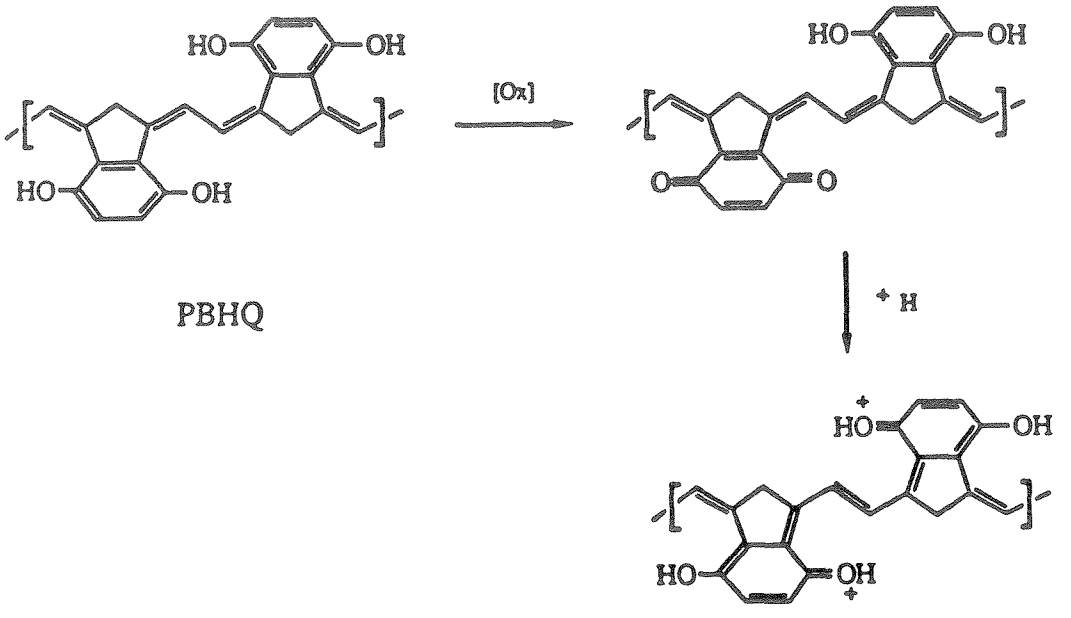

Scheme 5.9

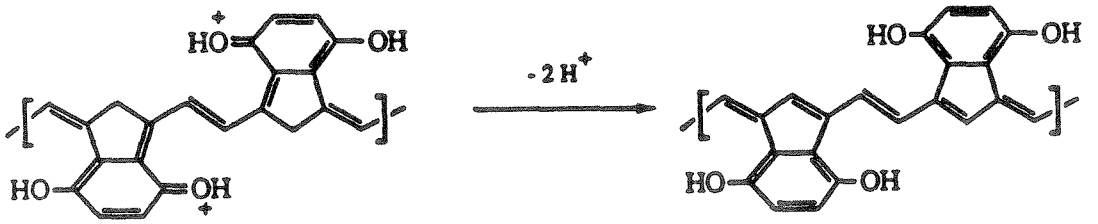

Scheme 5.10

The thermal chemistry appears to be promising and by impregnating catalysts in the film the elimination chemistry may be made to go in higher yields. In addition, the use of anhydrous acid may be a gentle means to affect chemistry analogous to the thermal chemistry.

Polymerization of Cyclobutanone Ketal:

The ROMP of the ketal of cyclobutanone (13) was also briefly investigated as a route to a conductive polymer precursor. This monomer is synthesized in a straightforward manner from 3-bromo-cyclobutanone as shown in Scheme 5.10.

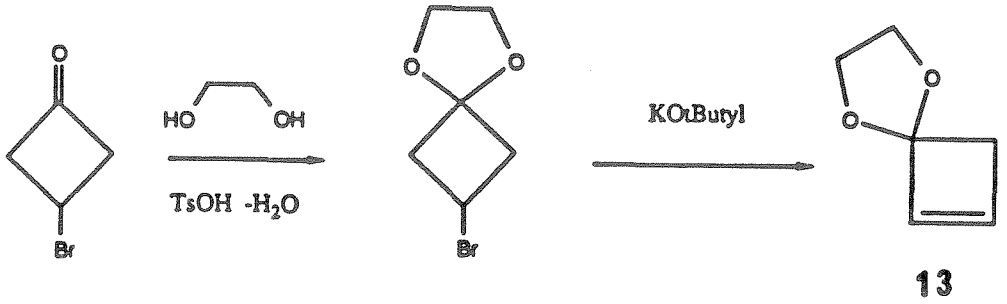

Scheme 5.11

The ROMP of **13** was found to proceed smoothy for both catalyst **9** and **10** to produce polymer **14** as shown in Figure 5.17. The structures of these polymers are complicated by head to tail and head to head isomers.

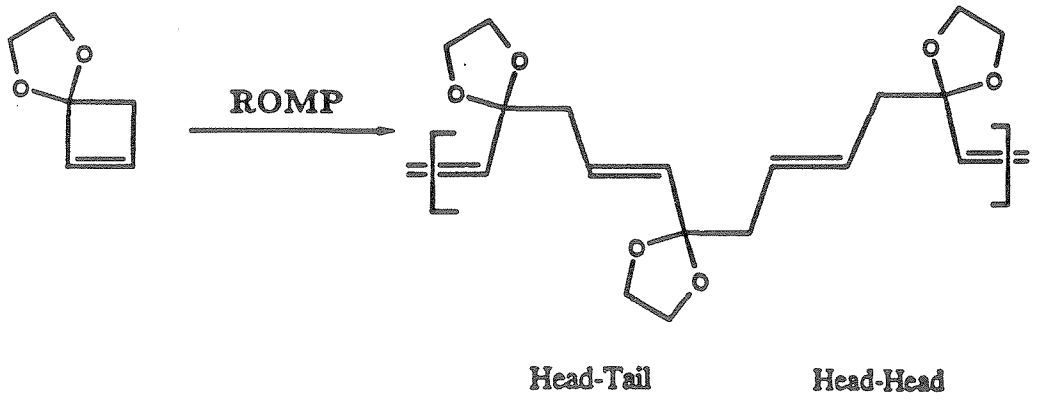

Figure 5.17. ROMP of 13 and isomers produced.

The polymer produced with **9** appears to have the least complicated structure. The ^{1}H NMR of this material is shown in Figure 5.18. There are two distinct allylic resonances in this structure. The material produced with **10** has an additional allylic resonance at 2.98 ppm in addition to those observed in **14** produced with **9**. Infrared analysis indicates that the polymer obtained with **9** has all *trans*-olefins. Hence, the observation of the two different allylic resonances in this material must reflect that both head to tail and head to head structures are present in the polymer; **14** synthesized with **10** has both *cis-trans*-isomers and head to tail isomers.

The polymer is readily deprotected with 10% TsOH in H_2O to produce **15** as shown below.

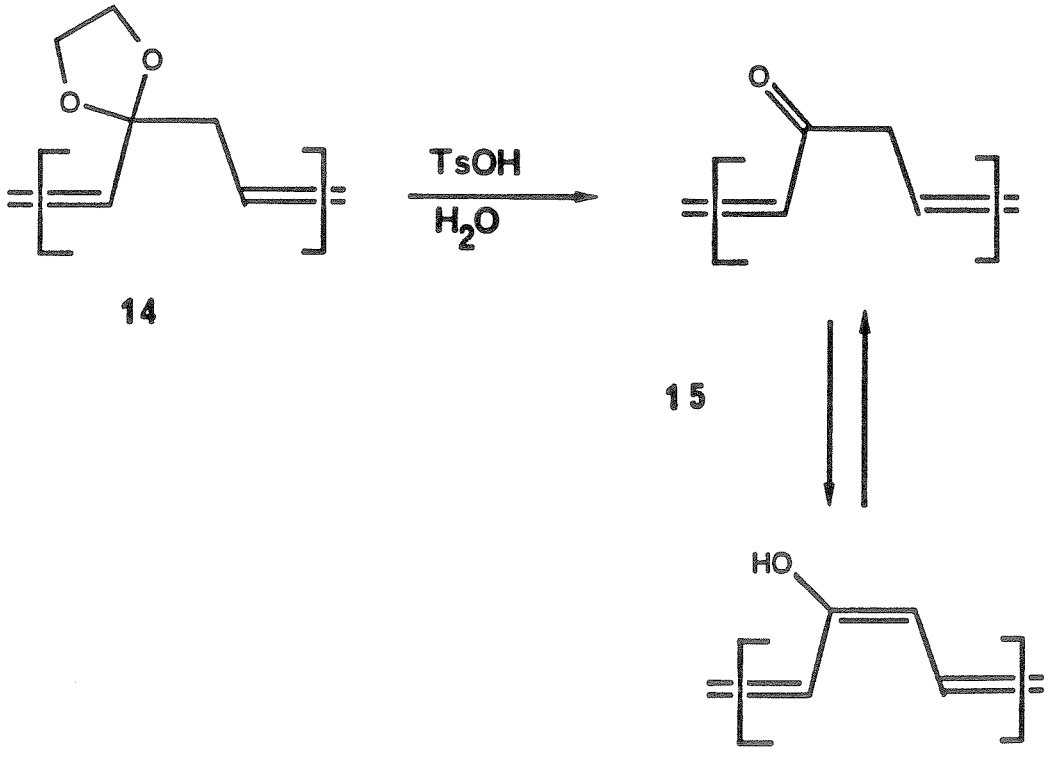

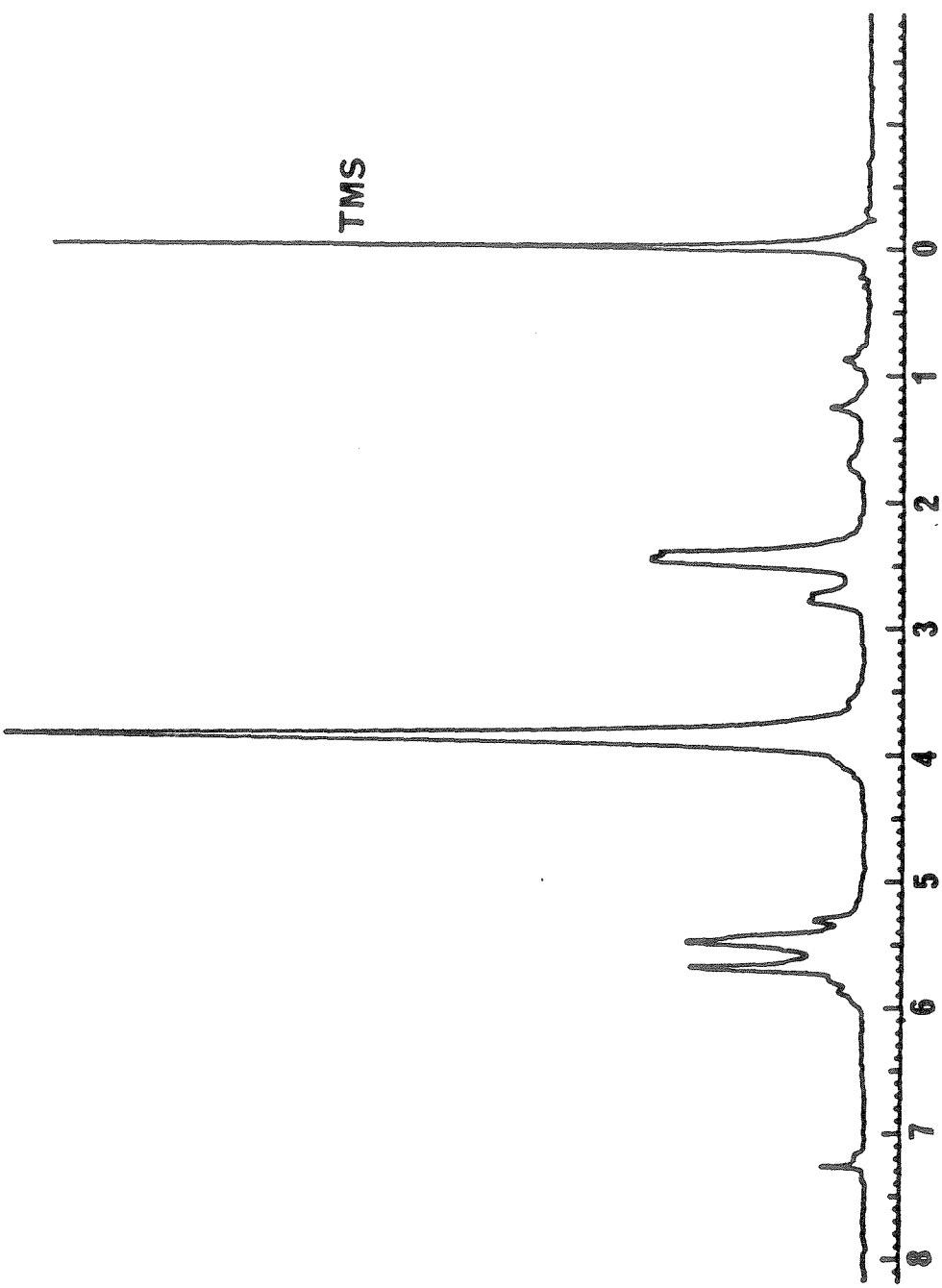

Figure 5.18. ^{1}H NMR of **14** polymerized with **9**.

15 was tan in appearance and insoluble in all solvents. Infrared analysis confirms the presence of carbonyl groups with a strong broad band from 1730 to 1620 cm^{-1}. This material turned dark brown when put in 15% KOH indicating that enolization created high conjugation lengths. Initially, this process was reversible and the color would change to light brown when put back in dilute acid. However, upon repeated cycling of this process the films became brown and exhibited little noticeable color change with pH. Treatment with 60% H_2SO_4 gave some indication that this material may be acid dopable. Films of **15** which were immersed in 60% H_2SO_4 became bronze and highly reflective by reflective light and were blue by transmitted light. Drying these films in vacuum (10^{-6} torr) over P_2O_5 resulted in loss of the luster of the bronze appearance and gave a material with a conductivity of 2 X 10^{-3} $\Omega^{-1}cm^{-1}$. Treatment of samples with an anhydrous base (KOt-butyl in THF) gave only light brown films. These films do not exhibit the color changes discussed above with pH. Hence, this treatment appears to decompose the polymer. The decomposition may be the result of Michael additions between polymer chains.

Oxidation of **15** with a variety of oxidants proved unsuccessful. Enolization appears to give decomposition; hence, an alternative procedure must be developed. One possible means of accomplishing this goal would be to enolize the polymer and trap the enol with a TMS group as shown in Scheme 11 below. The TMS group may then be removed and the polymer oxidized to form a conductive material. The head to tail ratio of these materials may also be improved by using a more bulky ketal.

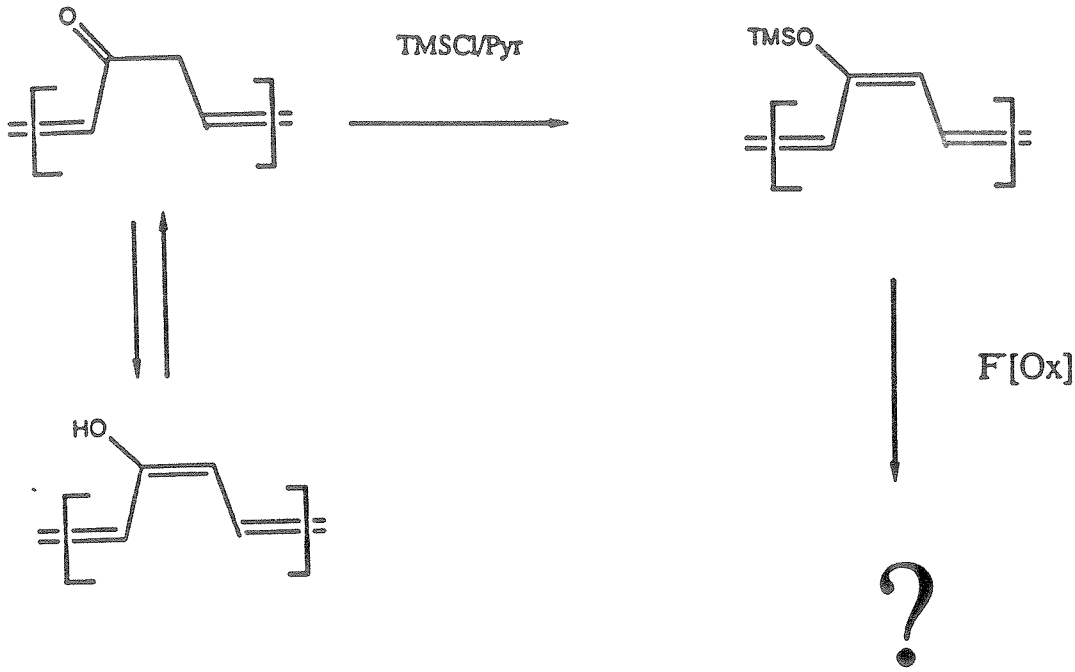

Scheme 5.12

Experimental Section:

General Procedures: All manipulations of air- and/or moisture-sensitive compounds were carried out using standard Schlenk or vacuum line techniques. The flush gas (argon) was purified by passage through columns of activated BASF RS-11 (Chemalog^{TM}) oxygen scavenger and Linde 4 Å molecular sieves. Manipulation of solids was performed in a Vacuum Atmospheres glove box equipped with a MO-40-1 purification train. The purification train was charged with activated Ridox^{TM} oxygen scavenger and Linde 11 Å molecular sieves. When dealing with moisture sensitive materials, all glassware was rinsed with base, dried in a 140°C oven, and subjected to vacuum while hot.

^{1}H and ^{13}C NMR were recorded on a Joel FX-90Q spectrometer (89.6 MHz ^{1}H, 23.53 MHz ^{13}C). Chemical shifts were referenced to the solvent (^{13}C NMR) or to residual protons in the solvent (^{1}H NMR). Infrared spectra were acquired on a Shimadzu IR-435 spectrometer. Infrared samples were free standing films of the polymer. UV-vis spectra were obtained on a HP-8451A diode array spectrometer. Samples for UV-vis analysis were films of $\approx$.1 micron thick.

The conductivity measurements were made with a home-built probe, described in Appendix B, or a commercial Sigmatone sheet resistivity probe. In the four point conductivity measurements,[38] current was supplied by a Power Designs 605 precision power source (.1-6 V), current was measured with a Keithley 160B digital multimeter (.1 to 10^{-10} amps.), and the voltage was measured with a Fluke 895A differential voltmeter.

CPMAS ^{13}C NMR were obtained on a home-built spectrometer at a carbon frequency of 35.36 Hz. A commercial Doty Scientific CPMAS probe was used. The samples were ground in Na_2SO_4 into a homogenous mixture and packed tightly in a 7 mm o.d. sapphire rotor (Doty Scientific) with Kelef end caps. Sample sizes

were 100-200 mg and the balance was Na_2SO_4. A Doty Scientific CPMAS probe was employed and spinning speeds of 3.5 to 5 KHz were obtained. Data collection was performed with a Nicolet 1280 computer and Nicolet NMC software. Chemical shifts were referenced to an external adamantane standard. The adamantane standard was used for setting the Hartmann-Hahn matching condition and the 90°C ^1H pulse which was typically $\approx 5\mu s$. Cross-polarization contact times were 2 or 3 ms. A "rolling baseline" in some samples was eliminated by leftshifting the free-induction decay by 0-100μs, or by using a baseline fit routine in the software.

Thermal analysis was performed on a Perkin Elmer DSC-7, TGS-2 thermogravimetric analyzer, and a 3600 data station. Scanning rates are specified in the figures. SEM photographs were obtained on an ETEC autoscan electron microscope. Samples were prepared by coating the materials with 100 Å of Au:Pd (80:20) with a Technics Hummer 5 sputter coater.

Raman spectra were obtained in a backscattering configuration with a Spex 1-m double monochromator instrument and photomultiplier tube operating in the photon counting mode. The excitation source was the 488 nm line of an Ar^+ laser with a nominal intensity less than 200 mwatts. The laser beam was focused to a spot $\approx$100 μm in diameter. A Spec SCAMP computer was used to drive the monochromator and collect data.

Thermolysis of **PBK** and **PNK** was conducted in a tube furnace under vacuum. The temperature was monitored with a thermocouple which was mounted in the furnace next to the tube. In addition, films were also thermolized in a dry box on a hot plate. The hot plate had been previously calibrated with a thermometer.

Materials: Solvents for the polymerizations were dried and deoxygenated. Benzene was dried and deoxygentated with sodium benzophenone ketyl. Pentane was purified prior to drying and deoxygenation by treatment with H_2SO_4

for 3 weeks. The titanocene metallacyle catalyst **9** was prepared by the literature methods[27]. Catalysts **10** and **11** were made by the published procedure[28] and purified by recrystallization from pentane (20°C to -50°C). The hexane for precipitation of the polymers was partially deoxygenated by bubbling argon through the solvent for a half an hour or more. ZnI_2 (Aldrich) was purified by heating at 100°C under vacuum for 12 hours. Cyclopentadiene was cracked and stored until ready for use at -50°C. The benzoquinone was recrystallized before use from ether. Phenylbenzoquinone and methylbenzoquinone were purchased from Aldrich and used without purification. Dimethylsulfate is a hazardous material and was used in a hood. 3-bromo-cyclobutanone was synthesized by the literature method.[29]

Synthesis of 3a, b, and c: This procedure is for **3a** in particular and will also work for 3b and 3c. Cyclopentadiene (18.32 g .277 mmole) and benzoquinone (30 g .277 mmole) were added together in 500 ml of ether at -15°. The reaction is allowed to warm to RT and then stirred at room temperature for 3 hours. The ether is then removed *in vacuo* to yield a slightly yellowed solid. 500 ml of methanol and a spatula scoop of $KHCO_3$ is then added to this material. The solution gradually turns dark brown over the course of approximately 10 minutes and all the solids are dissolved. The reaction mixture becomes warm as the Diels Alder adduct is converted to the hydroxyquinone dervative **4**. This mixture is stirred for 12 hrs and then the methanol is removed *in vacuo* to yield a black tar. **4** is pumped at 10^{-6} torr for 3 hours and then 500 ml of ether, Ag_2O (8.6 g 3.7 mmole), and 9 g $MgSO_4$ are added. This mixture is allowed to stir at room temperature for 5 hours. At this time, the reaction has become bright yellow in color, and filtration and removal of the solvent *in vacuo* yields crude **3a** as a yellow solid with slightly brown spots. This mixture is then sublimed at 60°C (10^{-6} torr) to yield 84% of pure **3a**. ^{1}H NMR ($CDCl_3$): 2.31 (2H d), 4.10 (2H, t), 6.57 (2H s), 6.84 (2H t) ppm. ^{1}H NMR ($CDCl_3$) of **3b**: 2.02 (3H d), 2.30 (2H

d), 4.08 (2H t), 6.42 (1H t), 6.89 (2H t) ppm. ^{1}H NMR ($CDCl_3$) of 3c: 2.34 (2H d), 4.16 (2H t), 6.64 (1H s), 6.90 (2H t), 7.42 (5H s) ppm.

Synthesis of 5: The hydroxyquinone **4** is produced exactly as was reported above in the synthesis of **3a**. 51.4 g (.295 mole) of **4** (crude product) is dissolved in 300 ml of ethanol with heating. Portions of dimethylsulfate (90.78 g .72 mole) and sodium hydroxide (32 g .80 mole) in 80 ml H_2O are added in alternate ($\approx$10 portions) over approximately 30 to 40 minutes. With each addition of reagent, the reaction is heated to reflux and some methyl ethyl ether is produced. After the addition is complete, 10 more grams of sodium hydroxide in 10 ml of H_2O are added with considerable exothermicity. The reaction is then refluxed for 2 hours, and then most of the ethanol is distilled off to leave approximately 100 ml of solvent and a considerable amount of brown residue. This mixture is allowed to cool and then given an aqueous ether workup. The ether layer is evaporated to a brown solid and then recrystallized to give 29 g (48%) of **4** as a white solid. This material was further purified by sublimation at 90 °C and 10^{-6} torr. ^{1}H NMR ($CDCl_3$): 2.04 (2H s), 3.57 (6H d J=1.9 Hz), 4.03 (2H d J=.4 Hz), 6.30 (2H d J=1.9 Hz), 6.68 (2H d J=.4 Hz) ppm. ^{13}C NMR ($CDCl_3$): 46.78, 55.68, 69.79, 109.23, 140.10, 142.64, 148.55 ppm. Infrared (neat): 2995 (m), 2950 (s), 2820 (m) 1602 (m), 1493 (s), 1445 (s), 1330 (w), 1297 (m), 1250 (s), 1165 (m), 1080 (w), 1040 (s), 997 (w) 965 (w), 897 (m), 827 (m), 800 (m) cm^{-1}.

Synthesis of 6: 12.5 g (61.8 mmole) of **5** is partially dissolved in 1% KOH in methanol (200 ml) and 40 ml THF. Two platinum gauze electrodes are immersed in the solution and the reaction is vented to a bubbler. A 6 volt power supply is hooked up to the electrodes with an in-line ammeter. The initial current was approximately 160 mA. The solution was then electrolyzed for 5 days while monitoring the reaction with TLC (ether:hexane 1:4). The R_f of **5** is .4 and the

product (5) decomposes and gives a streak from a R_f of 0 to .25. Continued electrolysis would not drive the reaction to completion. Hence, the reaction mixture was given an ether:aqueous (sat. K_2CO_3) workup with minimum air exposure and the electrodes were cleaned with a Bunsen burner. The ether extract was evaporated *in vacuo* and the resulting oil was redissolved in 200 ml of 1% KOH in methanol and electrolysis was continued. After 36 hours of more electrolysis, the reaction was determined to be complete by TLC and given an ether:aqueous (sat. K_2CO_3) workup. Again, care was taken to minimize air exposure. The ether was removed *in vacuo* to give a slightly yellowed tacky crystalline solid. This material was then put in a sublimator and sublimed rapidly at 80°C. The solid melted under these conditions and was stirred. Once sublimed, the white crystalline solid was then resublimed ≈5 - 6 times at 65°C. On the final sublimations, the solid on the bottom did not melt. ^{1}H NMR ($CDCl_3$): 2.13 (2H t), 3.12 (6H s), 3.30 (6H s), 3.83 (2H q), 6.09 (2H s), 6.84 (2H t) ppm. ^{13}C NMR ($CDCl_3$): 153.6, 142.2, 132.4, 95.1, 72.4, 50.9, 49.6 ppm. Melting point: 66-69°C . Elemental analysis calculated: C, 68.18; H, 7.65; found: C, 68.33; H, 7.50. Mass spec.: M^+ 264, M^{+1} 265 (22%), M^{+2} 266 (8.75%).

Synthesis of 7: The synthesis of **7** employed the same procedure as was used in the synthesis of **6**. The analogous precursor to **7** was obtained in 60% yield based on the starting quinone. The product was recrystallized from pet. ether and obtained as a white crystalline solid. This compound was then electrolyized in 1% KOH in methanol and THF. The current efficiencies for this process were high and the reaction took roughly half as long as the electrolysis of **5**. This product was then recrystallized from pet. ether and then sublimed once to give pure material. ^{1}H NMR ($CDCl_3$) 2.23 (2H m), 2.91 (6H s), 3.08 (6H s), 3.98 (2H t), 5.93 (2H t), 7.45 (2H m), 7.67 (2H m) ppm. ^{13}C NMR 49.8, 51.5, 72.0, 97.0, 126.1, 128.7, 137.7, 142.0, 155.0 ppm. Melting point: 107-108°C . Elemental analysis calculated: C, 72.61; H, 7.01; found: C, 72.70; H, 6.90.

Synthesis of 8: The fulvene derivative presents a problem in the fact that the initial Diels Alder reaction between the 6,6-dimethylfulvene and benzoquinone is a reversible reaction. If excess quinone is present during the enolization of the Diels Alder adduct, then redox reactions occur which produce hydroxy quinone and a [2.2.1] quinone derivative. Hence, this was avoided by using an excess of the 6,6-dimethylfulvene in the Diels Alder reaction. Evaporation of the solvent from this Diels Alder adduct results in the evaporation of 6,6-dimethylfulvene and shifts the equilbrium. After stirring at 3 hours triethyl amine was added to the Diels Alder reaction mixture. This mixture was then allowed to stir for 3 hours and the reaction became progressively darker. The solvent was then evaporated and the reaction mixture was dissolved in ethanol and then was subjected to the same reaction that was done for 5. The reaction mixture was extremely impure and after aqueous workup and drying, the mixture was given preliminary purification by eluting the product through a 3 inch pad of silica gel eluted with ether/pentane 1/3. The product was then recrystallized from methanol and sublimed at 110°C. Total yield was ≈20%. ^{1}H NMR ($CDCl_3$): 1.55 (6H s), 3.78 (6H s), 4.60 (2H t), 6.50 (2H s), 6.93 (2H t) ppm. ^{13}C NMR ($CDCl_3$): 18.966, 47.10, 56.33, 101.37, 109.56 139.45, 142.96, 148.10, 161.22. Elemental analysis calculated: C, 79.34; H, 7.44; found: C, 79.00; H, 7.15. This material was then subjected to electrolysis as was described for 6 and the crude product was isolated as a yellowed oil which was sublimed at 75°C to give a white product. This material was then resublimed 2 more times; however, the material became more yellow with the additional sublimation. ^{1}H NMR ($CDCl_3$): 1.99 (6H s), 3.15 (6H s), 3.21 (6H s), 4.31 (2H t), 6.03 (2H s), 6.94 (2H t) ppm. ^{13}C NMR ($CDCl_3$): 18.05, 49.45, 51.07, 95.07, 96.56, 133.15, 141.60, 153.43, 162.84 ppm. Melting point: 74-79°C .

General Polymerization of 6 and 7: Care was taken to exercize the best possible air sensitive technique in this transformation. The glassware was

pumped into a drybox while hot, and monomer and catalysts were loaded into separate Schlenk tubes in the drybox. The reactions were monitored by thin layer chromatography. This was performed by opening the reaction vessel with an argon purge, and taking an aliquot from the polymerization reaction with a long capillary tube that had just been taken from a hot oven. This aliquot was then spotted on a TLC plate. Developing the TLC plate in ether:hexane 1:4 shows the polymer to remain at the origin and streaking due to monomer decomposition with a R_f between 0 and .25. When no streaking was observed, the reaction was stirred for a half an hour more and then terminated. The best results for precipitation of the polymer were obtained by diluting the polymerization mixture with CH_2Cl_2 and adding it to hexane, which is $\approx$20 times the volume of the solution to be precipitated.

Synthesis of PBK: **6** (2.00 g 7.58 mmole) and **11** (43.4 mg .0758 mmole) were mixed together in 5 ml of benzene. The reaction was observed to become slightly warm after a couple of minutes and the color turned from a light yellow to a light orange. The reaction was noticeably viscous after 1 hour, and TLC indicated that the reaction was complete after 1.5 hours. After half an hour more stirring at room temperature, the polymerization was diluted with CH_2Cl_2 (20 ml) and precipitated in hexane as a slightly off white powder. The hexane was filtered away via a cannula with filter paper wired around the end. The powder was then pumped overnight at 10^{-6} torr and then taken into the drybox. The weight of the product was 2.1 g indicating that residual solvent was present in the polymer. NMR and elemental analysis samples were prepared by pumping on the polymer for 24 hr at 10^{-6} torr in a drying pistol heated with refluxing methanol. ^{1}H NMR ($CDCl_3$): 1.55 (w vbr), 2.25 (w vbr), 3.10 (s br), 3.16 (s br), 3.49 (m br), 3.70 (w vbr), 5.72 (m br), 6.01 (m br) ppm. ^{1}H NMR (C_6D_6): 1.85 (w vbr), 2.37 (w vbr), 3.14 (s br), 3.22 (s), 3.59 (w vbr), 3.98 (w vbr), 5.92 (m br), 6.12

(m br) ppm. ^{13}C NMR ($CDCl_3$): 36.8, 42.0, 46.5, 51.8, 96.1, 130.2, 132.8, 144.8 ppm. Infrared (film): 2950 (s br), 2833 (s s), 2200 (m s), 1672 (s br), 1642 (s s), 1614 (s s), 1492 (m s), 1462 (s br), 1389 (s s), 1348 (s s), 1301 (s br), 1252 (m s), 1202 (s s), 1075 (s br), 962 (s vbr), 911 (s s), 834 (m s), 730 (s s), 645 (w s) cm^{-1}. UV-vis in $CHCl_3$ λ_{max}= 243 nm ϵ= 8,400 $M^{-1}cm^{-1}$, λ= 289 nm ϵ= 3,200 $M^{-1}cm^{-1}$. Elemental analysis calculated: C, 68.18; H, 7.65; found: C, 68.13; H, 7.78. Catalyst **10** under similar conditions gives **PBK** with the following ^1H NMR (C_6D_6): 1.65 (w vbr), 2.18 (w vbr), 2.26 (s br) 4.11 (m br), 5.60 (w br), 5.81 (m br), 5.97 (m br) ppm.

Synthesis of PNK: To 2 g (6.36 mmole) of **7** is added 48.8 mg (.085 mmole) of **11** in 12 ml of benzene. **7** slowly dissolves over 3 to 4 minutes as the reaction proceeds, and the solution turns to a light orange tint. After 6 hours of stirring at RT, the reaction is diluted with approximately 10 ml of CH_2Cl_2 and precipitated as a white powder in 400 ml of rapidly stirred hexane. Workup such as was given for **PBK** gave **PNK** 2.05 g. ^1H NMR ($CDCl_3$): 1.87 (w vbr), 2.45 (w vbr), 2.91 (s s), 2.95 (s s), 3.56 (m br), 6.03 (m br), 7.36 (m br), 7.57 (m br) ppm. ^{13}C NMR ($CDCl_3$): 35.8, 46.9, 51.2, 51.6, 98.3, 125.9, 129.0, 129.6, 132.8, 145.8 ppm. Elemental analysis calculated: C, 72.61; H, 7.01; found: C, 71.65; H, 7.15.

General Hydrolysis of PBK and PNK: The hydrolysis reactions were done with absolutely no attempt to use air sensitive conditions. Films of **PBK** and **PNK** were usually studied, and all infrared analysis was performed on samples prepared in this manner. Samples for solid state ^{13}C NMR were more conveniently packed when they were powders, hence the samples for CPMAS experiments were powders. Hydrolysis of films was carried out in jars with a lid at ambient temperature. Film thicknesses were typically .001 to .0001 cm thick.

Formation of PBQ: A film (or powder) of **PBK** is immersed in 15% HCl and soaked for 36 hours. At this time the film is orange-brown by transmitted

light. CPMAS ^{13}C NMR: 188, 150, 137, 134, 47 ppm. Infrared: 3500 (m vbr) O-H (H_2O), 2920 (m s), 1655 (vs br), 1588 (m s), 1493 (s s), 1453 (s br), 1393 (w s), 1318 (s s), 1220 (s br), 1075 (m vbr), 967 (m s), 830 (m s) 673 (w s) cm^{-1}. Elemental analysis: calculated for $C_{11}H_8O_2$; C, 76.74; H, 4.66; found after drying at 65°C for 24 hours at 10^{-6} torr: C, 71.26; H, 5.62; data fit to $C_{11}H_8O_2(H_2O)_{.68}$: C, 71.66; H, 5.08; found with no drying: C, 69.48; H, 4.66; data fit to $C_{11}H_8O_2(H_2O)_{1.07}$: C, 69.01; H, 5.30.

Formation of PNQ: A film (or powder) of **PNK** is immersed in 15% HCl and soaked for 36 hours. The film is orange brown by transmitted light. CPMAS ^{13}C NMR: 183.6, 151.5, 133.6, 128.6, 47.6, 35.3 ppm. Infrared: 3500 (w s), 3100 (m s), 2920 (s br), 1666 (s br), 1602 (s s), 1453 (s br), 1236 (s vbr), 1075 (s vbr), 978 (s vbr), 874 (w s) 758 (s br), 665 (w s) cm^{-1}. Elemental analysis: calculated for $C_{15}H_{10}O_2$; C, 81.08; H, 4.50; found after drying at 65°C for 24 hours at 10^{-6} torr; C, 75.36; H, 5.02; data fit to $C_{15}H_{10}O_2(H_2O)_{.95}$; C, 75.28; H, 4.97.

Thermolysis of PBK and PNK: A tube with the polymer sample was put in a tube furnace and heated to 200°C under dynamic vacuum for 12 hours. These materials were burgundy-red in appearance. Analysis of the product from the thermolysis of **PBK** is the following. CPMAS ^{13}C NMR: 153 (s s), 141 (m br), 110 (w s), 56 (s s), 42 (m br). Infrared: see Figure 5.16. Elemental analysis: calculated for $C_{13}H_{12}O_2$; C, 78.00; H, 6.00; found C, 73.04; H, 6.52. Elemental analysis data is fit to a structure with 65% conversion to structure **11**. Analysis of the product from the thermolysis of **PNK** is the following. CPMAS ^{13}C NMR: 149 (m s), 129 (s s), 126 (s s), 61 (m s), 29 (m vbr). Elemental analysis: calculated for $C_{17}H_{14}O_2$; C, 81.6; H, 5.6; found; C, 79.24; H, 5.62.

Treatment of PBK with TsOH in C_6H_6: .5 g of **PBK** was dissolved in 50 ml of benzene at RT, and a spatula tip of TsOH:H_2O was added to the solution

with stirring. The solution became immediately red in color and solid polymer began to precipitate. After 12 hours of stirring, the solution was filtered to give a dark red insoluble solid. CPMAS ^{13}C NMR: 151 (s s), 133 (s br), 115 (m br), 98 (w br), 56 (s s), 44 (s br). Elemental analysis found: C, 71.65; H, 5.99.

Synthesis of Cyclobuanone Ketal: 16.8 g (.117 mole) of 3-bromo-cyclobuanone was added to 50 ml of ethylene glycol, 100 ml benzene, 150 ml of benzene, and 1 g of TsOH. This mixture was then refluxed overnight under Dien-Stark conditions. The water in the trap (3 ml) was then emptied and the trap was filled with activated molecular sieves for 6 hours. The reaction was given an aqueous (sat. K_2CO_3):benzene workup and dried over $MgSO_4$. The benzene was then distilled off to leave a slightly brown oil (21 g). ^1H NMR ($CDCl_3$): 3.70 (4H s), 4.10 (1H m), 2.57 (4H m) ppm. ^{13}C NMR ($CDCl_3$): 31.8, 48.7, 63.7, 64.3, 107.2 ppm. This material was then added to KO-tButyl (15.03 g .1341 mole) in THF (75 ml) at 0°C under argon and stirred for one hour. The reaction was then allowed to warm to RT and stir for 1 hour more. At this time ether (50 ml) was added and the excess base was precipitated. The reaction was filtered through a medium frit. This mixture was then distilled to approximately 10 mls of a yellowed solution and then transfered via cannula onto NaH which reacted with the residual t-butanol. This mixture was then stirred for 1.5 hours and then the volitile products were removed by vacuum transfer as a clear liquid. This solution was 6.5 g in total and was approximately 50% by weight **13**, with a balance of THF and benzene. Total yield from 3-bromo-cyclobutanone was ≈20% . ^1H NMR ($CDCl_3$): 6.03 (1H d J=3.0 Hz), 6.51 (1H d J=3.0 Hz), 3.99 (4H s), 2.8 (2H s) ppm. ^{13}C NMR ($CDCl_3$): 135.7, 141.3, 109.4, 31.2, 64.5 ppm.

Synthesis of **14**: 23.1 mg (.093 mmole) of **9** is dissolved in 5 ml of benzene and .8 ml of a 50% solution of **13** in THF and benzene is added. The reaction is stirred for 30 minutes at RT and then 4 ml of n-butanol is added to deactivate

the catalyst and then the polymer is precipitated in pentane; **14** is isolated as a slightly yellowed soft solid in approximately 70% yield. ^{1}H NMR ($CDCl_3$): 2.52 (m d), 2.82 (m d), 2.98 (w d), 3.98 (s s), 5.32 (w s), 5.47 (m s), 5.52 (m s), 5.71 (m s) ppm. ^{13}C NMR ($CDCl_3$): 133.0 130.81, 127.3, 125.87, 108.13, 64.65, 41.21, 36.25 ppm. Infrared: 2890 (s s), 2965 (s s), 1670 (w br), 1476 (w s), 1429 (w s), 1184 (s br), 1124 (s br), 1043 (s), 973 (s), 946 (s), 874 (w br), 800 (w br).

REFERENCES:

1. *Handbook of Conducting Polymers*; Skotheim, T. J. (ed.); Dekker: New York, 1986.

2. March, J. *Advanced Organic Chemistry* 3rd ed., McGraw Hill, 1986.

3. See Feast, W. J. in reference 1.

4. (a) Ivin, K. J. *Olefin Metathesis*; Academic Press, 1983. (b) Draguton, V.; Balabon, A. T.; Dimonie, M.; *Olefin Metathesis and Ring Opening Polymerization of Cyclo Olefins*; John Wiley and Sons, 1985.

5. (a) Gilliom, L. R.; Grubbs, R. H. *J. Am. Chem. Soc.* **1986**, 108, 733. (b) Schrock, R. R.; Feldman, J.; Cannizzo, L. F.; Grubbs, R. H. *Macromolecules* **1987**, 20, 1169.

6. Cannizzo, L. F.; Grubbs, R. H. *Macromolecules* in press.

7. Elias, H. *Macromolecules*; vol. 1, 2nd ed. page 155, Plenum Press, 1984.

8. (a) *Molecular Electronic Devices;* Carter, F. L. (ed.); Marcel Dekker, 1982. (b) *Molecular Electronic Devices;* Carter, F. L. (ed.); Marcel Dekker, 1987. (c) See the special issue on molecular electronics: IEE Proc. I **1983**, 130, 197-263.

9. Sze, S. M. *Physics of Semiconductor Devices;* 2nd ed., Wiley: New York, **1981**

10. Cannizzo, L. F.; Swager, T. M.; Grubbs, R. H. unpublished results.

11. See discussion in chapter 1.

12. See MacDiarmid, A. G. and Kaner, R. B. in reference 1.

13. Degrand, C.; Miller, L. L. *J. Electroanal. Chem* **1982**, 132, 163-176. Degrand, C.; Miller, L. L. *J. Electroanal. Chem* **1981**, 117, 267-281.

14. *The Chemistry of the Quinonoid Compounds;* Patai, S. (ed.), John Wiley and Sons, **1974**.

15. Catalysts that were employed without success were: **9**, **10**, $RuCl_3$, $IrCl_3$, $W(CO)_5CPhOMe$, $WOCl_4$:$EtAlCl_2$, WCl_6:$SnMe_4$, $ReCl_5$, $RuCl_3$:COD.

16. Brown-Wensley, K. A.; et al. *Pure and Appl. Chem.* **1983**, 55, 1733-1744 and references therein.

17. Swenton, J. S. *Acc. Chem. Res.* 1983, 16, 74-81. Belleau, B.; Weinberg, N. L. *J. Am. Chem. Soc.* **1963**, 85, 2525-2526.

18. Any attempts at separation on silica gel even with triethylamine as an eluent gave decomposition. The same was true for basic alumina.

19. Novak, B. M.; Grubbs, R. H. *J. Am. Chem. Soc.* **1988**, 110, 960.

20. Yannoni, C. S. *Acc. Chem. Res.* **1982**, 15, 201-208.

21. Eckert, H.; Yesinowski, J. P.; Sandman, D. J.; Velazquez, C. S. *J. Am. Chem. Soc.* **1987**, 109, 761.

22. The methoxy resonance at 56 ppm was distinctly larger for this material than that produced with concentrated HCl.

23. The materials are hydroscopic and to measure a reliable conductivity of the material and not the water in the material samples must be dried. Drying was best accomplished by putting samples in a vacuum chamber with P_2O_5 under 10^{-5} torr.

24. Billman, J. H.; Wolnak, B.; Barnes, D. K. *J. Am. Chem. Soc.* **1944**, 66, 652.

25. Marjit, D.; Bishui, P.K.; Banerjee, S. B. *Indian J. Phys.* **1972**, 46, 457.

26. Freeman, S. K. *Applications of Laser Raman Spectroscopy;* John Wiley and Sons, **1974**.

27. (a) Lee, J. B.; Ott, K. C.; Grubbs, R. H. *J. Am. Chem. Soc.* **1982**, 104, 7491. (b) Gilliom, L. R.; Grubbs, R. H. *Organometallics* **1986**, 5, 721. (c) Strauss, D. A.; Grubbs, R. H. *J. Mol. Cat.* **1985**, 28, 9 and references therein.

28. (a) Schaverin, C. J.; Dewan, J. C.; Schrock, R. R. *J. Am. Chem. Soc.* **1986**, 108, 2771. (b) Schrock, R. R.; Depue, R. T.; Feldman, J.; Schaverien, C. J.; Dewan, J. C.; Liu, A. H. *J. Am. Chem. Soc.*, **1988**, 110, 1423.

29. Sieja, J. B. *J. Am. Chem. Soc.* **1971**, 93, 2481-2483. With the modification that a photochemically assisted Hunsdiecker reaction was used, Meyers, A. I.; Fleming, M. P. *J. Org. Chem.* **1979**, 44, 3405-3406.

Appendix A

PROCEDURE FOR THE SYNTHESIS OF OSBORN'S CATALYST

A detailed experimental procedure for the synthesis of catalyst 4 has not yet been published.[1] This procedure is based on that which was supplied by J. Kress. The reaction scheme for the synthesis of this catalyst is shown below.

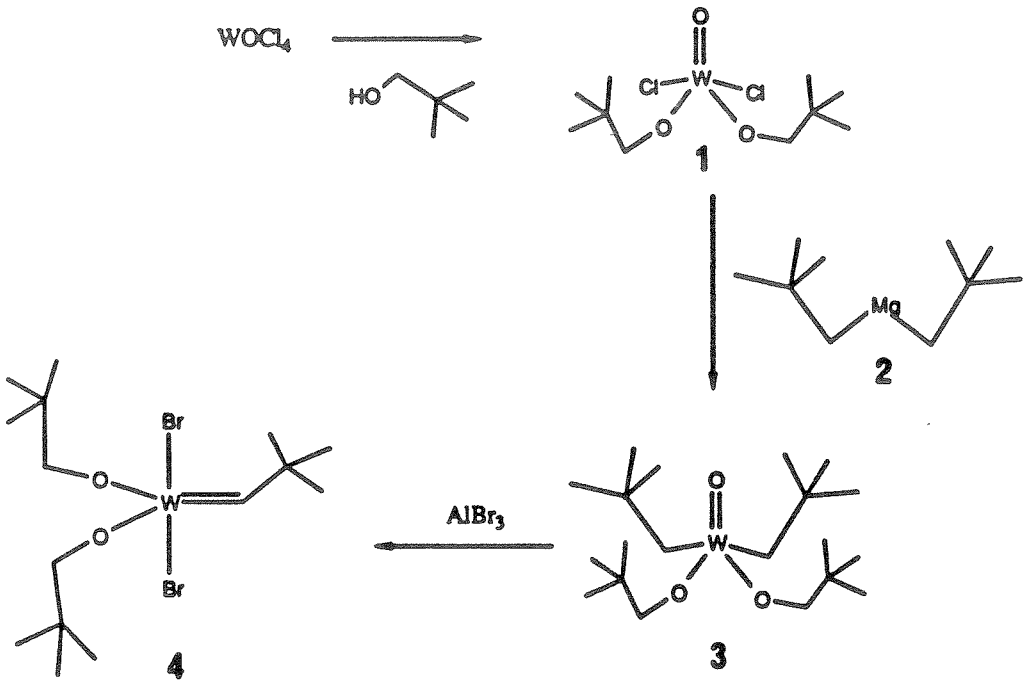

General Procedures: These procedures were given in Chapters 3 and 4.

Materials: Neopentyl chloride was purified by stirring over sulfuric acid, washed with a saturated K_2CO_3 solution, dried with $CaCl_2$, and distilled from CaH_2. $AlBr_3$ was purified by sublimation under dynamic vacuum.

Preparation of $WOCl_4$: Sodium tungstate trihydrate (80 g) was added to $SOCl_2$ (320 ml) and refluxed for 2-3 days or until no more gas SO_2 was being evolved. The excess $SOCl_2$ was then pumped off in vacuum to leave a red orange solid. The solid is sublimed (10^{-6} torr, 140°C) with a layer of glass wool over the crude material to catch ash. Multiple sublimations were also mecessary to get material with no ash. Total yield of $WOCl_4$ is approximately 70% .

Preparation of 1: 40 g of $WOCl_4$ is dissolved in diethyl ether (50 ml) and neopentanol in 50 ml diethyl ether is added with rapid stirring. The solution becomes cloudy and HCl is evolved. The product continues to precipitate and eventually the solution is a gel and cannot be stirred. This gel is allowed to sit for 3 hrs at room temperature with occasional physical stirring. The reaction is pumped on periodically to remove HCl and drive the reaction to completion. The reaction mixture is then evaporated to give a white material with a slight blue tint in quantitative yield.

Preparation of 2: A hot flask was charged with 8.2 gr magnesium dust; 200 ml of ether was added and 30 gr of neopentyl chloride was added slowly under inert atmosphere. The Grignard formation was initiated by adding a crystal of Iodine. Once the reaction had initiated, the addition of the neopentyl caused the reaction to reflux. When the addition was complete, the reaction mixture was refluxed for 18 hours. The mixture is filtered into a Schlenk flask by passing the solution through a cannula with filter paper wired around the inlet. Para-dioxane was added to the solution to give a white suspension which was further diluted with

400 ml ether to allow stirring. This was stirred overnight and then transferred under inert atmosphere into centrifuge tubes. Centrifuging the suspension in 50 ml portions gave a white cake of $MgCl_2$:dioxane and a slightly yellowed solution of the product. The ether was evaporated *in vacuo* to give a tacky solid, which was then loaded into a sublimator inside a dry box. Sublimation under dynamic vacuum gave **2** in a 60% yield.

Preparation of 3: 3.74 gr (.0225 mole) of **2** in 50 ml of ether is slowly added to a suspension of 10.0 gr (.0225 mole) of **1** in 40 ml of ether. A yellow color is observed upon immediate addition of **2** and dissolves upon further additon. The reaction is noticeably exothermic and $MgCl_2$ is observed to precipitate. The reaction is stirred under inert atmosphere for half an hour and then filtered. Rapid evaporation of the ether to $\approx$ 30% *in vacuo* cooled the solution down and produced yellow crystals. Further cooling to -30°C produced more crystals and the cold ether solution is then filtered away. Washing of these crystals with pentane at -50°C produced bright yellow crystalline material (65%) that is very pure by ^1H NMR. This procedure is found to be much more reliable than isolation of product by evaporation of the ether and recrystallization from pentane as was recommended by J. Kress. Quality crystals are hard to obtain by the latter method and the yields were lower. Solutions of **3** before recrystallization became progressively darker in time indicating decomposition. This decomposition is most likely the result of impurities and hence the rapid isolation of the crystals is effective because **3** is separated from the impurities before decompostion can occur.

Preparation of 4: $AlBr_3$ (.213 g) and **4** (.5 g) were combined in 25 ml of CH_2Cl_2 and then 18 μl of H_2O was added. The reaction turned slowly from a yellow color to a orange brown color. The reaction was then stirred for 20 hours and then pumped to dryness. **4** is then extracted from the aluminium oxides with pentane. Pumping down the extracts yields **4** as a relatively pure material.

References:

1. (a) Kress, J.; Osborn, J. A. *J. Am. Chem. Soc.* **1983**, 105, 6346. (b); Aguero, A.; Kress, J.; Osborn, J. A. Green, R. M. E.; Ivin, K. J.; Rooney, J. J. *J. Chem. Soc., Chem. Comm.* **1985**, 874. (c) Aguero, A.; Kress, J.; Osborn, J. A.*J. Chem. Soc., Chem. Comm.* **1985**, 793. (d) Kress, J.; Osborn, J. A. Green, R. M. E.; Ivin, K. J.; Rooney, J. J. *J. Am. Chem. Soc.* **1987**, 109, 899. (e) Kress, J.; Aguero, A.; Osborn, J. A. *J. Mol. Cat.* **1986**, 36, 1.

Appendix B

EQUIPMENT FOR CONDUCTIVITY MEASUREMENTS AND THE MANIPULATION OF AsF_5

Schematic drawings of the conductivity cell used for continuous monitoring of the conductivity with doping is shown in Figure B.1. The O-ring joints are important since grease absorbs and reacts with the dopants. The O-rings were Viton^{TM} and were changed regularly.

Figure B.2 is a drawing of the vacuum line that was constructed for the handling of AsF_5. AsF_5 is a particularly toxic material, and the vacuum line was in a hood with a charcoal filter. The O-rings were coated with Halocarbon grease obtained from Halocarbon Products Corporation, 82 Surlews Court, Hackensack, NJ (201-343-8703). This grease is a chlorofluorocarbon based material and is highly resistant to oxidative reagents. Coating the 0-rings with this grease was found to increase the resistance to decomposition by the AsF_5. The pressure transducer was a diaphragm type made specifically for corrosive gases. This transducer was an MKS Instruments AA01000A pressure transducer and it required a PdRC-1B readout/power supply unit. Pressures between 0 and 1000 torr may be measured with this unit to an accuracy of .1 torr. AsF_5 pressures were always maintained considerably below ambient atmosphere. The transducer was connected to the vacuum line with an all metal Swaglock union. The vacuum line was thoroughly dried with heat guns while applying vacuum before any AsF_5 was admitted into the system. The AsF_5 tank was connected to the vacuum line by an all metal path capable of holding vacuum. Hence, vacuum was usually applied all the way to the tank before admitting AsF_5 to the system. Once the line was filled with the desired amount of AsF_5 (100 to 400 torr), the cold finger was immersed in liquid nitrogen. The AsF_5 was then collected into the cold finger and dynamic vacuum is applied to the system in case of any air contamination. This procedure also allowed the AsF_5 to be isolated with a teflon valve from the rest of the system to allow any pumping down of other equipment such as a chamber with polymer or the conductivity cell of Figure B.1. One batch of AsF_5 was usually used for

multiple experiments. This was done because of the fact that the AsF_5 is not plesant to quench. Excess AsF_5 is quenched by condensing it in the trap between the vacuum line and the pump and then adding acetone to the mixture while it was still cold. White fumes are produced in this process.

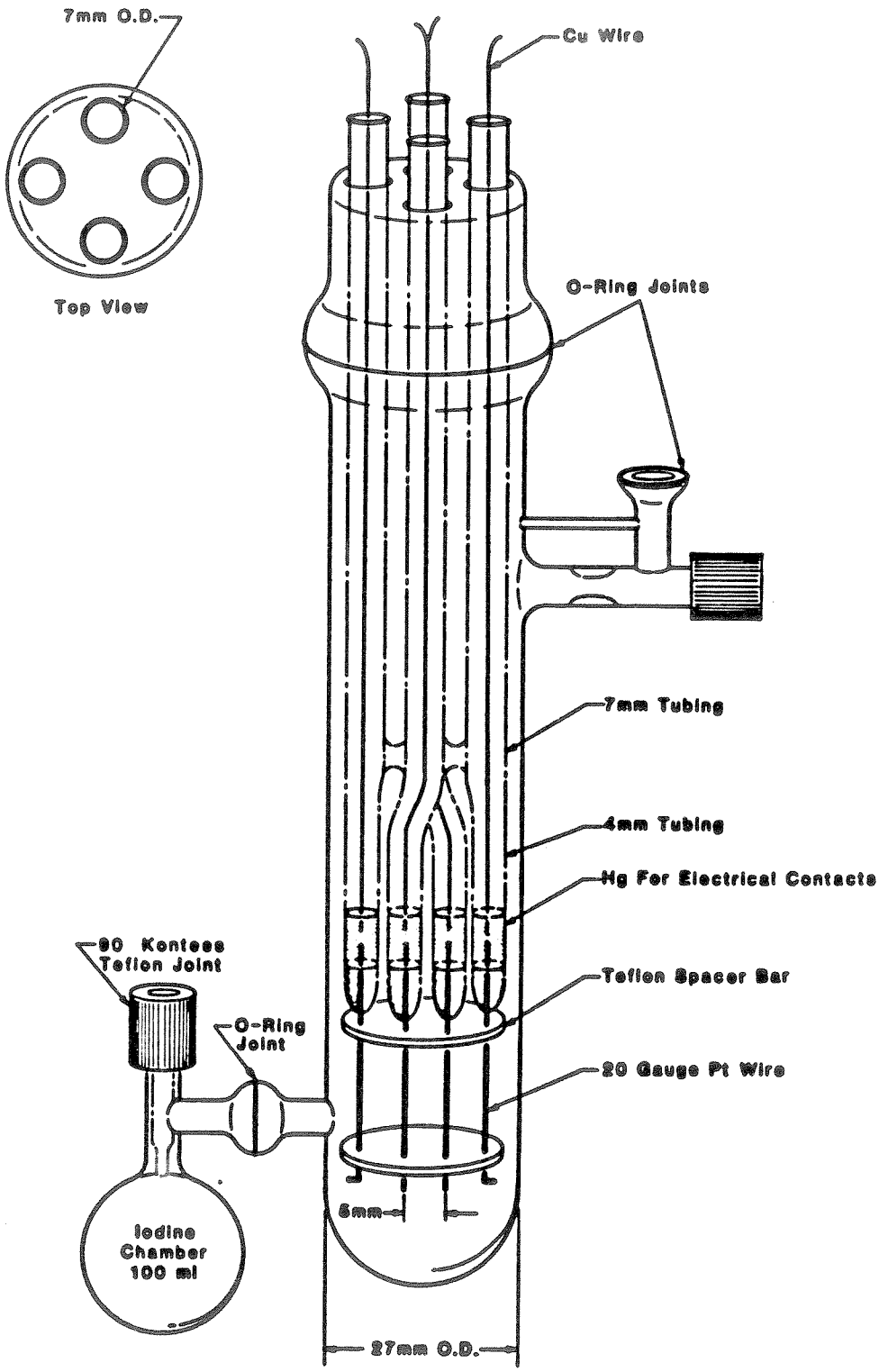

Figure B.1. Schematic drawing of a conductivity cell.

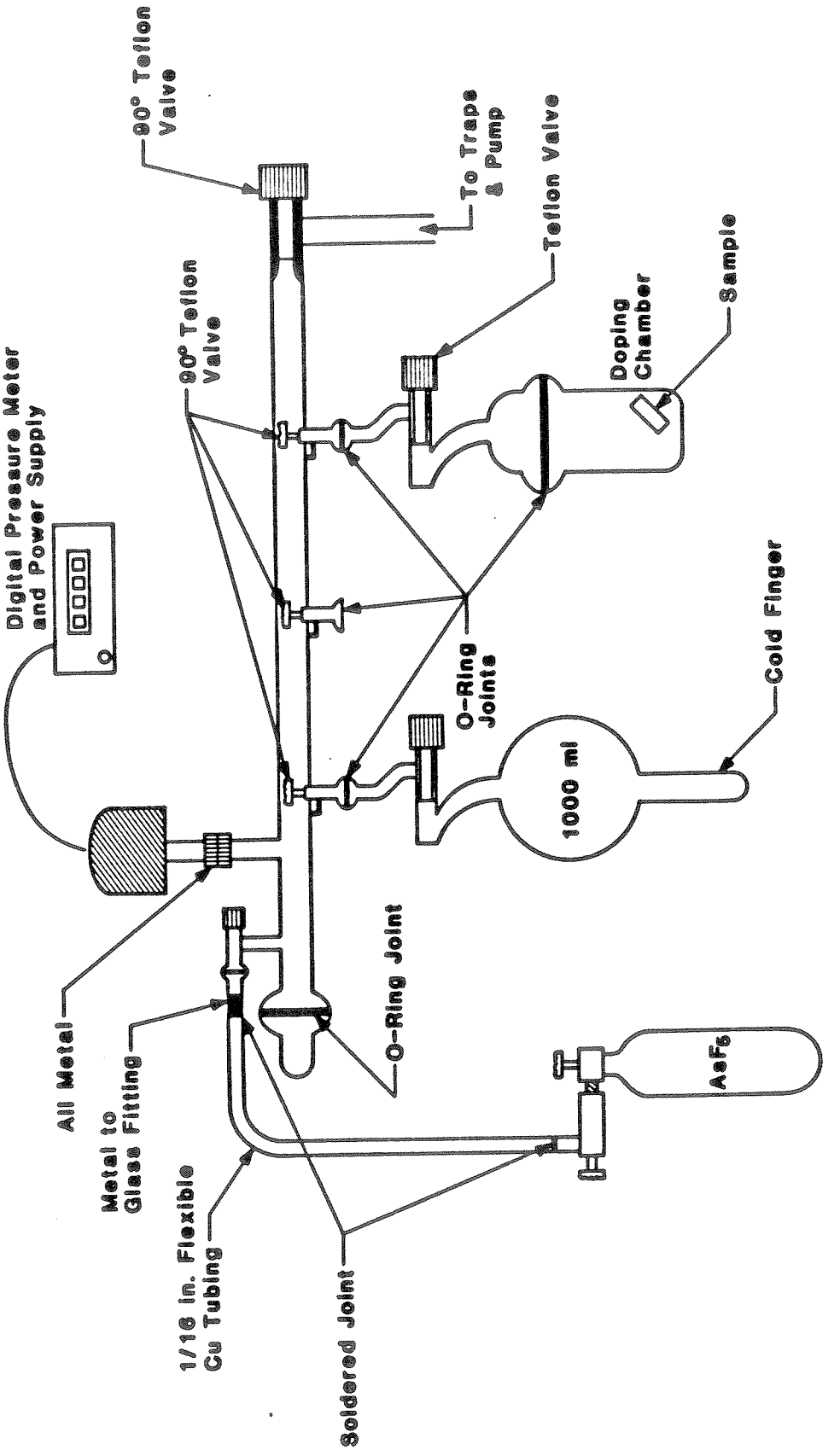

Figure B.2. Schematic drawing of a vacuum line for AsF_5 doping.